

General Disclaimer

One or more of the Following Statements may affect this Document

- This document has been reproduced from the best copy furnished by the organizational source. It is being released in the interest of making available as much information as possible.
- This document may contain data, which exceeds the sheet parameters. It was furnished in this condition by the organizational source and is the best copy available.
- This document may contain tone-on-tone or color graphs, charts and/or pictures, which have been reproduced in black and white.
- This document is paginated as submitted by the original source.
- Portions of this document are not fully legible due to the historical nature of some of the material. However, it is the best reproduction available from the original submission.

99626

FINAL TECHNICAL REPORT

S-047 EXPERIMENT

CEI NAS 9-7457-V.A.

FACILITY FORM 602

N69-24200

(ACCESSION NUMBER)	(THRU)
160	1
(PAGES)	(CODE)
OK 99626	13
(NASA CR OR TMX OR AD NUMBER)	(CATEGORY)

CR 99626

TABLE OF CONTENTS

	Page
I. Background	1
II. Supporting Theoretical Analysis	10
A. The Spacial Autocorrelation Coefficient in Objective Analysis	11
B. The Distribution of Bright Stars Observable from a Spacecraft Orbiting the Earth at a Small Inclination Angle	17
III. Hardware Requirements	19
A. General	19
B. Major Subsystems	19
IV. Phase C Summary, Conclusions and Recommendations	23
A. Chronology of the Experiment Technique	23
B. Contract Effort Summarized	25
C. Conclusions	28
D. Recommendations	28
Figures 1 through 32	
Appendix A - Refraction Star Tracker Specification including:	
Photographic Section	
Mechanical and Electronic Drawings	

I. Background

A. Introduction

Improvements in man's understanding of atmospheric processes and in his ability to forecast weather parameters through longer periods are known to be quite dependent upon data coverage. The initial conditions for numerical weather prediction models are still, to a surprising extent, composed of an initial guess field updated by observations. However, such observations are not forthcoming over much of the Earth's oceanic surfaces, with the exception of satellite visual and infra-red photography. Thus the useful quantitative parameters for weather forecasting or research on a hemispheric scale are in good supply only over certain land regions such as Europe and the United States. To sound the atmosphere in data sparse areas, new satellite techniques are needed which will produce data in volume for numerical prediction, for GARP (Global Atmospheric Research Program) in the mid-1970's, and for WWW (World Weather Watch), which is already under way.

B. Display of the Refraction Technique

Such a technique was proposed in 1961 by Prof. L. M. Jones of the University of Michigan High Altitude Engineering Laboratory. It consists of probing the atmosphere by measuring the refraction of a star ray passing through with a minimum tangent height (r_0). (Fig. 1). This refraction angle (R_s) is measured by a star-tracker as a function of time (t). From geometric considerations and the fact that the satellite platform is to be highly stable, $\theta(t)$ is obtained. These quantities yield the zenith angle, $z_s(t)$.

Employing Snells' Law, which states that the triple product of the index of refraction (μ), $r(t)$, and $\sin z_s(t)$ is constant along the refracted ray path, we find that certain simplifications can be made at the tangent point, where $\sin z_s(t) = 0$, and at the satellite, where $\mu \approx 1$. Therefore

$$r_s(t) \sin z_s(t) = \mu_0 r_0(t) \quad (1)$$

Subscript zero refers to the tangent height and $r_s(t)$ is obtained by satellite tracking. $\mu_0 r_0$ has been named the impact parameter, η_0 , by us.

From knowledge of $R_s(t)$ and $\eta_0(t)$, $R_s(\eta_0)$ is determined. As may be seen in Eq. (2), this function is desired for the computation of μ by numerical quadrature.

$$\mu = \exp \left[-\frac{1}{\pi} \int_{\eta}^{\infty} (\eta_0^2 - \eta^2)^{-\frac{1}{2}} R(\eta_0) d\eta_0 \right] \quad (2)$$

Choosing η , one finds $\mu = \psi(\eta)$ and then secures r from the expression, $r = \eta / \mu$. The remaining relationships used to get the common atmospheric parameters are:

$$\text{Dale and Gladstone's Law, } \rho = \frac{\mu - 1}{K} \quad (3)$$

ρ = density

K = constant

$$\text{Hydrostatic Law, } \frac{dP}{dh} = -\rho g \quad (4)$$

P = pressure

h = height

g = gravity acceleration

$$\text{Gas Law, } P = \rho R^* T \quad (5)$$

R^* = gas constant

T = temperature

The ρ - field is expected to attain more importance in the future, but P - and T - fields are nevertheless obtainable from use of the last two Laws, with little error.

C. Details of Star-tracking from a Spacecraft

From a polar orbit which assures global data excepting over the sun-lit pole, the star-tracker is pointed aft and programmed to pick up a star ray penetrating the Earth's dark hemisphere (Fig. 2). First contact is made at 40 - 50 km tangent height, but as the satellite proceeds in orbit, the star appears to set, i. e., it is occulted by the Earth. The measurements of $R_s(t)$, $\theta(t)$, and $r_s(t)$ are made about twice per second, and the size of R_s varies from 4 arc seconds at 50km to 40 arc minutes at 5 km. Successful data-gathering below 5 km is improbable because of cloudiness, which obstructs ray penetration, attenuation due to ray scattering and a prismatic dispersion effect. Keeping the azimuth angles within 30° of aft conserves tracking time and permits the recording of about 50 R_s values in each of 80 or so scans per orbit. Tracking time is about 30 sec per star. The resulting N. Hemisphere coverage (Fig. 3) for a particular day shows the repetitive pattern. The longitudinal spacing between pattern repetition is about 27° when the orbital altitude is 1100 km. Clearly, a wealth of upper air data is attainable when stars of magnitudes greater than 4.5 are tracked, as in this case.

The equipment in the spacecraft includes, besides the star-tracking telescope, a clock, a data recorder, and a telemeter. On the ground, a command and data acquisition station would pass updated sets of star coordinates to the satellite. It would also receive data in brief periods amounting to a few seconds per orbit. About 1/4 million bits are involved in these transmissions. A data processing program was written in 1964 which retrieves density, pressure and temperature more than twice as fast as acquired.

D. Theoretical Justification for the Refraction Solution

Eq. (2) is a mathematical inversion of the classical refraction integral for a ray passing completely through the atmosphere with impact parameter η_c . The latter integral is

$$R = 2 \eta_c \int_{\eta_c}^{\infty} \frac{d\mu}{\mu (\eta^2 - \eta_c^2)^{1/2}} \quad (6)$$

The inversion was discovered in the field of seismology, and it has the desirable features of uniqueness and exactness. The uniqueness implies, in the refraction case, that knowledge of the function $R(\eta_c)$ yields any and all densities within the scan altitude limits. The two features combined permit (1) simple, precise evaluation of $R(\eta_c)$, (2) direct reduction of simulated $R(\eta_c)$ data to ρ , P , and T , and (3) definitive evaluation of errors.

E. Analysis of Errors

The following possible errors have been investigated: (1) measurement of refraction angle at the spacecraft; (2) truncation of pressure at an upper level; (3) nonspherical stratification of the refraction angle about the tangent point; (4) satellite tracking inaccuracy. They will now be considered in turn.

(1) Using the CIRA 1961 atmosphere as a model, Eq. (6) was evaluated numerically to obtain a set of refraction angles. Various Gaussian-scatter standard deviations were then tested, retrieving ρ , P, and T to compare with the model. The second star-tracking parameter which affects the data reduction is readout frequency. Accordingly, this quantity was also varied in the analysis.

(2) When using Eq. (4) to retrieve $P(h)$, an initial estimate of P (or T) is required at the uppermost level where results are to be secured. As one proceeds downward in the integration process, an error in the initial estimate of P will "integrate out" in about 10 km, i.e., it will be overshadowed by the refraction angle measurement errors.

(3) Within the visual and near-IR range of wavelengths, the refractive effect is concentrated quite well at the ray tangent point. This result has been found by an analytic treatment of the lower spacial derivatives of ρ and T around the tangent point under the influence of extreme atmospheric gradients. Thus the refraction angle is found to be symmetric around the tangent point, with negligible departures. To be otherwise would violate one of the basic assumptions of the classical refraction equation.

(4) Since the meteorological parameters obtained from refraction data are, to some extent, averaged values over tens of kilometers in a network which usually has several hundreds of kilometers between observation points, horizontal errors in satellite positioning can be tolerated of the order of 10 km. However, inaccuracies in vertical positioning are transmitted undiminished as height errors into the P- and T-profiles. The P-profile

is especially sensitive to this effect, although the error is systematic in the horizontal and can probably be removed through calibration with radio-soundings.

Numerical results for the error analysis are presented in Figs. 4 and 5 for T-errors and P-errors. The scatter of the refraction angle has a standard deviation of 4 arc seconds, and a 5% RMS pressure error is assigned to the initial value of P at 40 km in both instances. The outcome is entirely comparable in accuracy to radiosondes, indicating that a viable system is assured if the equipment specifications of Figs. 4 and 5 are met. The accuracy requirements for T and P compiled recently by COSPAR Working Group Six for GARP are somewhat more stringent in the lower stratosphere, probably demanding a 2 arc second star tracker to fulfill them.

F. Adverse Atmospheric Effects

A study of atmospheric effects known to operate upon the stellar image received at the satellite has yielded assessments of such diverse factors as (1) molecular scattering, (2) differential refraction (the phenomenon of prismatic dispersion), (3) absorption by gaseous constituents, (4) scintillation, (5) quivering, and (6) clouds.

(1) Molecular scattering has a notable dependence upon wavelength (λ) in the range 0.3 to 1.0 μ . The transmission factors for various λ in this range are shown in Fig. 6 for tangent ray heights between 5 km and 40 km. An analytic model atmosphere was investigated to obtain these results, following the analysis of an isothermal atmosphere.

Water vapor can add important attenuation due to scattering. Its occurrence is largely confined to layers below 10 km, although water vapor penetrates above this level in significant quantities at times, mainly in the tropics.

Dust is another important scatterer because of its tendency to stratify at times in the stratosphere.

(2) Differential refraction shows little wavelength dependence (Fig. 7). However, it is responsible for some of the shifting in the image's center of gravity during occultation. As may be seen in Fig. 7, the transmission suffers a rather great diminution from 30 km to 10 km. Satellite altitude is of major importance in this respect, with a lower orbit enjoying higher transmission. The altitude used here is 1100 km.

(3) Absorption by ozone in the Chappuis band centered near 0.6μ was found to be inconsequential. This constituent is the principal absorber in the visual range.

(4) The scintillation, or fluctuation of starlight intensity, is related to the telescopic aperture, zenith angle, and meteorological conditions along the ray path. The star-tracker must have an aperture large enough to control adverse scintillation, as the other two factors are not controllable.

(5) Quivering of the stellar image turns a point image into a spot with a diameter of 2 - 4 arc seconds. It is also controlled by a sufficiently large lens size.

(6) Through the collection of thousands of aircraft reports at 10 - 12 km, the vertical distribution of clouds has been better determined by us. With a few exceptional cases, it is generally true that clouds will not interfere with refraction scans down to 10 km. The principal exception is the Intertropical Convergence Zone of tropical latitudes; a second is certain instability lines in low- and middle-latitudes. Lower probing down to about 5 km is often not restricted by clouds, but is impaired by the other adverse effects.

G. Signal/Noise Ratio

The reduction of the signal received behind the photocathode tube may be summarized in a graph of photocathode magnitude against tangent ray height (Fig. 8). Thus, taking into account the spectral response of two sensors, as well as molecular scattering, differential refraction, and ozone absorption, a decline in apparent stellar magnitude is to be expected amounting to 5 to 7 when tracking down to 5 km.

The noise consists of 4 components. They are the airglow, which predominates; zodiacal light; aurorae; and stellar background. Minimum noise levels have been computed for these factors, excluding the highly variable aurorae, which generally lie above the field of view.

Signal/noise ratios were calculated for equipment specifications, utilizing the above information.

H. Downward Extrapolation to 500 mb.

Recognizing the difficulty of retrieving the atmospheric parameters at the critical 500-mb level (~ 5.5 km) by the refraction method,

error studies were completed dealing with downward extrapolation of the data obtainable at higher levels. Outside of the tropics, 90 percent or more of the variance of the 500-mb geopotential is explained by an extrapolation from 300 mb (~ 9 km) in January, slightly less in July, and 50 - 80 percent of the variance is explained when extrapolating from 200 mb (~ 12 km) to 500 mb. Furthermore, these values are upheld, outside of the 0° - 20° latitude band, when the regression coefficients are all expressed as functions of latitude. This work was completed for one-half of the N. Hemisphere.

II. Supporting Theoretical Analysis

During the contract period, supporting studies have been conducted to assist with hardware design. Generally, the results are incorporated into engineering decisions. Two results have application to the technique theory and are of independent interest. They have not been otherwise published and are presented here for documentation purposes.

A. The Spatial Autocorrelation in Objective Analysis

Introduction

The kind of information obtainable from stellar refraction is similar to that which is currently produced by radiosondes, but two important differences in air-sampling locations should be noted. First, the data from star-tracking would be mainly from the upper troposphere and lower stratosphere, in the upper altitude range of radiosoundings. Second, the geographical locations of refraction data points would not be fixed, in the sense that land-based radiosonde stations are fixed. The latter difference leads one to consider how to incorporate such data into charts being analyzed objectively, as by a computer program. If the data are to help form the basis for a field of grid values, as is commonly the case, then the question can be enlarged to include all kinds of measurements pertinent to the parameter being analyzed.

Some recent advances in the field of objective analysis have been made by Gandin [1963] , Peterson [1967] , and Alaka [1969] . In all of these investigations, the method of "optimum interpolation" holds a prominent place among the various schemes to give data values appropriate weights when transferring data to grid points. Kolmogorov 1941 is credited with the origination of the idea of "optimum interpolation" and Gandin is responsible for much of its development. Kruger's unpublished comparative study of four methods, namely, those of Gandin, the National Meteorological Center in Washington, D. C. , and (two) of the Canadian Central Analysis Office showed "optimum interpolation" to be about on a par with one of the Canadian methods and clearly superior to the other two, in sparse data regions.

In the "optimum interpolation" method, the weighting functions are obtained by autocorrelation techniques and they are applied under the assumption that the meteorological fields are homogeneous and isotropic with respect to the spacial autocorrelation function. Mathematically, this means that for homogeneity,

$$[f'(\vec{r}_i)]^2 = \text{constant for all } i, \quad (1)$$

and for isotropy

$$\frac{\partial f'(\vec{r}_i)}{\partial \theta} = \text{constant for all } i. \quad (2)$$

f' = deviation of an element from its norm

\vec{r}_i = point vector on the isobaric surface

θ = degrees from north on the isobaric surface

Since these assumptions are basic to "optimum interpolation" and an intensive search did not reveal any published test results in the literature, an examination was conducted on 500 mb height data for three sites in the Northern Hemisphere. The purpose of the test was to find, through graphical displays, the degree of homogeneity and isotropy apparent in the data.

Grid Network and Data

A grid-point network was used which had a 500 km separation between points at the three sites selected. 500 mb height data* for the Januarys of

* Sometimes referred to as Project 433-L grid data.

of 1956, 1957, and 1958 were processed, the data consisting of interpolated grid-point values from subjectively analyzed charts of the National Weather Analysis Center. The information was available on punched cards, and no expense was incurred in this respect. July data were also processed for the same years, but for one site, only.

Computation of the Spatial Autocorrelation Coefficient

The spatial autocorrelation function, $\mu(\rho)$, was normalized, as may be seen in the following expression,

$$\mu_j(\rho) = \left[\frac{1}{N} \sum_{i=1}^N \Phi_{ij} \Phi_{io} - \Phi_j \Phi_o \right] [\sigma_j \sigma_o]^{-1} \quad (3)$$

where

$$\sigma_j = \left[\frac{1}{N} \sum_{i=1}^N \Phi_{ij}^2 - \left(\frac{1}{N} \sum_{i=1}^N \Phi_{ij} \right)^2 \right]^{1/2}$$

ρ = distance from base point

N = 186 observations

Φ = geopotential height

σ = standard deviation of

subscript zero refers to base point, or "site"

subscript j refers to grid-point

The sites selected were as follows, and will be referred to by site number.

1. (42N, 101 W), in Nebraska, U.S.A.
2. (46N, 35W), 1550 km east of Newfoundland in the Atlantic Ocean

3. (60N, 125W), near Fort Nelson, British Columbia

From each base point, the μ_j were computed by an IBM 7090 to a distance of 5800 km (Site 1), 4700 km (Site 2), and 3800 km (Site 3), excepting in those directions where data boundaries cut off the calculations.

Results

The μ_j were displayed in three ways. The first mode of representation can be found in Gandin's book, p. 49, as a collection of curves of μ against ρ . However, the scatter was not shown therein, and it is evidently rather large beyond 500 km at Sites 1 and 2 (Figs. 1, 2) and even at 500 km at Site 3 (Fig. 3). The curves drawn on these figures were fitted by inspection to a standard empirical formula, $\mu(\rho) = e^{-a\rho} \cos(b\rho)$.

The large amount of scatter in these diagrams was studied further through curves of μ versus ρ for 8 directions from the base point (Figs. 4, 5), and two-dimensional displays of $\mu(\rho)$ centered upon the base point (Figs. 6-9). True homogeneity and isotropy would be indicated by coincident curves and concentric circles, respectively, in these two types of figures. Qualitatively, rather large departures from homogeneous and isotropic conditions are quite evident to all sites in these graphs. No quantitative measure of these statistical concepts was found in the literature, however, so here the matter rests. There is tenuous evidence of relationships between the patterns of Figs. 6-9 and the mean flow fields at 500 mb for the same periods. More base points need to be explored to firmly establish such relationships.

Conclusions

The assumption of statistical isotropy and homogeneity in geopotential

height data at 500 mb, as defined by Eqs. 1 and 2, is not on firm ground.

Diagrams of the normalized autocorrelation coefficient, $\mu(\rho)$, show departures from true isotropic and homogeneous conditions at three widely separated base points in the Northern Hemisphere. These results relate particularly to the method of "optimum interpolation" in objective analysis, which employs the above assumption in forming spacial fields of $\mu(\rho)$.

References

- Alaka, M. A., Theoretical and Practical Considerations for Network Design,
Paper Ob 1.2, American Meteorological Society Symposium on
Meteorological Observations and Instrumentation, Washington, D.C.,
February 10 - 14, 1969.
- Gandin, L. S., Objective Analysis of Meteorological Fields, GIMIZ,
Gidrometeorologicheskoe Izdatel' stvo, Leningrad, 1963.
- Kolmogorov, A. N., Interpolated and Extrapolated Stationary Random Sequences,
Izvestiya AN SSSR, Seriya Matematicheskaya, 5, 1, 1941.
- Peterson, Daniel, A Study of Interpolation and Smoothing Operators in
Objective Analysis, EE 148 DC 7 35028, New Mexico U., Bureau
of Engineering Research, 15 December 1967.

B. THE DISTRIBUTION OF BRIGHT STARS OBSERVABLE FROM A SPACECRAFT ORBITING THE EARTH AT A SMALL INCLINATION ANGLE

When only the brighter stars can be tracked in an occultation experiment, as is presumed to be true for manned capsules, the distribution of available stars is inevitably uneven and weighted heavily toward Gould's Belt. A computer program at hand based upon a magnetic tape version of the Albany (Boss) Catalog was used to obtain an accurate estimate of this distribution. Inputs for the IBM 7090 program were the orbital elements of the satellite and the celestial coordinates of stars brighter than magnitude 2.0. The output was the geographical position of stars observable on the night side of Earth within 30° of due aft.

The two launch dates selected for testing were March 21 and September 21, both midnight launchings. The orbital inclination was 27° in either case, this being the estimate for Apollo Applications A at that time. The resulting geographical positions were plotted on a global chart, and the following features were noted.

March 21 launch: 12 stars were located, all clustered in the Indian Ocean - Western Australia region of the Southern Hemisphere. The probable lack of routine radiosonde reports in this region was considered to be quite disadvantageous, as a comparison of stellar refraction data (in terms of density and temperature profiles) with a radiosounding would be desirable.

September 21 launch: 4 stars were located near 20° N in the Western Hemisphere. These data points were more amenable to radiosonde comparison,

especially the ones near the Dominican Republic and Hawaii.

The conclusion reached by this investigation is that a fraction of stars brighter than magnitude 2.0 will be available for tracking on the night side aft of the spacecraft, even in an orbit of low inclination. However, in tropical regions a large proportion of the stellar refraction profiles, and their corresponding atmospheric parameter profiles, would not be close enough to a radiosonde station to permit a comparison test. Thus if this kind of test is desired, careful preplanning is needed with attention being given to launch date, time of attempted observation, and upper cloudiness forecasts.

III. Hardware Requirements

A. General

Having thus shown the meteorological import attached to refraction angle measurements of the type mentioned, and having conducted a definitive error analysis, the overall performance specifications were set and the task of designing a state-of-the-art star-tracker was begun.

The performance goals, overall, may be summarized:

- Star-tracking with angular error less than 2 arc-seconds RMS.

- Readout frequency greater than 10/second.

- Acquisition of any star brighter than the third visual magnitude.

- Tracking of any star brighter than the 4.5 visual magnitude when attenuated an additional 5 magnitudes, with stated accuracy.

- Operation from astronomical twilight to astronomical twilight on the dark side of any orbit.

- Continued tracking through any cirrus layer causing occultation of less than 0.5 second.

B. Major Subsystems

The major subsystems involved are:

- Acquisition telescope

- Data telescope

- Acquisition tracker

- Data tracker

- Gimbals

- Gyro

Command logic unit

Astronaut control unit

A description of the primary requirements is given for each subsystem:

1. Acquisition telescope

Field of view - 2° (or more)

Transmission - 60%

Refracting optics

Diameter - 2.5 inch

Shutter to prevent contamination

2. Data telescope

Field of view - 16 arc-minutes

Diameter - 10 inches

Transmission - 60%

Reflecting, folded or catadioptric optical system

Thermal gradient control of folded optics

Shutter to prevent contamination

3. Acquisition tracker

F 4012, S20 phototube (image dissector) with .020 square aperture

Square raster scanning system with 10% overlap

Atwill scanning detector system

Error signal (Atwill) generation at 200 Hz

Error signal error (Atwill) less than 3% in either axis

4. Data tracker

F 4012, S20 phototube (image dissector) with .020 square photo cathode

Square raster scanning system with 10% overlap

Atwill scanning detector system

Error signal (Atwill) generation at 200 Hz

Error signal error (Atwill) less than 3% in either axis

5. Gimbals

Two-axis freedom

No static friction permissible

Allowable spring torque = -5 lb-in/radian

Caging requirement for launch and astronaut boresight coincidence

Torquing capability to maintain required pointing accuracy under prescribed star angle acceleration plus spacecraft acceleration

6. Gyro requirements are detailed in the Star-Tracker Specification, below.

7. Command Logic Unit:

Upon astronaut command to track, the logic must:

- a) Select the brightest star in the acquisition telescope field-of-view by raster scanning and memorize its position.
- b) Point the telescope so as to center the image in the field-of-view.
- c) Switch to Atwill scan and center the image precisely.
- d) Begin raster scan in data tracker.
- e) Upon location of image in data tracker switch gimbal control to data tracker

f) Point telescope to center image in the data telescope field-of-view.

g) Switch to Atwill scan and center the image precisely.

The above sequence should take less than three seconds.

8. Astronaut Control Unit

This Unit will be located in the Command Module and will be comprised of a zero-reader, switches, and boresighted telescope.

It enables the astronaut to warm-up the equipment, select a star and point the spececraft so as to acquire it, command the tracker to track and monitor shut-down or occultation, and secure the equipment when finished.

This Unit cannot be designed until the interfaces are defined and ICD's issued.

IV. Phase C Summary, Conclusions & Recommendations

A. Chronology of the Experiment Technique

1. The refraction star-tracking technique was conceived in 1961 and feasibility studies began in 1962.

2. The analytic solution of density as a function of height from measurements of refraction angle was demonstrated in 1964.

3. Error analyses were completed in 1965.

4. Experiment definition studies were carried out in 1965 and 1966 and 1967.

5. A Phase "C" proposal was submitted on 9 June 1967 for equipment to be flown on the Apollo Applications A mission.

6. A contract was awarded on 6 September 1967 (NAS 9-7457) for a portion of the proposed Phase "C" effort, excluding the construction of a qualifiable prototype, and including a brassboard instrument. A six-month period was indicated.

a) During the contract period the anticipated funding for Phase "D" was sharply reduced and the time schedule was drastically stretched.

b) During the contract period the spacecraft integration contract was cancelled. Because of this, the carrier vehicle was not designed and the interface control documentation was not issued.

c) During the contract period the flight mission was cancelled.

d) The University, working in close harmony with the Manned Spacecraft Center, proposed stretching the NAS 9-7457 contract period to 1 July 1968 with no cost increase. This request was granted.

e) The University was advised to proceed with the design in as reasonable a manner as possible, considering the lack of interface control. NASA supplied interface design parameters and approximate design details.

f) As 1 July 1968 approached it was evident that follow-on funding would not be available on that date. Accordingly, the Principal Investigator redoubled efforts to complete the engineering design and brassboard construction to a milestone point prior to the loss of personnel. This was accomplished. As a result, the planning documents for the cancelled mission, which were clearly of diminished importance, were deferred and completed by the Principal Investigator after the loss of other project personnel.

7. As of 14 March 1969:

a) The key personnel are on leave of absence from the University activities. Non-key personnel have been discharged. The Principal Investigator is employed on a different, related contract on another project.

b) The brassboard and mockup hardware items are completed and located in the University star-simulation facility. It has been formally requested that they remain in the University

NASA facility property account pending a resumption of hardware implementation for flight.

c) The documentation has been completed and is being delivered in March 1969.

B. Contract Effort Summarized

The bulk of contract effort was expended in the design and fabrication of the brassboard prototype instrument. This effort may be roughly divided into five categories:

Supporting theoretical analyses

Background analysis and critical systems engineering decisions

Critical component selection

Detail electronic design and fabrication

Detail mechanical design and fabrication

1. Supporting analysis is included in the remainder of the report, such as Figs. 18, 19, 20, or in Section II above.

2. An extremely critical decision on the overall system was required. The measurement of refraction angle can be made by comparing the present location of a star with its former unrefracted location by means of an inertial reference (gyroscope); or it can be done by including both the subject star and an unrefracted star in the field-of-view, and measuring the change in angle between them as the first is refracted. The former method requires a telescope in gimbals and gyros; the latter, a large field-of-view with certain pattern recognition features, great resolution and rapid scanning, but no gimbals or gyros. We refer

to the latter as "electronic gimbaling". The electronic gimbaling can be used on one star, with gyros but no gimbals, or if the spacecraft motion were known (as through auxiliary star trackers) on one star with no gyros and no gimbals.

The decision to proceed with a conventional gimballed telescope and gyros was made after a great amount of study, analysis, consulting help, investigation of test results, and comparisons with operating instruments. Electronic gimbaling was very attractive because of its simplicity and consequent economy. However, the required accuracy lay somewhat beyond the anticipated state-of-the-art at the time of Phase 'D' implementation. Improvements in electronic gimbaling were occurring rapidly, therefore the time of Phase "D" implementation played an essential role in what otherwise would have been a straightforward engineering decision.

Having been now indefinitely delayed, the Phase "D" schedule may some day dictate that due to advances in electronic gimbaling the current design is not optimum. Such vagaries could not and were not considered by the designers.

3. Other important but less critical decisions involved the selection of gimbal bearings, phototube type, basic telescope optical design, and gimbal torque motor size. These component selections were rather fundamental to the systems design.

Once the phototube type was chosen for performance characteristics based on supporting analysis of spectral characteristics of starlight

having passed through the atmosphere on a tangent path, and the optical system was chosen, the gimbal bearings and torque motor sizes were chosen from error rate network analyses.

The approach to such analyses is illustrated by an example in figures 18 through 32. Supporting analysts calculated average probable refraction angles, rates, accelerations, and times for a typical occultation, as shown in figures 18, 19, and 20. The telescope and star-tracker system characteristics were simulated by the systems in Figures 21 and 22. The error rate network design procedure is shown in figures 23 through 30. Then, knowing the Apollo stability limit cycle in the fine control mode and the minimum attitude stabilizing thrust (15 ms linear duration to produce 6 arc-minute/sec rate change), the transient response of the overall system is shown in figures 31 and 32.

By use of such an approach, the flex-pivot was chosen over such possibilities as ball-bearings and the 60 oz-in torque motor was selected. The size of flex-pivot was likewise determined, although based on a 1g test demonstration. If 0g conditions were assumed the specification could have been less rigid, but the instrument would not have been susceptible to ground performance test.

4. The electronic circuit design and some construction details are illustrated in the attached specification drawings.

5. The mechanical design is illustrated in the attached specification photographs and drawings.

C. Conclusions

1. The brassboard instrument was successfully designed and constructed. It was not completely tested. Sweep circuitry and command logic was tested and performs according to expectation. The alignment of sweep with aperture at telescope focus was not accomplished satisfactorily and requires adjustment rather than redesign. The servo system is analytically correct but has not been tested with simulated star motion.

2. The planning functions were completed. Because of the lack of firm interface controls some documents are preliminary. The cancellation of the proposed mission greatly diminished the interest in and value of these documents.

3. The very rigid performance requirements were met in the design somewhat more readily than had been anticipated. This has increased the feasibility of the technique.

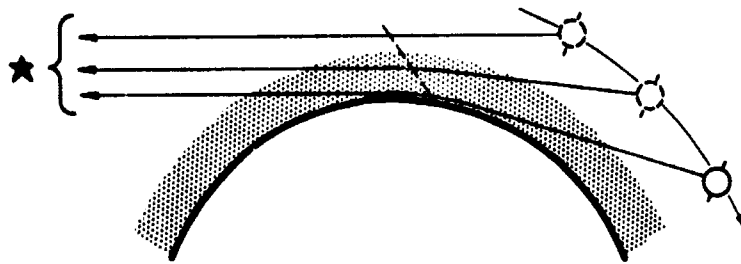
4. The failure to provide a follow-on contract for flight equipment has threatened the permanent loss of the project of several key persons.

D. Recommendations

1. The brassboard instrument should be thoroughly tested in the University star-simulation facility. Its performance has a potential impact on star-tracking technology as well as the refraction technique.

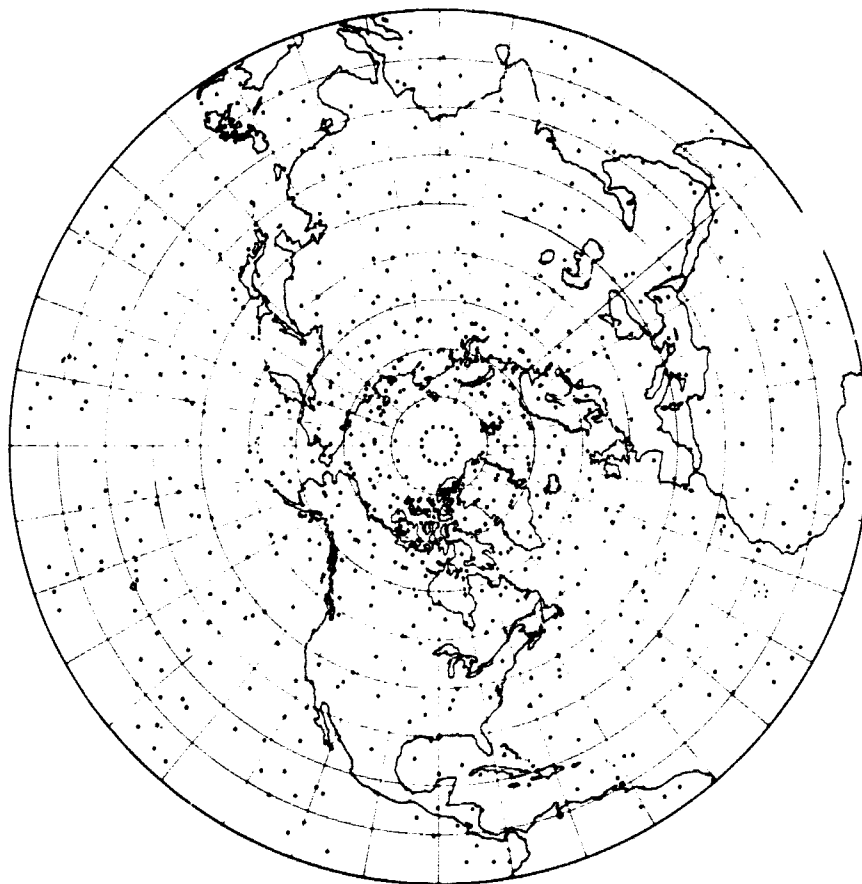
2. The stellar refraction technique remains at this report date the only technique seriously proposed which can obtain unambiguous,

accurate, atmospheric structure data by remote sensing. Its cloud cut-off altitude of 300 to 500 mb appears to be insufficient reason not to utilize the technique for structure of the atmosphere from that level to 24 km, in view of its unique advantages.



**SCHEMATIC ILLUSTRATION OF
A REFRACTION SCAN**

Figure 2



**EACH DOT REPRESENTS AN ATMOSPHERIC SOUNDING.
OBSERVATIONS FOR A 24 HOUR PERIOD ON DEC. 21
1100 KM, CIRCULAR, SUN-SYNCHRONOUS ORBIT.
SINGLE TELESCOPE.**

Figure 3

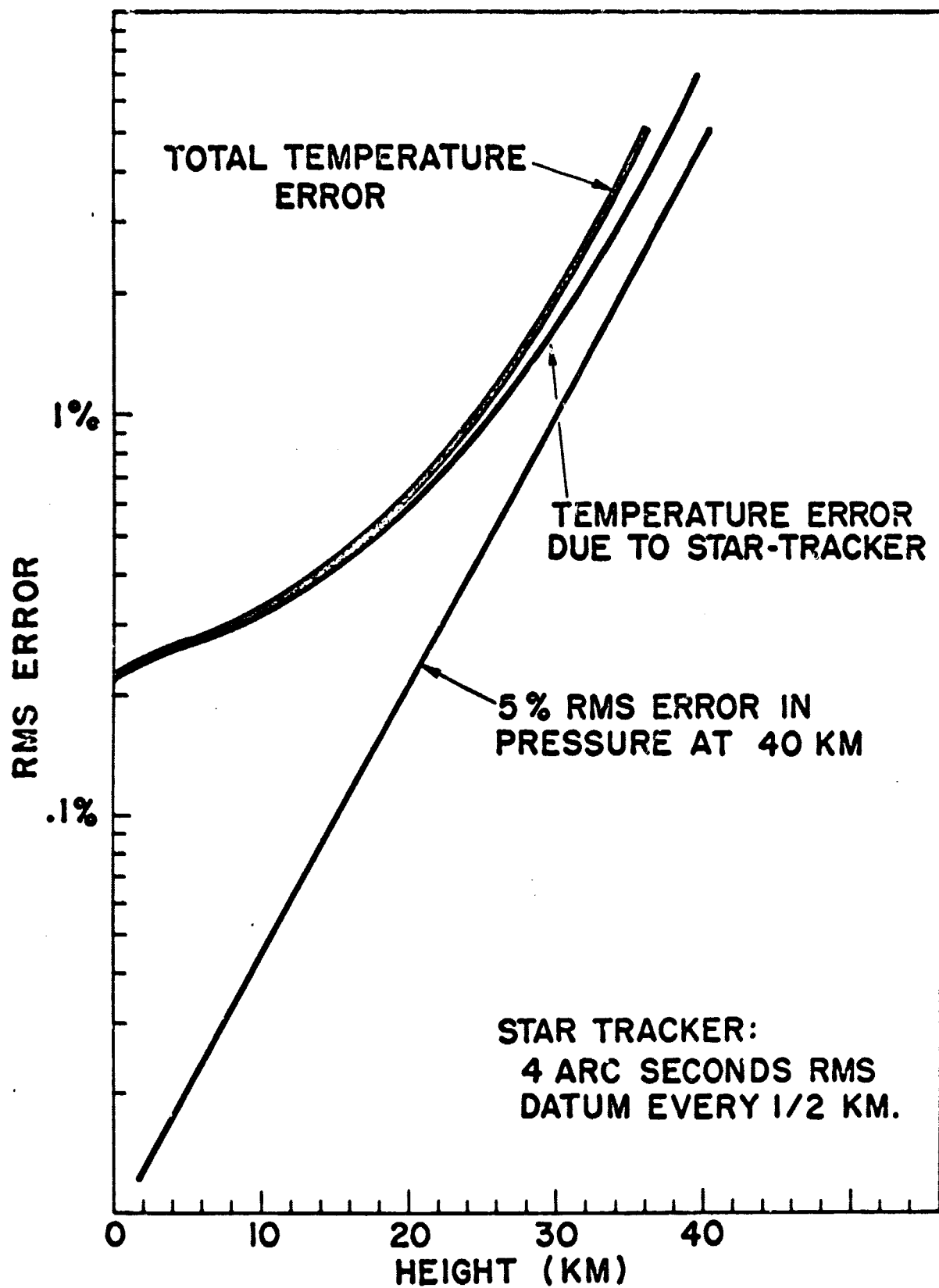


Fig. 4 Total temperature error for 4-arc-second star-tracker.

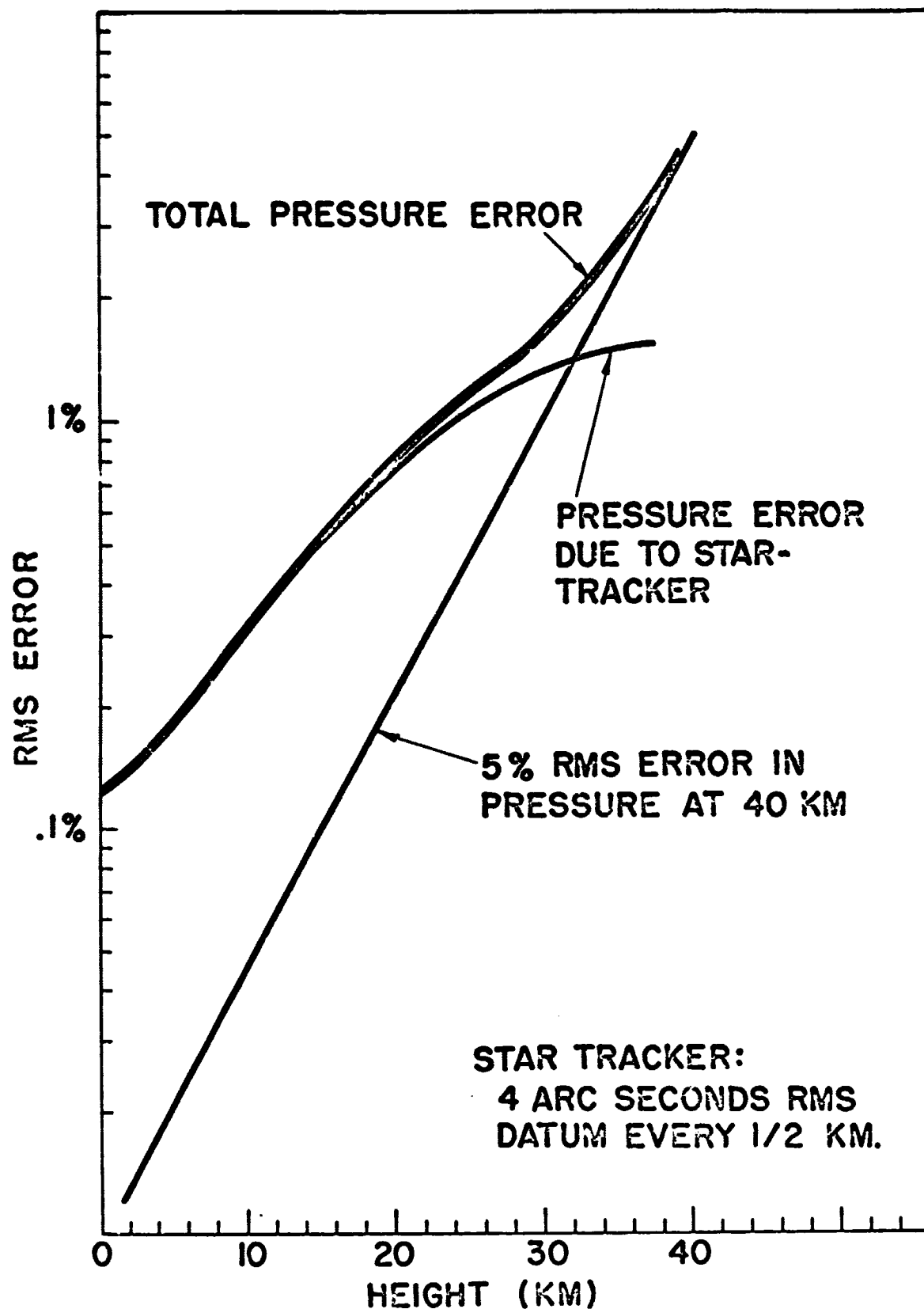


Fig. 5 Total pressure error for 4-arc-second star-tracker.

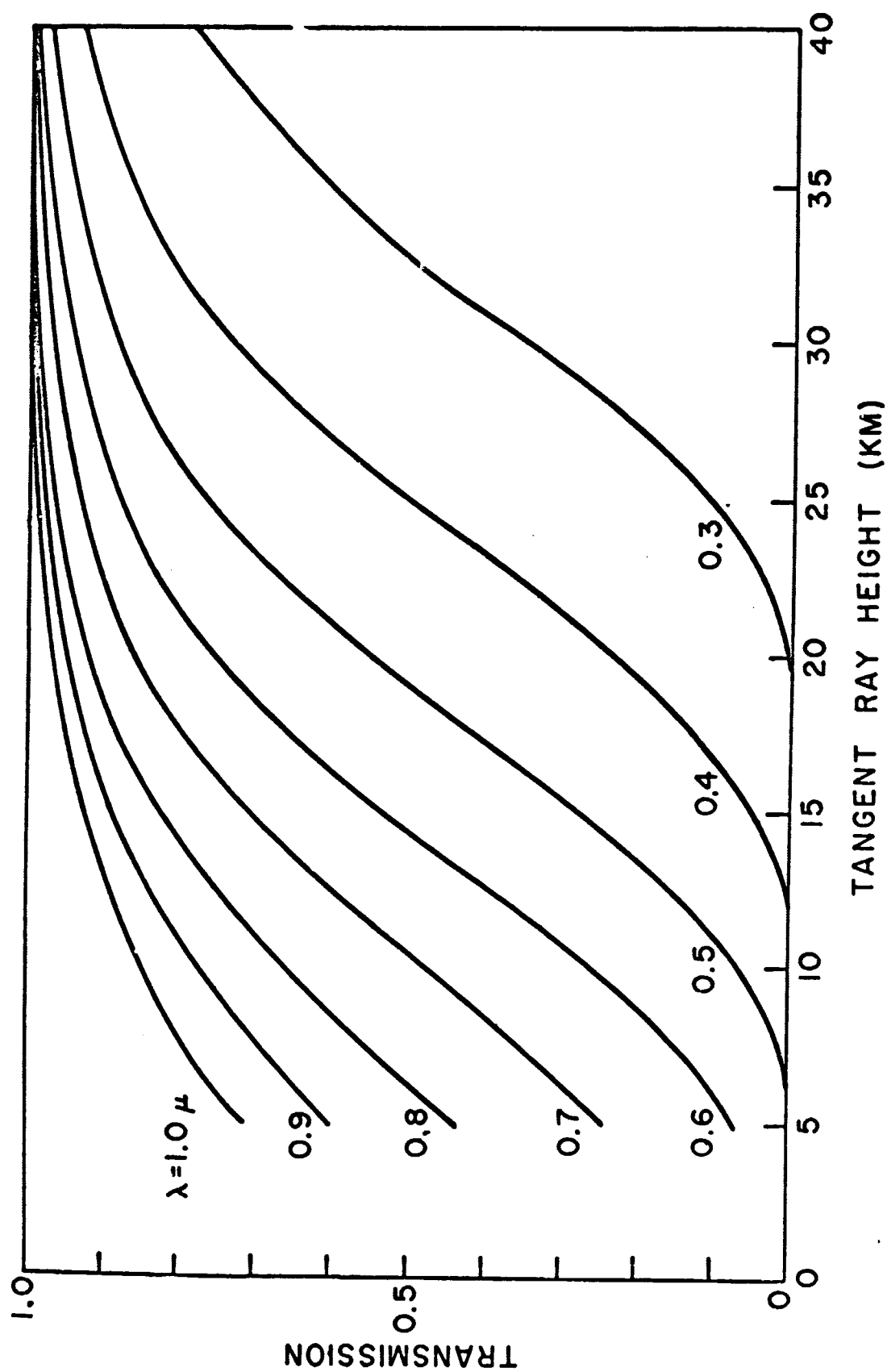


Fig. 6 Intensity reduction due to molecular scattering in an analytic model atmosphere.

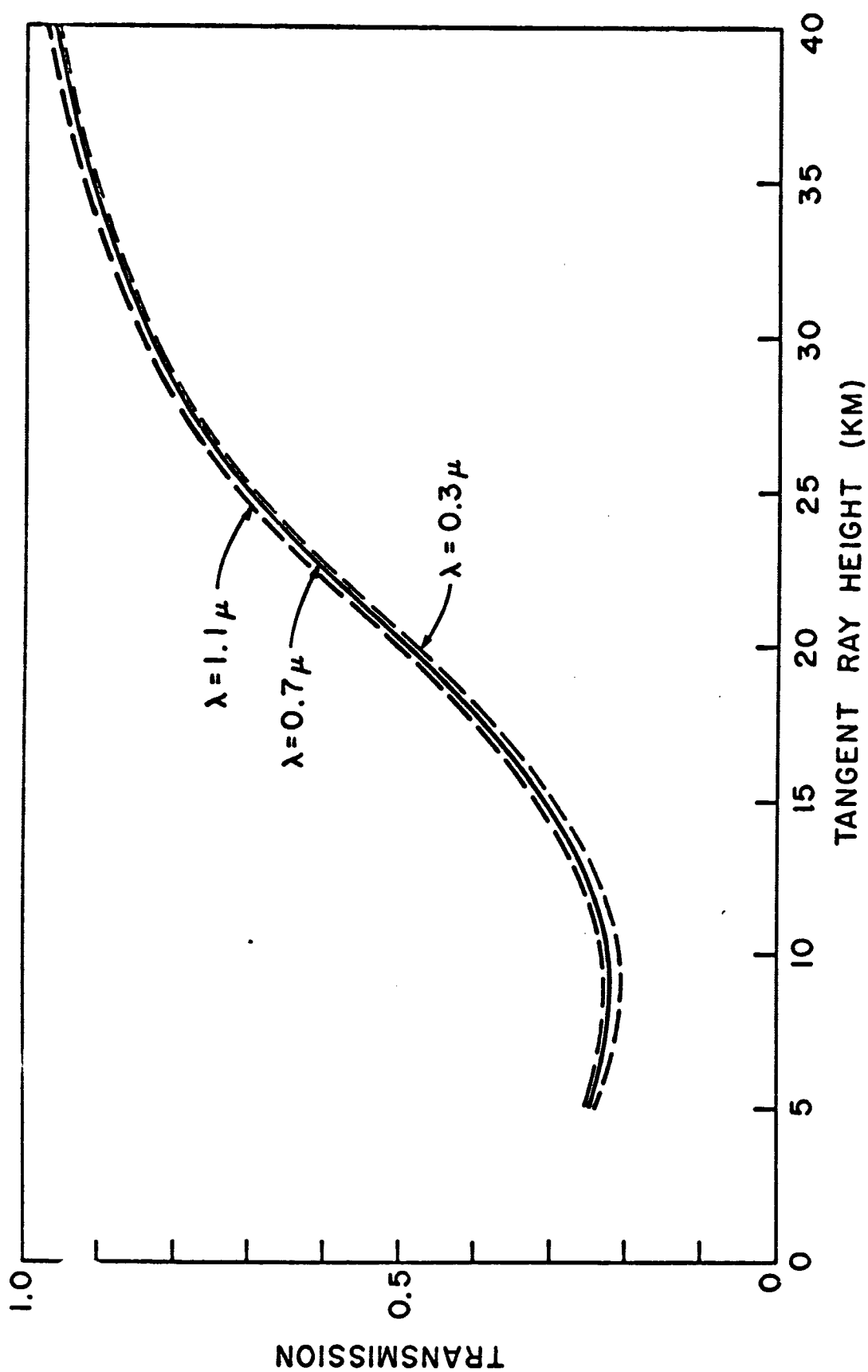


Fig. 7 Intensity reduction due to differential refraction in an analytic model atmosphere.

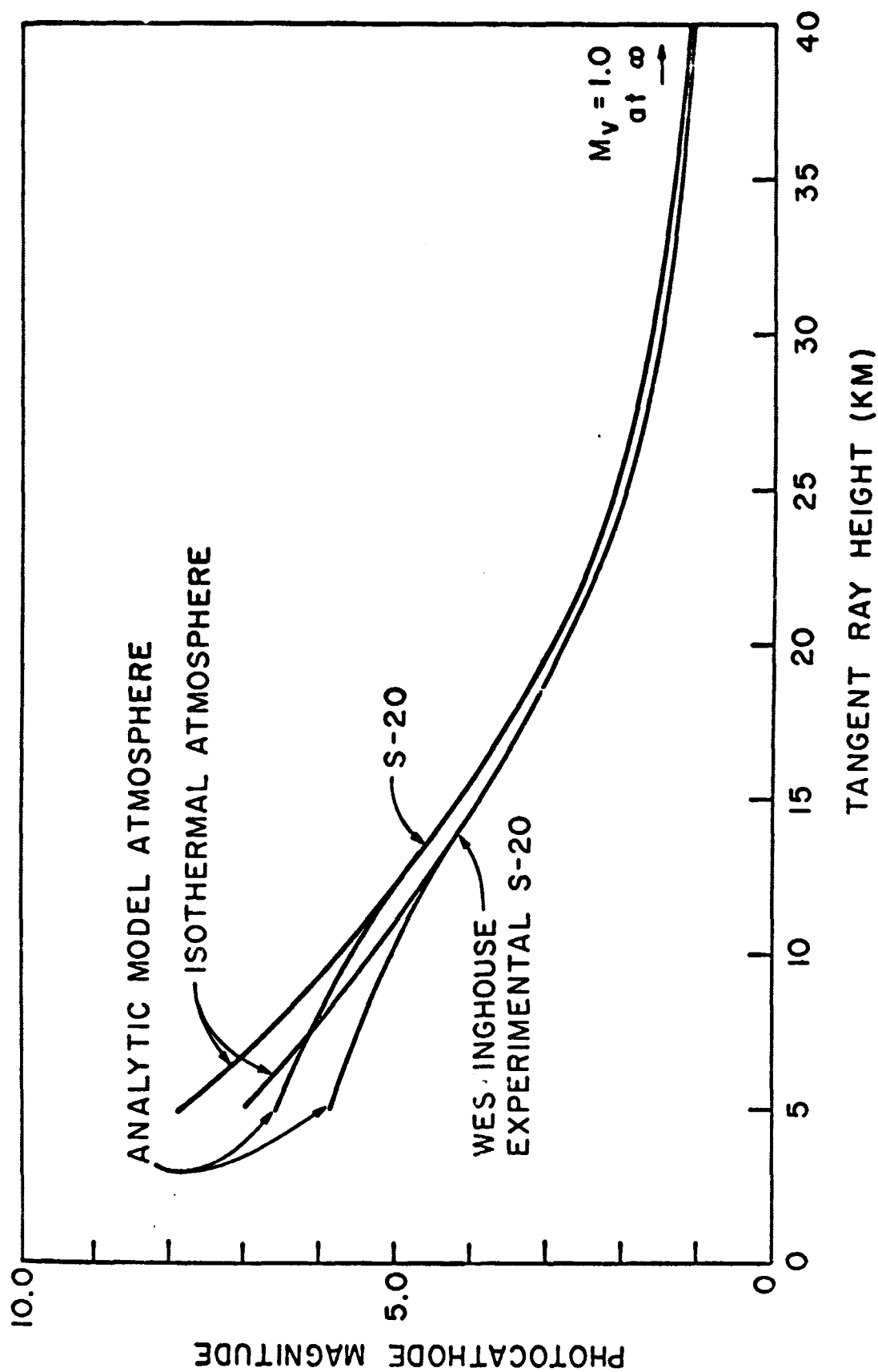


Fig. 8 Photocathode magnitude as a function of tangent ray height for the S-20 and Westinghouse Experimental S-20. The initial photocathode magnitude of +1.0 is arbitrarily assigned equal to +1.0 visual magnitude. The spectral type is G0.

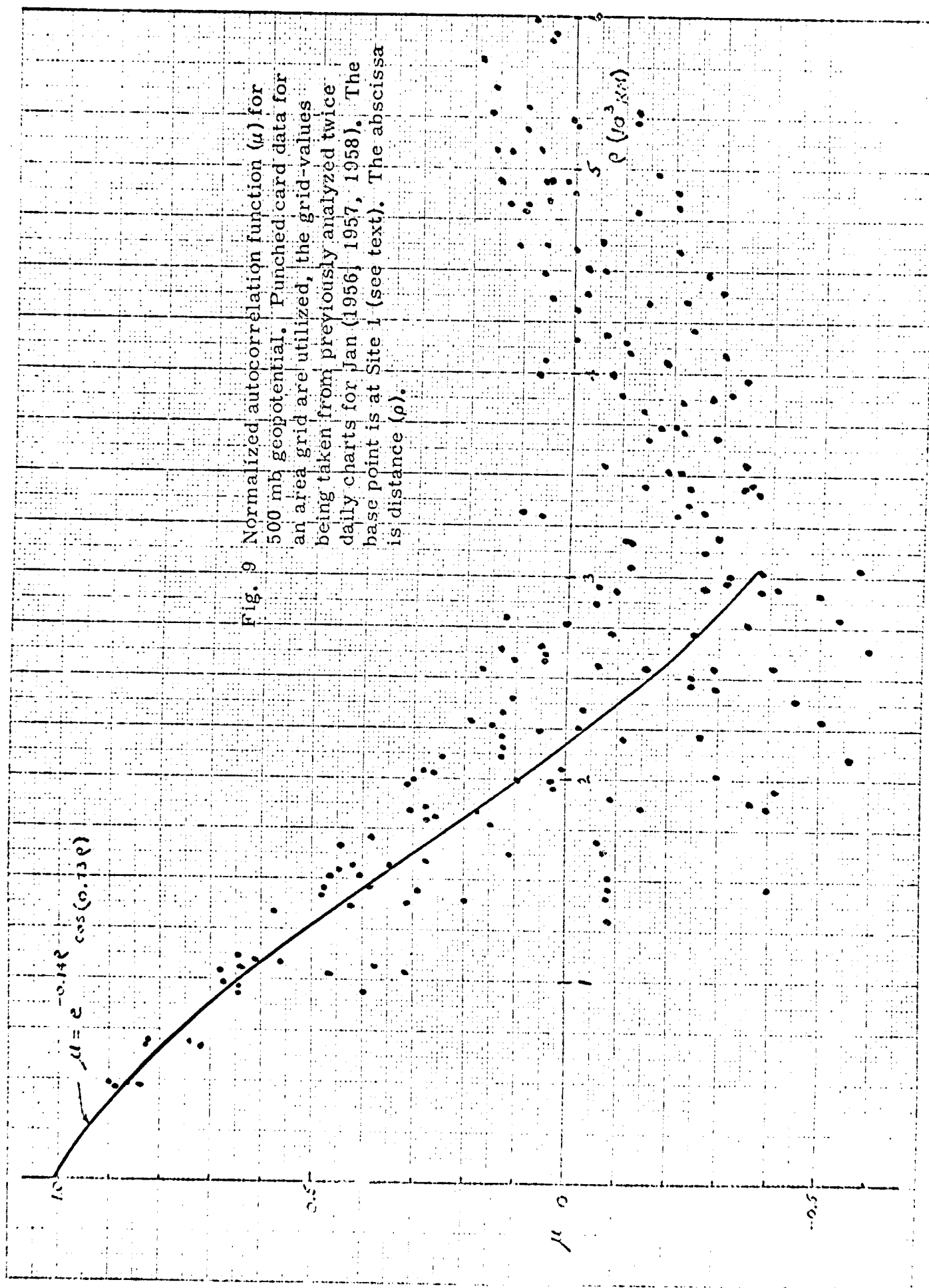


Fig. 9 Normalized autocorrelation function (μ) for 500 mb geopotential. Punched card data for an area grid are utilized, the grid-values being taken from previously analyzed twice daily charts for Jan (1956, 1957, 1958). The base point is at Site 1 (see text). The abscissa is distance (ρ).

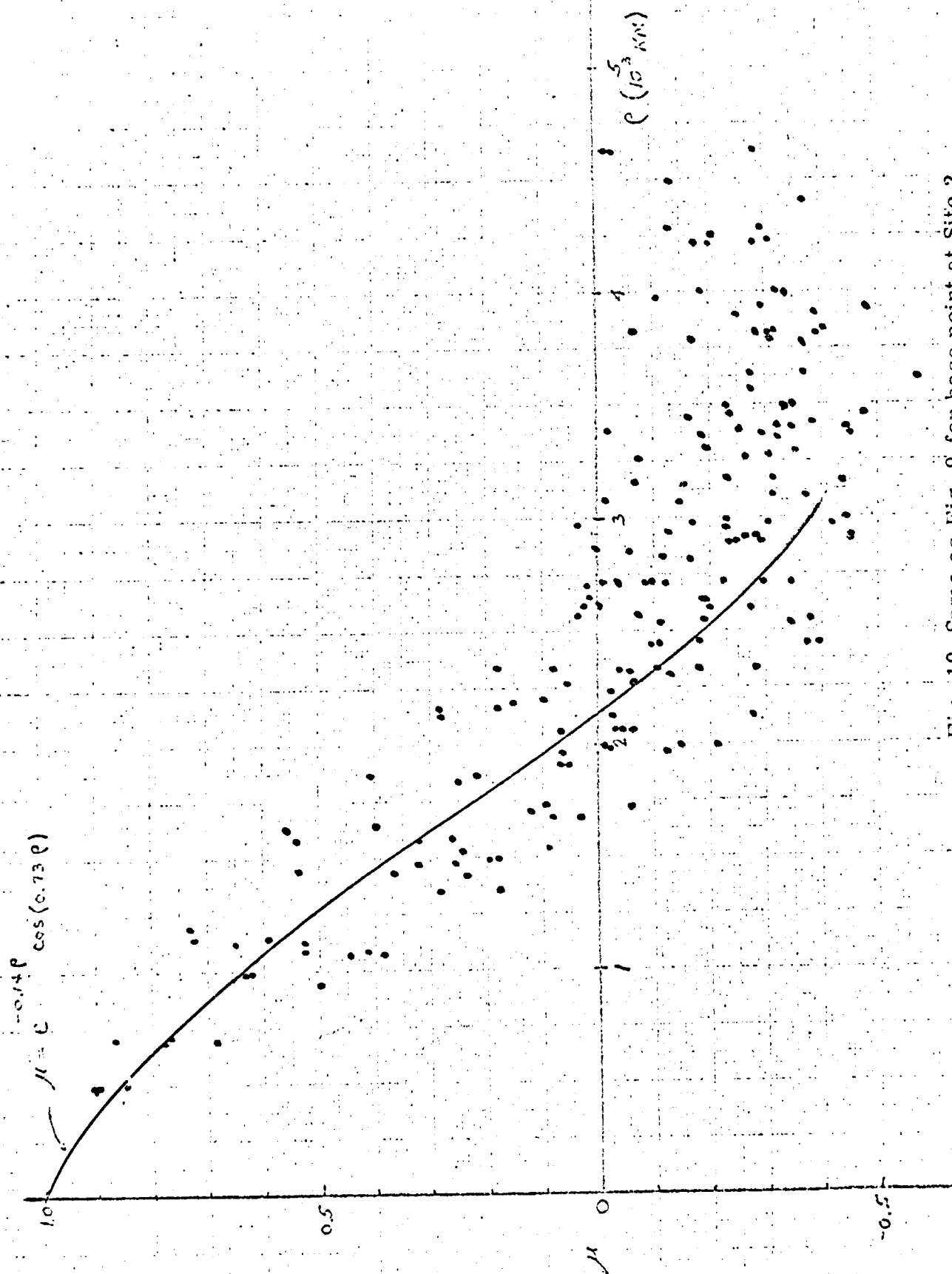


Fig. 10 Same as Fig. 9 for base point at Site 2.

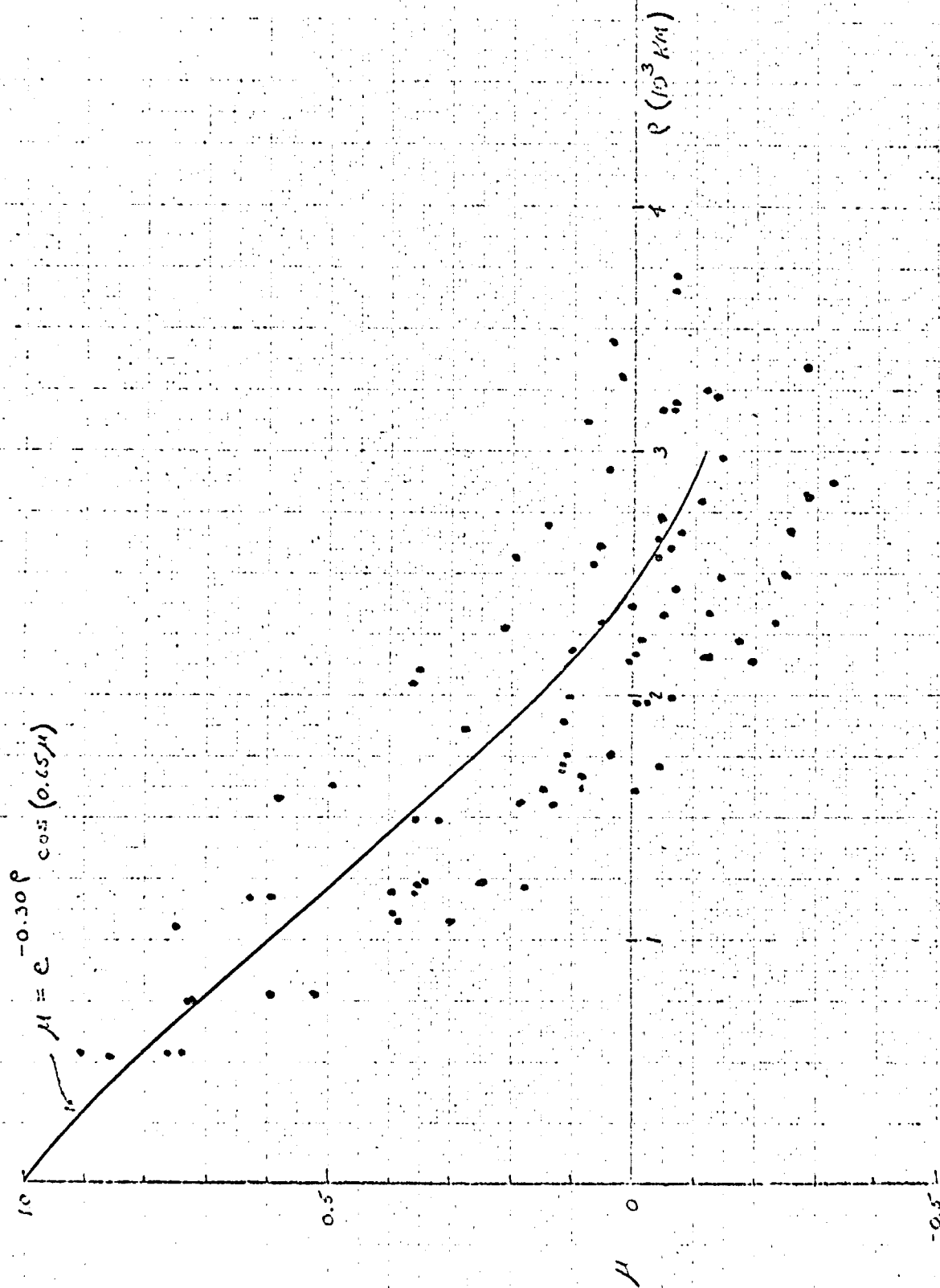


Fig. 11 Same as Fig. 9 for base point at Site 3.

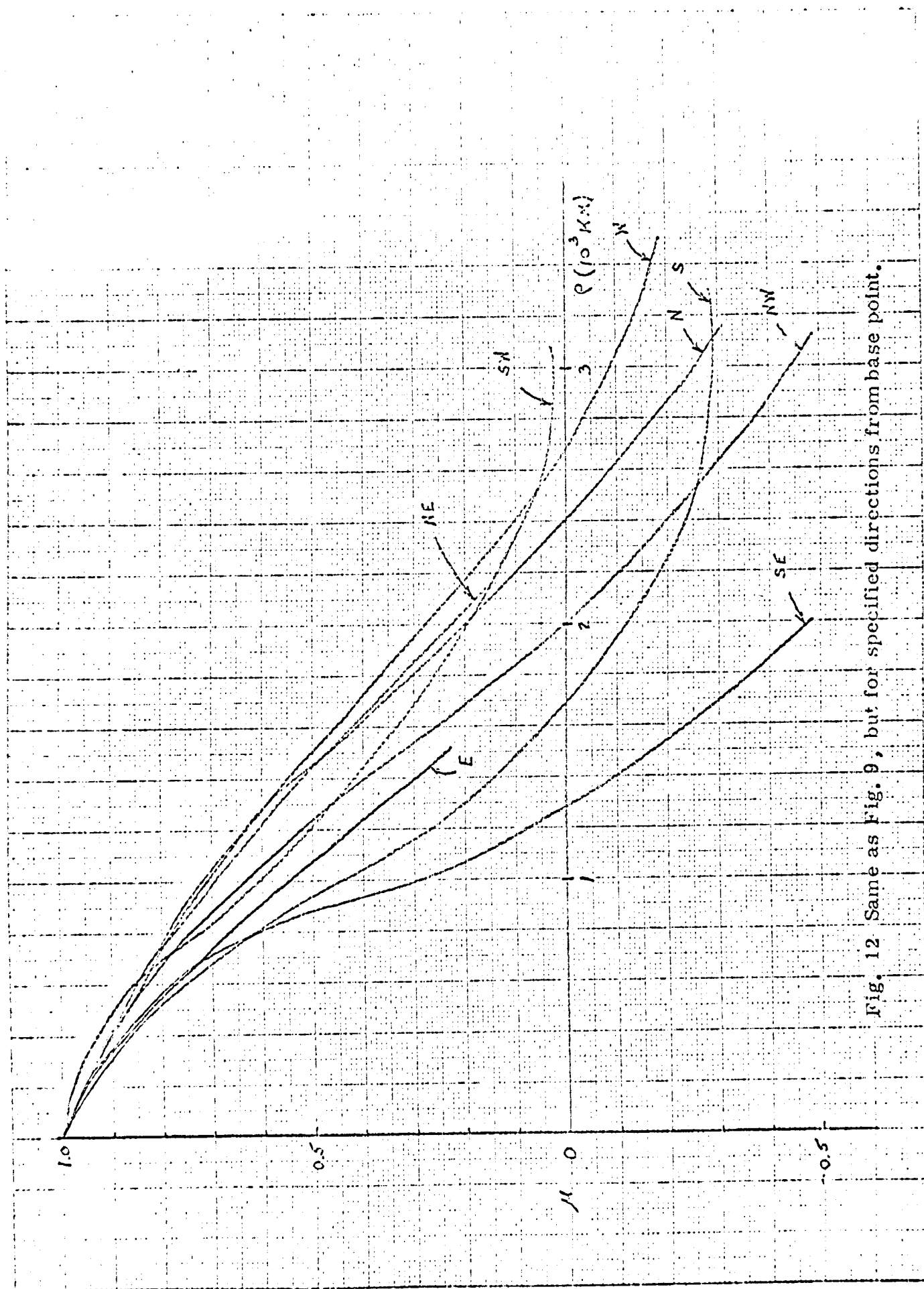


Fig. 12 Same as Fig. 9, but for specified directions from base point.

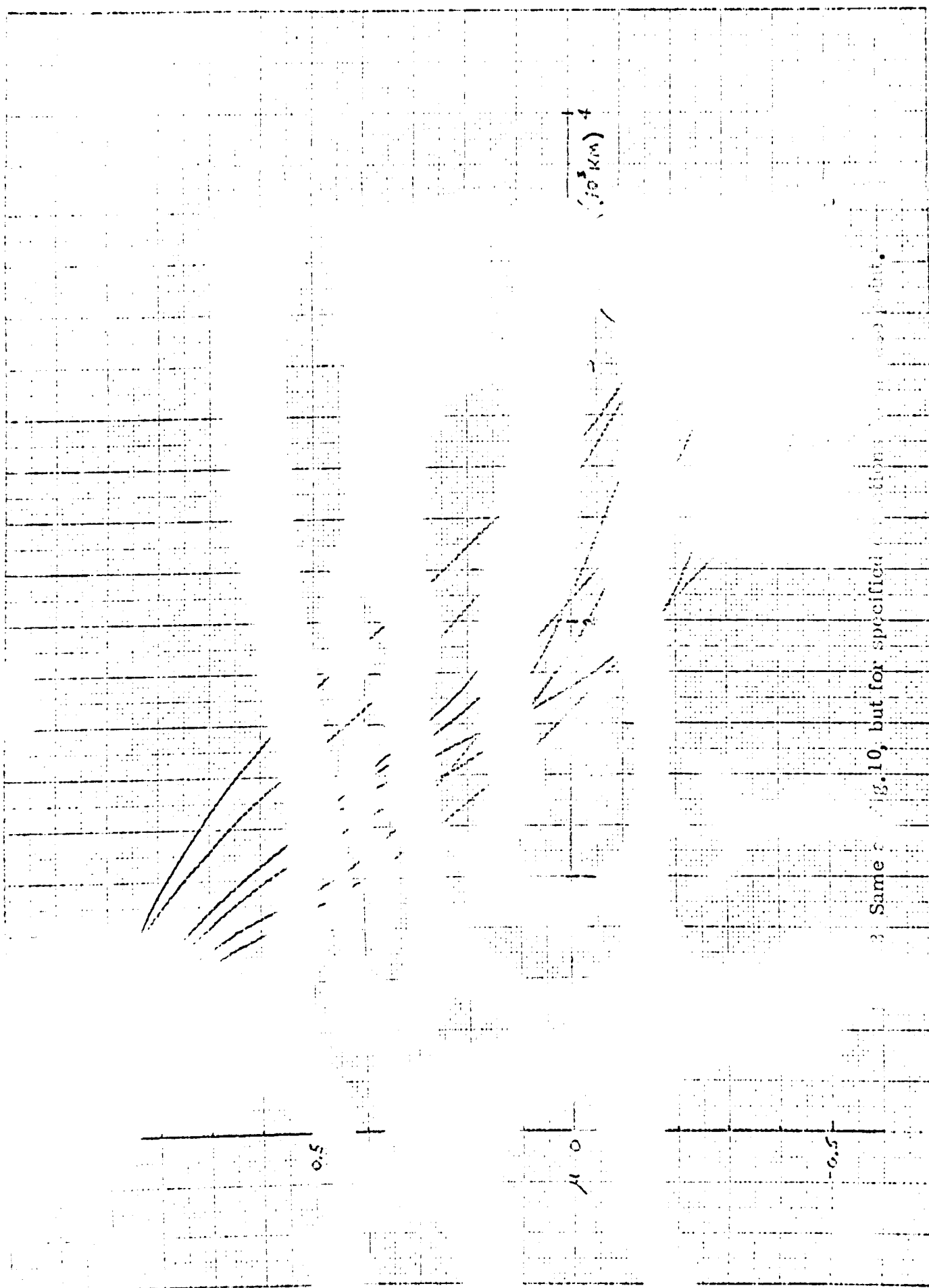


Fig. 10, but for specified conditions of the plot.

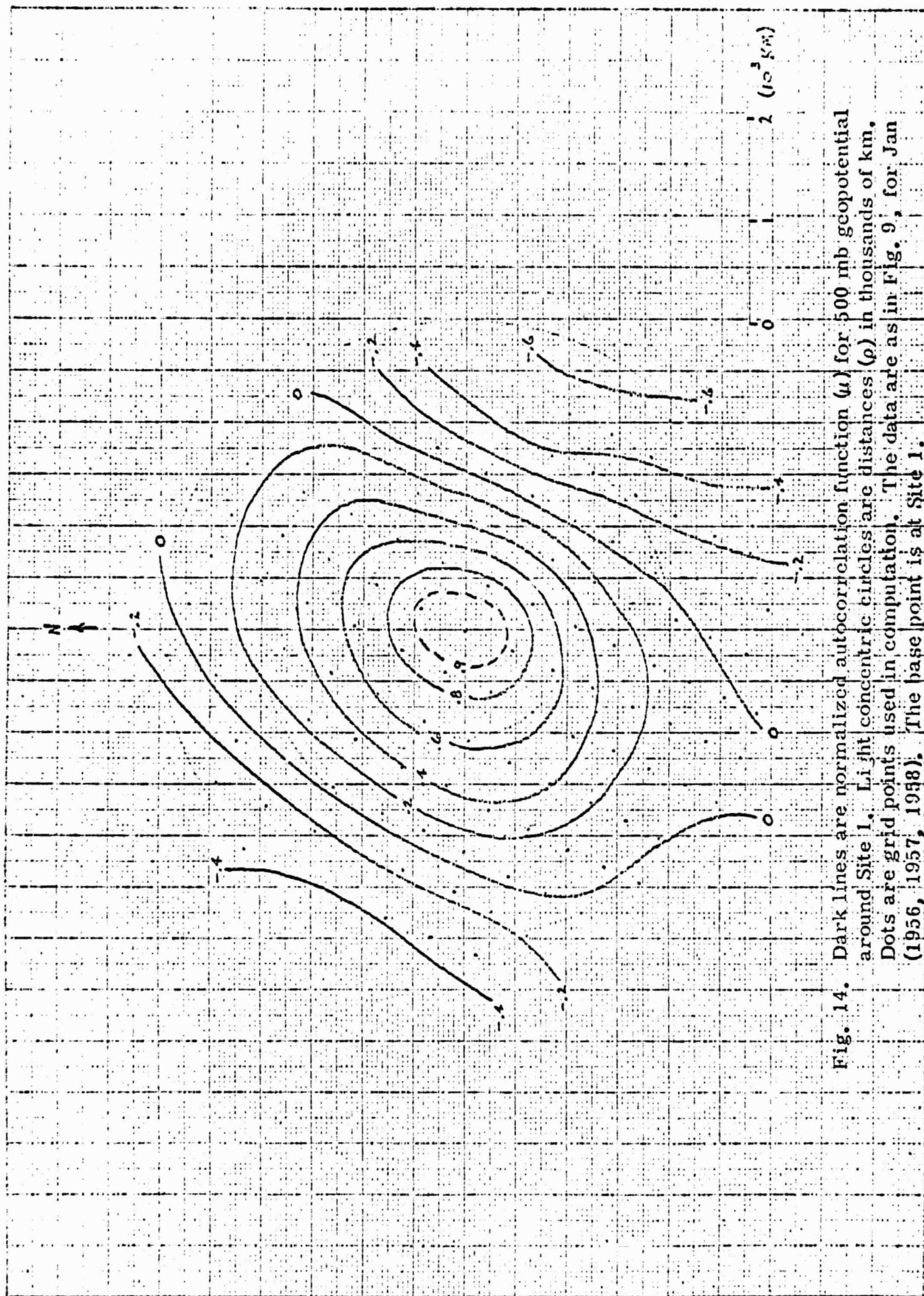


Fig. 14. Dark lines are normalized autocorrelation function (u) for 500 mb geopotential around Site 1. Light concentric circles are distances (ρ) in thousands of km. Dots are grid points used in computation. The data are as in Fig. 9, for Jan (1956, 1957, 1958). The base point is at Site 1.

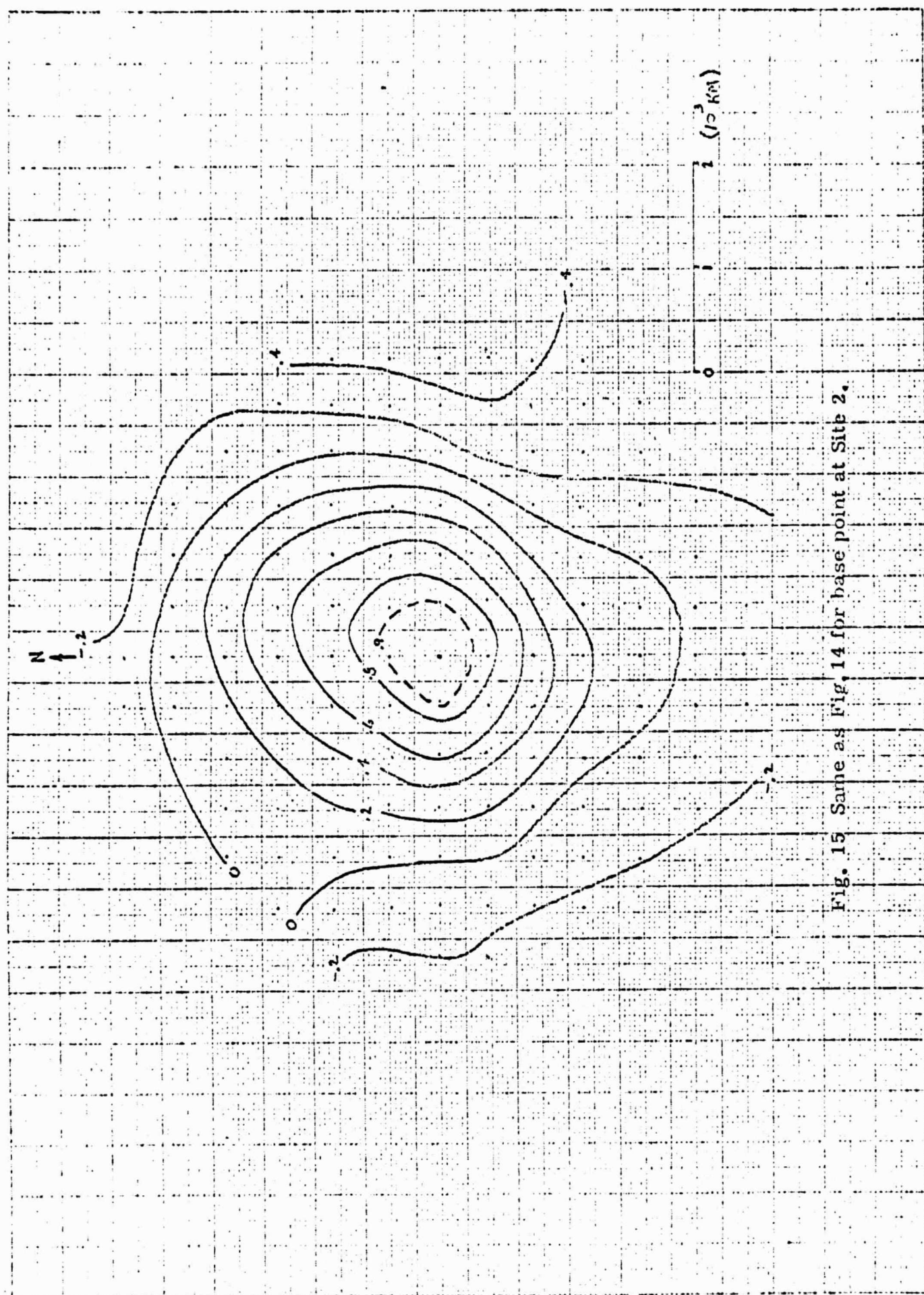
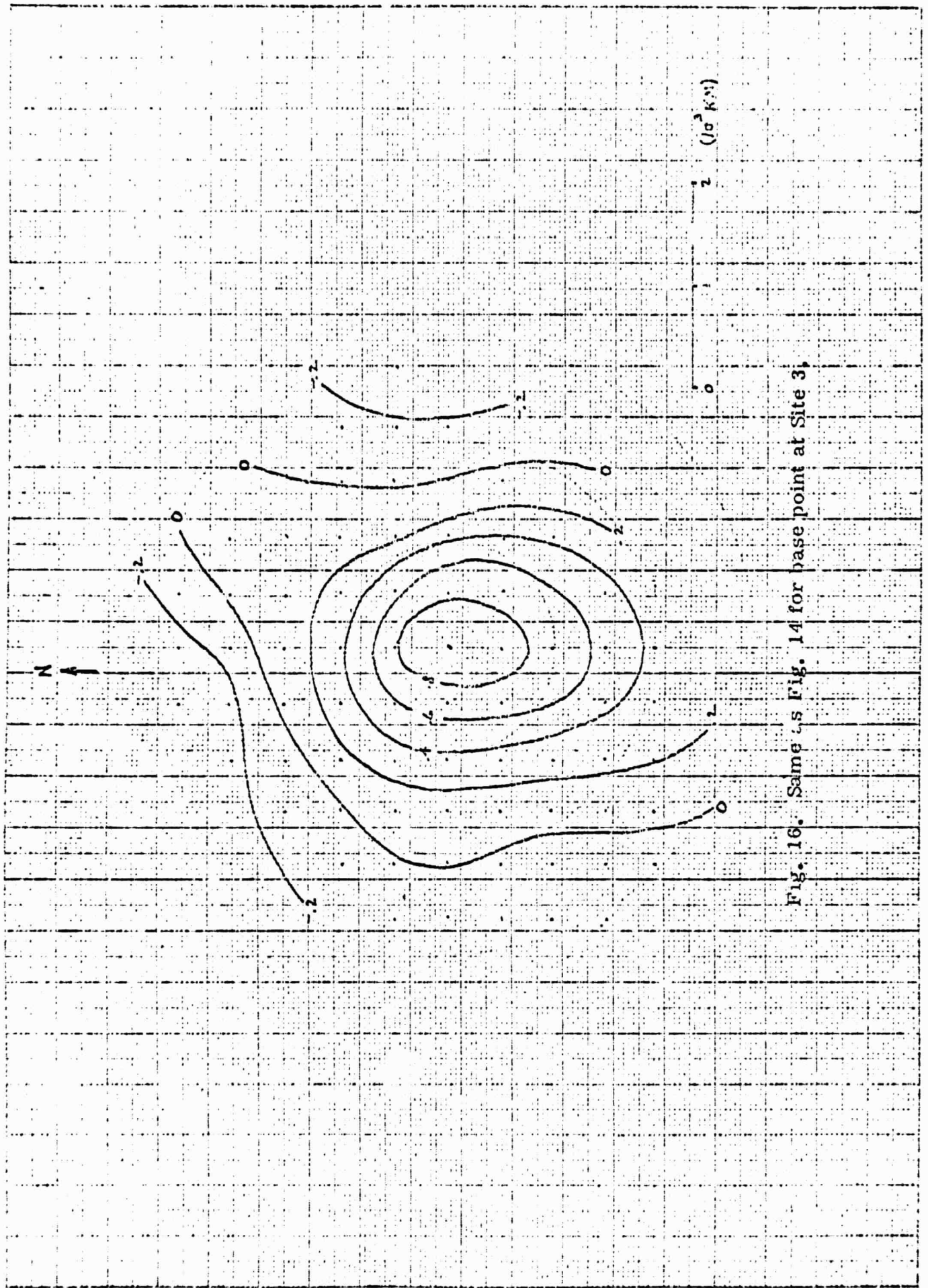


Fig. 15 Same as Fig. 14 for base point at Site 2.



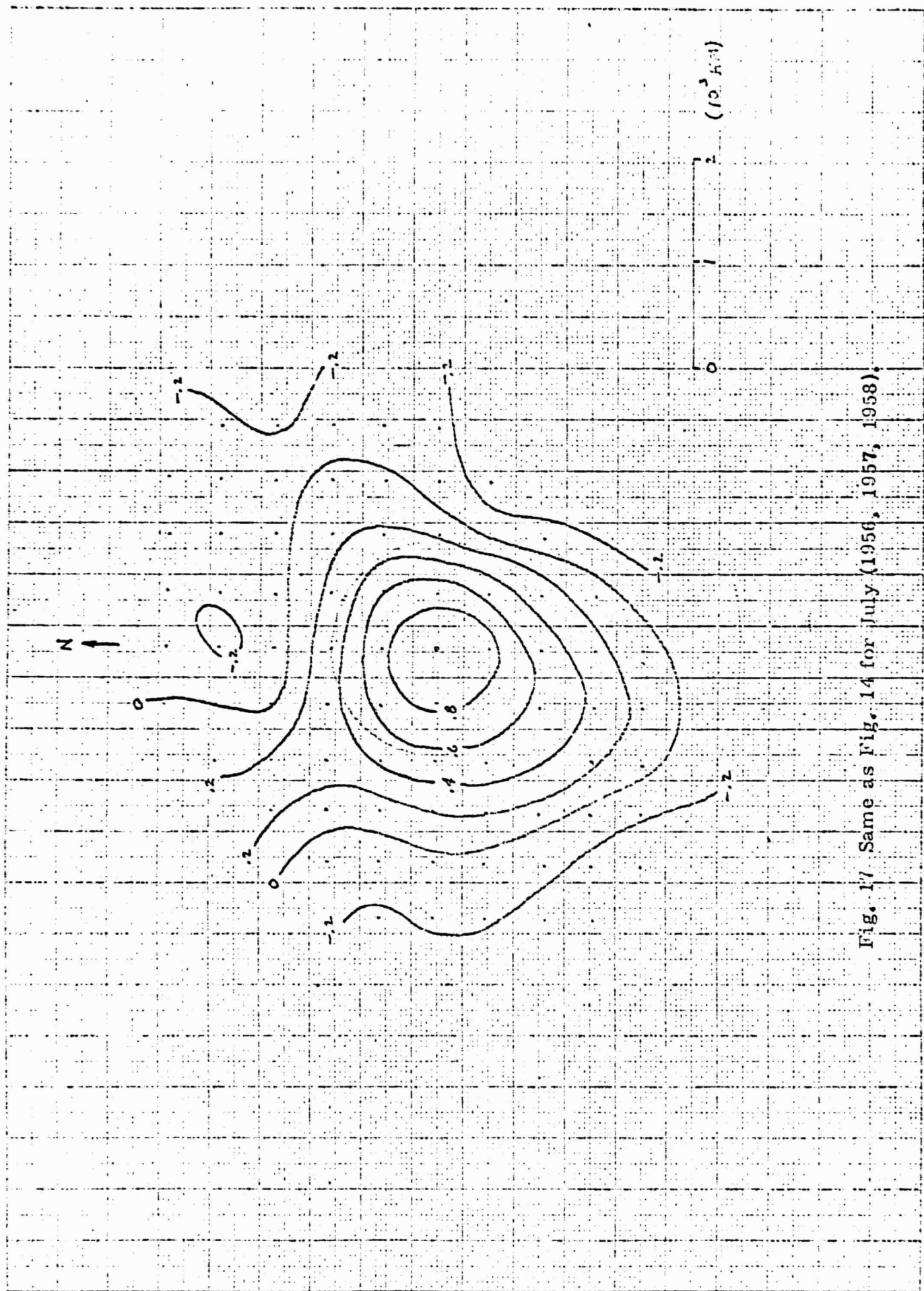


Fig. 17 Same as Fig. 14 for July (1956, 1957, 1958).

Fig. 18

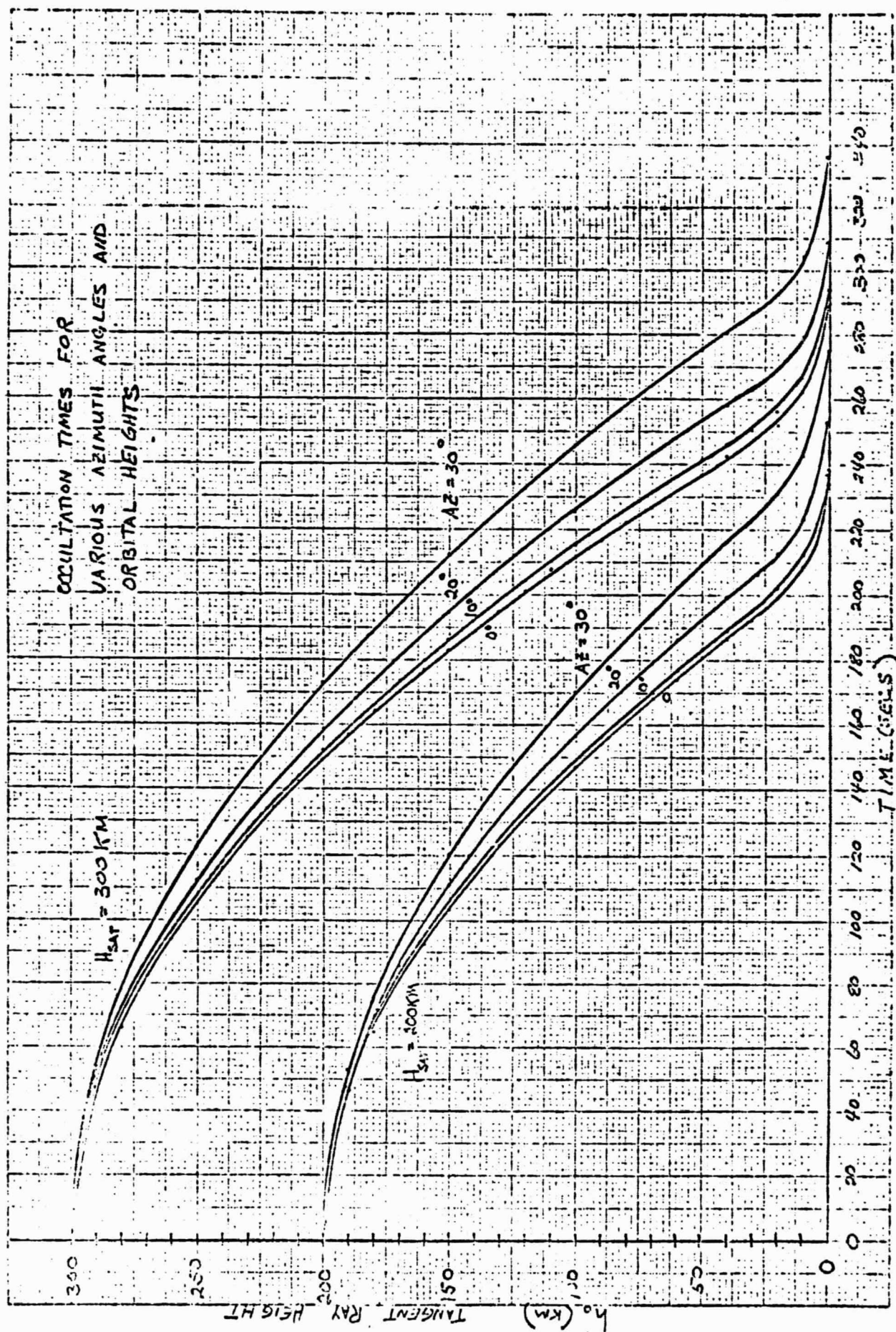
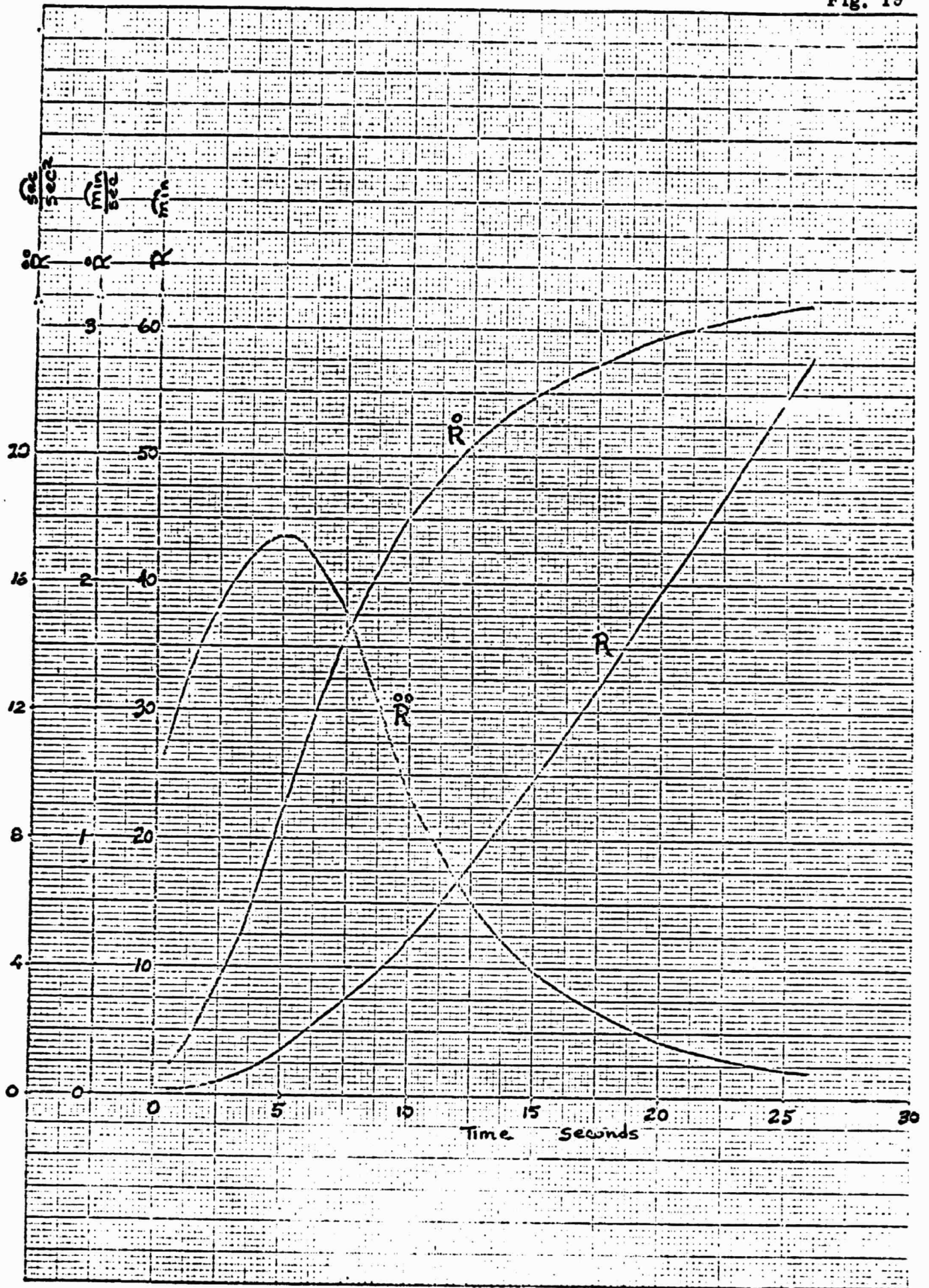
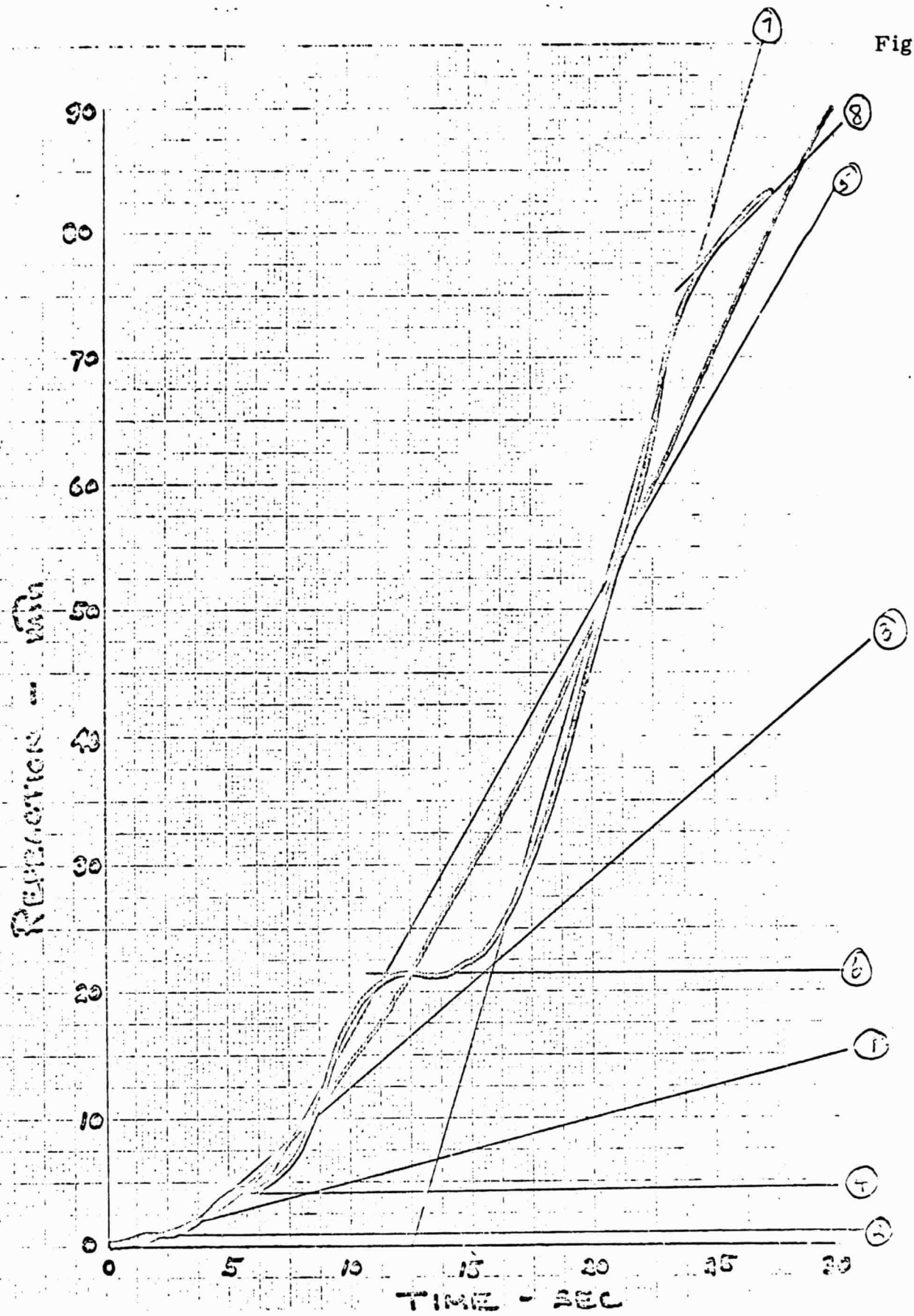


Fig. 19



"REPRODUCIBILITY OF THE ORIGINAL PAGE IS POOR."

Fig. 20



Telescope

$$T = I s^2 \theta_0$$

$$\bar{T} T_{max} = I s^2 \bar{\theta}_0 \theta_{0 max}$$

$$\bar{\theta}_0 = \frac{T_{max}}{I \theta_{0 max} s^2} \bar{T}$$

$$\bar{\theta}_0 = \frac{6}{s^2} \bar{T}$$

where $T_{max} = 60$ oz inches

$$\theta_{0 max} = \frac{2\pi}{360} \text{ rad.}$$

$$I = 3 \text{ slug ft}^2$$

Therefore

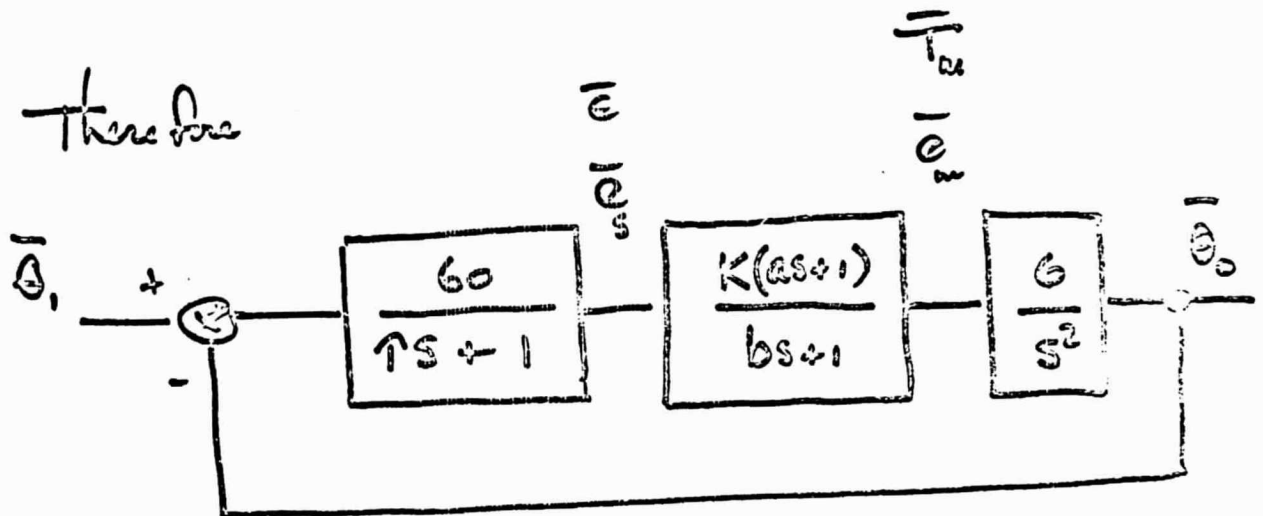


Fig. 21

Star Tracker



$$\theta_{i, \max} = 60 \text{ mrad}$$

$$\epsilon_{\max} = 1 \text{ mrad}$$

Fld of View

$$(\theta_i - \theta_o) K = \epsilon$$

$$\bar{\theta}_i \theta_{\max} = \bar{\epsilon} \epsilon_{\max}$$

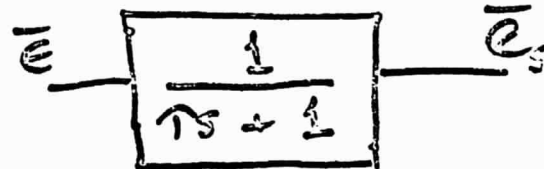


$$e_s = K \epsilon$$

$$\bar{e}_s e_{s \max} = K \bar{\epsilon} \epsilon_{\max}$$

$$K = \frac{e_{s \max}}{\epsilon_{\max}}$$

Volts / Angle



Network : Amplifier

$$\frac{\bar{e}_m}{\bar{e}_s} = \frac{K (as + 1)}{(bs + 1)}$$

$$e_m = K e_s$$

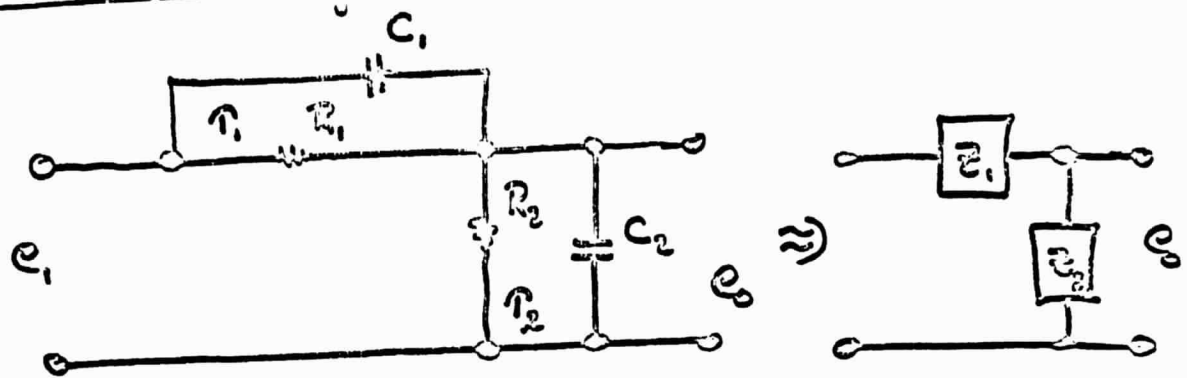
$$K = \frac{e_{\max}}{e_{s \max}}$$

$$K e_m = T_m$$

Fig. 22

Error Rate

Network Design



$$\frac{e_2}{e_1} = \frac{Z_2}{Z_1 + Z_2} \quad Z_1 = \frac{R_1}{\tau_1 p + 1}, \quad Z_2 = \frac{R_2}{\tau_2 p + 1}$$

$$= \frac{\frac{R_2}{\tau_2 p + 1}}{\frac{R_2}{\tau_2 p + 1} + \frac{R_1}{\tau_1 p + 1}} = \frac{R_2 (\tau_1 p + 1)}{(R_2 \tau_1 + R_1 \tau_2) p + R_1 + R_2}$$

$$= \frac{\left(\frac{R_2}{R_1 + R_2} \right) (\tau_1 p + 1)}{\left(\frac{R_2 \tau_1 + R_1 \tau_2}{R_1 + R_2} \right) p + 1}$$

Choose $R_1 = .1 \text{ meg}$ $R_2 = .01 \text{ meg}$
 $C_1 = 10 \mu\text{fd}$ $C_2 = 1.0 \mu\text{fd}.$

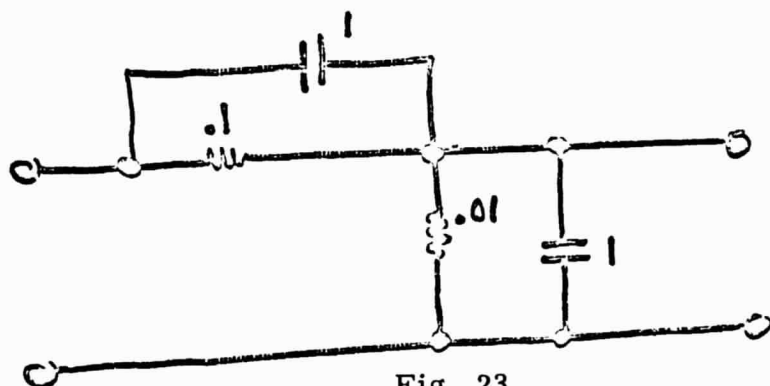
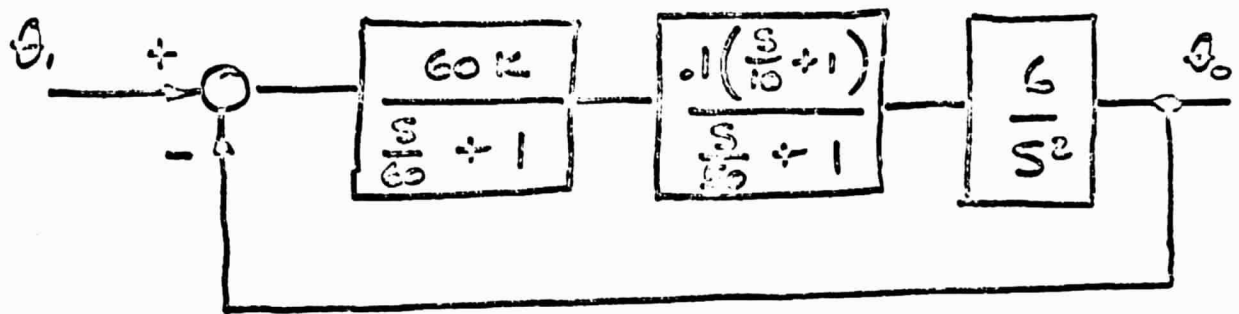


Fig. 23

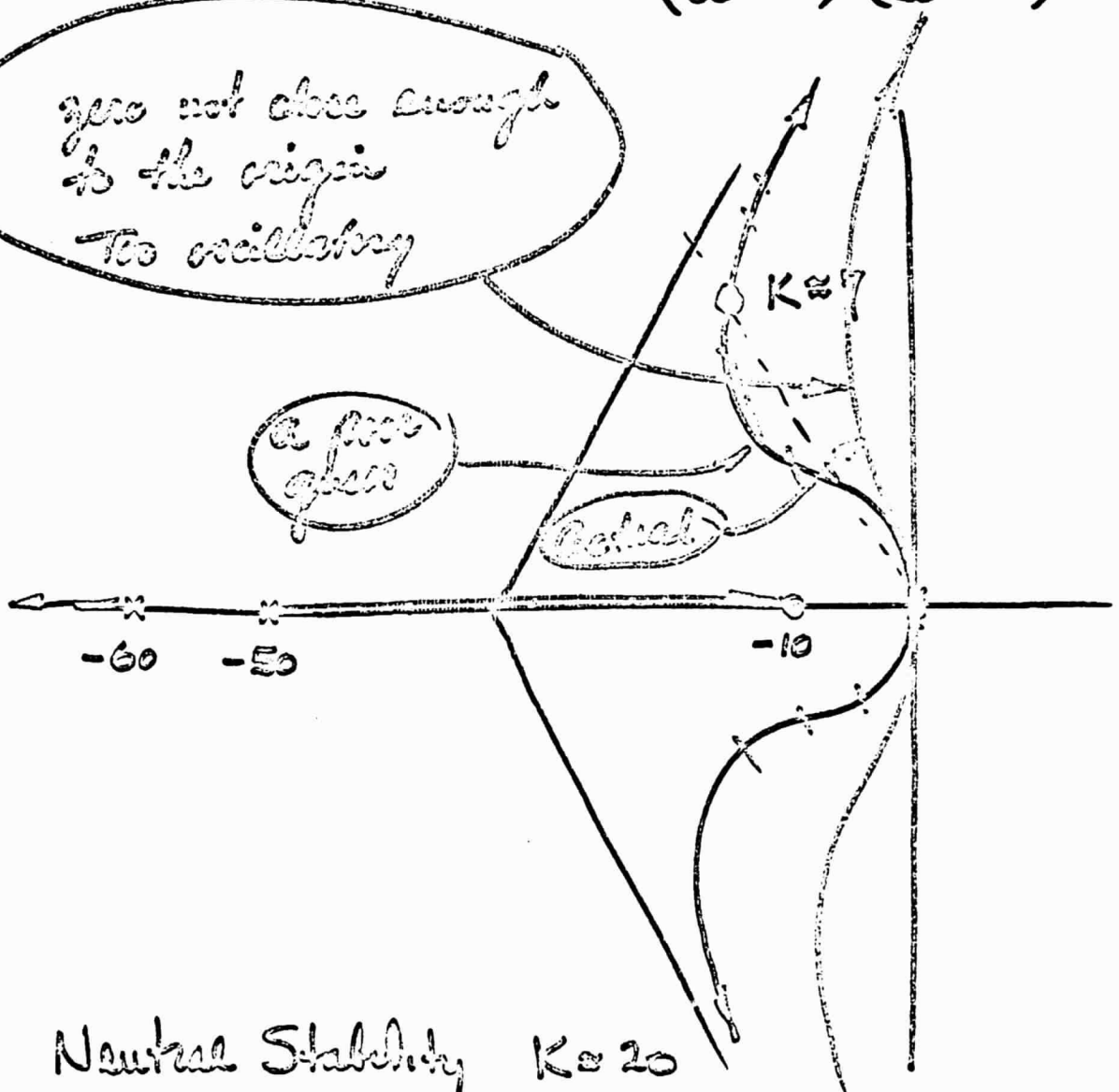


$$Y = \frac{36K \left(\frac{s}{10} + 1 \right)}{s^2 \left(\frac{s}{60} + 1 \right) \left(\frac{s}{10} + 1 \right)}$$

zero not close enough
to the origin
Too oscillatory

a free
zero

Roots

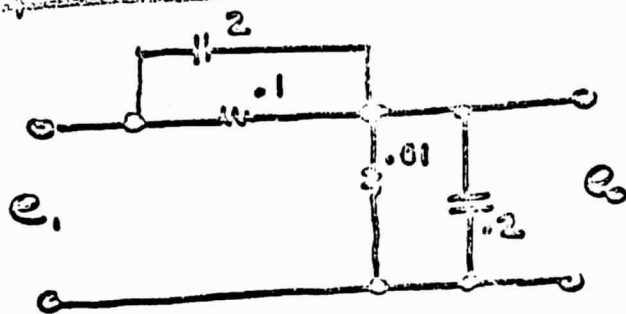


Neutral Stability $K=20$

Complex poles $\zeta = \frac{1}{2}$ for $K=7$

Fig. 24

Try Network



$$\frac{e_2}{e_1} = \frac{.09 \left(\frac{s}{5} + 1 \right)}{\frac{s}{50} + 1}$$

$$Y = \frac{6K(5.4) \left(\frac{s}{5} + 1 \right)}{s^2 \left(\frac{s}{50} + 1 \right) \left(\frac{s}{60} + 1 \right)} = \frac{3600K(5.4)(s+5)}{s^2(s+50)(s+60)}$$

Fig. 25

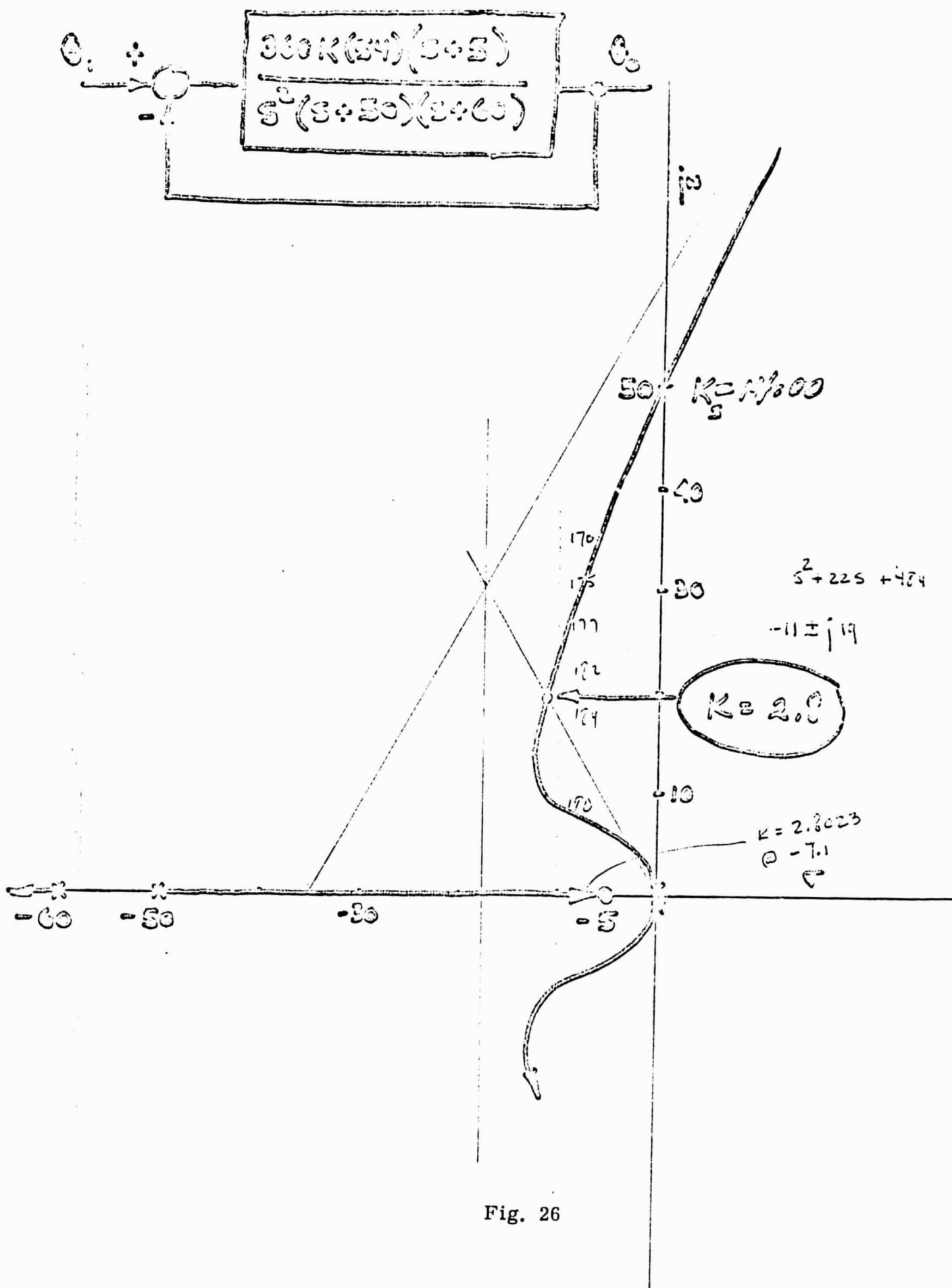
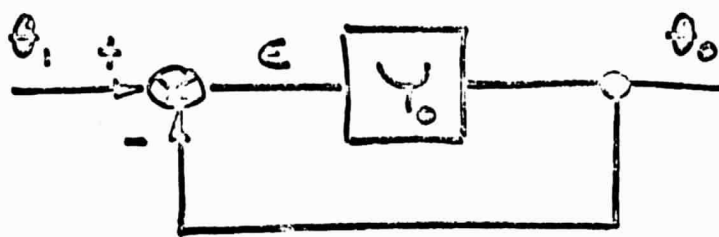


Fig. 26



$$\frac{\epsilon}{\theta_i} = \frac{1}{1 + Y_o}$$

$$\epsilon(j\omega) = Z(j\omega) \theta_i(j\omega)$$

$$Y_o = \frac{360(2.8)(54)(s+5)}{s^2(s+50)(s+60)}$$

$$Y(j\omega) = \frac{A(5+j\omega)(5-j\omega)}{[+ \omega^2(+ \omega^2 - 3000) - j\omega^3 110](5-j\omega)}$$

$$= \frac{A(25 + \omega^2)}{5(\omega^4 - 3000\omega^2) - 110\omega^3 - j\omega^3(\omega^2 - 3000 + 550)}$$

$$= \frac{A(25 + \omega^2)}{-15\omega^2(7\omega^2 + 1000) - j\omega^3(\omega^2 - 2450)}$$

$$A = 360(2.8)(54)$$

$$= 5.43 \times 10^4$$

Since $\frac{C}{O_1} = \frac{1}{1 + Y_0}$ and

$$Y_0 = \frac{-A(25 + \omega^2)}{15\omega^2(7\omega^2 + 1000) + j\omega^3(\omega^2 - 2450)}$$

$$= \frac{-\frac{A(25 + \omega^2)}{15\omega^2(7\omega^2 + 1000)}}{1 + j\frac{\omega(\omega^2 - 2450)}{15(7\omega^2 + 1000)}}$$

As $\omega \rightarrow \infty$ $Y_0 \rightarrow -\frac{K}{j\omega^3} = j\frac{K}{\omega^3}$

$\omega \rightarrow 0$ $Y_0 \rightarrow -\frac{K}{\omega^2}$

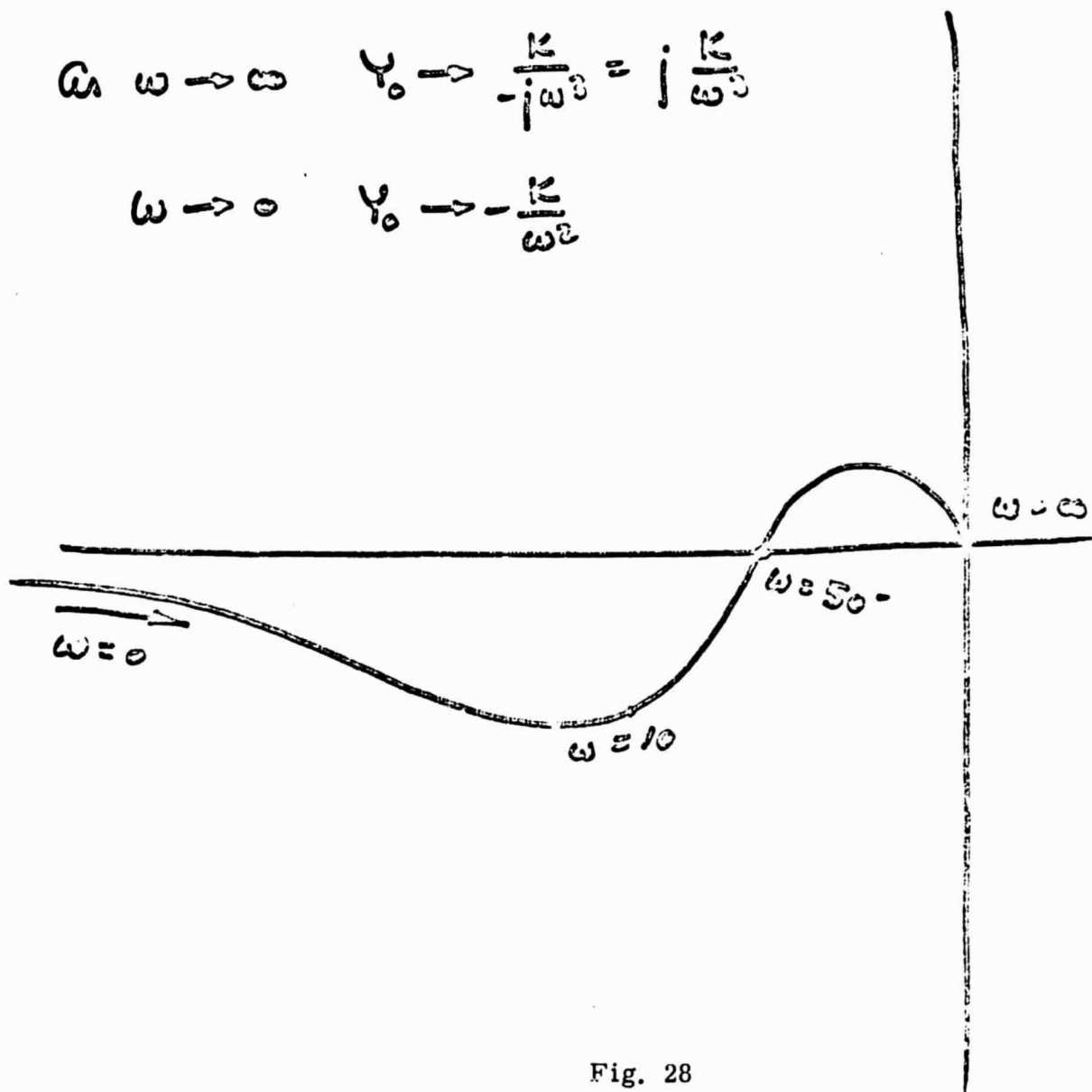


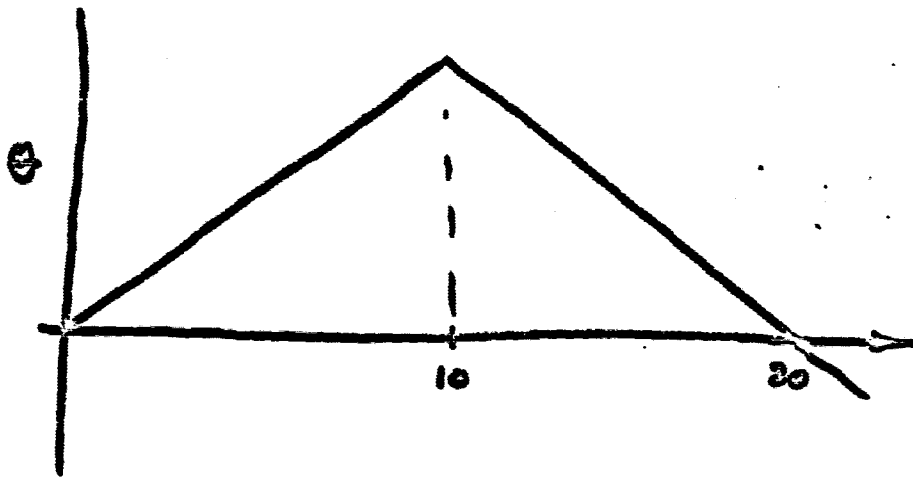
Fig. 28

$$Y = \frac{M}{1 + jy}$$

ω^2	jy	M
400	.719	1.01
225	.864	
100	.902	2.66
64	.879	
25	.688	6.1617
9	.459	12.86
1	.162	93.46
.09	.049	1×10^3
.01	.0163	9053
.0009	.0049	1.0×10^5
.0001	.00163	9.05×10^5

Fig. 29

Transient Response to Apollo Limit Cycle



$$\theta = \frac{t}{20} \quad 0 < t \leq 10 \text{ sec}$$

$$\theta = 1 - \frac{t}{20} \quad 10 < t < 20$$

$$\theta(s) = \frac{1}{20s^2} - e^{-10s} \frac{2}{40s^2} = \frac{1}{20s^2} (1 - 2e^{-10s})$$

$$\epsilon(s) = \frac{\theta(s)}{1 + Y(s)} = \frac{s^2(s+50)(s+60) \theta(s)}{(s+7.1)(s+81)(s^2+22s+484)}$$

$$= \frac{.05(s+50)(s+60)}{(s+7.1)(s+81)(s^2+22s+484)}$$

$$= \frac{A}{s+7.1} + \frac{B}{s+81} + \frac{Cs+D}{s^2+22s+484}$$

$$A = +0.00406$$

$$B = -0.0000837$$

$$C = -0.00398$$

$$D = -0.01544$$

Fig. 30

Evaluation of C and D

$$As^3 + Bs^3 + Cs^3 = 0$$

$$C = -A - B$$

$$= -0.00398$$

$$484(81)A + 484(7.1)B + 7.1(81)D = 150$$

$$D = -0.01544$$

$$\frac{D}{s^2 + 22s + 484} = \frac{D}{(s+11)^2 + (19.1833)^2}$$

$$f(t) = \frac{D}{19.1833} e^{-11t} \sin(19.1833t)$$

$$\frac{-0.00398(s+11) + 0.02834}{(s+11)^2 + (19.1833)^2}$$

$$e^{-11t} \left[+5.318 \sin \omega t - 14.328 \cos \omega t \right] \quad \text{Answer}$$

$$\omega = 19.1833 \frac{\text{rad}}{\text{sec}} = 3.05 \text{ cps}$$

Fig. 31

Response due to minimum Amplitude Control Impulse

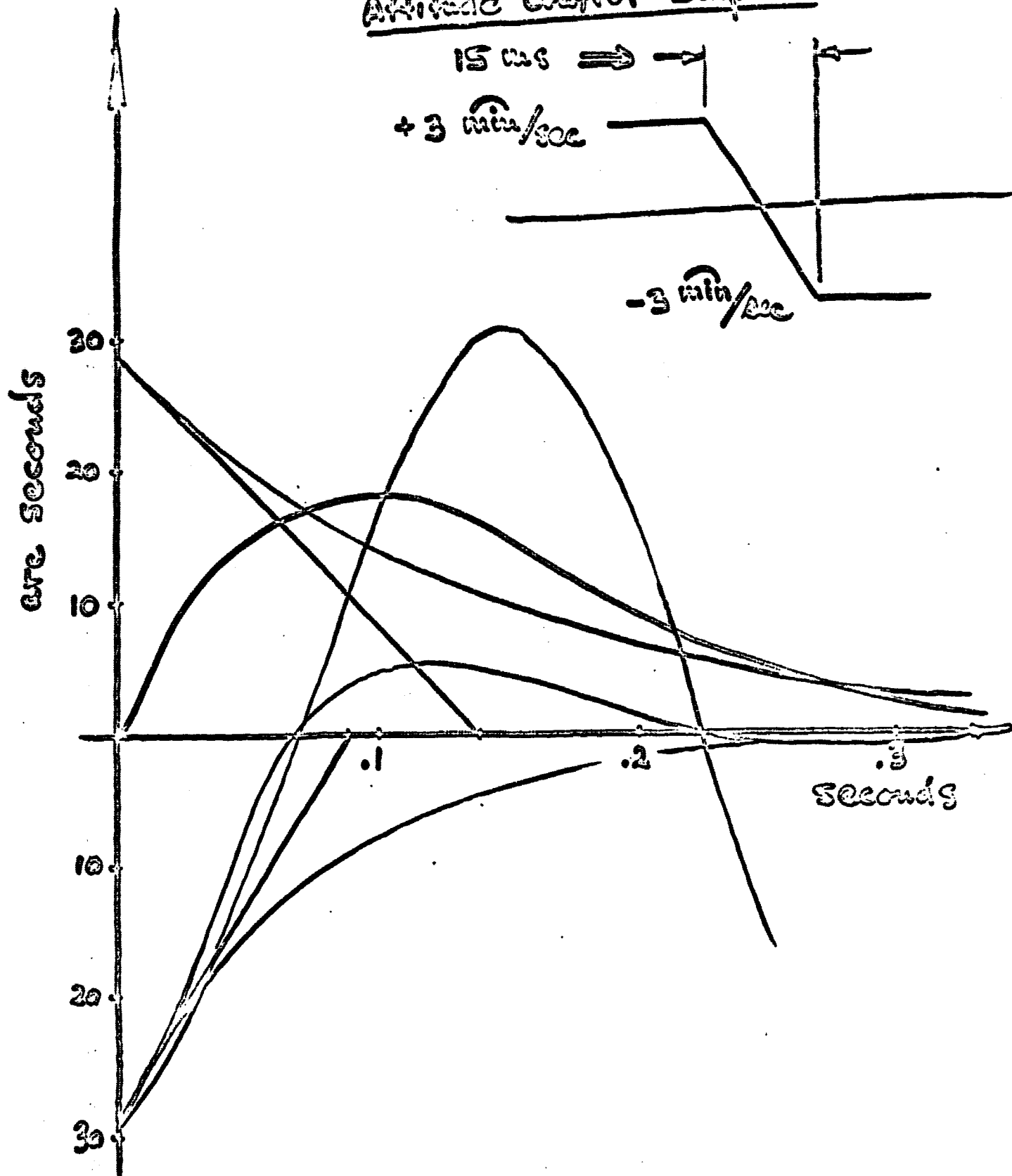


Fig. 32

Specification No. S-047-1

Revision No. N/A

Release Date 1 July 1968

PRELIMINARY
CONTRACT END ITEM DETAIL SPECIFICATION
(PRIME EQUIPMENT)

PERFORMANCE/DESIGN
and
PRODUCT CONFIGURATION
REQUIREMENTS

CEI NO. NAS 9-7457 - IV.A.

STELLAR REFRACTION STAR-TRACKER
S-047 EXPERIMENT APOLLO APPLICATIONS "A"

Approved by Not for bids

Date 1 July 1968

Contract No. NAS 9-7457

Specification No. S-047-1

Release Date 1 July 1968

1. SCOPE

This part of the specification establishes the requirements for performance, design, test and qualification of one type of equipment identified as the "Stellar Refraction Star Tracker" CEI NAS 9-7457-IV.1.

2. APPLICABLE DOCUMENTS

PROJECT DOCUMENTS

University of Michigan ORA Tech Rpt 04963-3-T

University of Michigan ORA Tech Rpt 06647-1-T

DRAWINGS

H1-52001	Motor, Inland T-2170
H1-52002	Rotor shaft
H1-52003	Dummy shaft
H1-52004	Flex-pivot
H1-52005	Ring, rotor clamp
H1-52006	Field cup
H1-52007	Pivot mount
H3-52003	Atwill demodulator
H3-52004	Atwill scan generator & torque compensator
H3-52005	Tube-data scope
H3-52006	Base-data scope
H3-52007	Mount-mirror
H3-52010	Atwill scan generator
H3-52011	Horizontal & vertical raster scan generator
H3-52016	Peak light intensity hold detector
H3-52017	Focus regulator and deflection coil drivers

H3-52018	Data telescope logic card
H3-52021	Torque motor drive amplifier
H3-52022	Pre-amplifier, signal dissector
H3-52023	Inner gimbal
H3-52025	Vertical raster scan generator
H3-52026	Horizontal raster scan generator
H5-52001	Middle gimbal
H5-52002	Outer gimbal
GPI C543003439	Schematic diagram, gyroscope intergrating
GPI C162564002	Envelope drawing, gyroscope integrating

SPECIFICATIONS

MIL-E-5272 Amendment 1 "Environmental Testing, Aeronautical &
Associated Equipment, General Specification for Kearfott
C182564252 "Test Instruction, Gyroscope Integrating"

STANDARDS

MIL-STD-810A "Military Standard - Environmental Test
Methods for Aerospace and Ground Equipment"
MIL-STD-826A "Military Standard - Electromagnetic
Interference: Test Requirements and Test Methods"
MIL-STD-143A "Military Standard - Specifications and Standards,
Order of Precedence for the Selection of"
MIL-STD-129D "Military Standard - Marking for Shipment
and Storage" (As changed)

BULLETINS

NASA-MSD-DS-21 Rev. A. "Meteoroid Environment - Near-Earth
and Cis-Lunar"

OTHER PUBLICATIONS

NASA-MSC-D-NA-0002 "Procedures & Requirements for the
Flammability and Offgassing Evaluation of Manned Spacecraft
Non-Metallic Materials"

NASA-MSC-PA-D-67-13 "Apollo Spacecraft Non-Metallic
Materials Requirements"

NASA-NPC-500-10 "Apollo Test Requirements"

NASA-NPC-200-1A "Quality Program Provisions for Space
System Contractors"

NASA-NPC-200-3 "Inspection System Provisions for Suppliers
of Space Materials, Parts, Components, and Services"

NASA-NPC-200-4A "Quality Requirements for Hand Soldering of
Electrical Connections"

NASA-NPC-250-1 "Reliability Program Provisions for Space
System Contractors"

NASA-NPC-500-1 "Apollo Configuration Management Manual"

NASA-MSC-Supplement #1 to NPC-500-1 Revision B

3. REQUIREMENTS

3.1.1 Functional Characteristics

The subject equipment must:

- a) Be attached to rigid spacecraft structure in a manner and position known to the astronaut and subject to monitor by the astronaut on remote indicating instrument in the command module.
- b) Have functional telescopic optics capable of viewing a field 1° by 1° (square) or 1° diametrically (circular)

- c) Have associated sensing and modulation electronics capable of detecting the most intense optical signal in the telescopic field-of-view
- d) Have gimbals between the rigid telescopic optical system and the spacecraft allowing $2^\circ \pm 0.1^\circ$ relative motion in any axis
- e) Have a suitable detection and demodulation system to detect the vector position of the most intense visual signal from the center of the optical field-of-view, and the capability of recording this vector position by independent measurement at least once per 0.1 second. The vector must be recorded with an overall error in spherical coordinates not to exceed two seconds of arc RMS. This signal will be called the "off-axis error signal "
- f) Have suitable feedback electronic system and a suitable gimbal torque system such that the off-axis error signal shall tend toward zero at all times while in operation, under conditions of spacecraft motion not to exceed 2 arc-minutes per second plus motion of the celestial source not to exceed 2 arc-minutes per second
- g) Have a two-axis gyroscopic system rigidly attached to the telescope frame which detects motion of 0.1 arc second or more, providing that:
 - 1) Motion of the telescope has not exceeded 1° per second in any axis for 2.5 minutes preceding measurement
 - 2) Motion of the telescope does not exceed 3 arc-minutes per second during measurement

The gyroscopic system must be capable of being caged and uncaged and must be operable at any acceleration less than 0.1g while uncaged

- h) Have a gyroscope system (g) above) which records the motion in each axis to the precision stated at least once per 0.1 second
- i) Have the ability to record the off-axis error signal as in c) above whenever the maximum intensity of optical signal available at the telescope entrance exceeds that of a 4.5 visual magnitude stellar source. Within two seconds of time after developing the initial off-axis error signal (star acquisition) the system must be operable whenever the signal exceeds in intensity that of a 9.5 visual magnitude stellar source

- j) Have the capability of protecting the optical surfaces from space contamination as provided by future criteria at all times while not in operation
- k) Have optical systems which provide the signals as required above whenever the sun is more than 18° below the sensible horizon
- l) Have a suitable control system actuated by the astronaut so that, realignment with the spacecraft, optical contamination protection, and electrical power turn-off can be commanded by the astronaut and completed within 2.0 seconds after command

3.1.2 Operability

The equipment shall be operable over two thousand sequences each lasting at least 5 minutes and shall have a useful life of not less than 500 hours.

All other reliability, maintainability, and environmental requirements shall be identical to those specified for the Apollo spacecraft in the referenced publications above.

No special requirements exist for the equipment, other than those listed.

3.2.2 Component Identification

3.2.2.1 Government-Furnished Property List

None

3.2.2.2 Engineering Critical Components List

- a) ITT F 4012 S-20 Phototube (2 ea)
- b) Kearfott C172564002 Gyro (or equivalent) (2 ea)
- c) Optical elements, Celestron 10 or equivalent
- d) Inland motor, torque, T-2170 (2 ea)
- e) Bendix Flex-Pivot 5010-600 (4 ea)

3.2.2.3 Logistics Critical Components List

Items 3.2.2.2 a) and b)

3.3 Design and Construction

3.3.1 The general design is exemplified by the comprehensive photographs attached.

The performance requirements listed above will be met by equipment fabricated in accord with the following specified drawings:

U-M H1-52001 thru 52007

U-M H3-52003 thru 52007

U-M H3-52010, 52011

U-M H3-52016, 52017, 52018

U-M H3-52021, 52022, 52023

U-M H3-52025, 52026

U-M H5-52001, 52002

ITT F 4012 S-20 and

Inland T-2170, provided that a gyroscope system be available meeting the following performance specification:

a) Gyro transfer function

The gyro open loop transfer function shall be 108.5 millivolts (mv) root mean square (RMS) ± 15 percent output per milliradians displacement about the input axis when the signal generator excitation, and spin motor excitation are held at the nominal value specified and the gyro is at operating temperature.

b) Output axis freedom

The gimbal freedom about the output axis shall be mechanically limited to 3.6 ± 0.25 degrees in both directions from signal generator null position.

c) Characteristic time

The characteristic time as determined by dividing the gimbal moment of inertia about the output axis by the damping coefficient shall be 6.4 milliseconds ± 15 percent at the operating temperature.

d) Angular momentum

The gyroscope, integrating shall be designed to have a nominal angular momentum of 227,000 gram (GM) centimeter (CM) squared per second ($\text{GM CM}^2/\text{sec}$) at synchronous speed of 24,000 revolutions per minute (RPM).

e) Output axis inertia

The gimbal output axis inertia shall be approximately 117 grams centimeter squared (GM CM^2).

f) Open loop gain

The open loop gain shall be 12.4 ± 10 percent at operating temperature.

g) Operating temperature

The gyroscope operating temperature shall be 165 ± 5 degrees fahrenheit (F).

h) Signal generator null

With the gyro at operating temperature and standard excitation applied to the spin motor, signal primary and operating heater, the null or minimum signal secondary voltage shall not exceed 1.0 MV RMS.

i) Warmup time

The time required for the gyroscope to reach operating temperature from 70°F. as indicated by the sensor resistance shall be approximately 4 minutes.

j) Rate mode output signal noise

The maximum value of noise measured in the output signal of a gyro operated in a rate mode shall not exceed an equivalent peak input rate of 8 degrees per hour when measured under the following conditions.

Amplifier-gyro constant: closed loop velocity error coefficient, $(KV \frac{1}{SEC}) = 80 \pm 5\%$

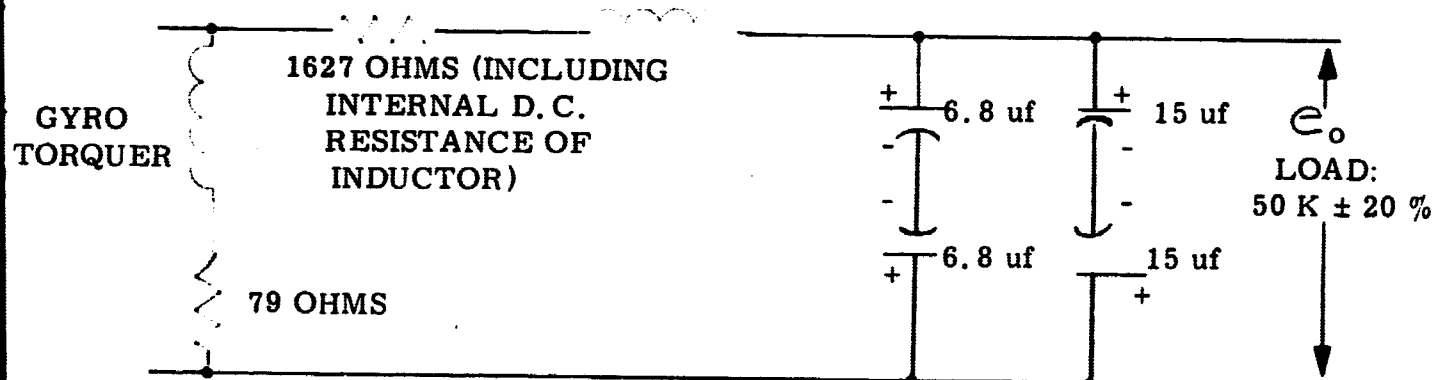
Loop damping constant: 0.7 ± 0.1 of critical

Loop natural frequency: $112.5 \text{ RAD/SEC} \pm 20\%$

Frequency response of measuring equipment
60 CPS minimum

A filter with the configuration shown below shall be inserted between the gyro output signal and the instrumentation

10 H



The above noise filter includes effects of both mechanical and electrical disturbance phenomena directly attributable to the gyro only in normal closed loop operation.

k) Acceleration insensitive drift rate

The maximum value of acceleration insensitive drift rate with the gyro at null and with no external compensation applied shall be $2^{\circ}/\text{HR}$.

l) Acceleration insensitive drift rate shift

The maximum change in acceleration insensitive drift rate, runup to runup, and with the gyro cooled to 70°F , for 16 hours between operating periods shall be $\pm 0.5^{\circ}/\text{HR}$ from the initial trimmed value for 3 runs.

m) Acceleration sensitive drift rate (mass unbalance drift rate)

The maximum acceleration sensitive drift rate under any condition of storage or operating environment shall be $1.0^{\circ}/\text{HR/G}$ along the input axis (IA) and spin reference axis (SRA).

n) Acceleration sensitive drift rate shift

The maximum change in acceleration sensitive drift rate shift, runup to runup, with the gyro cooled to 70°F , for 16 hours between operating periods shall be $0.5^{\circ}/\text{HR/G}$ from the initial value for 3 runs.

o) Random drift rate

The computed random drift (1 sigma value) for any operating position of the gyro for one-half hour shall not exceed $0.05^{\circ}/\text{HR}$.

p) Anisoelastic drift rate

The G^2 component of drift as computed from total drift rate data obtained with applied vibration over the frequency range of 30 to 1500 cps shall not exceed $0.02^{\circ}/\text{HR/G}^2$ peak; over the frequency range of 30 to 2000 cps shall not exceed $0.05^{\circ}/\text{HR/G}^2$ peak, except for isolated narrow frequency bands of less than 5 cycles.

q) Maximum torquing rate

The gyro shall be capable of a torquing rate equivalent to or exceeding an angular velocity about the input axis of $4.5^{\circ}/\text{sec}$.

r) Spin motor characteristics

The gyro spin motor shall be a synchronous, hysteresis type.

Excitation voltages: The spin motor excitation voltage shall be 26 ± 0.3 volts (V) RMS, 400 ± 0.04 cps, three phase sinewave.

Spin motor power: Starting power shall be 4.5 watts (w) maximum and running power at synchronous speed shall be 3.5 watts (w) maximum.

Spin motor current: Starting current shall be 0.154 amps maximum and running current at synchronous speed shall be 0.134 amps max.

Motor rundown time repeatability: The wheel rundown time, as measured by the elapsed time required for the back EMF to change from 20 cps to 0 cps shall not deviate by more than ± 15 seconds from the value recorded at gyro acceptance. The wheel rundown time shall be determined at gyro operating temperature, after the spin motor has been running for a minimum period of one hour.

s) Signal generator

The signal generator shall be an air core differential transformer.

Excitation: The excitation voltage on the primary winding shall be 13 ± 0.26 volts (v) RMS, 800 ± 0.08 cps, single (1) phase. The 400 cps motor supply and the 800 cps signal generator supply shall be phase locked.

Sensitivity: The sensitivity of the signal generator shall be 8.75 ± 0.9 MV per MR gimbal displacement with excitation at nominal.

Linearity: The linearity of the signal generator shall be ± 1 percent of full scale reading for gimbal travel up to ± 3.6 degrees.

Primary impedance: The primary impedance shall be $22.5 + j77$ ohms ± 10 percent at 800 cps and 70°F .

Secondary impedance: The secondary impedance shall be $46 + j7$ ohms ± 10 percent at 800 cps and 70°F .

Phase angle: The phase angle of the signal generator primary voltage shall be 11.0 ± 3 degrees when operating into an 5k ohm load minimum, when the gyro is at 70°F .

Signal generator input current: The input current to the signal generator primary shall be 0.210 amps maximum.

t) Torque generator

The torque generator shall be a permanent magnet D'arsonval type.

Torquer scale factor: The torque generator scale factor at signal generator null shall be 134 ± 13 degrees/HR/MA DC.

Torquer linearity: The torquer linearity at gimbal null shall be $\pm 0.05\%$ for rates from 0 to 100°/HR. This linearity error is the maximum deviation from the best straight line.

Torquer resistance: The torquer control field DC resistance shall be 38 ohms ± 10 percent at 70°F.

Control field time constant: The control field time constant shall be 55 microseconds ± 10 percent at 70°F.

Torque generator maximum current: The maximum current applied to the torquer generator secondary shall be limited to 250 milliamps.

u) Temperature sensing element

The temperature sensing element shall be adjusted to have a DC resistance of 780 ohms at operating temperature.

v) Heater windings

Control heater: (Operating heater)

Resistance: The control heater DC resistance shall be 31.4 ± 3.1 ohms at 70°F.

Power: The maximum control heater power shall be 30 watts when excited with 28 volts DC.

Warmup heater:

Resistance: The warmup heater DC resistance shall be 132 ± 13 ohms at 70°F.

Power: The maximum warmup heater power shall be 112 watts when excited with 115 volts, 60 cps, single phase.

3.3.2. Selection of specifications and standards shall be in accord with MIL-STD-143A.

3.3.3 Materials are specified in the materials and parts specifications. In those instances where substitution or qualification is required the materials shall be suitable, best commercial quality, non-toxic, light weight and non-flammable when possible.

3.3.4. All parts not covered by appropriate drawings attached hereto, are standard commercial parts. In most cases the parts are available from the Apollo Qualified Parts List. For the parts not so covered, qualification or redesign as per the Materials and Parts Specification shall be made.

3.3.5. Materials susceptible to humidity degradation or which are fungus nutrients shall not be used. If a substitute for a fungus nutrient material is not commercially available, the material shall be treated with a fungicide retaining efficacy for five years. The fungicide will require qualification and testing for offgassing properties.

- 3.3.6. The corrosion of metal parts shall be precluded by appropriate plating or anodizing. The corrosion which might be caused by dissimilar metallic junctions has been prevented by proper design with the exception of fasteners which have been for strength and weight considerations been exclusively restricted to stainless steel. Protective coating of the fastener-part interfaces is required and inspection and storage specifications must reflect this requirement in their provisions.
- 3.3.7. No special provisions for interchangeability and replaceability have been made.
- 3.3.8. Workmanship reflecting evidence of excellent shop practice is required throughout. Correct and uniform torquing is required on all parts and there shall be no evidence of scars, burrs, or scratches resulting from assembly operations.
- 3.3.9. Electromagnetic interference shall be a subject of integration test only. Integration specifications have not been issued. Testing provisions of MIL-STD-826A are fully applicable.
- 3.3.10. Identification and marking shall follow provisions of MIL-STD-129D and changes thereto, and as supplemented by MSC directives.

4. QUALITY ASSURANCE PROVISIONS

4.1 Test/Verification

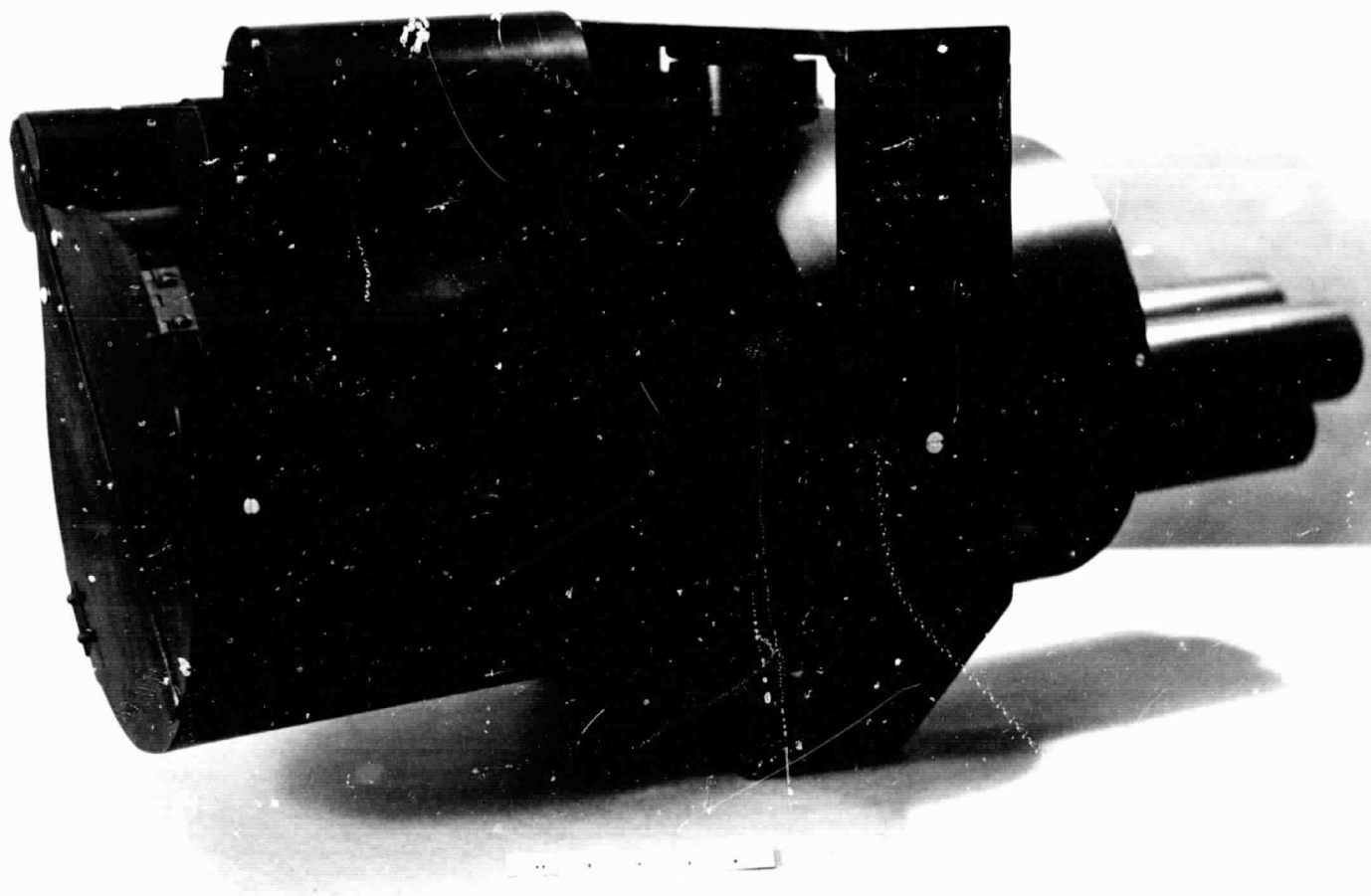
- 4.1.1 Engineering test and evaluation shall be performed in compliance with University of Michigan systems engineering group standards and conducted in the University facilities.
- 4.1.2 Qualification testing shall be conducted at the appropriate local manufacturers test facilities and in compliance with the qualification test standards established by The University quality and reliability program groups.
- 4.1.3 Engineering critical component qualification shall be conducted as follows:
 - Item: a) Manufacturer's plant
 - b) Manufacturer's plant
 - c) University of Michigan or local facility
 - d) University of Michigan
 - e) University of Michigan

4.2 Integrated Test Requirement

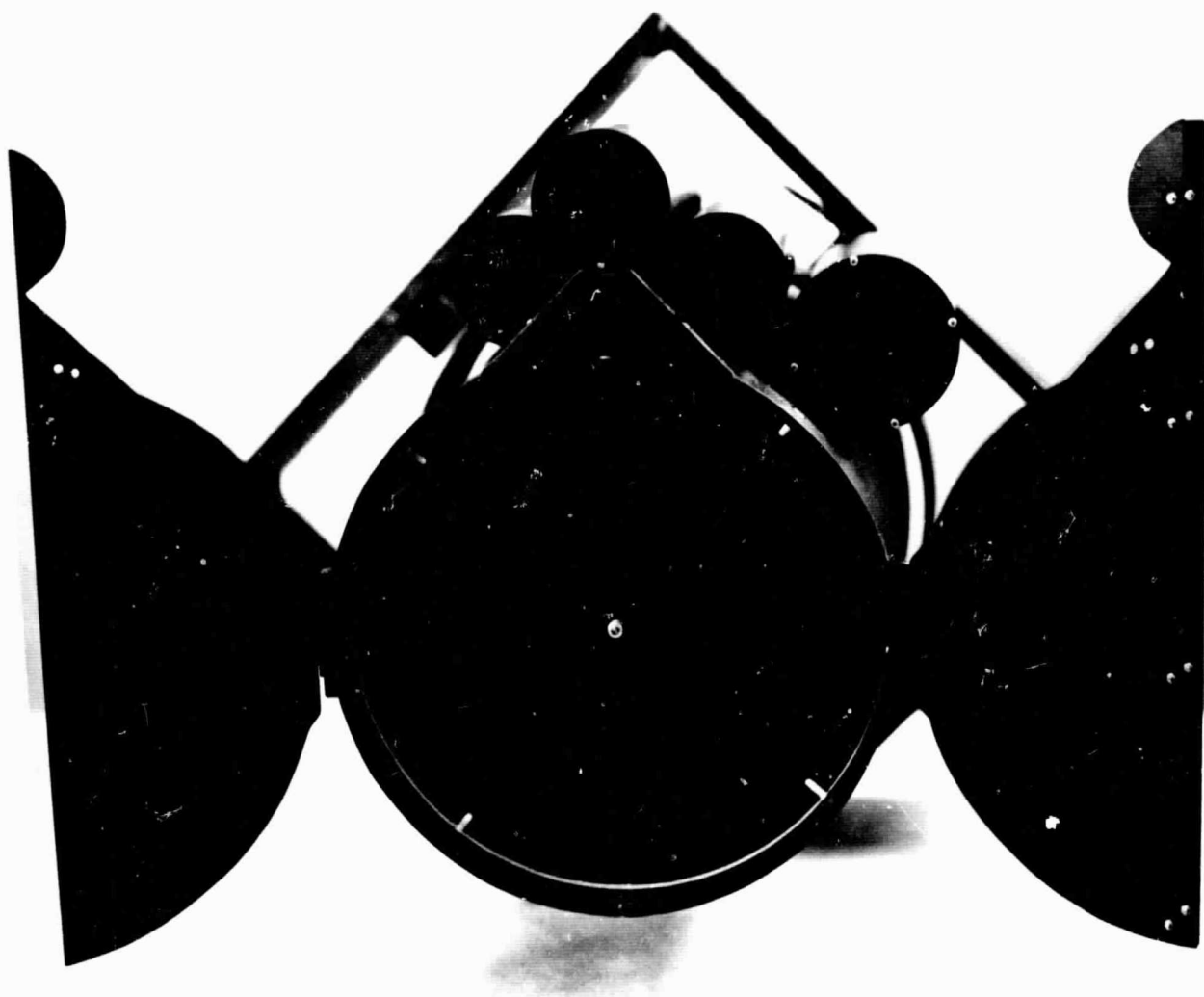
Not applicable

5. Notes

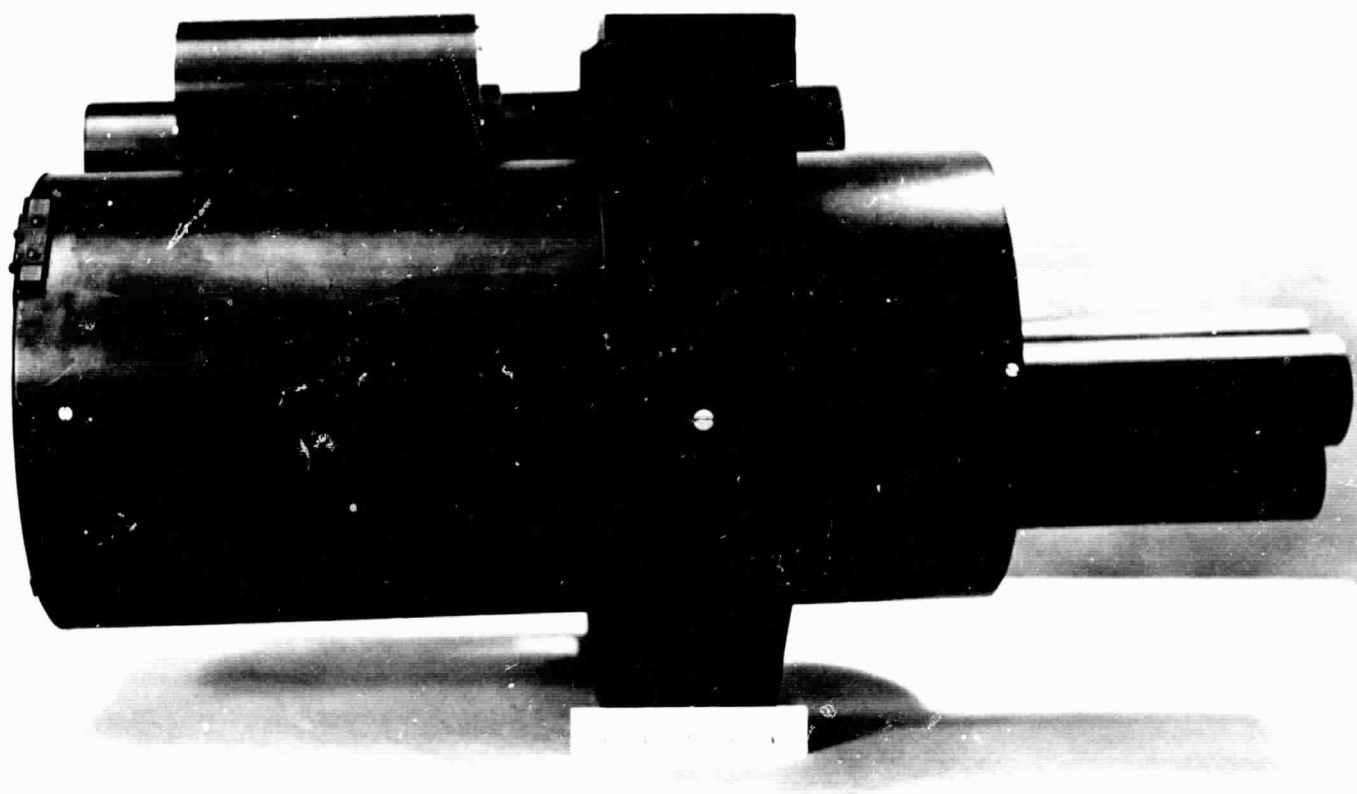
None



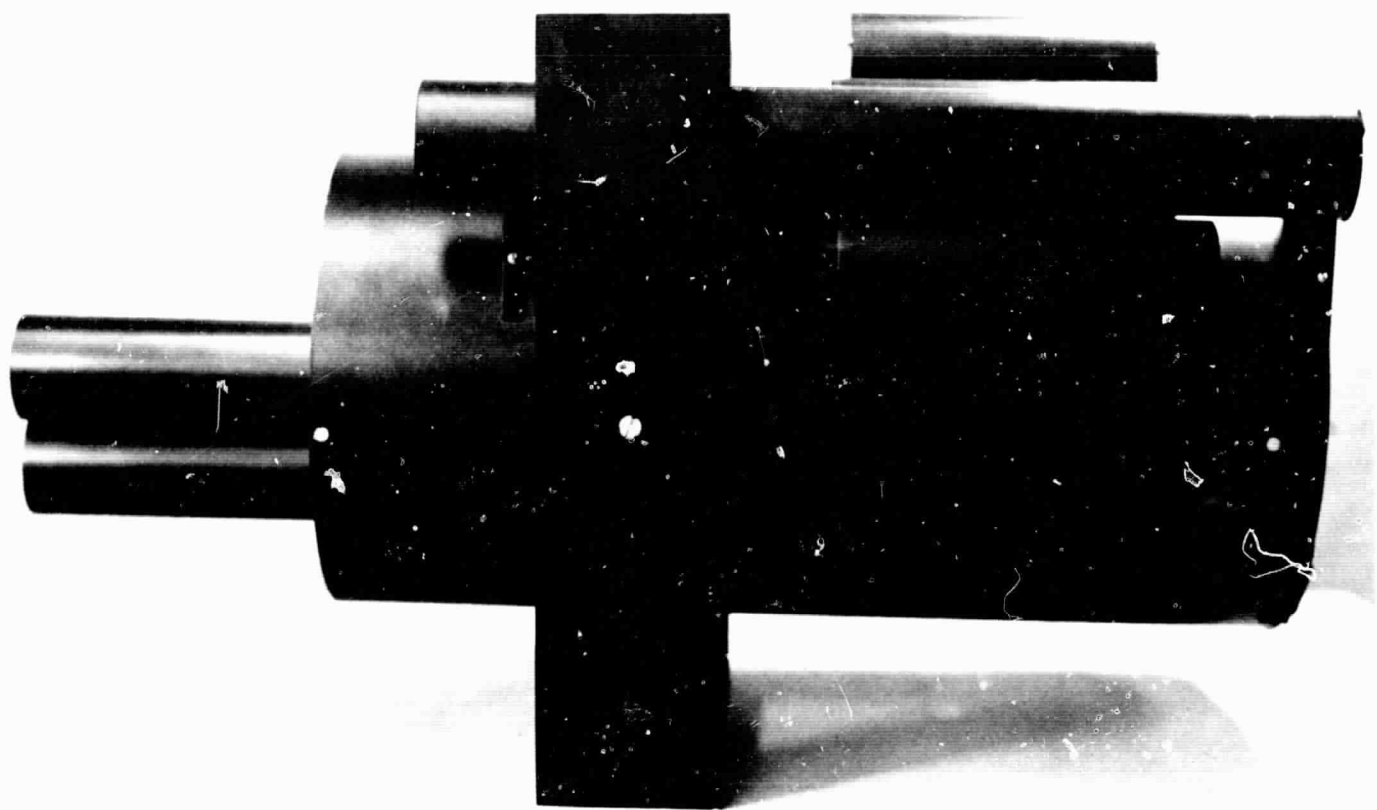
MOCKUP - QUARTER VIEW



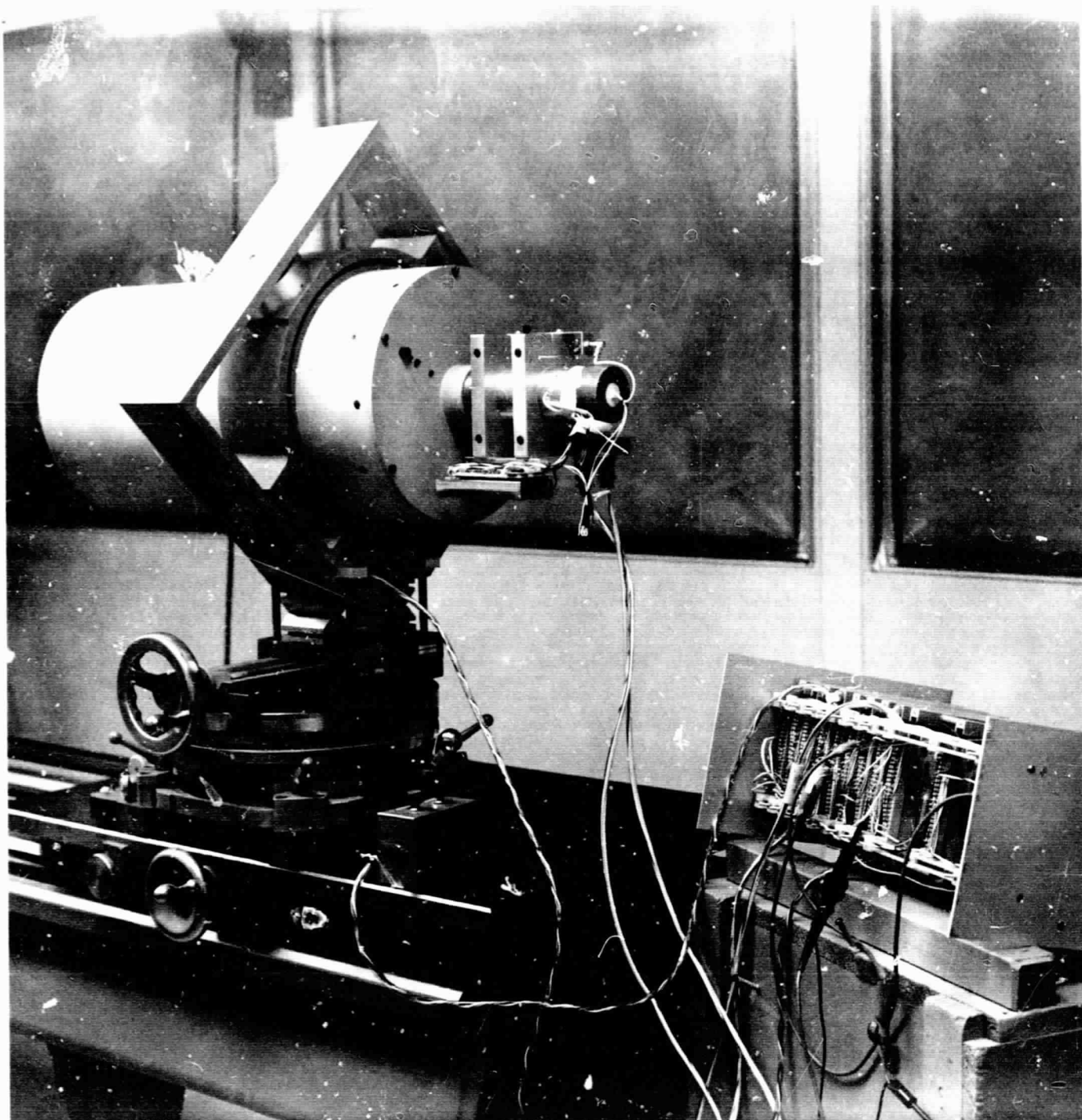
MOCKUP - FRONT VIEW



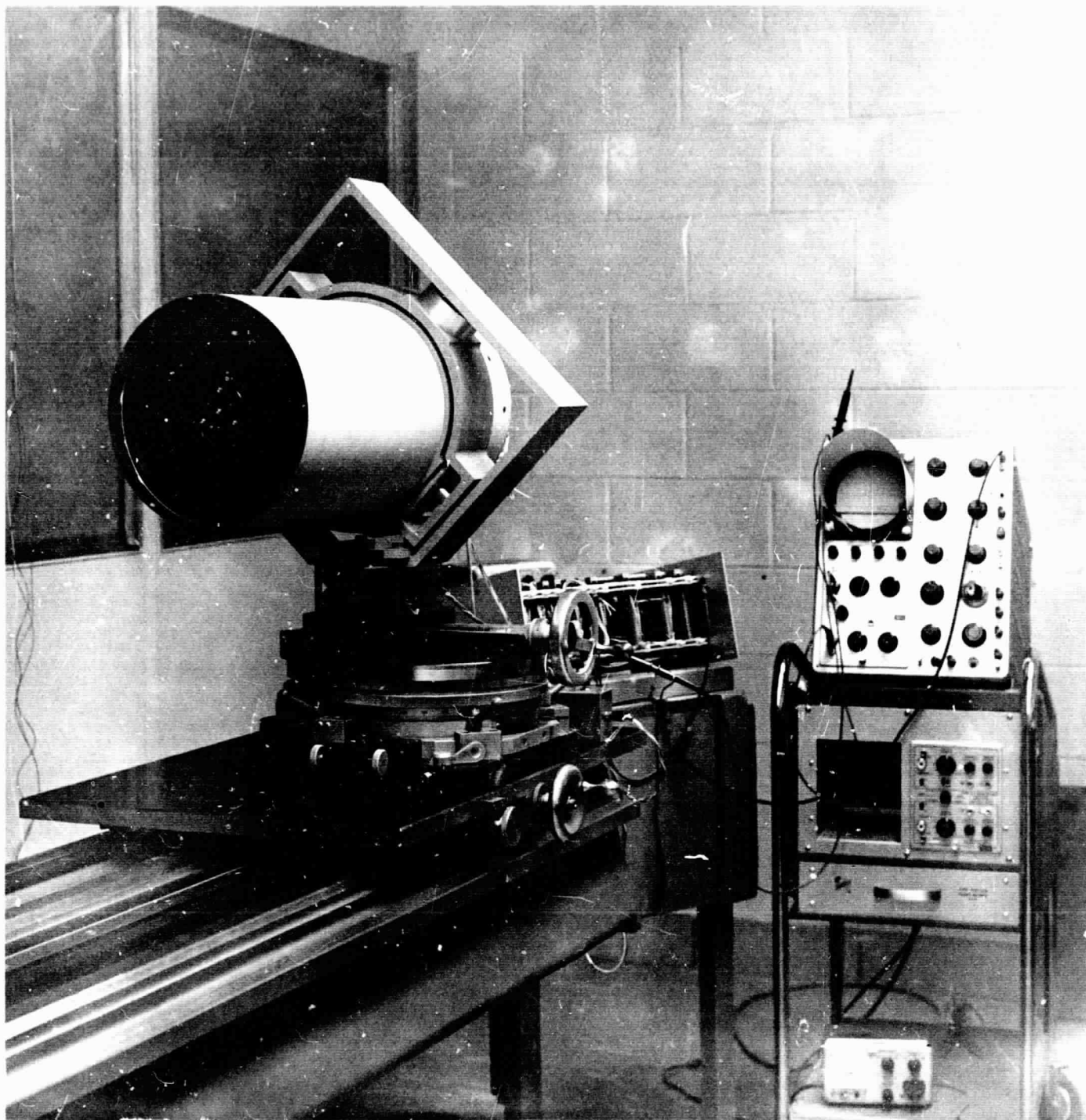
MOCKUP - LEFT SIDE



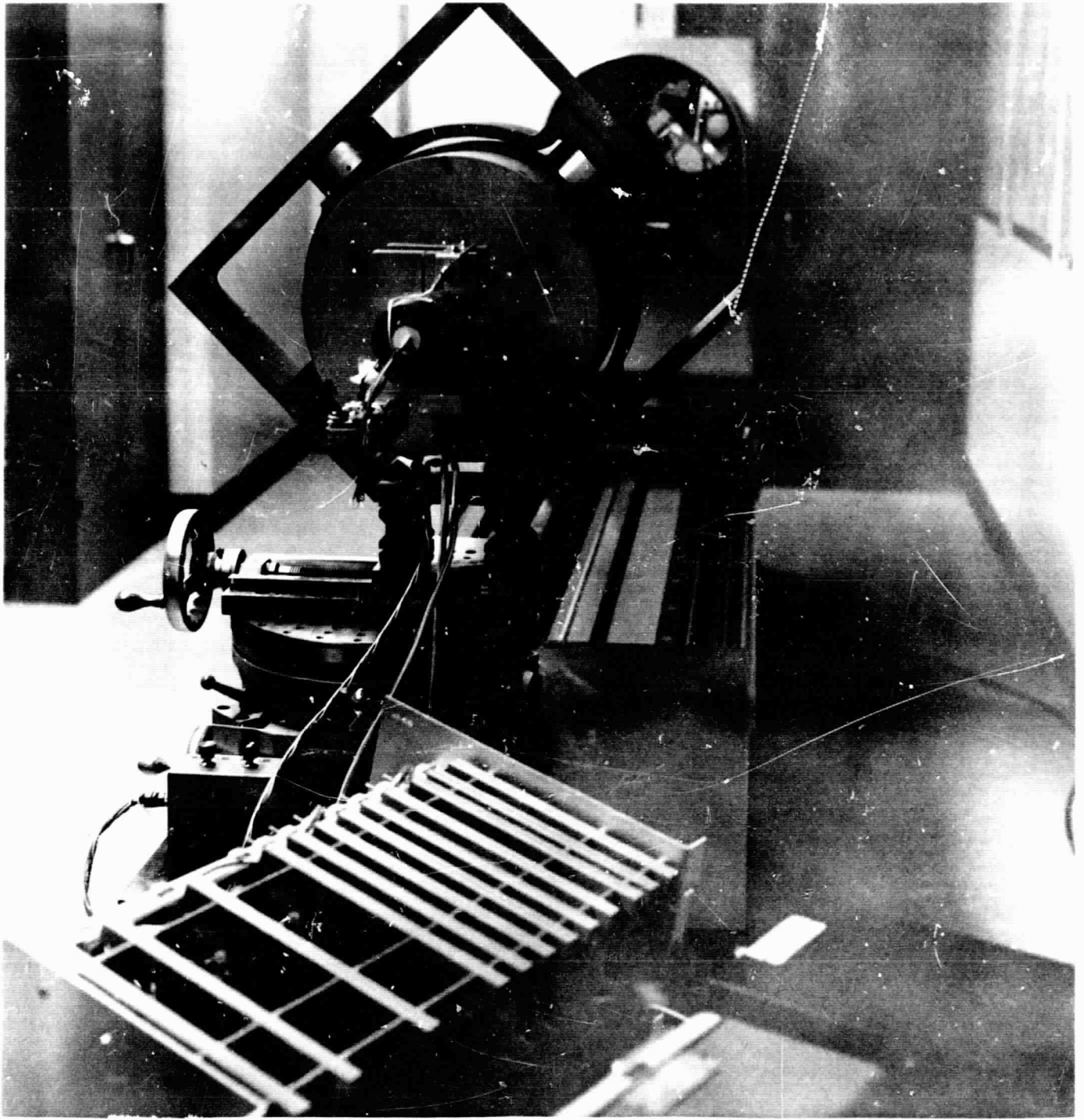
MOCKUP - RIGHT SIDE



BRASSBOARD - REAR QUARTER VIEW



BRASSBOARD - FRONT QUARTER VIEW



BRASSBOARD - REAR VIEW SHOWING
LENS BENCH

ALL DIMENSIONS PLUS ON MINUS

ACTUAL DIMENSIONS:

28120	.500
28123	.500
28120-28125	.501

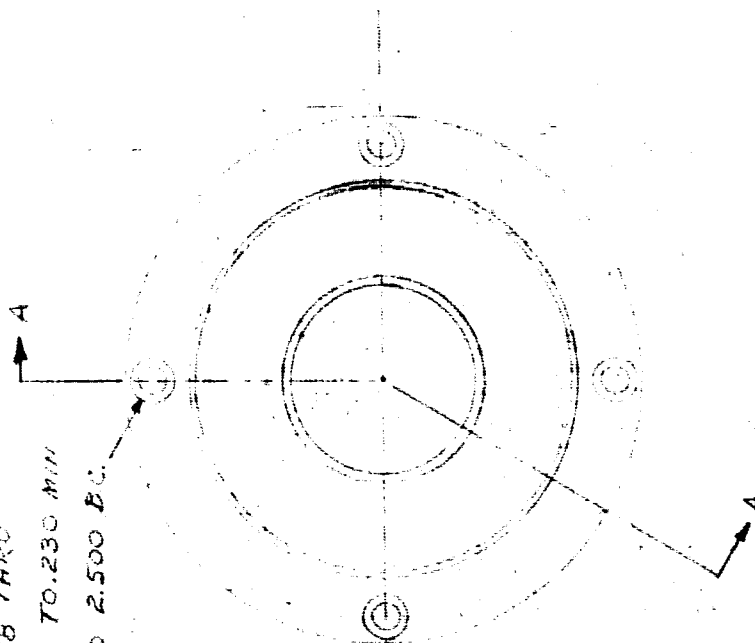
$$\left. \begin{array}{l} .245 \\ .245 \\ .245 \end{array} \right\} \begin{array}{l} .242 \\ .239 \\ .239 \end{array}$$

1.0004
1.0002
1.0004

021 MOUNTING
041 DIMENSION

[illegible]

4 HOLES $\frac{1}{8}$ " THRU
C'SINK 92° TO.230 MIN
EQ SPACED 2.500 BC.



SECTION A-A

DATE	1-17-68	DR. BY	F 3	SCALE	FULL	MATERIAL	PROJECT NO.	01114	FOR ASSEMBLY
NAME	MOTOR T-2170								

HIGH ALTITUDE ENGINEERING LABORATORY
DEPARTMENT OF AERONAUTICAL ENGINEERING
UNIVERSITY OF MICHIGAN
ANN ARBOR.
MICHIGAN

DRAWING NO.	H1-52001
-------------	----------

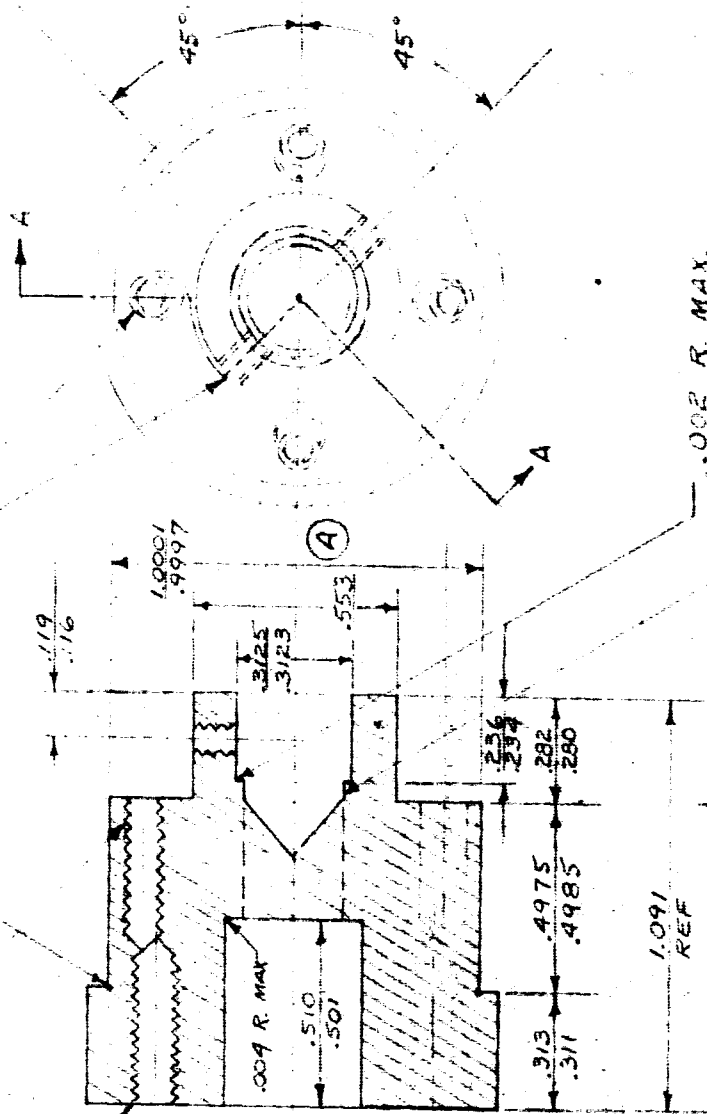
UNLESS OTHERWISE SPECIFIED

ALL DIMENSIONS PLUS OR MINUS

D & T 5-40 (4) HOLES
EQ. SPACED ON .8125 B.C.
TAP 3/8 DEEP

D & T 2-56 (2) HOLES
RELIEF. NO RADII.

D & T 6-32 UNC 3/4 DEEP
(4) HOLES EQUALLY SPACED
ON .750 ± .001 B.C.



SECTION A-A

"I" DRILL (.272)
OPTIONAL DRILL THRU

NOTE (A): THIS DIMENSION
TO BE .001 LESS THAN MATING
HOLE IN H1-52005

NOTES: 1. SURFACES WHICH ARE
DIMENSIONED 1.0001, .3125, .3754,
TO BE
CONCENTRIC WITHIN .0002.
2. BREAK EDGES.
3. TAPPED THREADS
TO BE OF MIL-SPEC QUALITY.

HIGH ALTITUDE ENGINEERING LABORATORY
DEPARTMENT OF AERONAUTICAL ENGINEERING
UNIVERSITY OF MICHIGAN
ANN ARBOR, MICHIGAN

NAME ROTOR SHAFT

SCALE 2 X FULL PROJECT NO. 01114
DR. BY F-3 GND. BY FOR ASSEMBLY

DATE 1-17-68

DRAWING NO. H1-52002

ALL DIMENSIONS PLUS OR MINUS

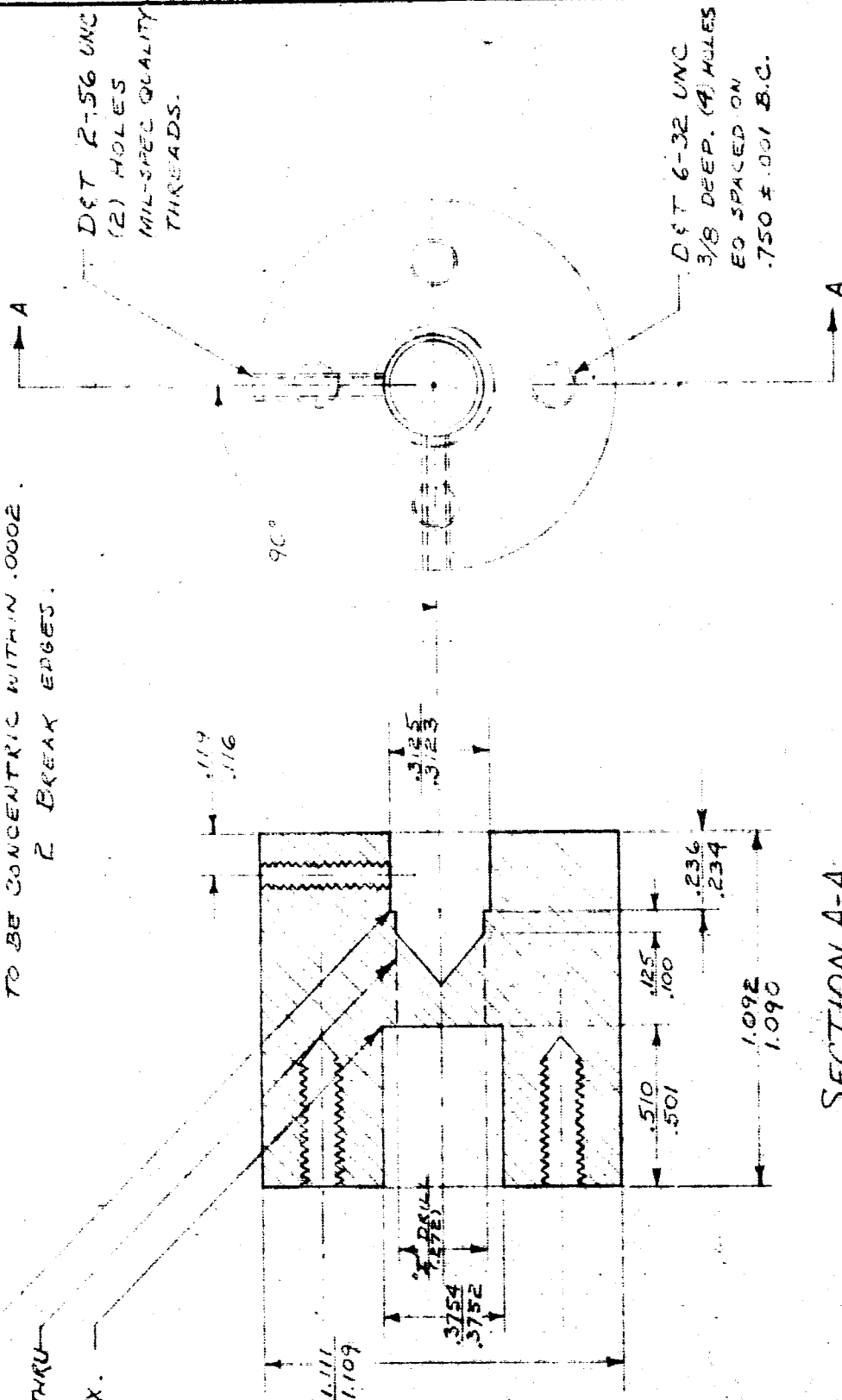
UNLESS OTHERWISE SPECIFIED

NOTES: 1. PRECISION HOLES (2)
TO BE CONCENTRIC WITHIN .0002.
2. BREAK EDGES.

.002 R. MAX.

OPTIONAL D. THRU

.004 R. MAX.



HIGH ALTITUDE ENGINEERING LABORATORY
DEPARTMENT OF AERONAUTICAL ENGINEERING
UNIVERSITY OF MICHIGAN
ANN ARBOR, MICHIGAN

NAME DUMMY SHAFT

PROJECT NO. 01114

MATERIAL 7075-T6

SCALE 2 X FULL

FOR ASSEMBLY

DR. BY F 3

DATE 1-19-68

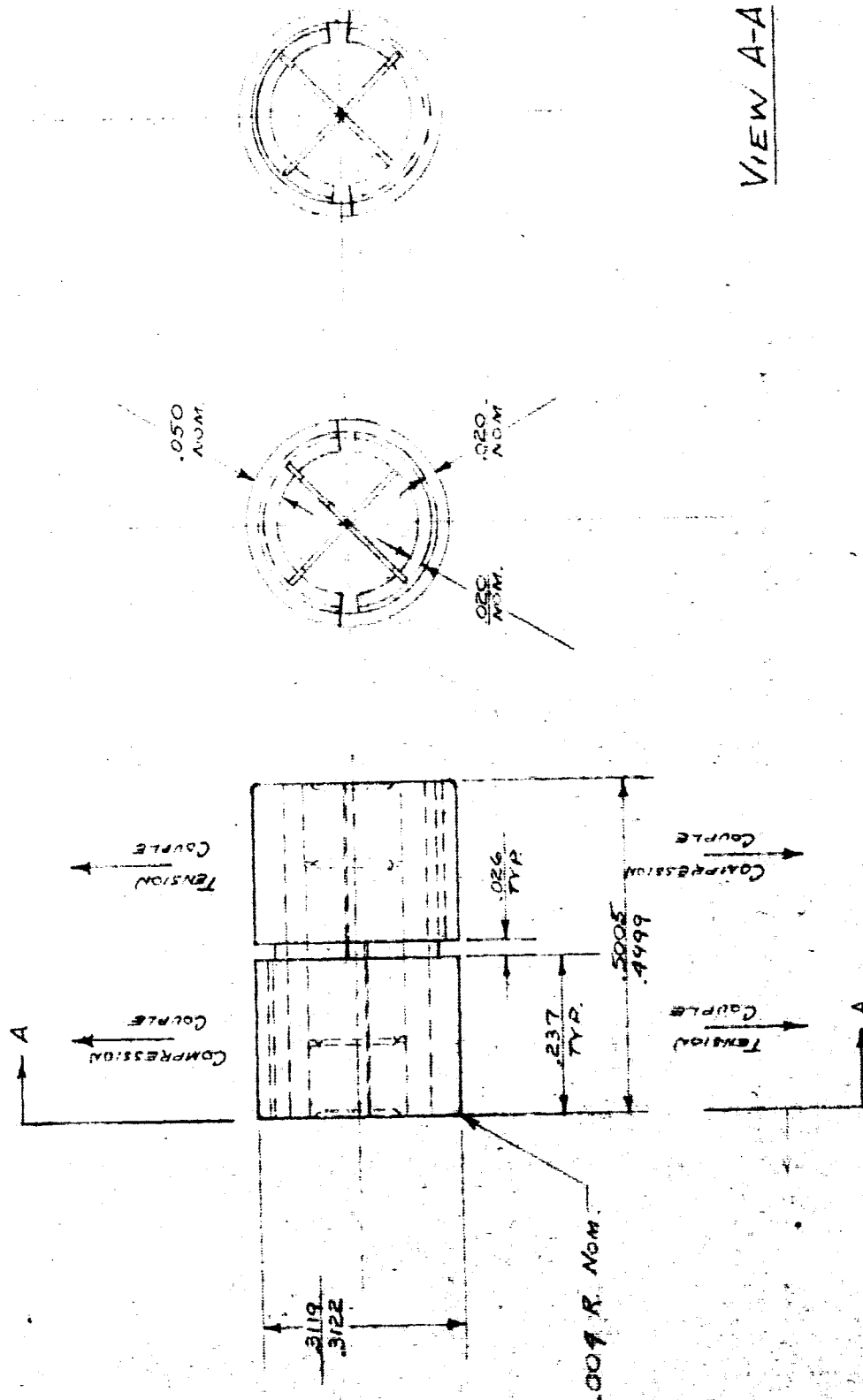
DRAWING NO. H1-52003

UNLESS OTHERWISE SPECIFIED

ALL DIMENSIONS PLUS OR MINUS

BENDIX-UTICA DIVN
PART 5010-600

COMPRESSION LIMIT : 55 LB.
TENSION LIMIT : 78 LB.
SPRING RATE - NO LOAD: 1.64 LB-IN/RADIAN
MAX DEFLECTION : $\pm 15^\circ$



VIEW A-A

HIGH ALTITUDE ENGINEERING LABORATORY
DEPARTMENT OF AERONAUTICAL ENGINEERING
UNIVERSITY OF MICHIGAN
ANN ARBOR, MICHIGAN

NAME FLEX-PIVOT

SCALE 1 X FULL
MATERIAL CRS
PROJECT NO. 0119
FOR ASSEMBLY

DRAWING NO.: H1-52004

DATE 1-19-68

CHANGES

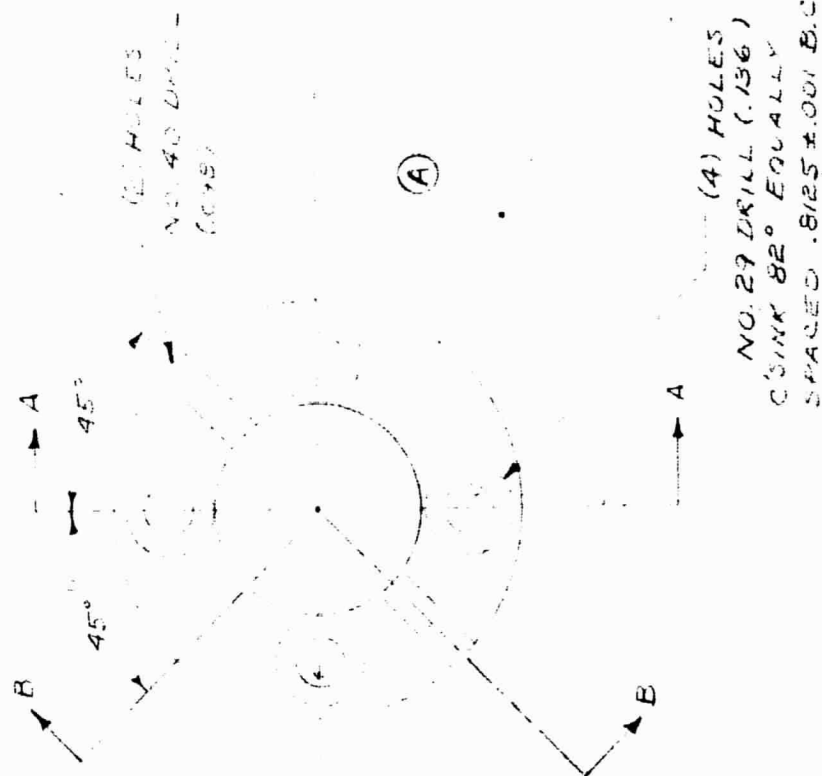
UNLESS OTHERWISE SPECIFIED

ALL DIMENSIONS PLUS OR MINUS

Notes:

1 BREAK EDGES.

2. ALL HOLE LOCATIONS $\pm .001$ UNLESS SPECIFIED



NOTE B THIS DIM.
TO BE .001 LARGER
THAN MATING DIM.
ON PART HI-52002

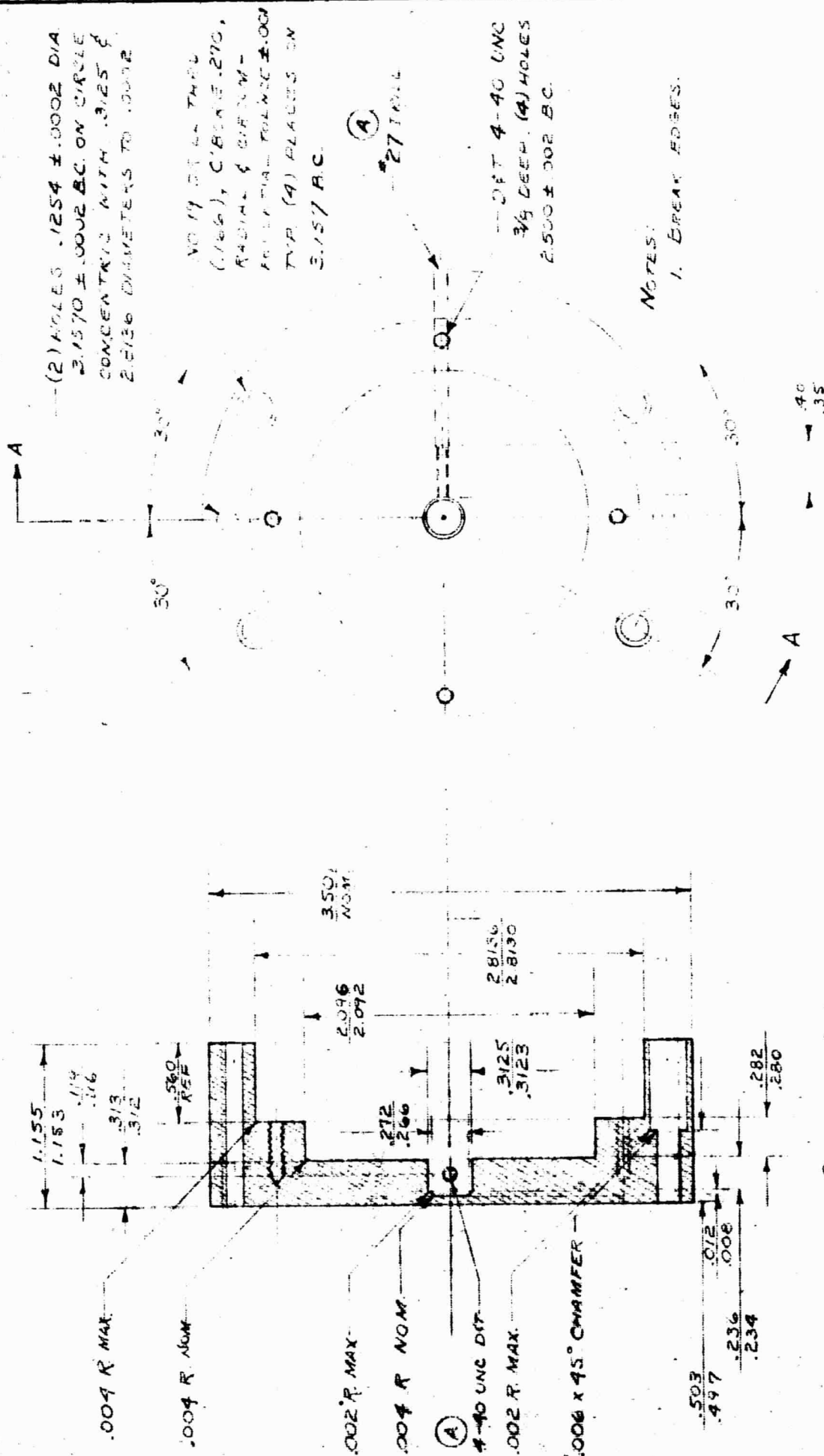
SECTION B-E

SECTION A-A

[illegible]

UNLESS OTHERWISE SPECIFIED

ALL DIMENSIONS PLUS OR MINUS .002



SECTION A-A

HIGH ALTITUDE ENGINEERING LABORATORY				DRAWING NO.: H1-52006
DEPARTMENT OF AERONAUTICAL ENGINEERING				
UNIVERSITY OF MICHIGAN				
ANN ARBOR, MICHIGAN				
NAME		FIELD CUP		PROJECT NO. 0114
SCALE		FULL		
MATERIAL		7075-T6		FOR ASSEMBLY
DR. BY		F3		
DATE		1-19-68		
CHANGES				
1ST				
2ND				
3RD				
4TH				
5TH				
6TH				
7TH				
8TH				
9TH				
10TH				
11TH				
12TH				
13TH				
14TH				
15TH				
16TH				
17TH				
18TH				
19TH				
20TH				
21ST				
22ND				
23RD				
24TH				
25TH				
26TH				
27TH				
28TH				
29TH				
30TH				
31ST				
32ND				
33RD				
34TH				
35TH				
36TH				
37TH				
38TH				
39TH				
40TH				
41ST		WAS 41 D. C 2-56		
42ND		3-12-68		

UNLESS OTHERWISE SPECIFIED

ALL DIMENSIONS PLUS OR MINUS

(2.) 40463 1254 \pm .0002
D.A. 3.1570 \pm .0002 A.C.
ON CASES CONCENTRATED
WITH .3025 HOLE TO .0002

NO. 19 CARL - THAO
(1960), DE. 13, V- P
270 N. V. 2004 - 10
T. 1004 V. 1004
3157 P. C. 1004 P. 1004

7-4614 987
A
100706 100706



2000

2000-00-00

CE R. MAX.

004 F. NOM.

012
008

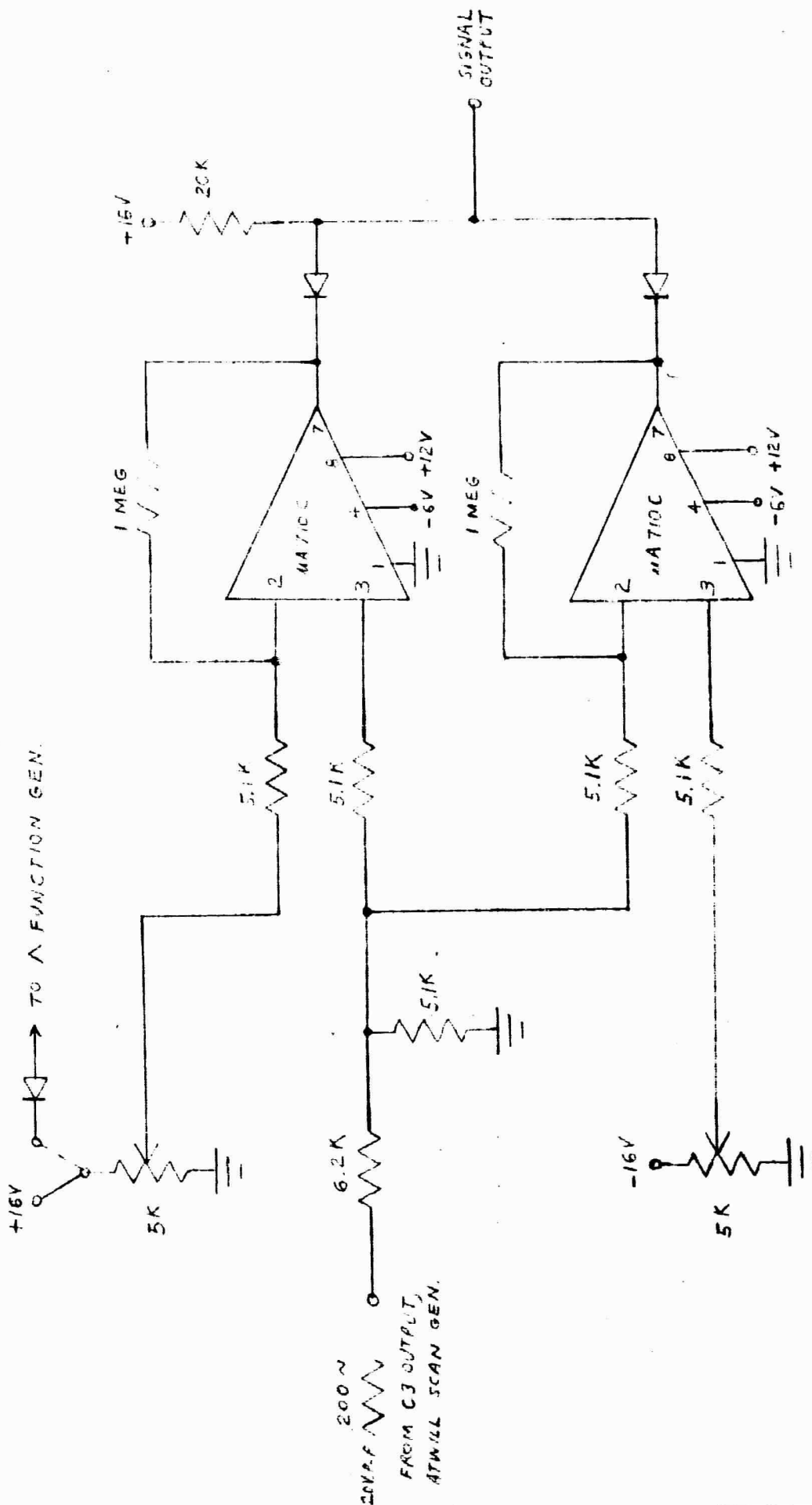
D					<h1>HIGH ALTITUDE ENGINEERING LABORATORY</h1> <p>DEPARTMENT OF AERONAUTICAL ENGINEERING UNIVERSITY OF MICHIGAN ANN ARBOR, MICHIGAN</p> <p>DRAWING NO: H1-52007</p>
C					
B					
A	1045410 6 2-10	3-20-60			
ET					

NAME <i>Pivot Mount</i>		PROJECT NO. <i>0114</i>	
SCALE <i>Full</i>	MATERIAL <i>7075-T6</i>	FOR ASSEMBLY	
DR. BY <i>FB</i>	C'D. BY		
1-20-60			

DATE	CHANGES

UNLESS OTHERWISE SPECIFIED

ALL DIMENSIONS PLUS OR MINUS



HIGH ALTITUDE ENGINEERING LABORATORY
DEPARTMENT OF AERONAUTICAL ENGINEERING
UNIVERSITY OF MICHIGAN
ANN ARBOR, MICHIGAN

TEST CIRCUIT -
NAME PRE-AMP SIGNAL SIMULATOR

PROJECT NO.
0114

MATERIAL

SCALE
NONE

DR. BY T.R.P.

FOR ASSEMBLY

O.K.D. BY

DATE
4-29-68

CHANGES

LET.

DRAWING NO.
H1-52008



OPERATE - CLEAR CONTROL BOX

HIGH ALTITUDE ENGINEERING LABORATORY

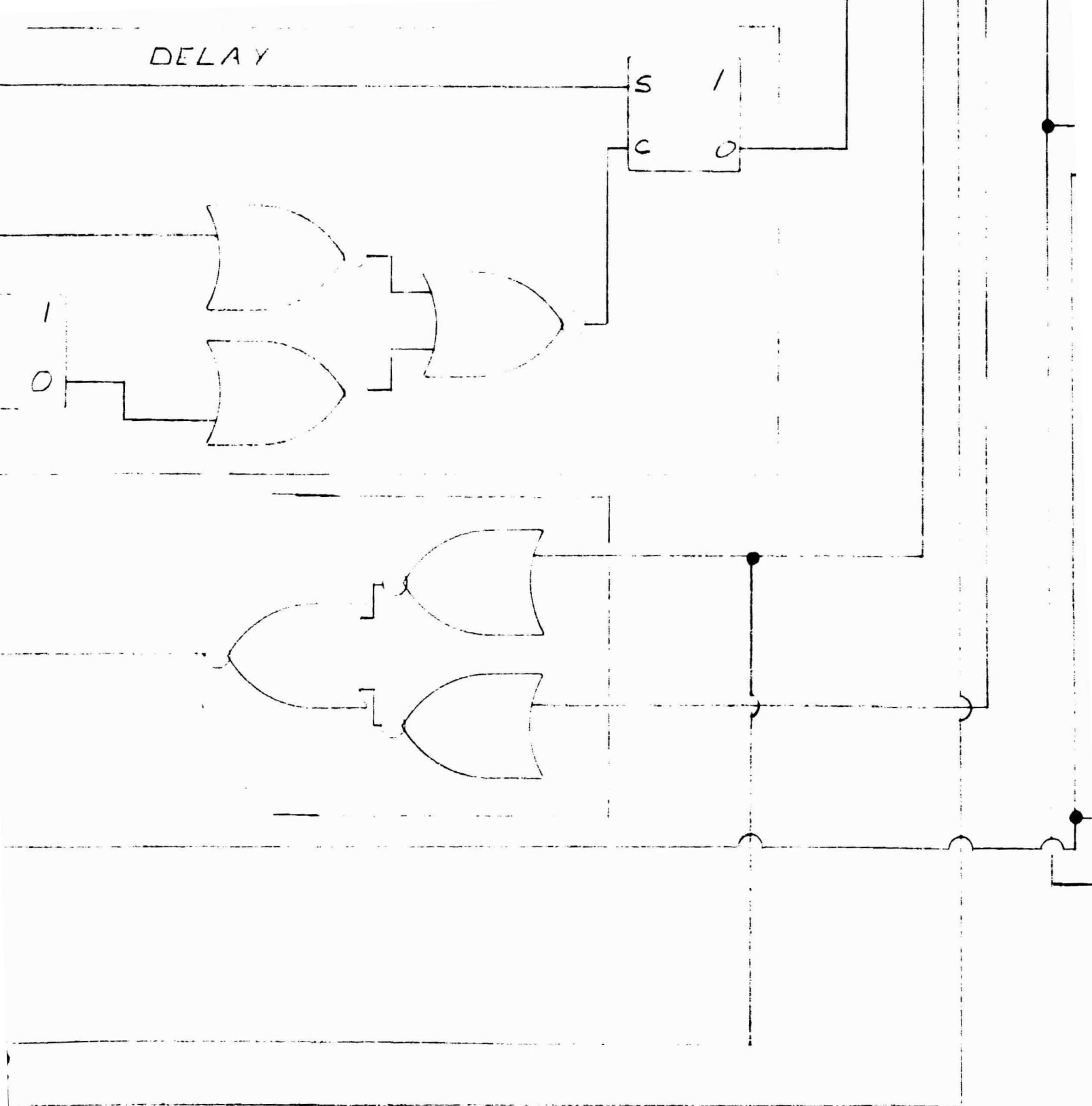
DEPARTMENT OF AERONAUTICAL ENGINEERING
UNIVERSITY OF MICHIGAN

**ROBBY AND
MICHAEL**

DRAWING

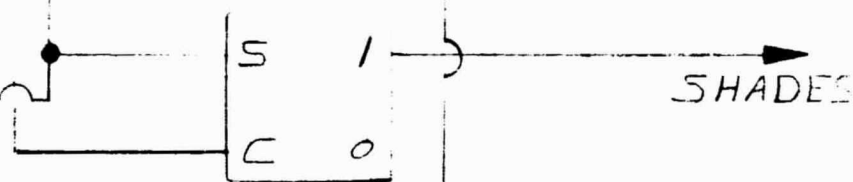
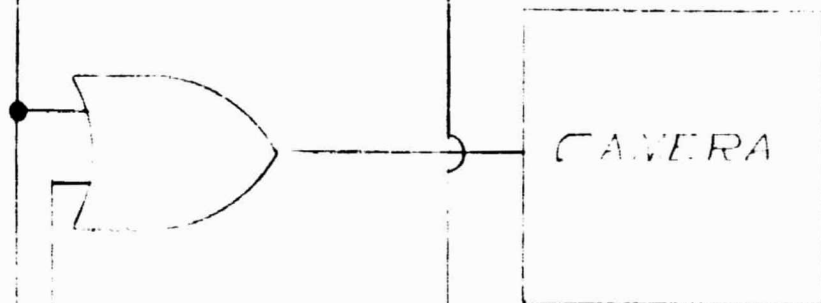
60025-1H

DELAY



FOLDOUT FRAME 2

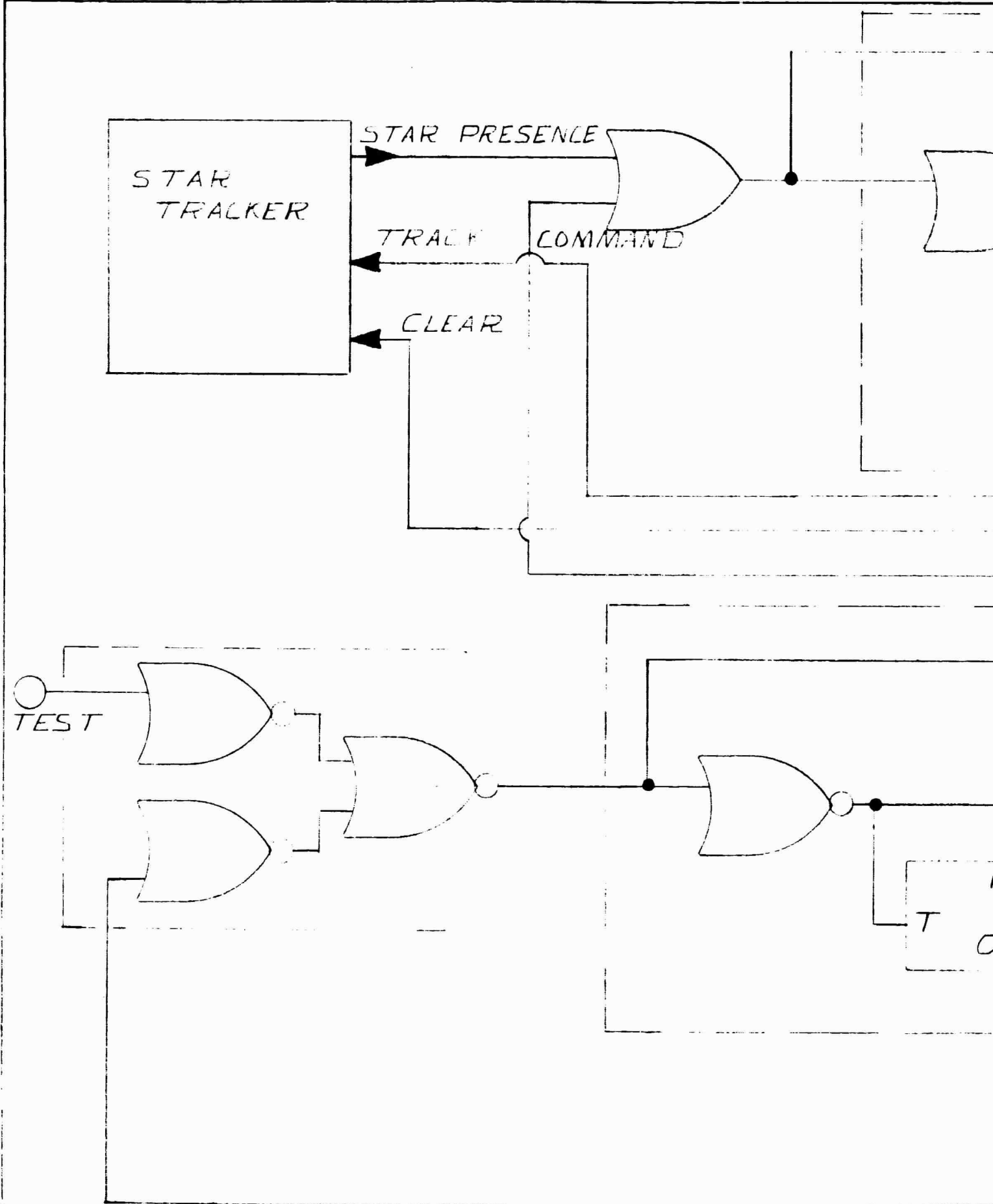
		SCALE	NONE
		PROJ. NO	06647
		DRAWN BY	J.C. POUSAN
		DATE	4-7-66
		FOR ASSEMBLY	
		DESIGNED BY	D.E. HADDOL
LET.	CHANGE	DATE	WEIGHT CAL. ACT.



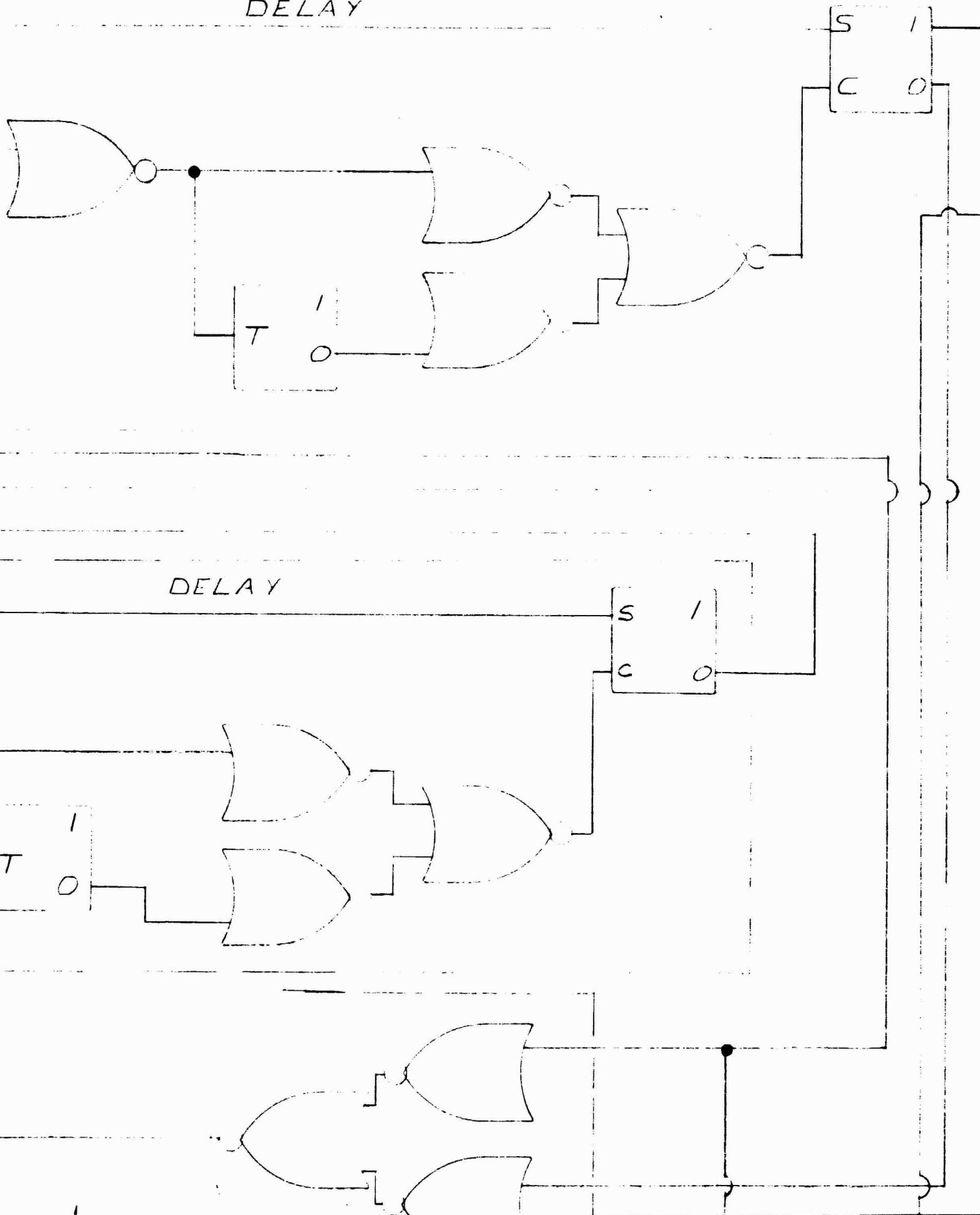
FOLDOUT FRAME 3

E	HIGH ALTITUDE ENGINEERING LABORATORY UNIVERSITY OF MICHIGAN DEPARTMENT OF AERO. AND ASTRO. ENGINEERING ANN ARBOR MICHIGAN
#7	
POUSAK	
-66	NAME ELECTRONIC GIMBAL CONTROL SYSTEM
ADDOLI	DRAWING NO. H3-52001

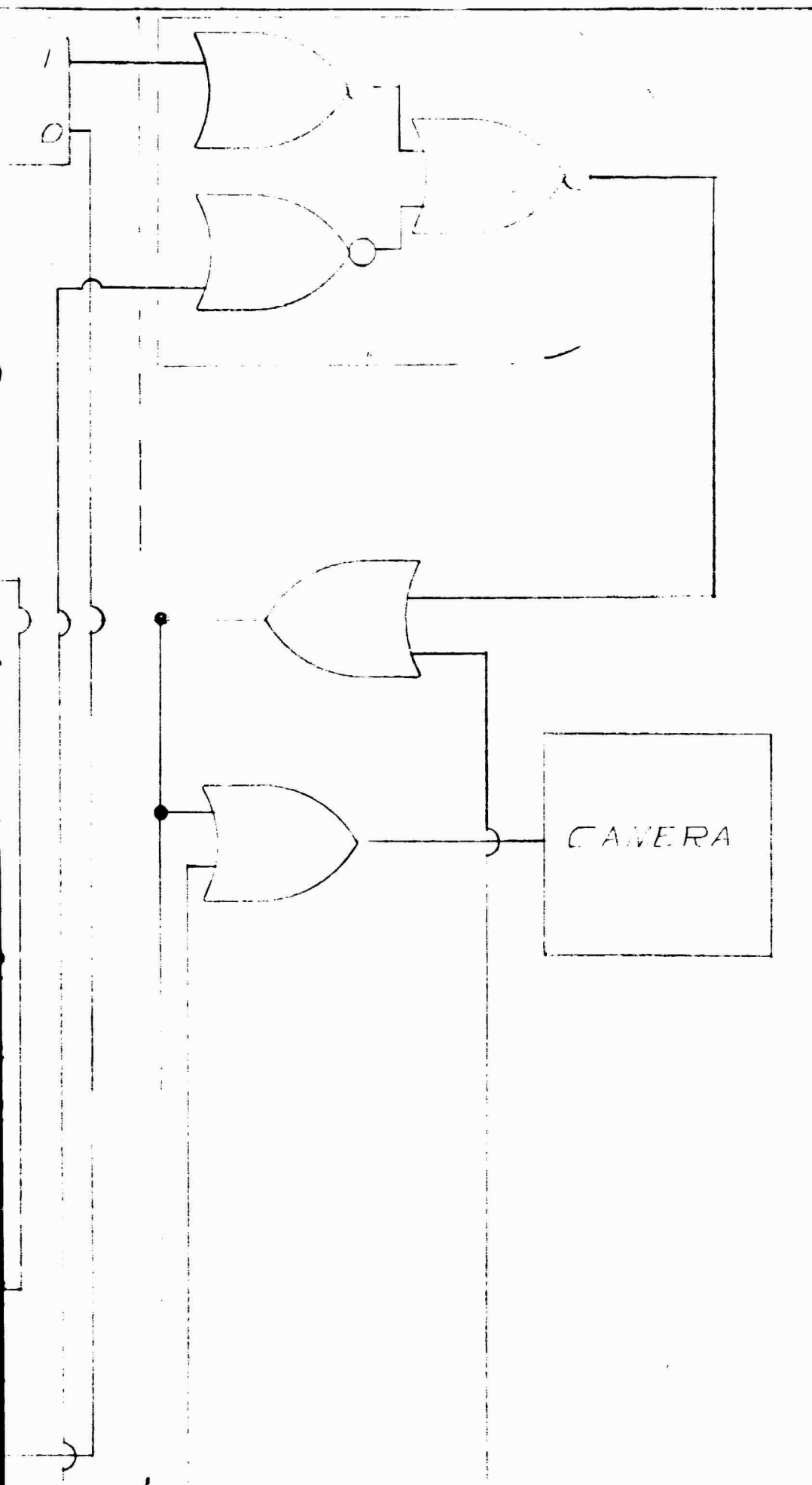
FOLDOUT FRAME 4

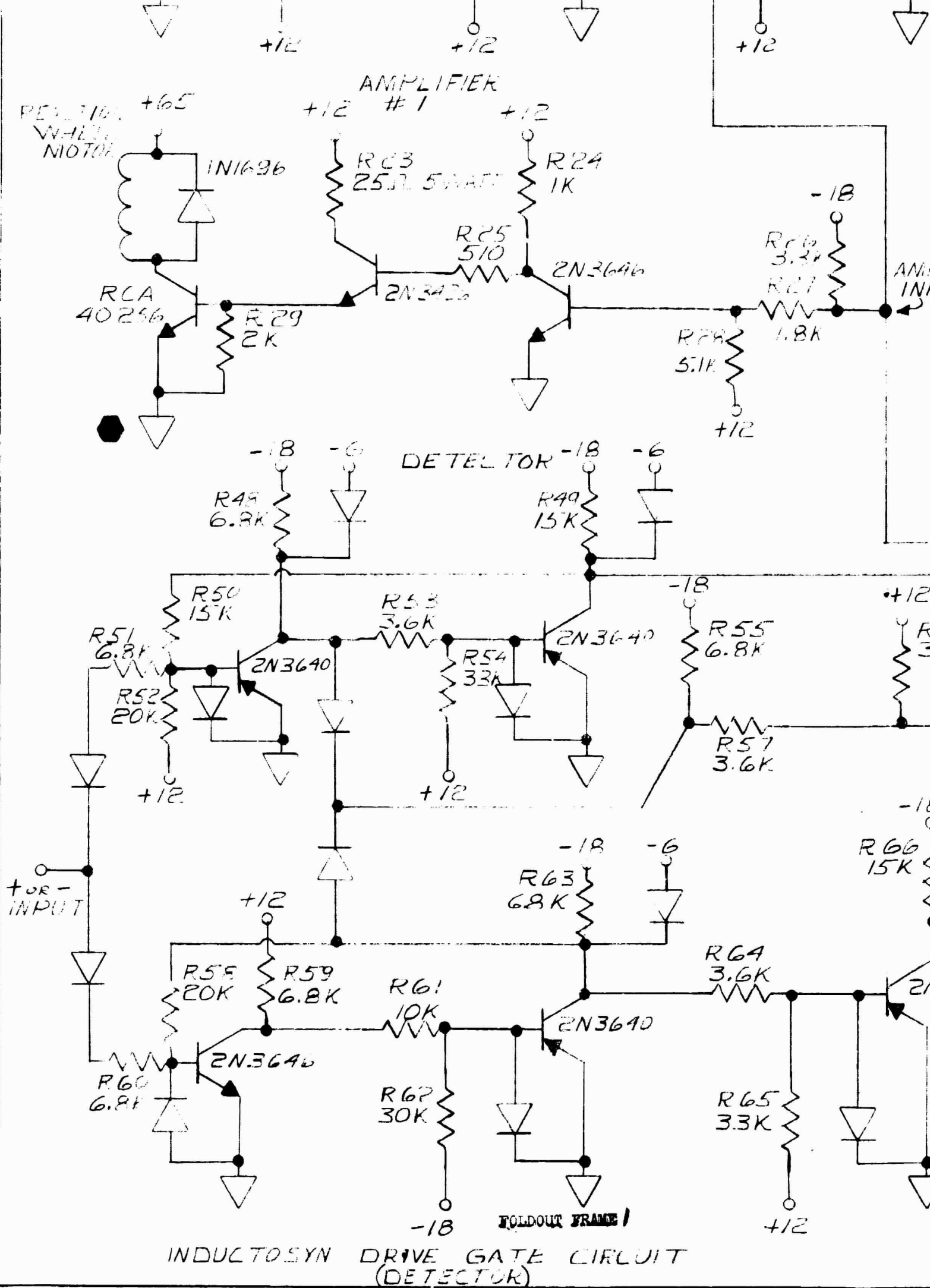


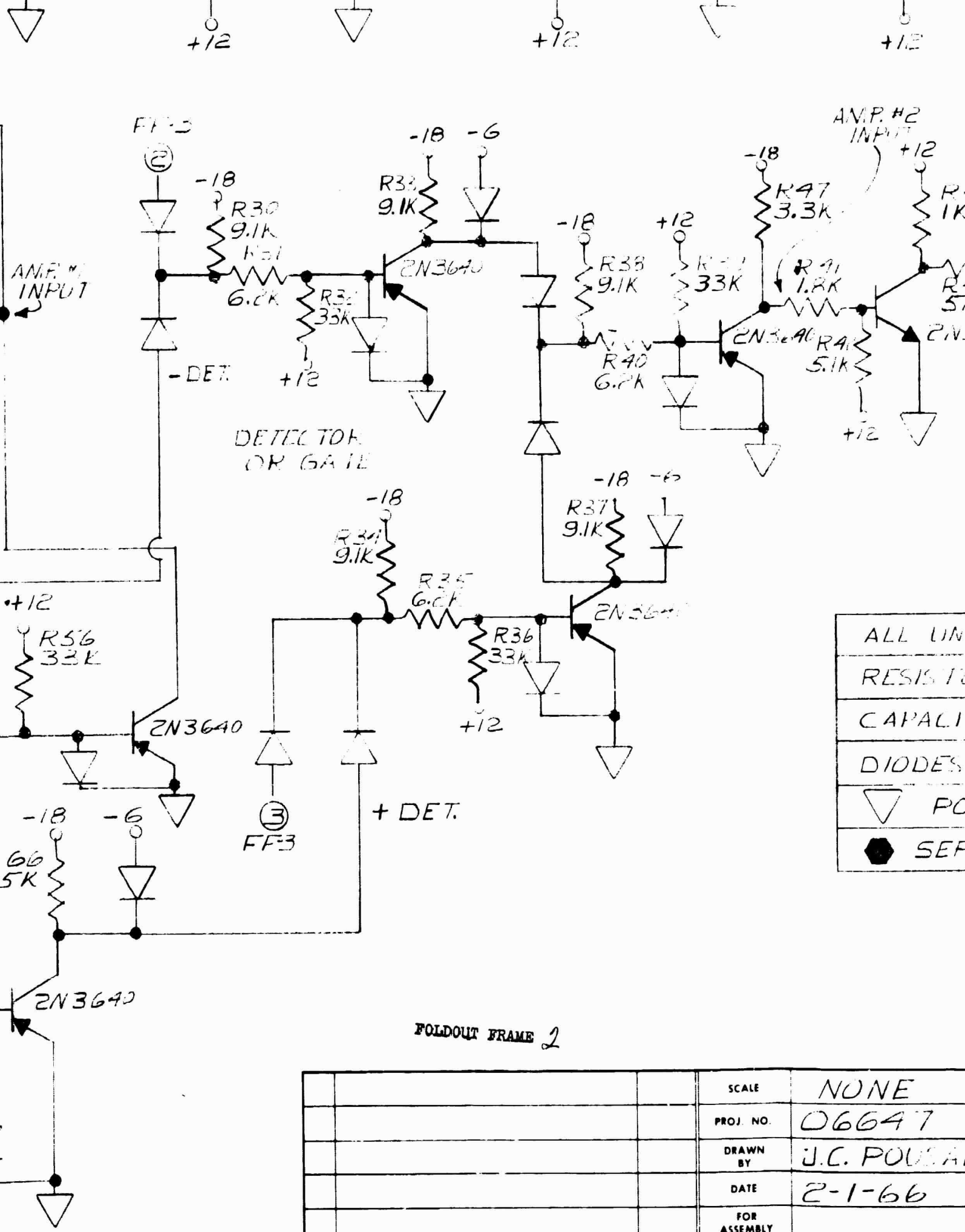
DELAY



FOLDOUT FRAME 6



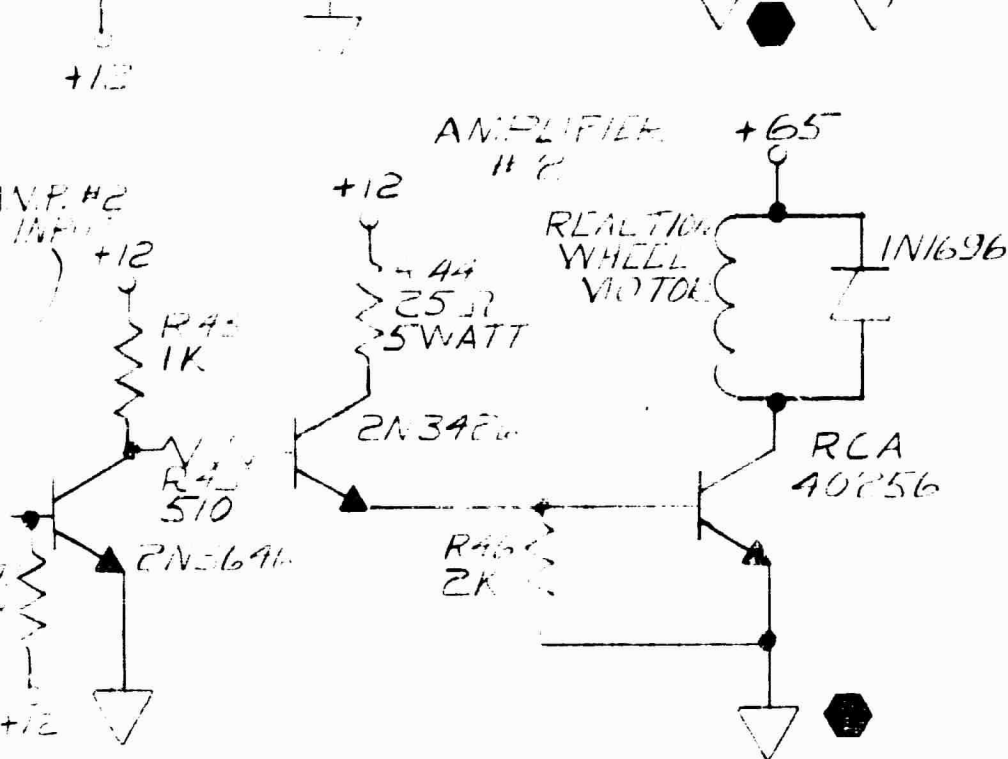




ALL UN
RESIST
CAPACI
DIODES
PC
SEP

FOLDOUT FRAME 2

			SCALE	NONE
			PROJ. NO.	06647
			DRAWN BY	J.C. POUSA
			DATE	2-1-66
			FOR ASSEMBLY	
			DESIGN BY	D. HADDOLPH
LET.	CHANGE	DATE	WEIGHT	CAL. ACT.



ALL UNLESS OTHERWISE SPECIFIED

RESISTORS $\frac{1}{2}$ WATT 5%

CAPACITORS 50VDC, $\pm 10\%$, IN MFD.

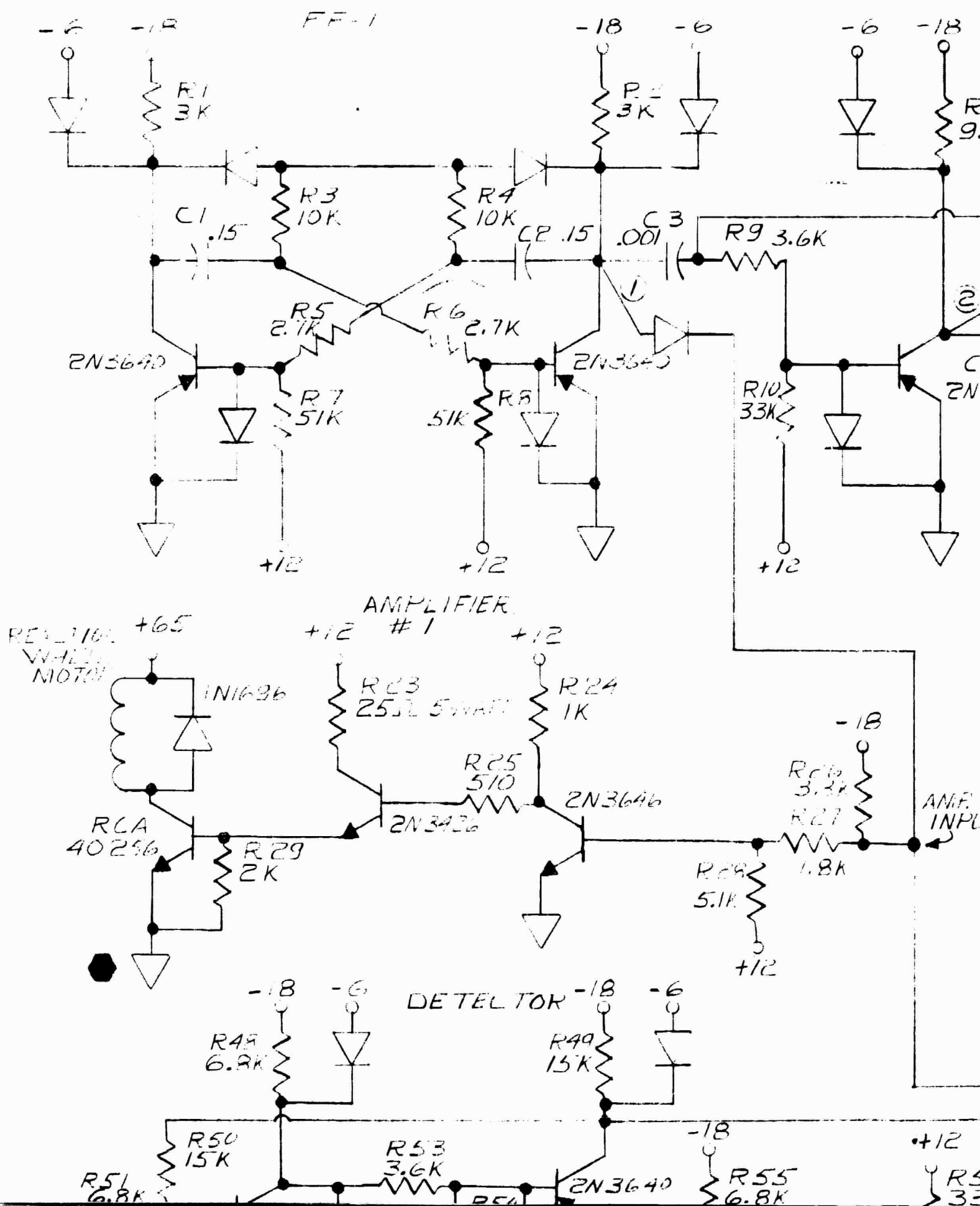
DIODES G.E. IN4154

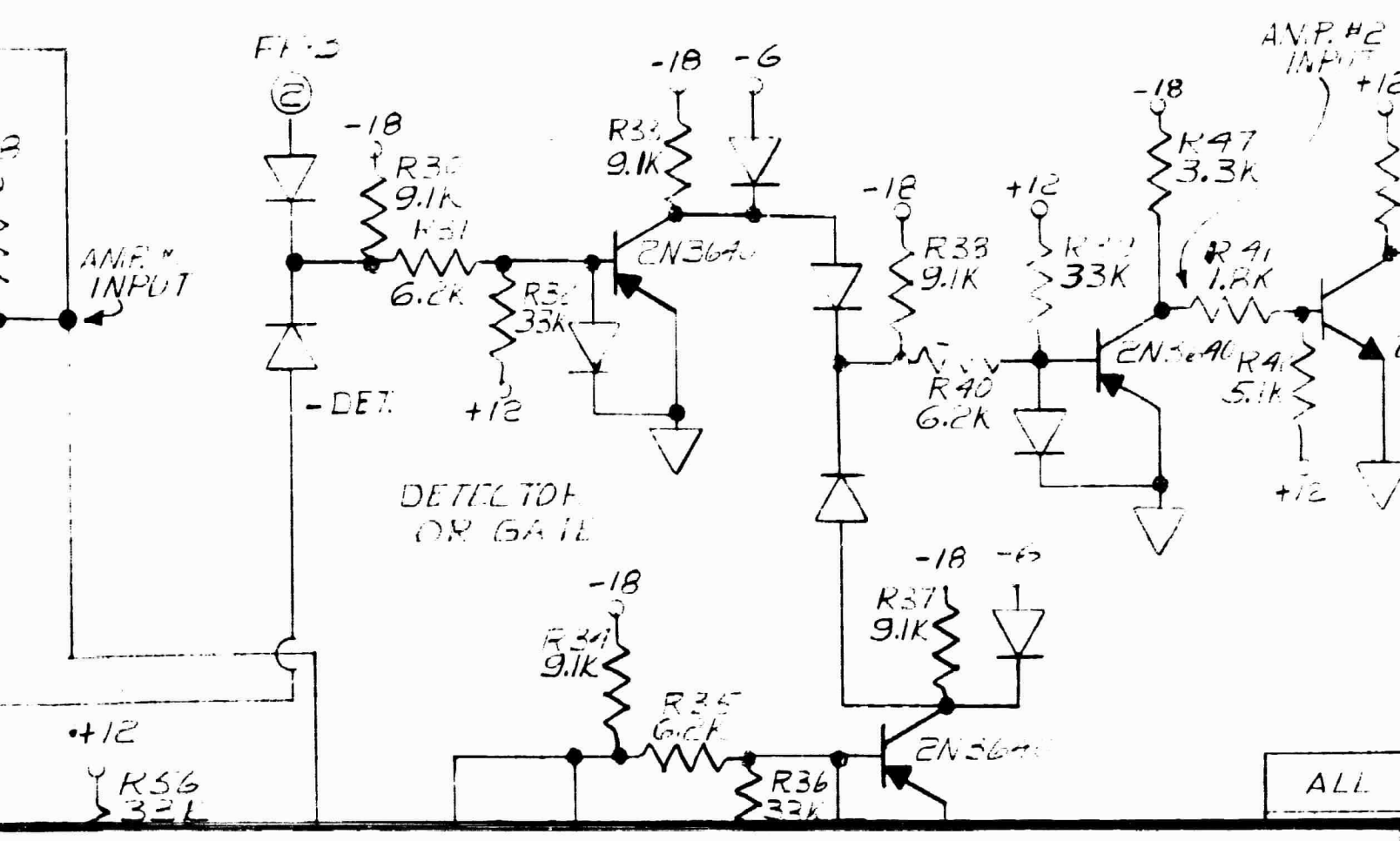
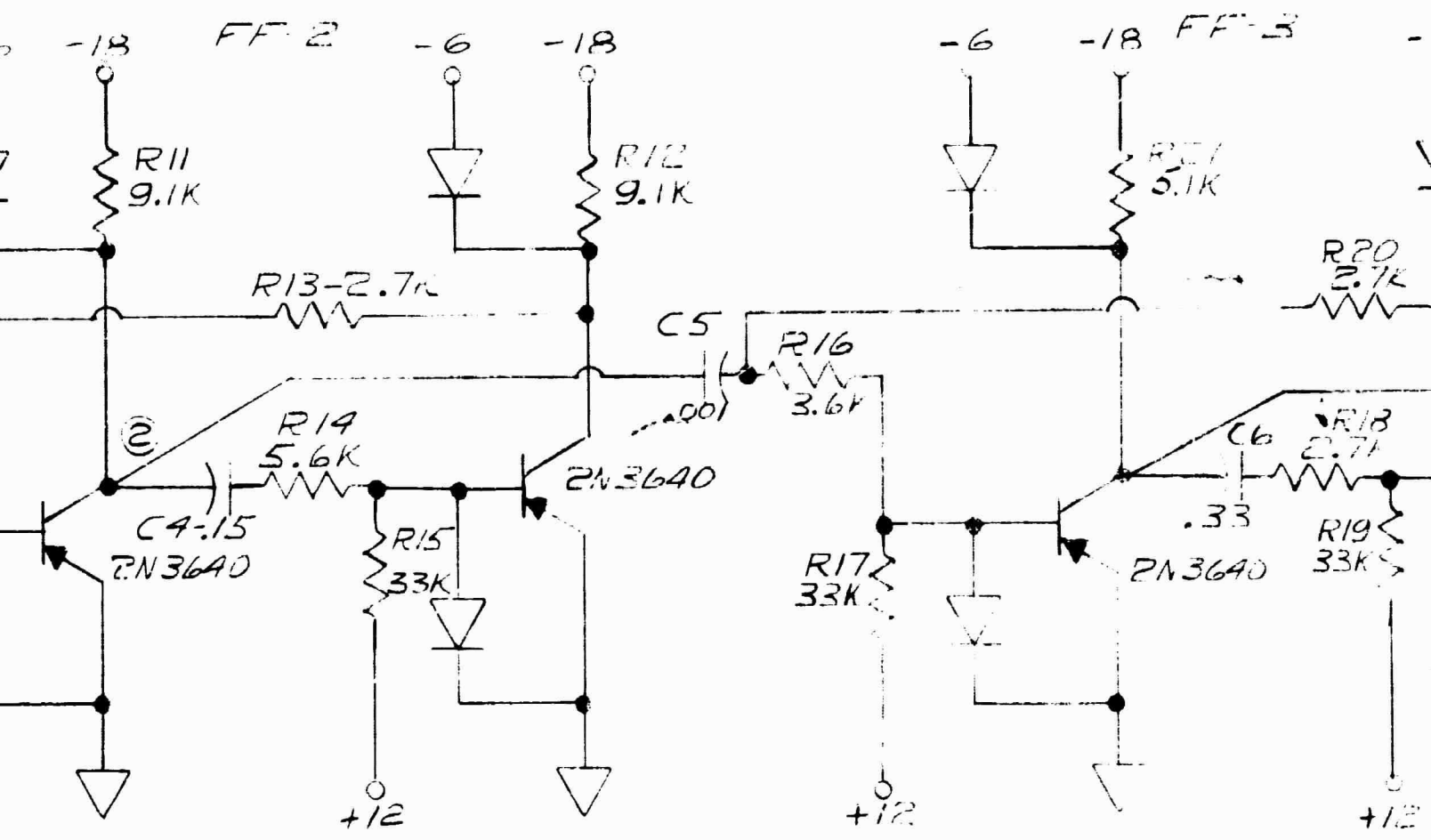
▽ POWER GROUND

⬡ SEPERATE POWER GROUND

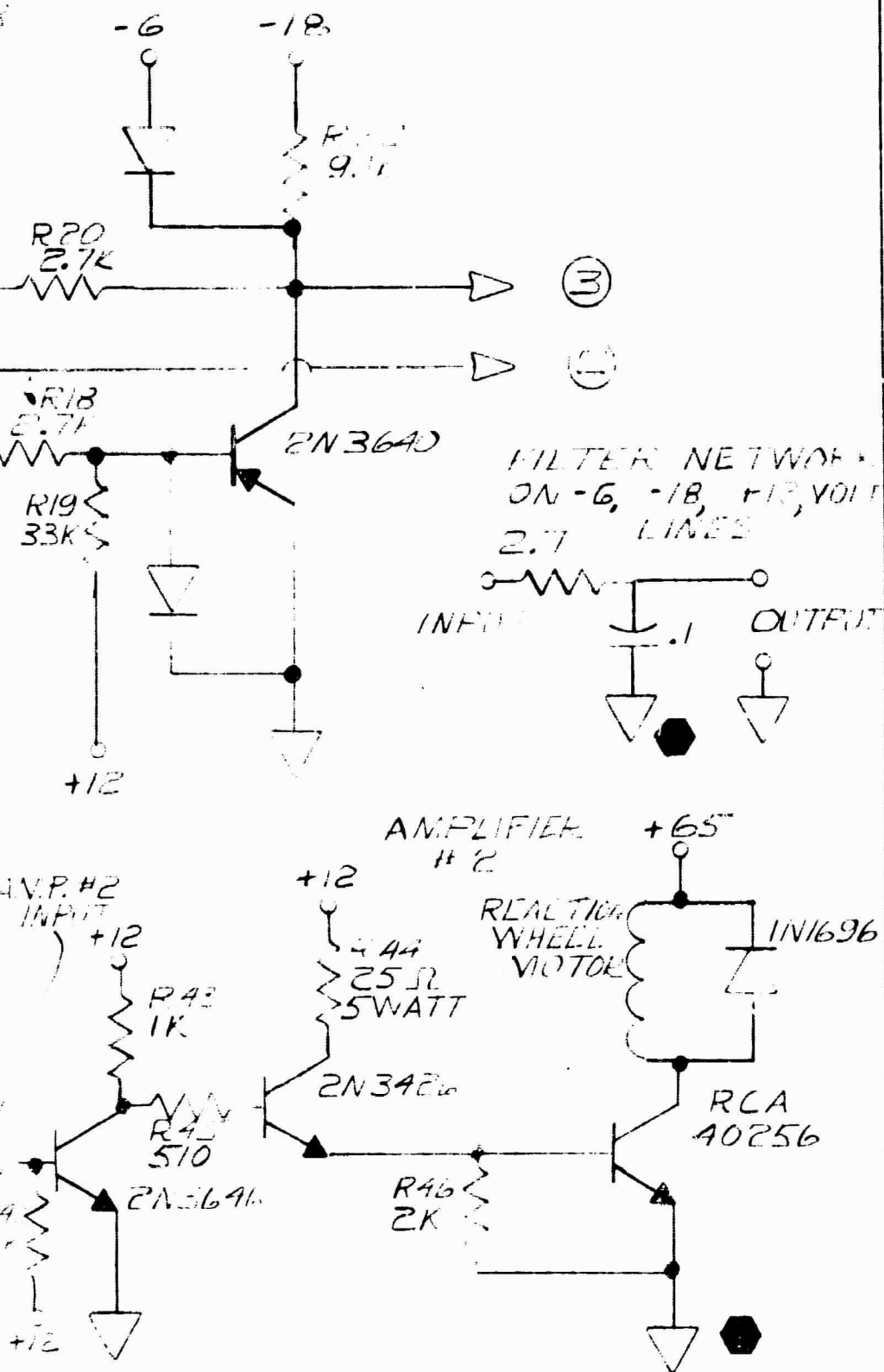
FOLDOUT FRAME 3

ONE	HIGH ALTITUDE ENGINEERING LABORATORY UNIVERSITY OF MICHIGAN DEPARTMENT OF AERO. AND ASTRO. ENGINEERING ANN ARBOR MICHIGAN
6647	
POLAR	
1-66	NAME REACTION WHEEL DRIVE CIRCUIT
HADDOLK	DRAWING NO. H3-52002





FOLDOUT FRAME 6



ALL UNLESS OTHERWISE SPECIFIED

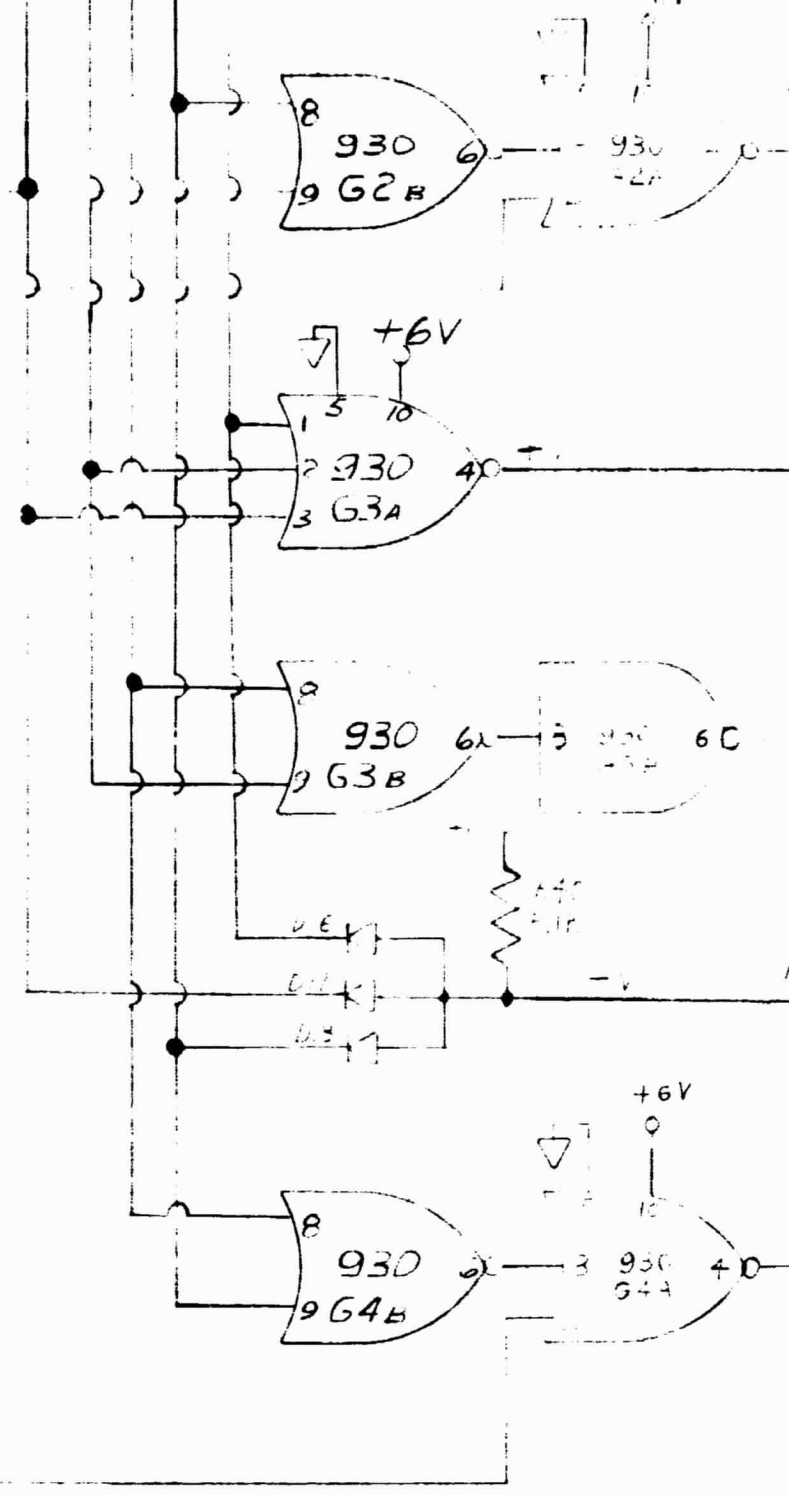
$\bar{B} \rightarrow$ 02

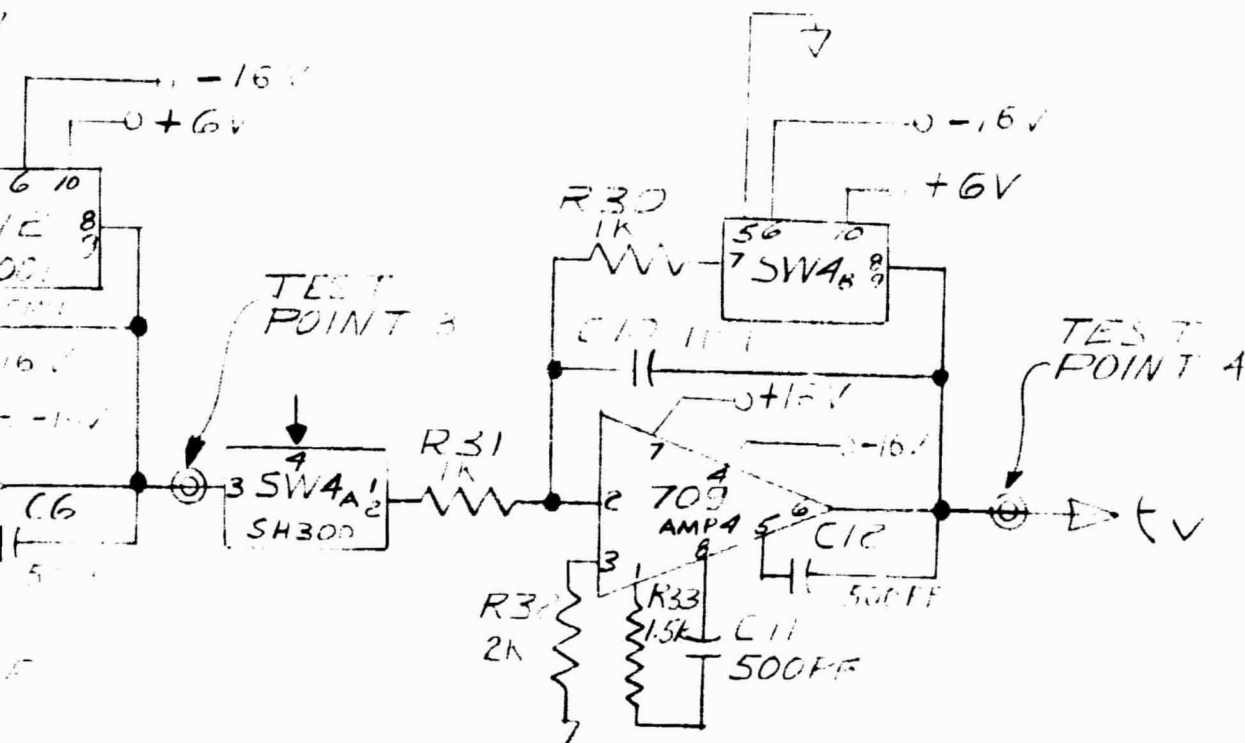
$\overline{SW} \rightarrow$

- | P3 | | |
|----|---|--------------|
| 1 | A | ϵ_H |
| 2 | B | KEY |
| 3 | C | STAR SIGNAL |
| 4 | D | B |
| 5 | E | \bar{C} |
| 6 | F | \bar{B} |
| 7 | H | C |
| 8 | J | -4V |
| 9 | K | -10V |
| 10 | L | -14V |
| 11 | M | GND |
| 12 | N | +14V |
| 13 | P | +12V |
| 14 | R | +10V |
| 15 | S | +6V |
| 16 | T | |
| 17 | U | |
| 18 | V | |
| 19 | W | |
| 20 | X | SW |
| 21 | Y | |
| 22 | Z | ϵ_V |

2.2KΩ
C13

FOLDOUT FRAME





ALL RESISTORS 1/4 WATT 5%

ALL DIODES IN486F

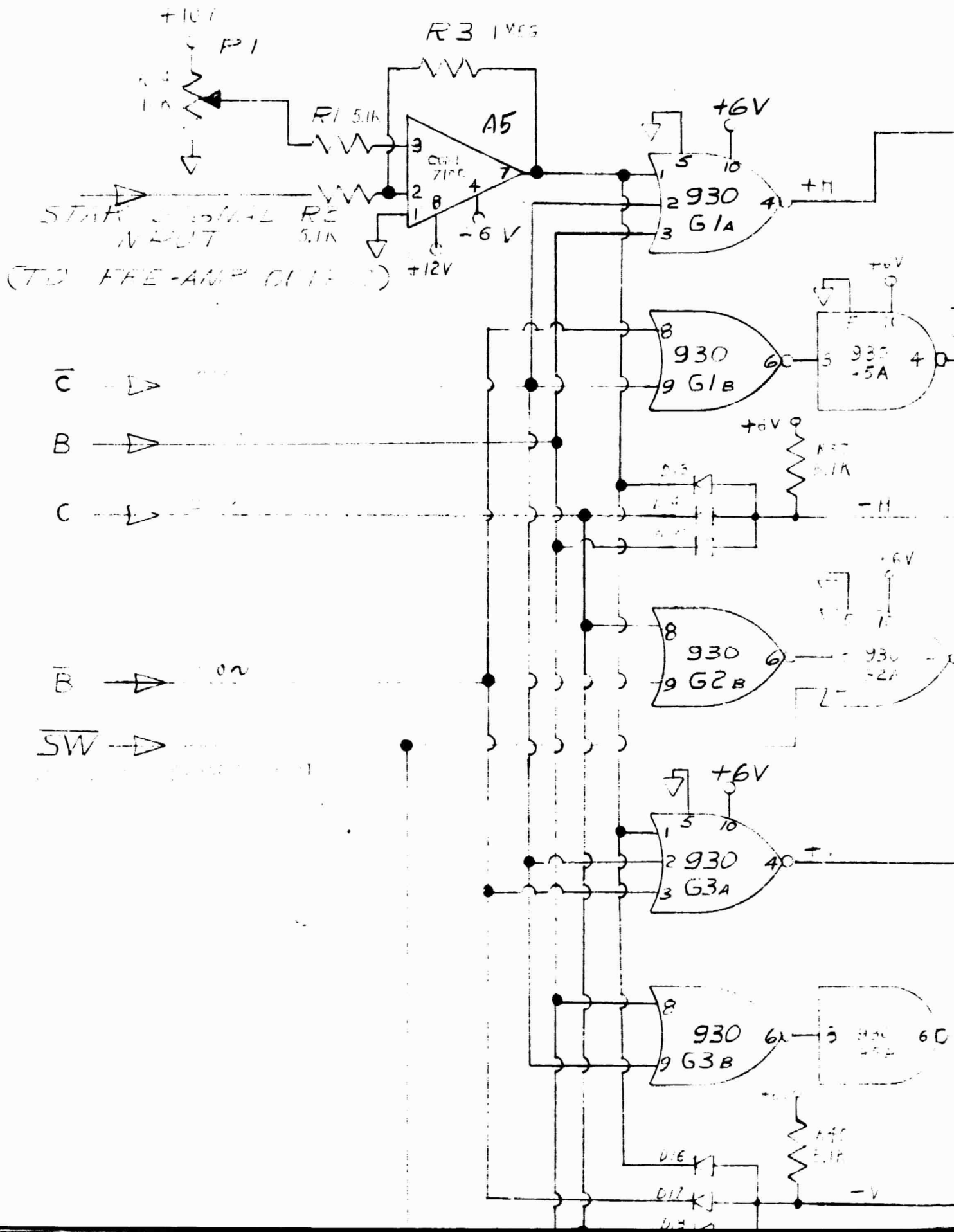
→ GROUND SYMBOL

SUPPLY VOLTAGES BROUGHT OUT
TO TEST POINTS

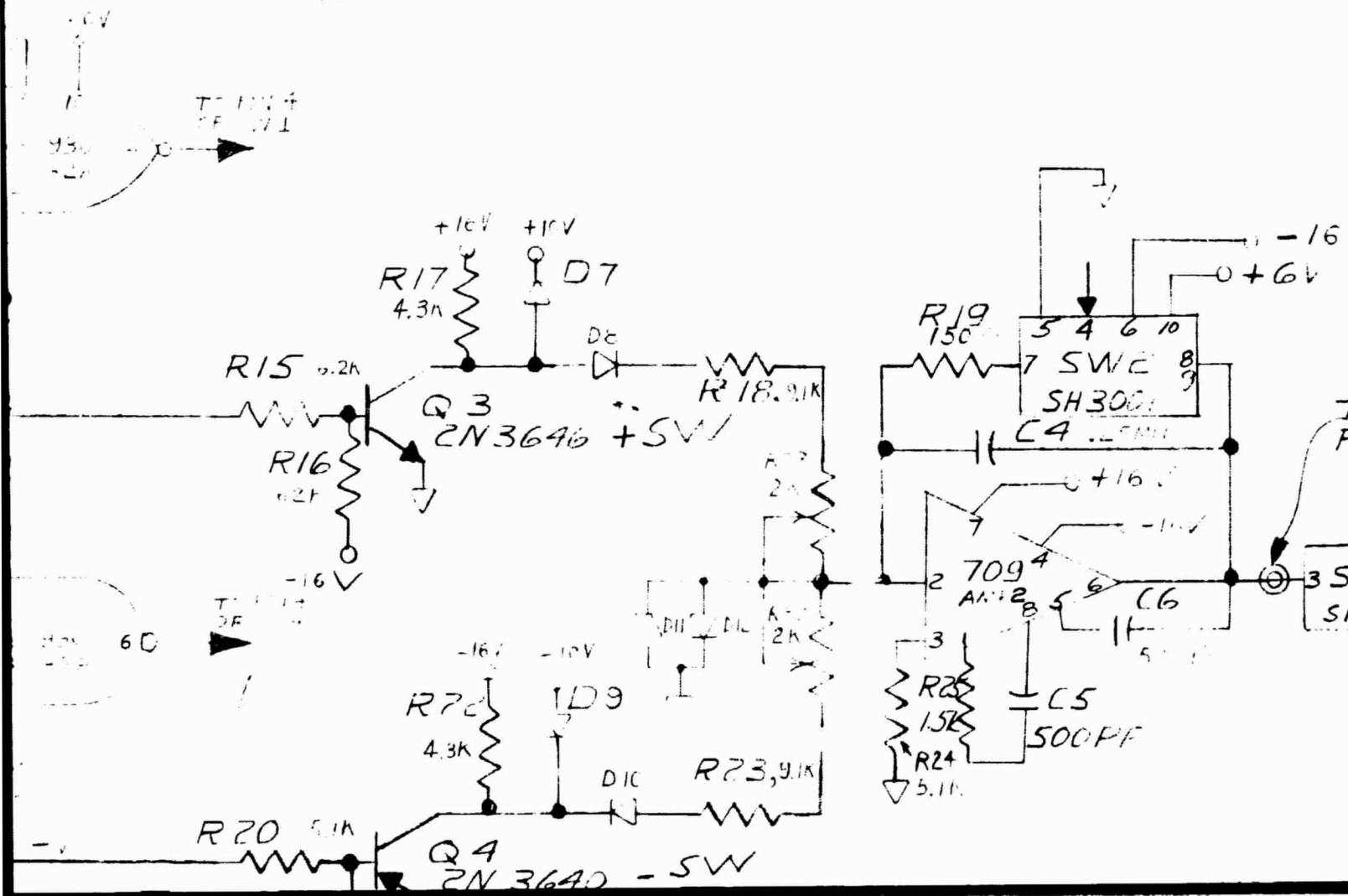
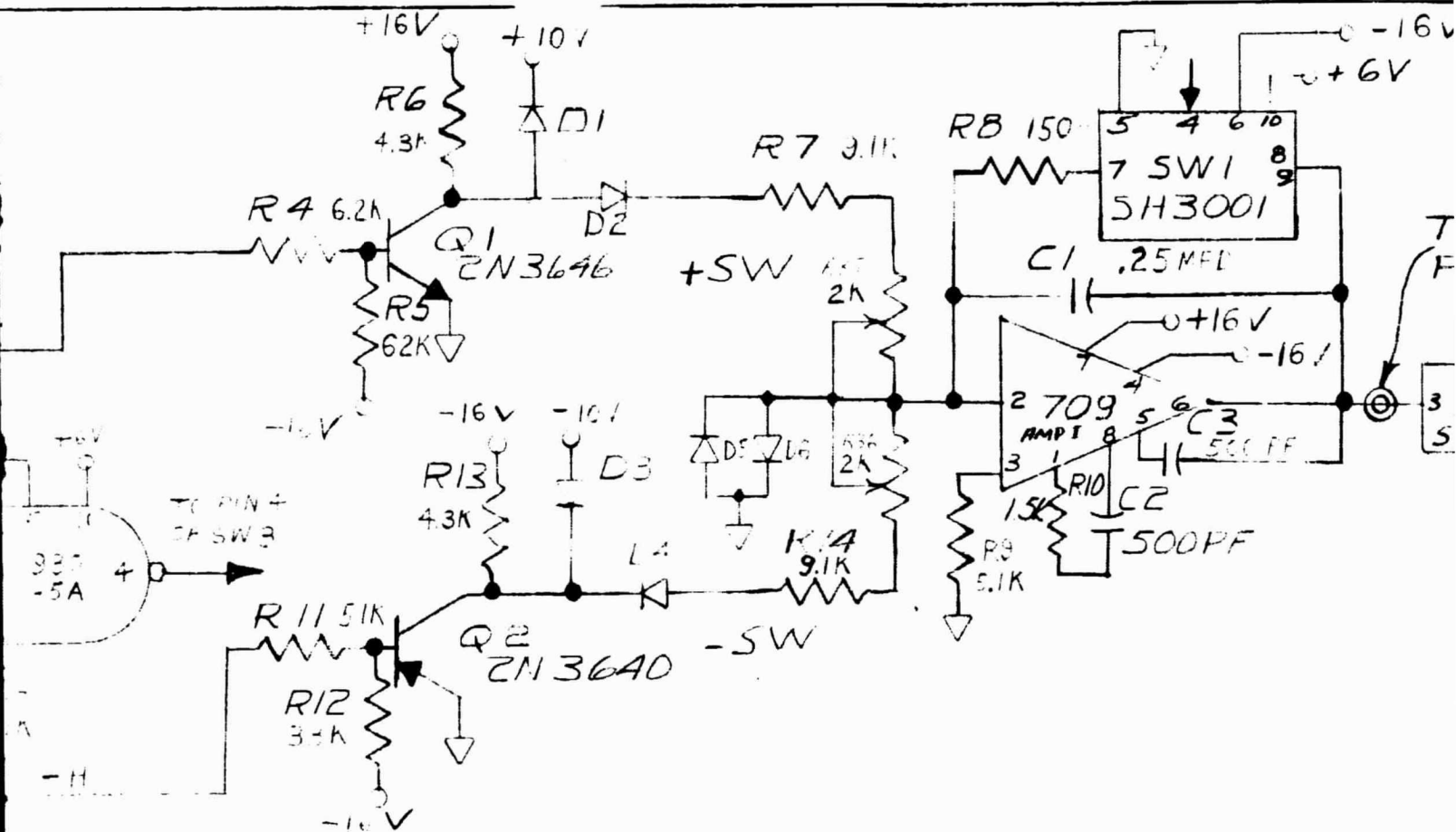
FOLDOUT FRAME 3

SCALE	NONE	HIGH ALTITUDE ENGINEERING LABORATORY UNIVERSITY OF MICHIGAN DEPARTMENT OF AERO. AND ASTRO. ENGINEERING ANN ARBOR MICHIGAN
PROJ. NO.	06647	
DRAWN BY	J. POUSAK	
DATE	8-9-66	
FOR ASSEMBLY		NAME ATWILL DEMODULATOR
MATERIAL		DRAWING NO. H3-52003
WEIGHT CAL. ACT.		

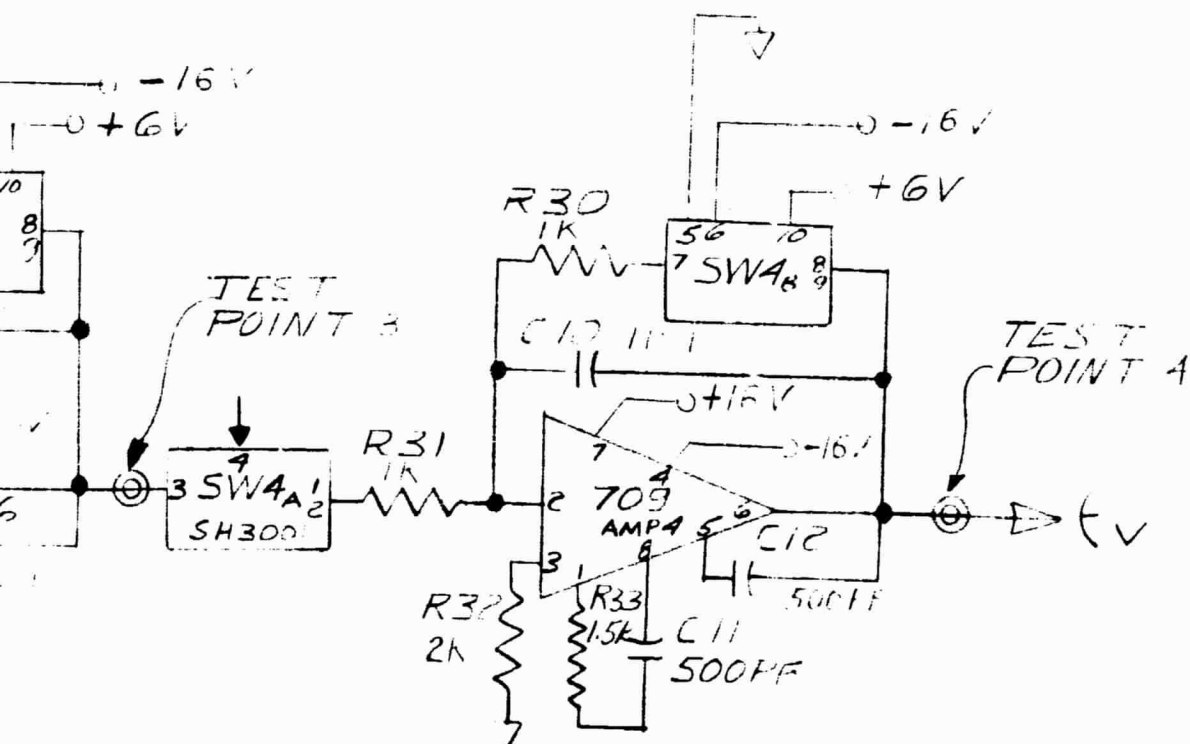
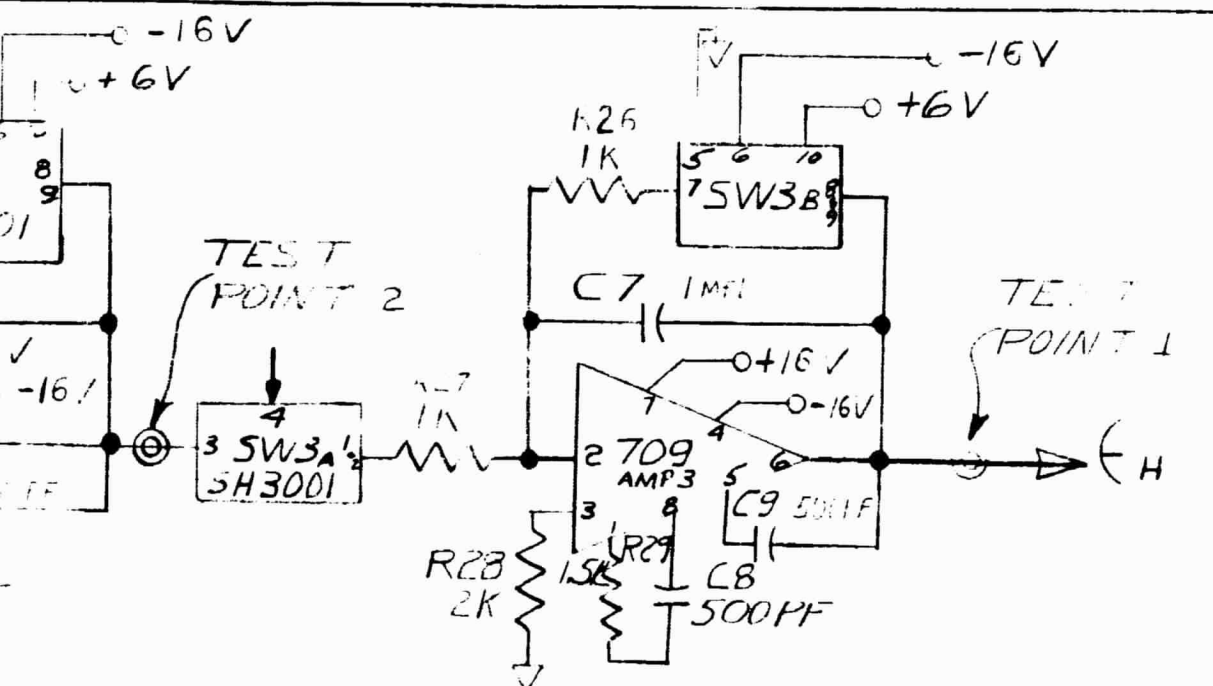
FOLDOUT FRAME 4

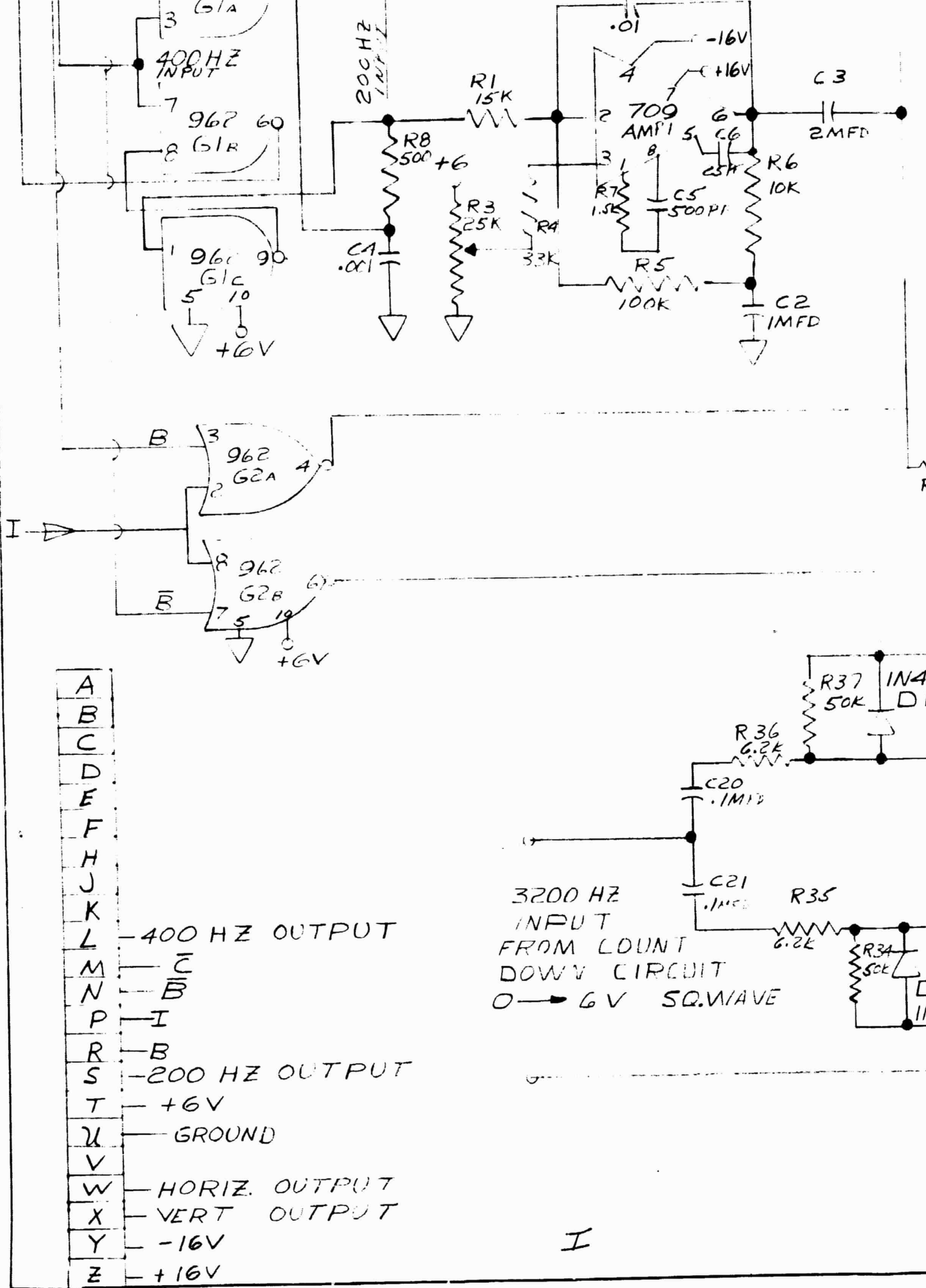


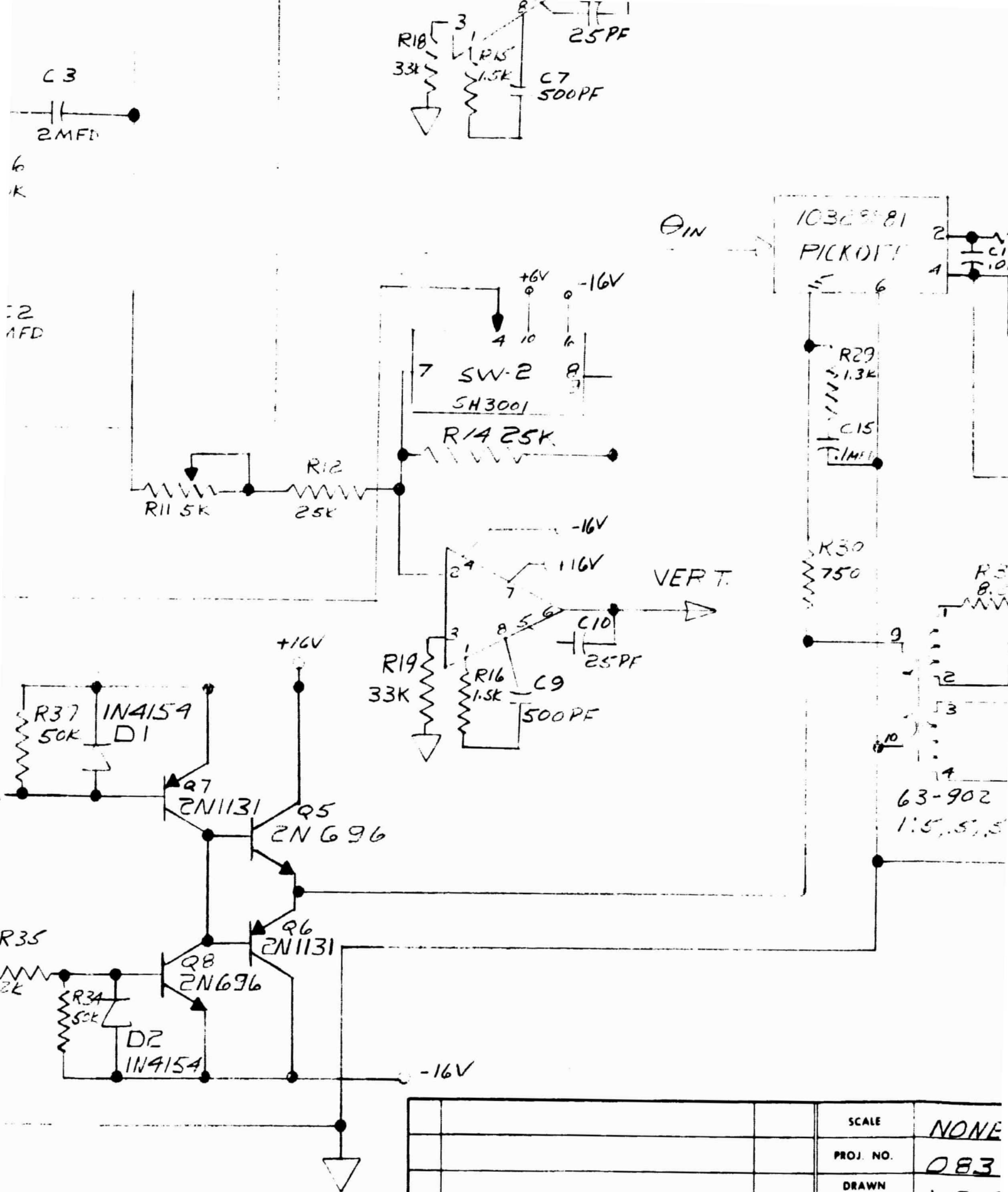
FOLDOUT FRAME 5



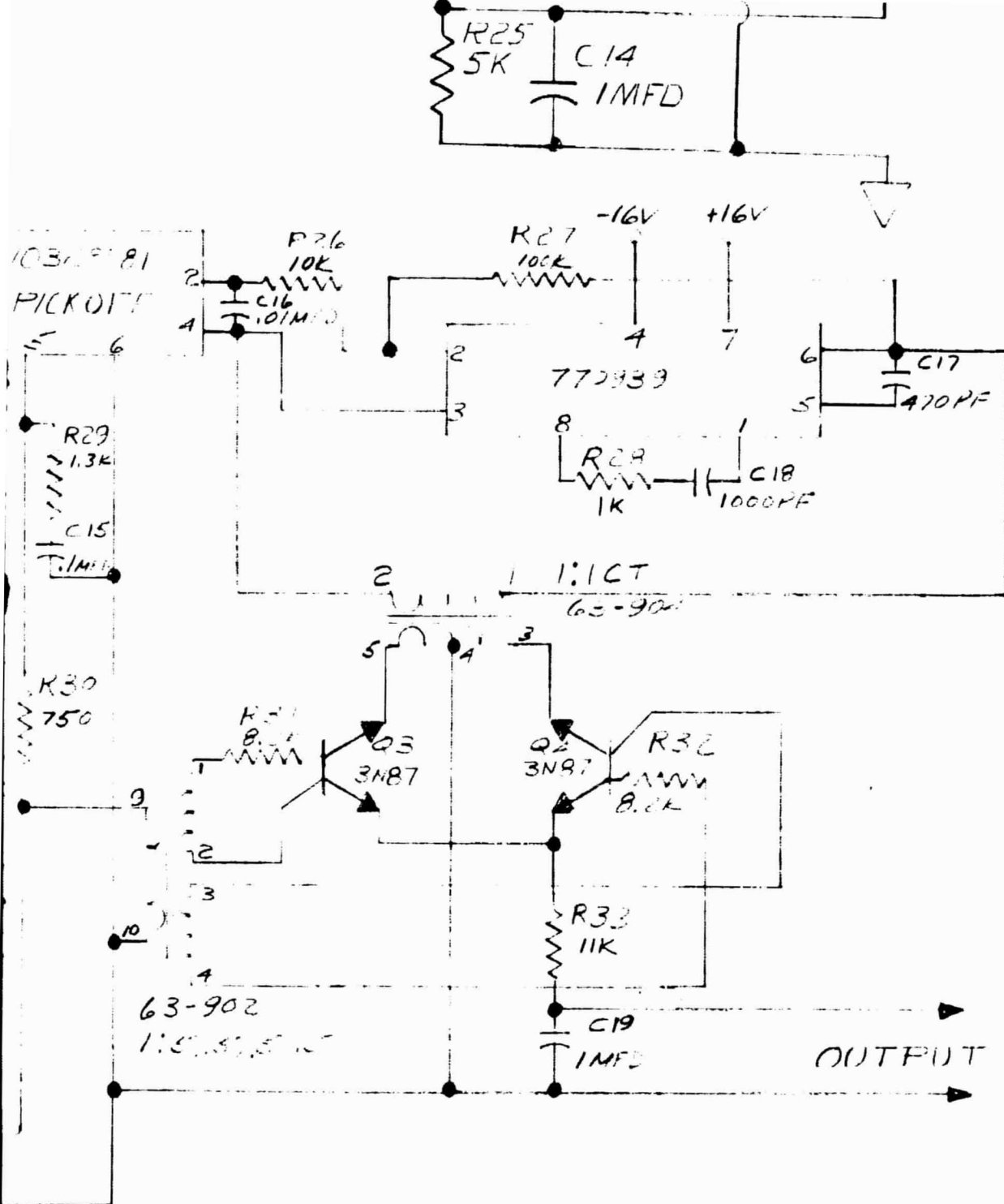
FOLDOUT FRAME 6







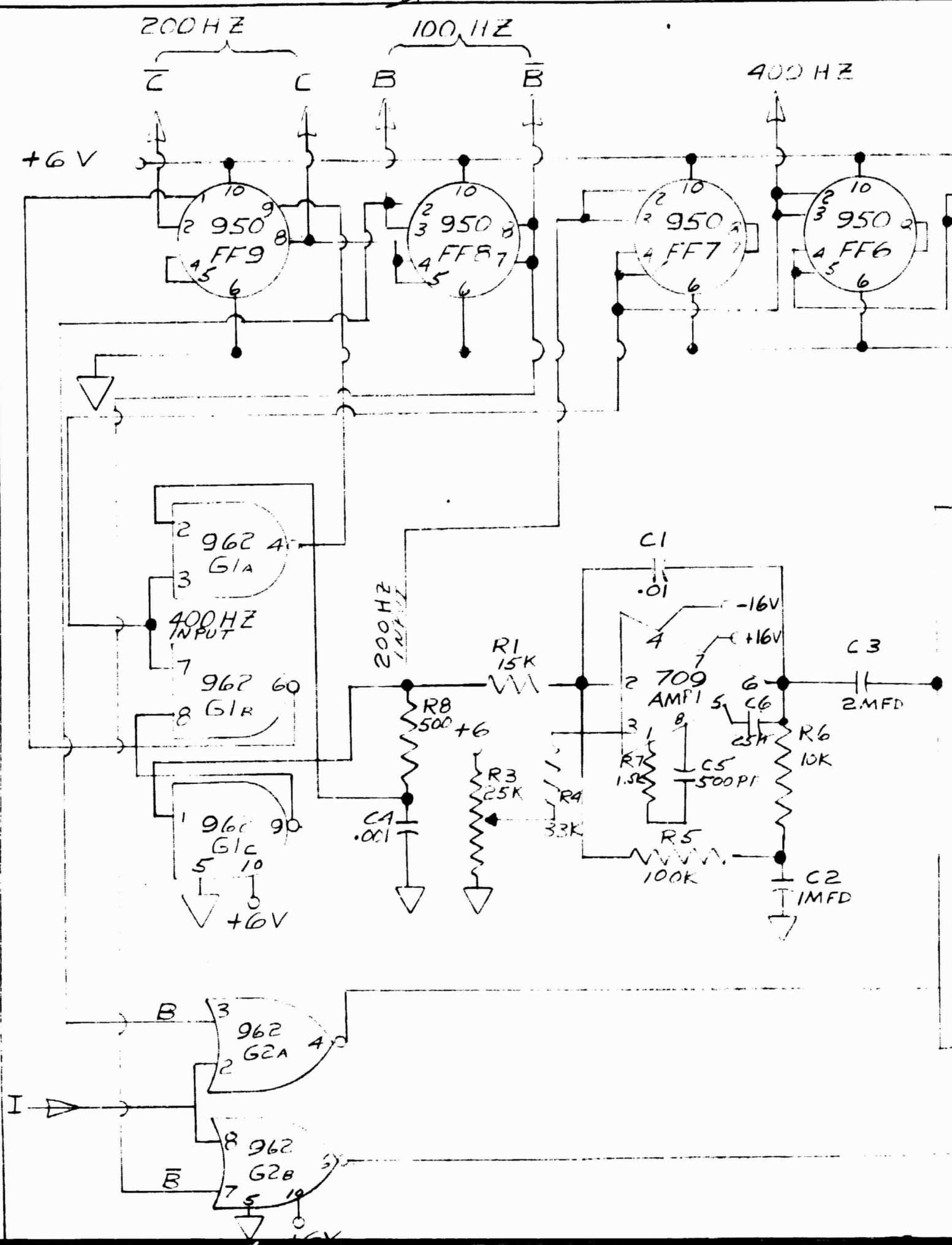
		SCALE	NONE
		PROJ. NO.	083
		DRAWN BY	J.C. F
		DATE	10-6
		FOR ASSEMBLY	
		MATERIAL	
LET.	CHANGE	DATE	WEIGHT CAL. ACT.



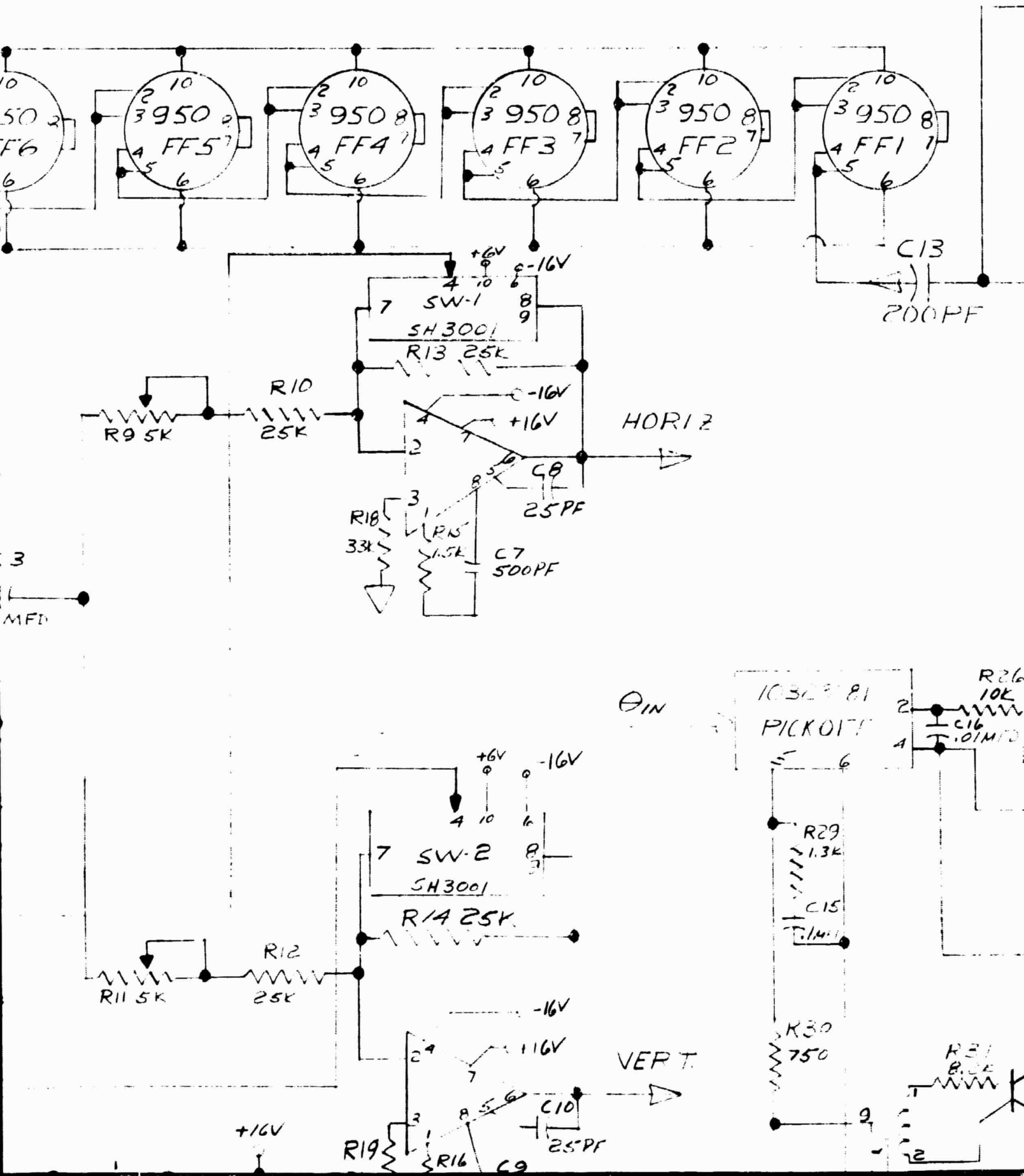
SCALE	NONE	HIGH ALTITUDE ENGINEERING LABORATORY UNIVERSITY OF MICHIGAN DEPARTMENT OF AERO. AND ASTRO. ENGINEERING ANN ARBOR MICHIGAN
PROJ. NO.	08370	
DRAWN BY	J.C. POUSAK	
DATE	10-6-66	
FOR ASSEMBLY		
MATERIAL		NAME ATWILL SCAN GENERATOR + TORQUE COMPENSATOR
TE	WEIGHT CAL ACT.	DRAWING NO. H3-52004

III

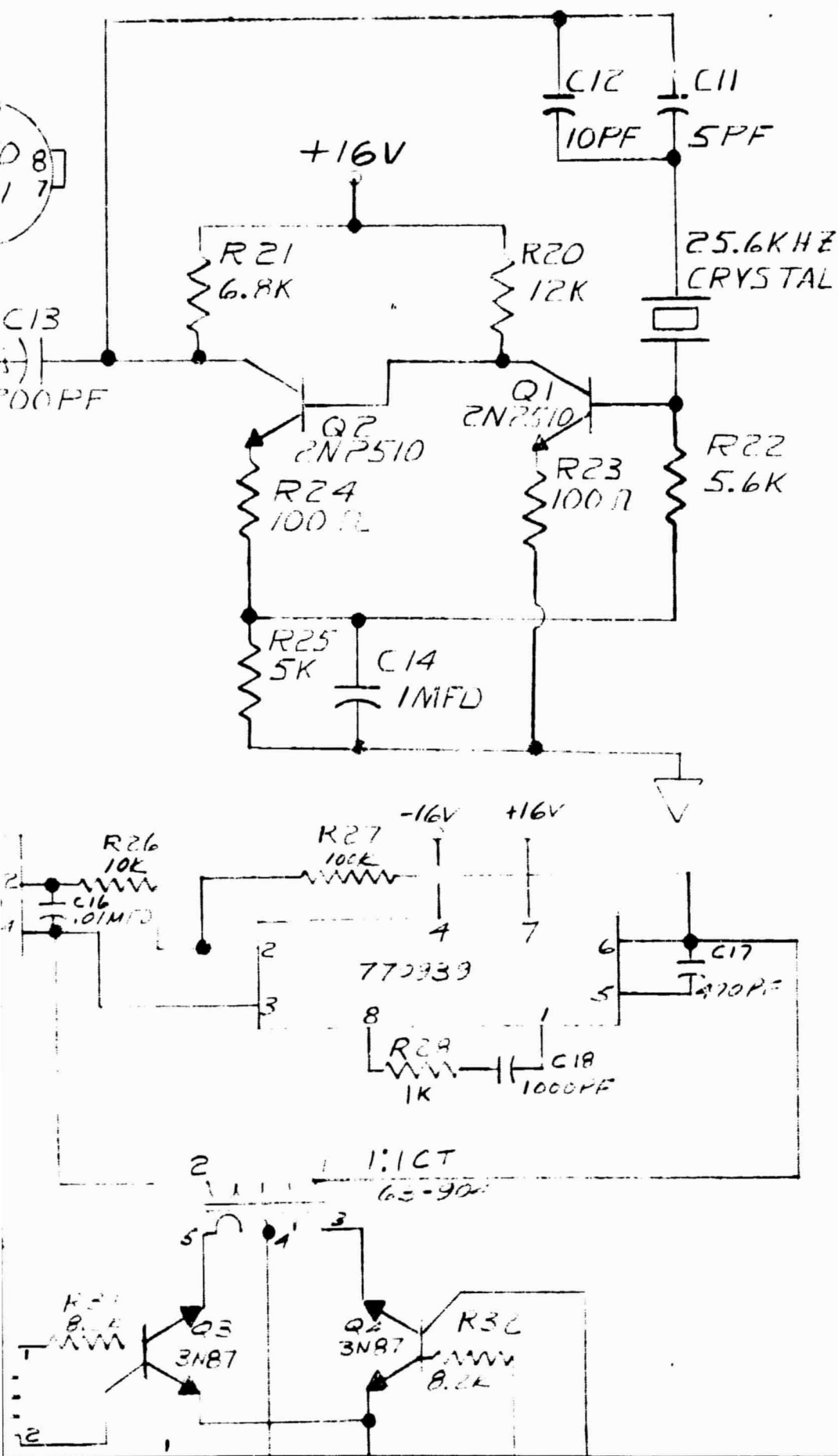
IV



IV



VI



1004
1004

1004
1004



NOTES

1004
1004

SECTION A-A

1004

1. BREAK EDGES.
2. FINISH V FLAT 4.000 ANGLE. COATING NOT TO EXCEED .0004.
3. DIM. 1.00 ± .001 (1.00 ± .001 INCHES).
4. HOLE V. DIM. 1.000 ± .001 INCHES.
5. DIM. 1.00 ± .001 INCHES (1.00 ± .001 INCHES).
6. 1/4 IN. 1.00 ± .001 INCHES (1.00 ± .001 INCHES).
7. 1.00 ± .001 INCHES (1.00 ± .001 INCHES).
8. SEE NOTE 4. ON H3-SECTION 6 (PAGE BEFORE DRILLING).

I

100

→ A

II

Handwritten notes at the top of the page, mostly illegible.

Handwritten notes in the upper middle section.



Small handwritten mark.

Handwritten 'A' with an arrow pointing to it.

Handwritten '1'.

<i>On - Hall</i>	HIGH ALTITUDE ENGINEERING LABORATORY UNIVERSITY OF MICHIGAN DEPARTMENT OF AERO. AND ASTRO. ENGINEERING ANN ARBOR MICHIGAN
<i>5114</i>	
<i>p 3</i>	
<i>1-3-60</i>	NAME <i>TUBE - DATA SCOPE</i>
<i>AZ-30</i>	DRAWING NO. <i>143-52006</i>

Handwritten 'III'.

Handwritten '1'.

IV

1.3
1.3

1.6
1.6

1.6

1.6
CHART 1.6

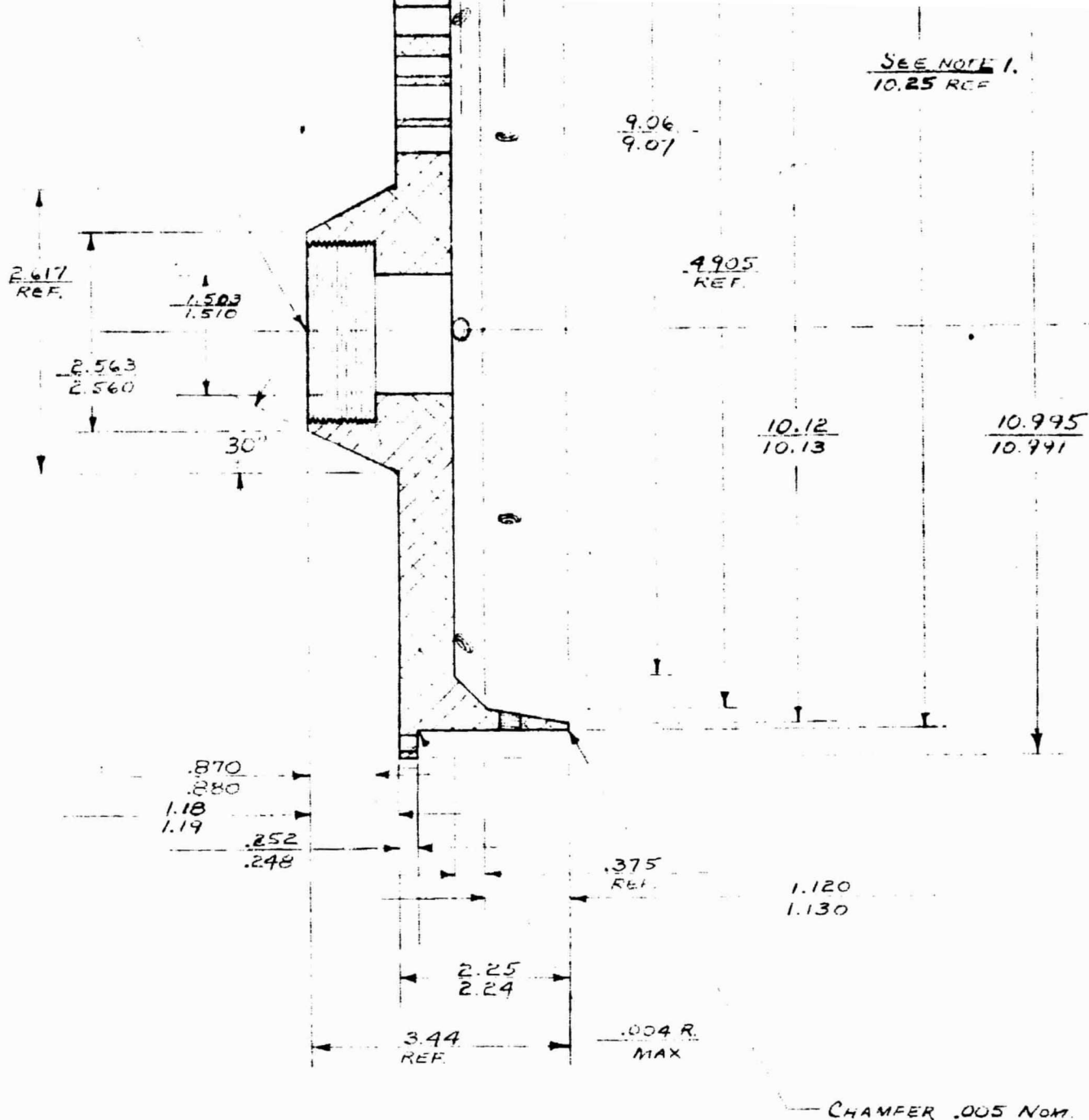
12.0

12.0

1.6
1.6

1.6
1.6

1.6
1.6



SECTION A-A

NOTES:

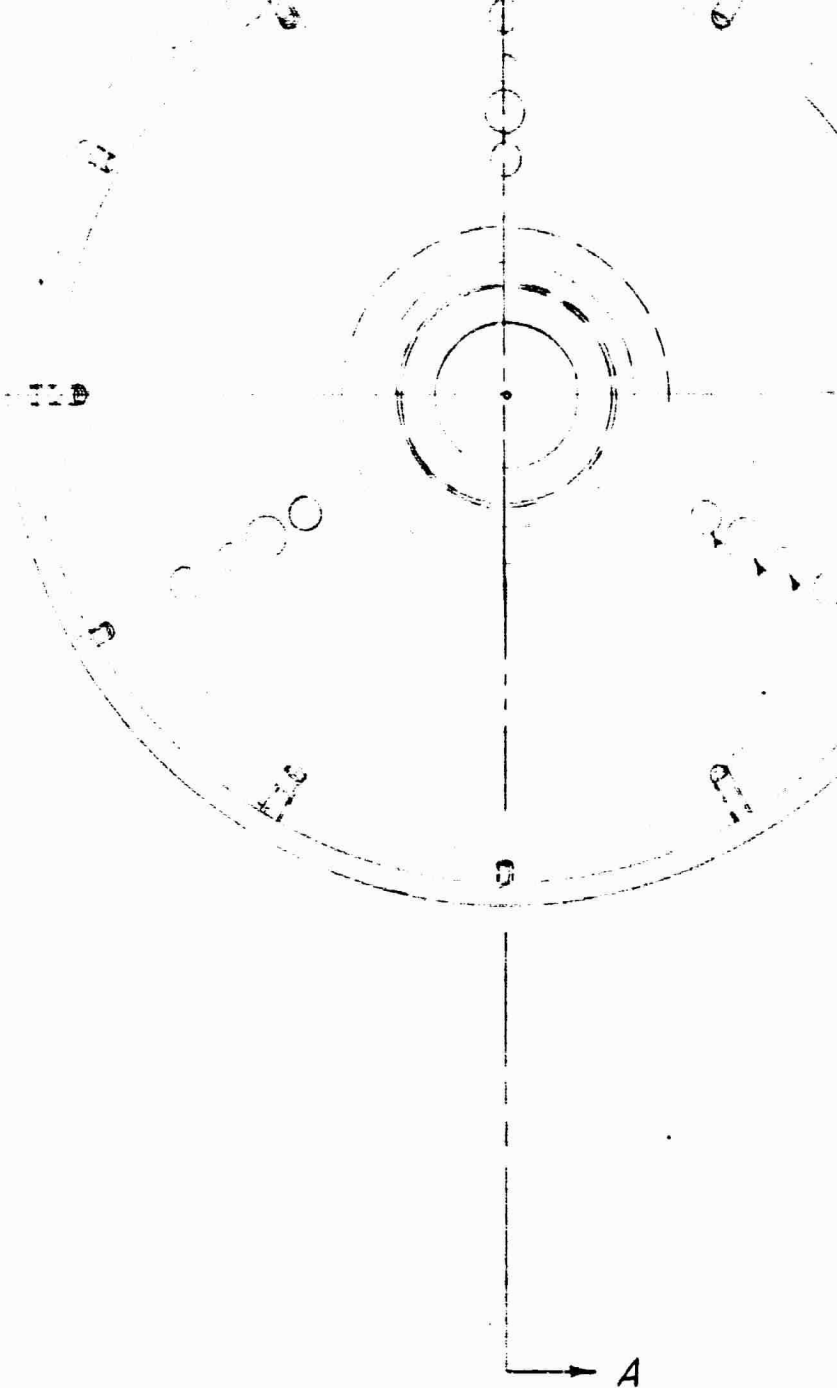
1. DIM. TO BE .001 LESS THAN MATING PART. (H3-52005)
MATING PART DIM. 10.246-10.254.
2. BREAK EDGES.
3. FINISH IN FLAT BLACK ANODIZE. COATING NOT TO EXCEED .0004.
4. ASSEMBLE TO H3-52005 (TUBE) FOR DRILLING ON 10.625 DIA.
APPLY TAPPING HOLES IN H3-52005 ON 10.625 DIA. ASSEMBLE
WITH (6) 10-24 SCREWS FOR RADIAL HOLE LOCATION
& PILOT DRILLING. SCRATCH FIDUCIAL MARK.

I

0.995
0.941

NOM

004.
5 DIA.
HOLE



			SCALE	ONE - 1/2"
			PROJ. NO.	01114
			DRAWN BY	F ³
			DATE	3-13-60
			FOR ASSEMBLY	
			MATERIAL	AZ-31
			DATE	3-25-68
			WEIGHT	
			CAL. ACT.	
LET.	CHANGE	DATE	WEIGHT	

II

(A)

DRILL THRU 61 HOLES EQUALLY
SPACED ON 10.625 \pm .003 B.C.
#10 DRILL (.194)

(5) HOLES $\frac{2}{64}$ D. THRU 8.040 \pm .003 B.C.

(3) HOLES $\frac{1}{64}$ D. THRU 6.875 \pm .005 B.C.

(3) HOLES "X" D. THRU 6.000 \pm .005 B.C.

(3) HOLES $\frac{5}{16}$ D. THRU 4.125 \pm .003 B.C.

ALL EQUALLY SPACED

$\frac{17}{64}$ HOLES DIA. .265 - .271

FEATURES BACKS.

ONE-HALF

01114

F³

3-13-68

AZ-31

HIGH ALTITUDE ENGINEERING LABORATORY
UNIVERSITY OF MICHIGAN
DEPARTMENT OF AERO. AND ASTRO. ENGINEERING
ANN ARBOR MICHIGAN

NAME

BASE-DATA SCOPE

DRAWING
NO.

H3-52006

III

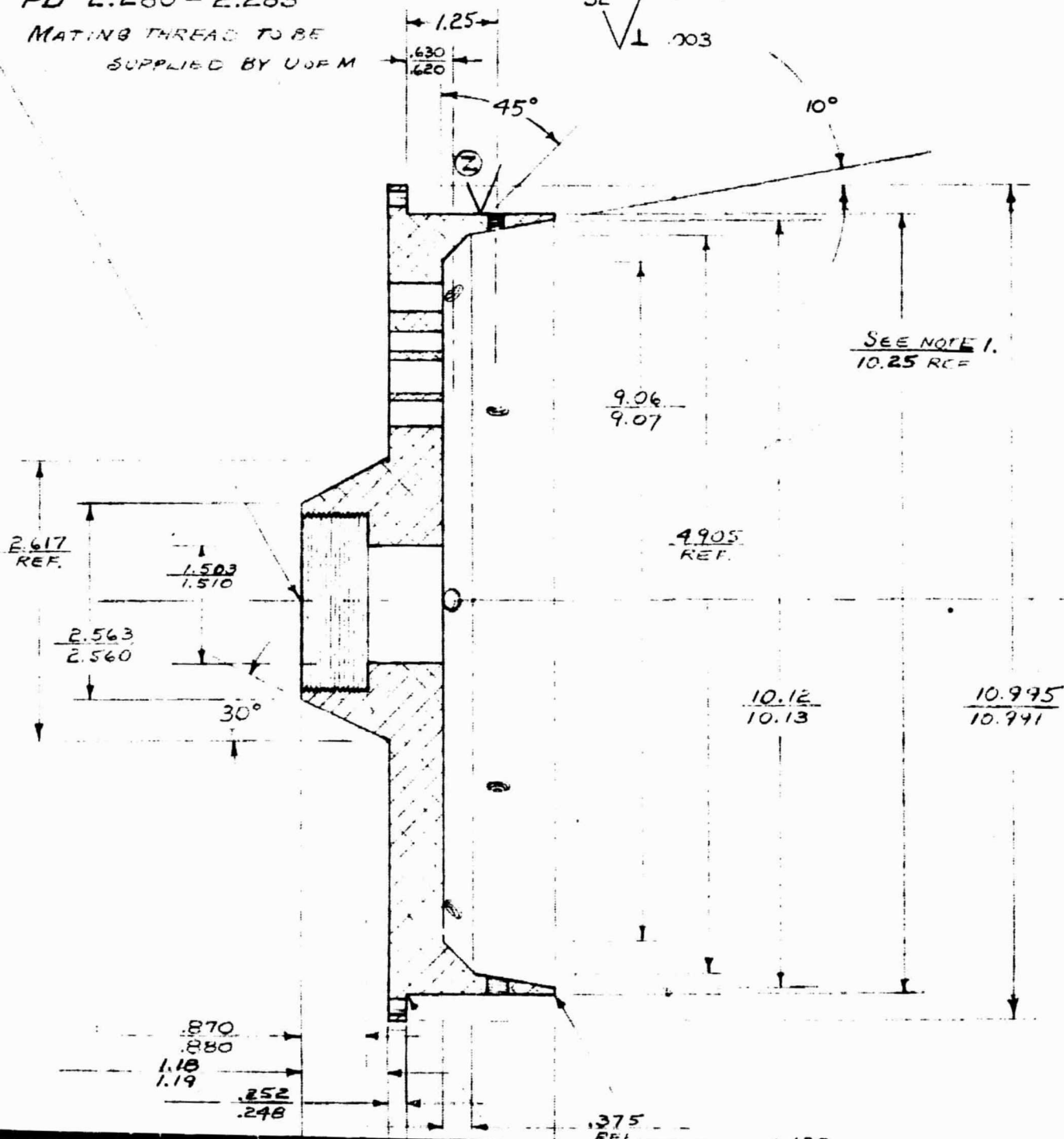
TV

2 5/16 - 20 UNS - 3B
PD 2.280 - 2.285

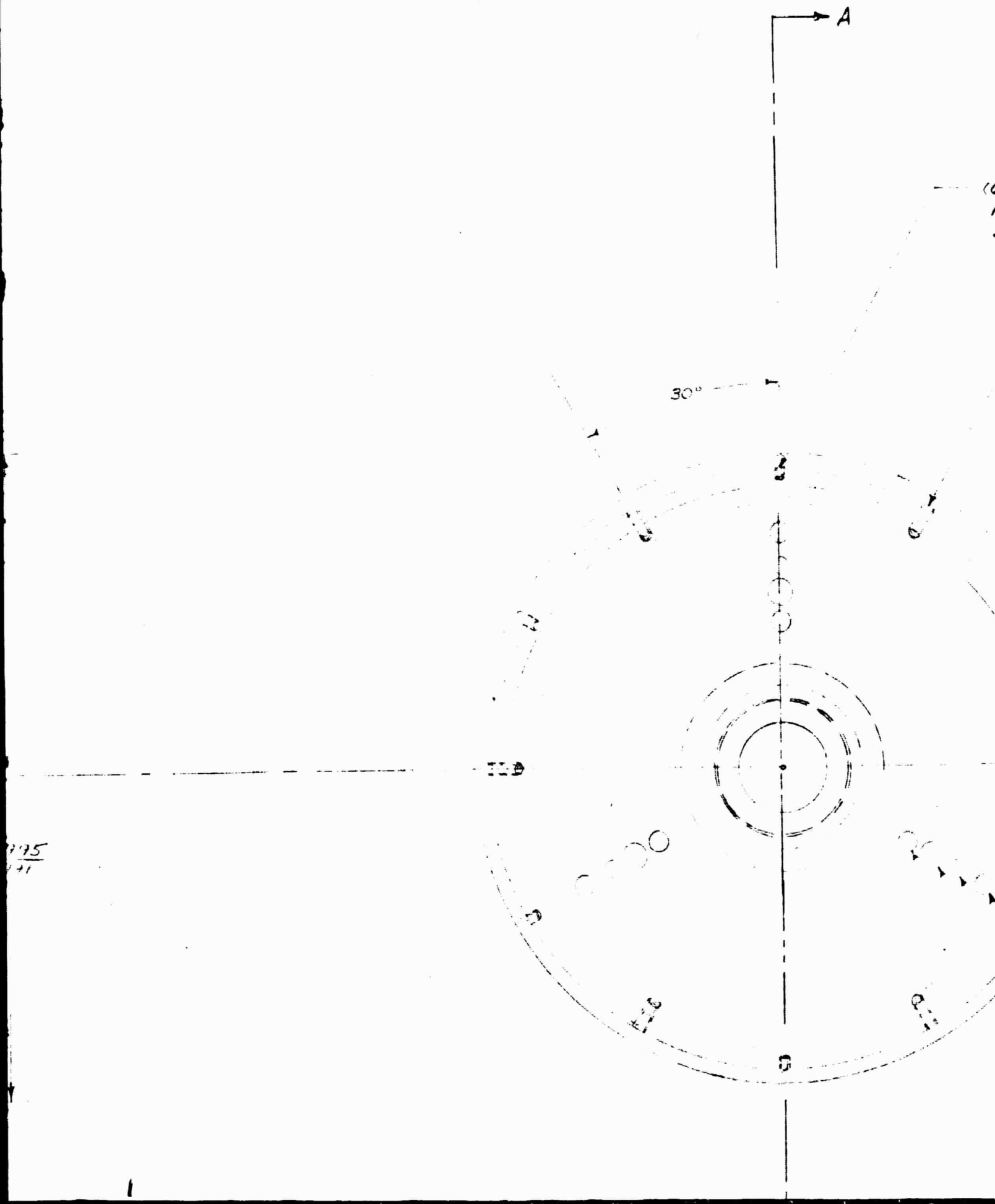
MATING THREAD TO BE
SUPPLIED BY UOPM

(Z)

32 $\sqrt{\frac{.001-1}{.010}}$
1 .003



V



VI

(6) HOLES EQUALLY SPACED ON RADII.
10-24 UNC-2B DRILL & TAP.
SEE NOTE 4.

(6) HOLES EQUALLY SPACED ON RADII.
10-24 UNC-2B DRILL & TAP.
SEE NOTE 4.

(A)

DRILL THRU (6) HOLES EQUALLY
SPACED ON $10.625 \pm .003$ B.C.
#10 DRILL (.194)

- (5) HOLES $\frac{25}{64}$ D. THRU $8.040 \pm .003$ B.C.
- (3) HOLES $\frac{17}{64}$ D. THRU $6.875 \pm .005$ B.C.
- (3) HOLES "X" D. THRU $6.000 \pm .005$ B.C.
- (3) HOLES $\frac{5}{16}$ D. THRU $5.125 \pm .003$ B.C.

2.507

3.007

1.625

1.267

.255

.150

.048

10°

		SCALE	FULL
		PROJ. NO.	01114
		DRAWN BY	F ³
		DATE	3-20-68
		FOR ASSEMBLY	
		MATERIAL	AL. ALLO
LET.	CHANGE	DATE	WEIGHT CAL. ACT.

II

FULL	<p align="center"> HIGH ALTITUDE ENGINEERING LABORATORY UNIVERSITY OF MICHIGAN DEPARTMENT OF AERO. AND ASTRO. ENGINEERING ANN ARBOR MICHIGAN </p>
01/14	
E3	
3-20-68	
AL. ALLOY	NAME <i>MOUNT-MIRROR</i>
	DRAWING NO. <i>H3-52007</i>

III

~~IV~~

8.992

1.499

1.262

.235

5°

1.625

IV

#1 DRILL THRU. (3) HOLES
EQUALLY SPACED ON $6.000 \pm .003$ B.C.
CHAMFER 45° .010 NOM.

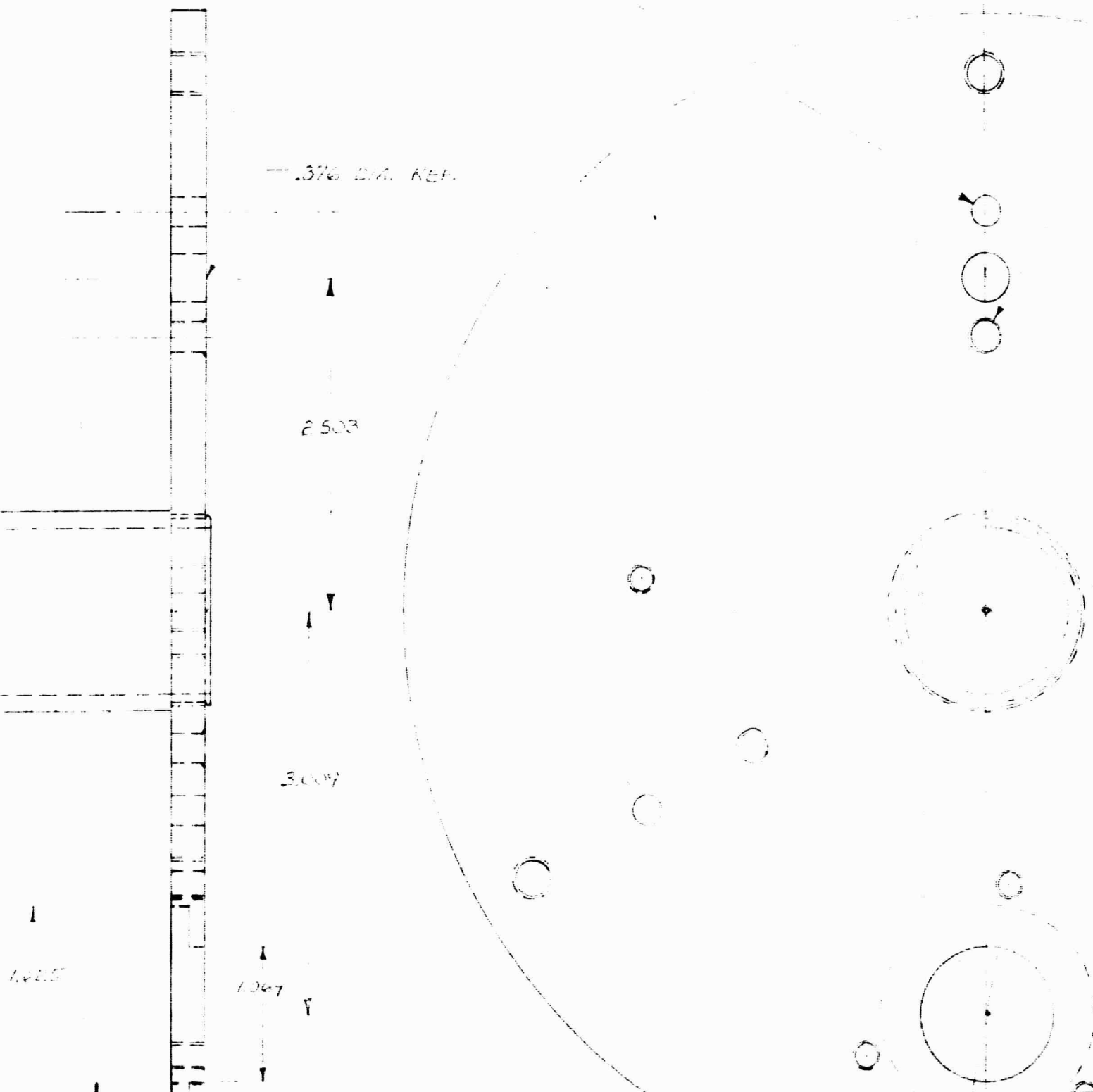
.376 DIA. REF.

2.503

3.007

1.067

1.065



I
IV

B.C.

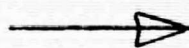
#7 DRILL THRU. (3) HOLES
DIA LIMITS .196 - .202
EQUALLY SPACED ON 9.125 ± .003
B.C. 120° C SINK TO .23 DIA.
TAP WITH HELI-COIL #3 FFB-112.



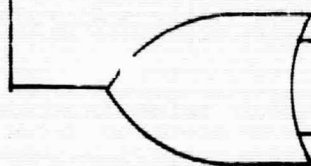
17-32
5.55 P.C. REF.

View 4 (3 holes
on 9.125 P.C. DIA.)

INPUT



DETECTOR



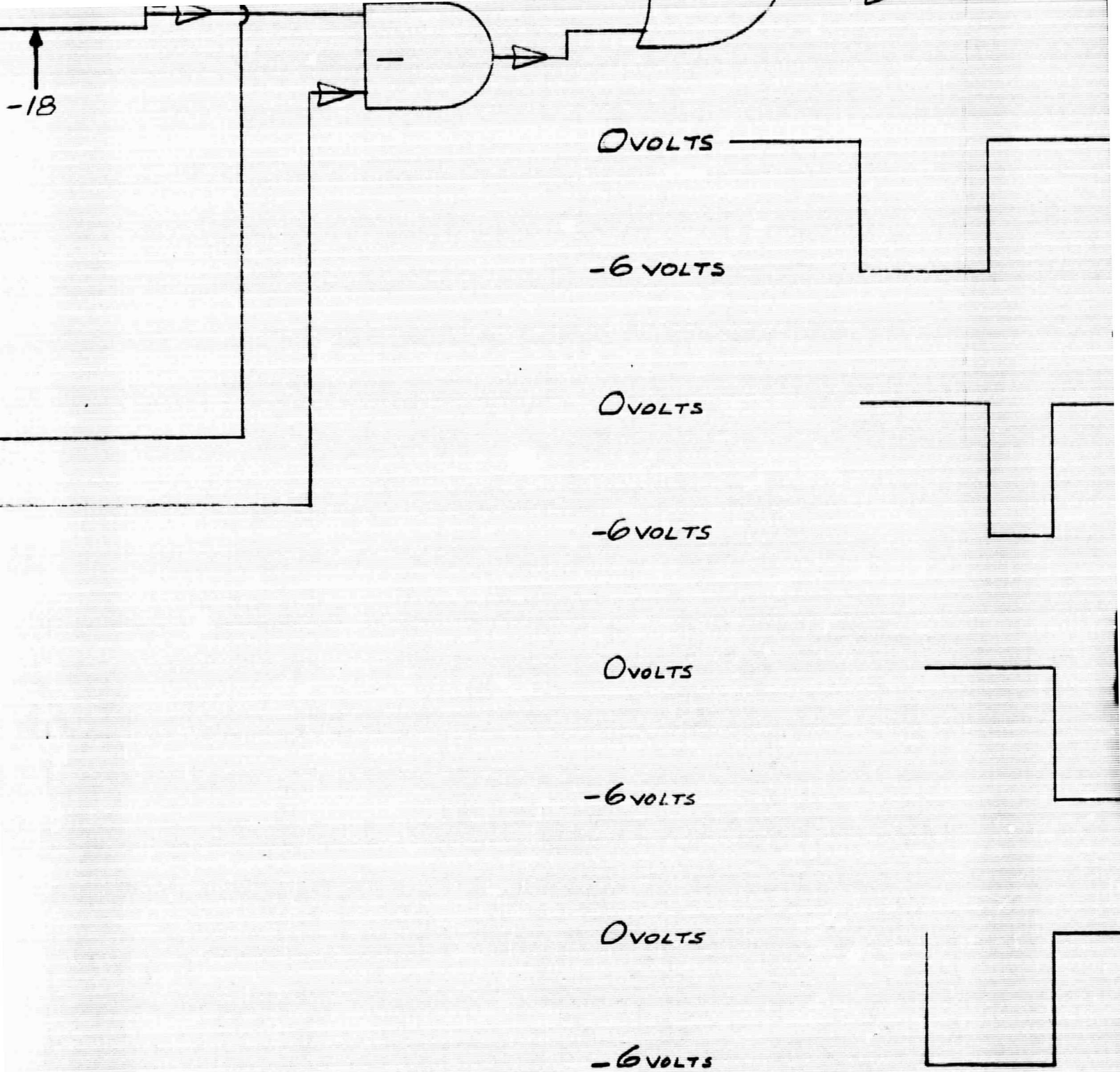
+

-

-18

-18

I



		SCALE	NONE
		PROJ. NO.	06647
		DRAWN BY	J.C. POUSA
		DATE	2-1-66
		FOR ASSEMBLY	
		DESIGN BY	D. HADDON
LET.	CHANGE	DATE	WEIGHT CAL. ACT.

IV

ANAL
2

2.5ms

FF-1
(1)

FF-2
(2)

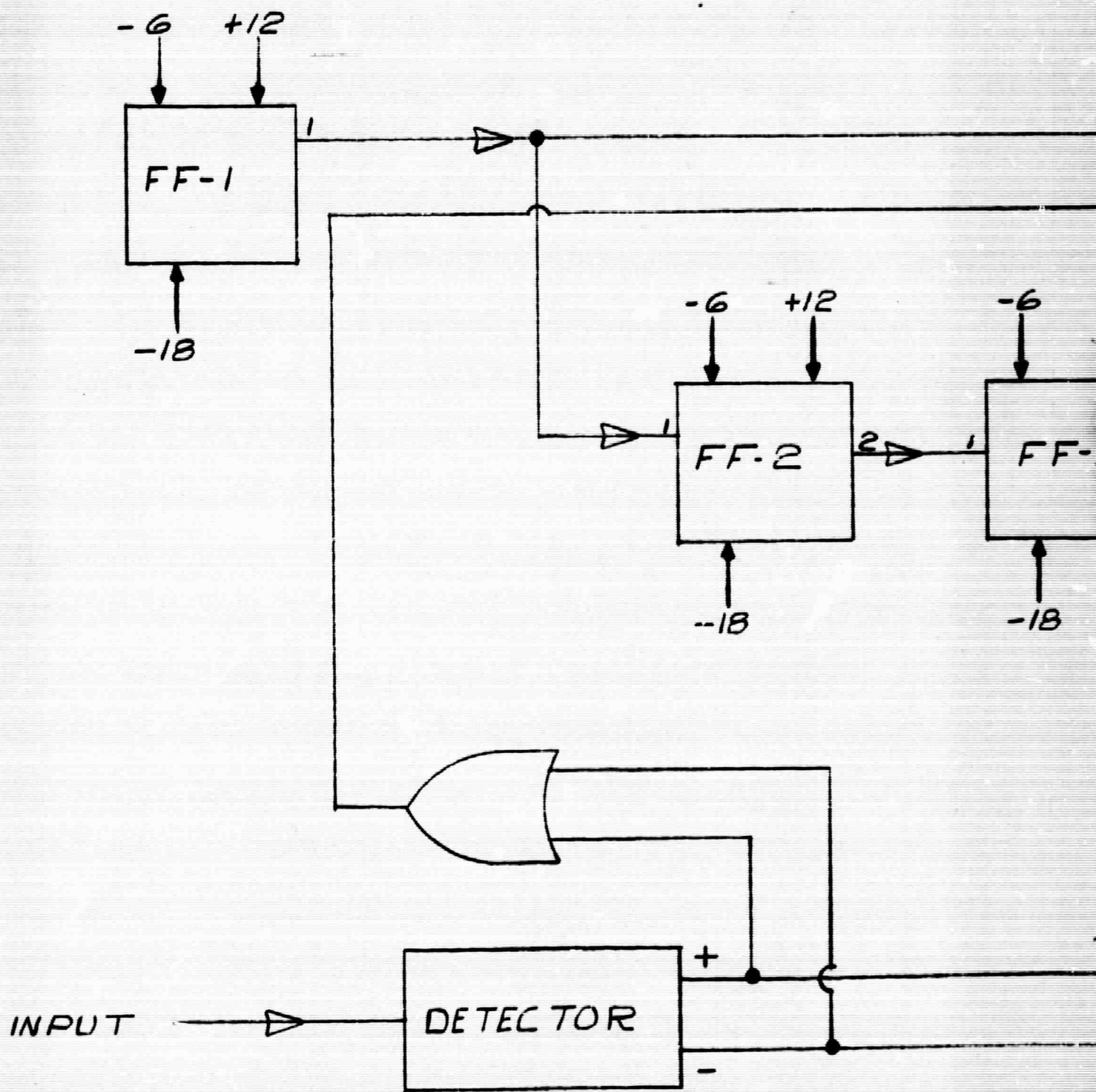
FF-3
(2)

FF-3
(3)

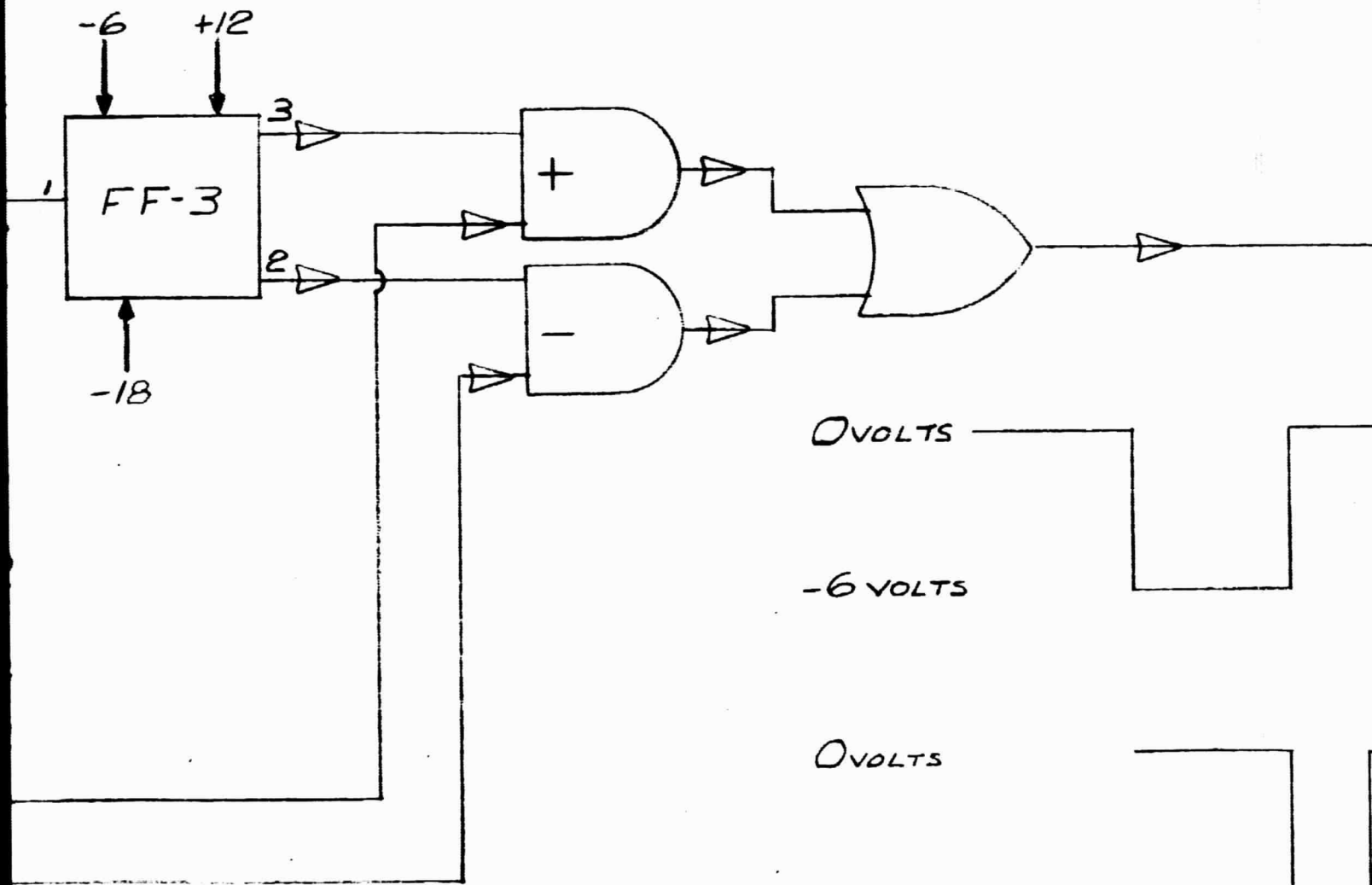
	NONE	HIGH ALTITUDE ENGINEERING LABORATORY UNIVERSITY OF MICHIGAN DEPARTMENT OF AERO. AND ASTRO. ENGINEERING ANN ARBOR MICHIGAN
	06647	
	J.C. POUSAK	
	2-1-66	
		NAME LOGIC CIRCUITS WAVE FORM FOR REACTION WHEEL
	D. HADDOCK	DRAWING NO. H3-52008

III

IV



IV



0 VOLTS

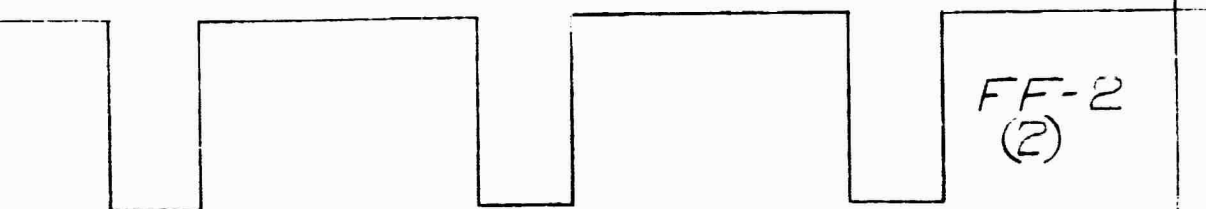
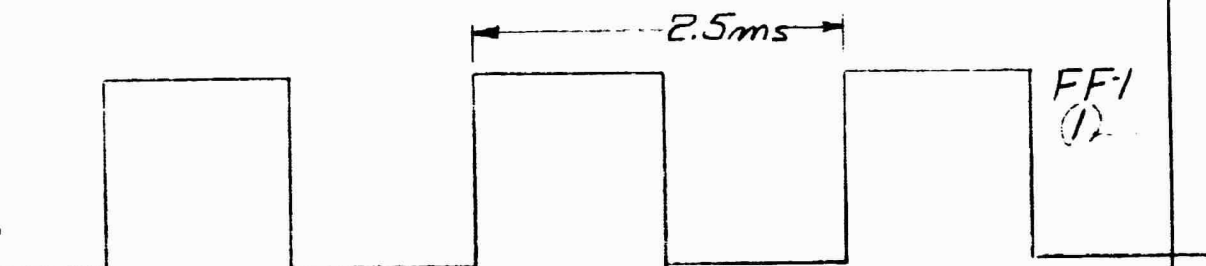
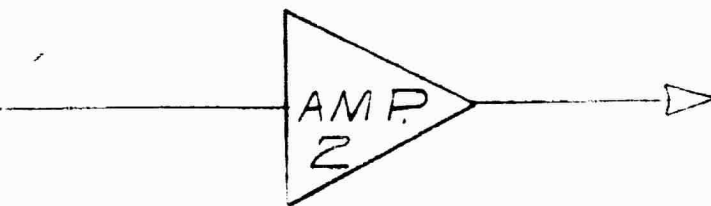
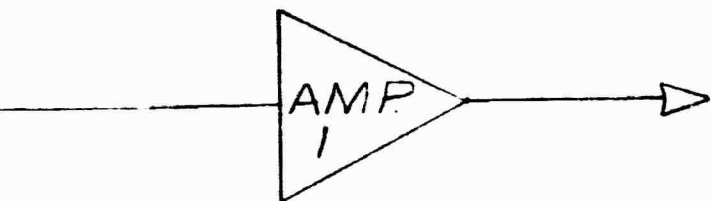
-6 VOLTS

0 VOLTS

-6 VOLTS

0 VOLTS

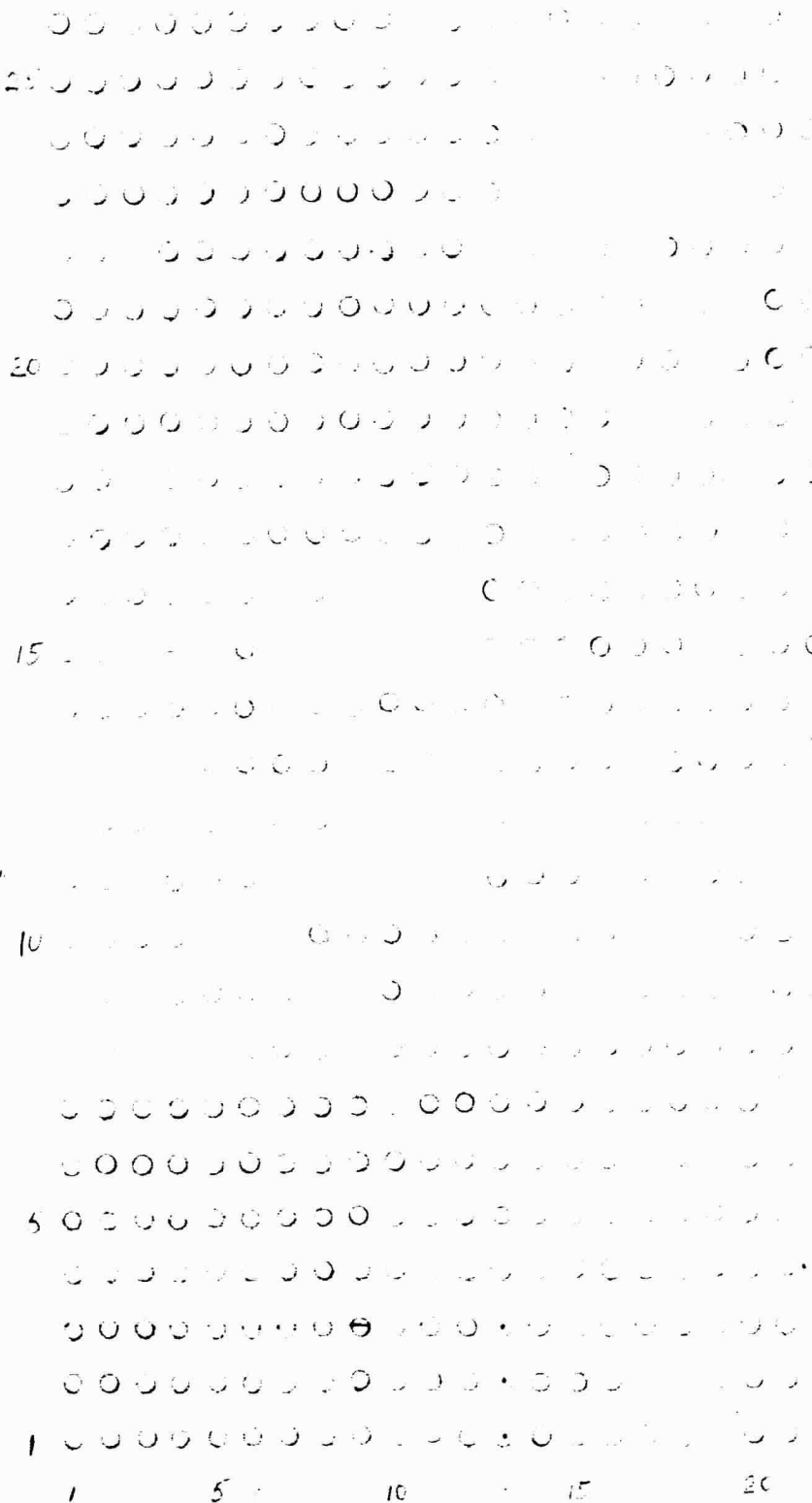
VI



22
21
20
19
18
17
16
15
14
13
12
11
10
9
8
7
6
5
4
3
2
1

3.6"

5"



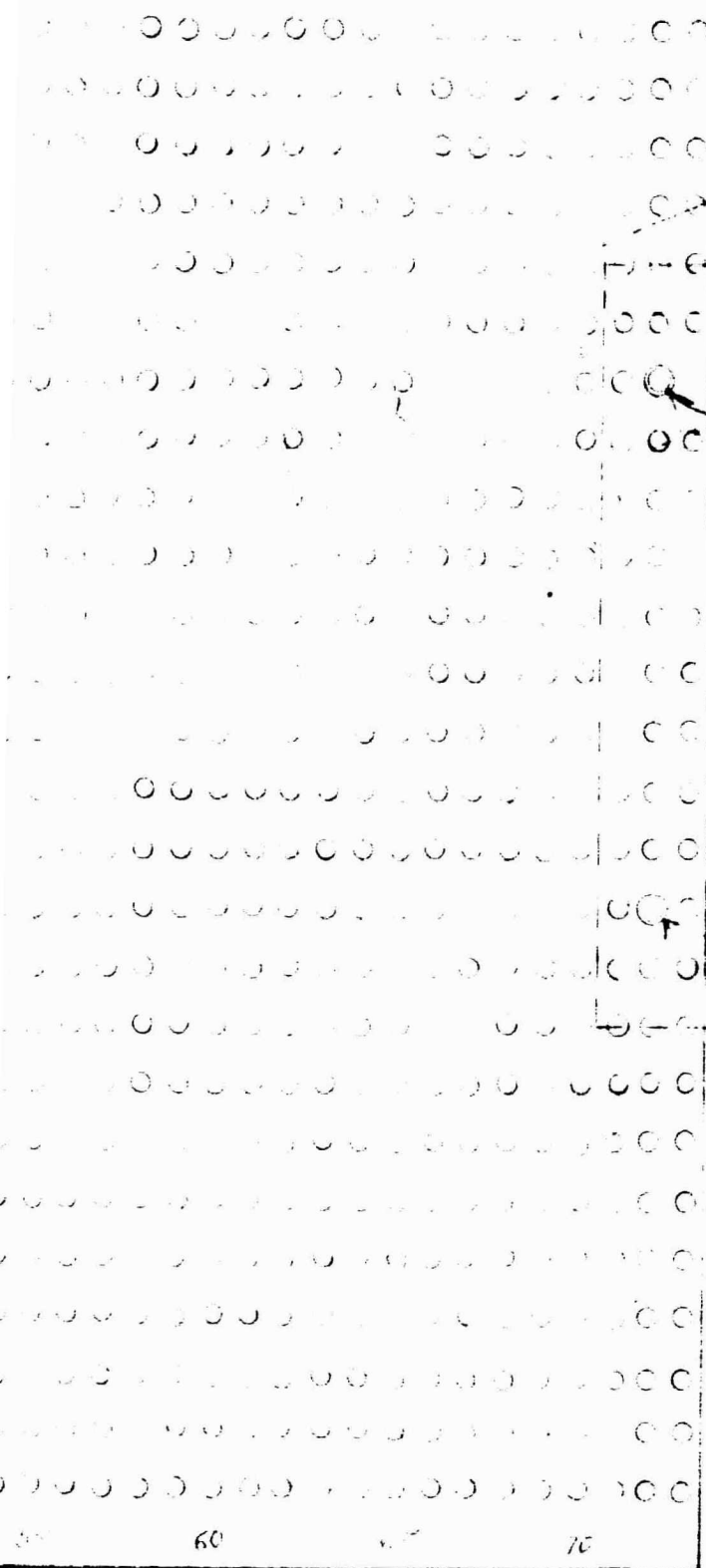
I

20 25 30 35 40 45 50 55 60

8"

			SCALE	2 TIM
			PROJ. NO.	0664
			DRAWN BY	J.C. PC
			DATE	8-22-
B	HANDLE POSITION CHANGED	3-15-68	FOR ASSEMBLY	
A	REVISED	2-23-68	MATERIAL	
LET.	CHANGE	DATE	WEIGHT CAL. ACT.	

IV



H 20/12
PRILE FOR 2-55

HAN LE

H 11/75
PRILE FOR 2-55

2 TIMES	HIGH ALTITUDE ENGINEERING LABORATORY UNIVERSITY OF MICHIGAN DEPARTMENT OF AERO. AND ASTRO. ENGINEERING ANN ARBOR MICHIGAN
06647	
J.C. POUSAK	
8-22-66	
	NAME VERO BOARD LAYOUT - COMPONENT SIDE
	DRAWING NO. H3-52009

III

IV

A

	1	5	10	15	20
30	○	○	○	○	○
	○	○	○	○	○
	○	○	○	○	○
	○	○	○	○	○
	○	○	○	○	○
	○	○	○	○	○
25	○	○	○	○	○
	○	○	○	○	○
	○	○	○	○	○
	○	○	○	○	○
	○	○	○	○	○
	○	○	○	○	○
20	○	○	○	○	○
	○	○	○	○	○
	○	○	○	○	○
	○	○	○	○	○
	○	○	○	○	○
	○	○	○	○	○
15	○	○	○	○	○
	○	○	○	○	○
	○	○	○	○	○
	○	○	○	○	○
	○	○	○	○	○
	○	○	○	○	○
10	○	○	○	○	○
	○	○	○	○	○
	○	○	○	○	○
	○	○	○	○	○
	○	○	○	○	○
	○	○	○	○	○

- 22
- 21
- 20
- 19
- 18
- 17
- 16
- 15
- 14
- 13
- 12
- 11
- 10
- 9
- 8
- 7
- 6
- 5

3.6"

5"



21

43

30

24.

40

43

50

55

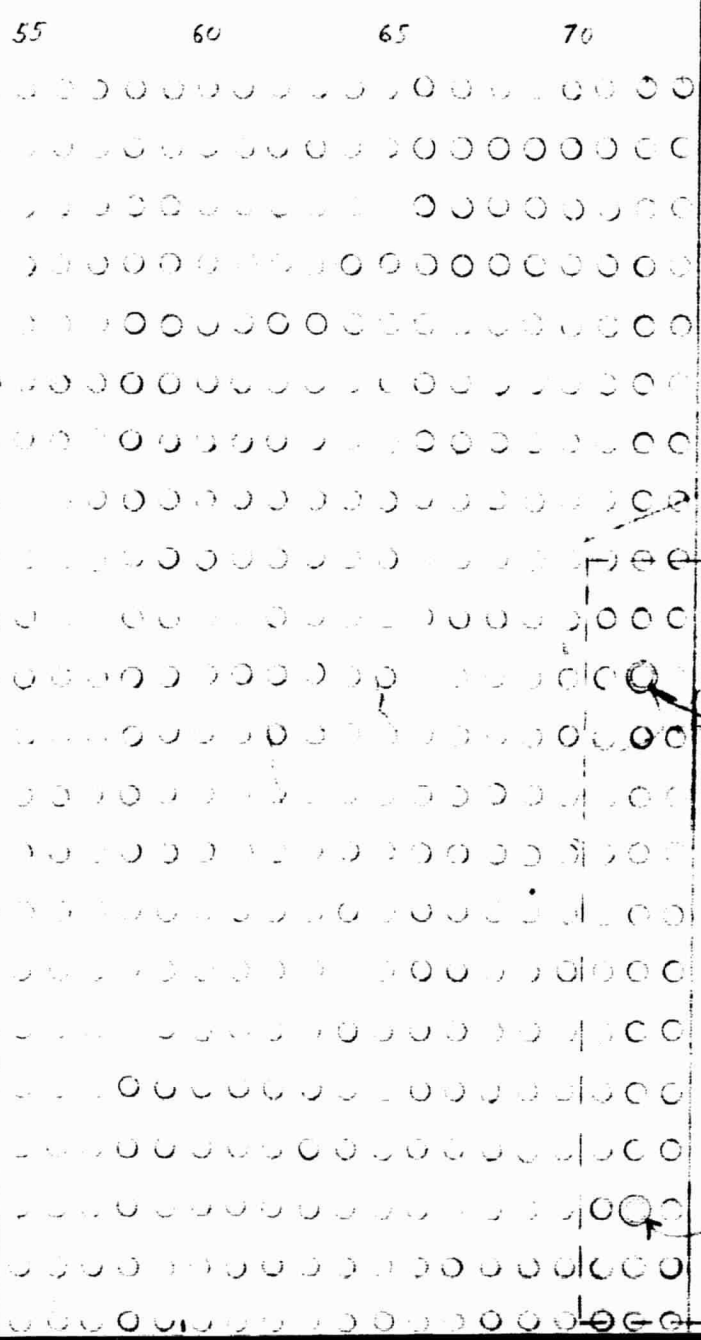
1. The first part of the document discusses the importance of maintaining accurate records of all transactions and activities. It emphasizes the need for transparency and accountability in financial reporting.

2. The second part outlines the various methods and tools used to collect and analyze data. This includes the use of surveys, interviews, and statistical software to ensure the reliability and validity of the findings.

3. The third part presents the results of the study, highlighting the key findings and trends observed. It discusses the implications of these results for the field and provides recommendations for future research.

4. The final part of the document concludes the study and summarizes the overall contributions. It reiterates the significance of the research and expresses gratitude to the participants and funding sources.

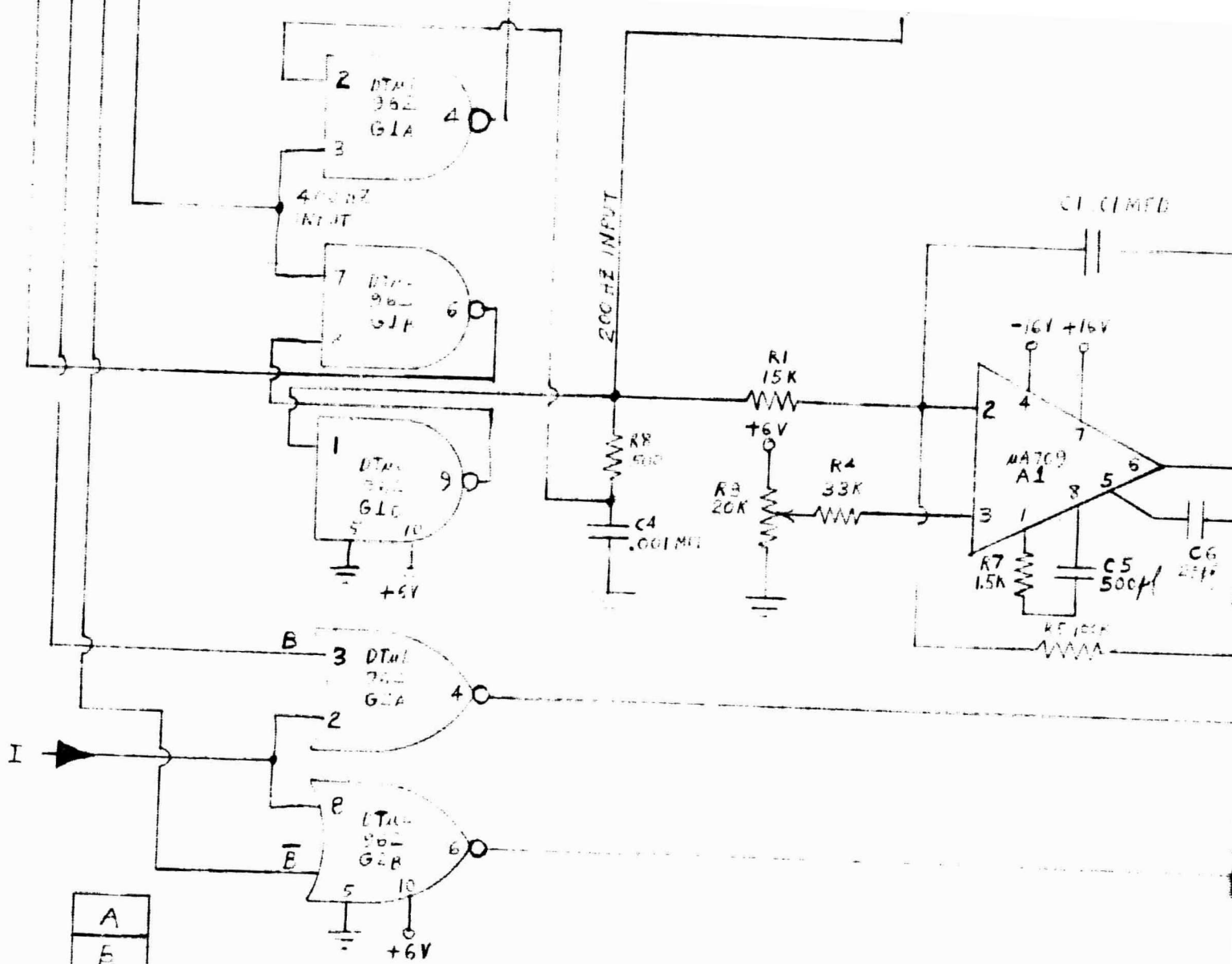
~~VI~~



HOLE #20/12
DRILL FOR 2-5%

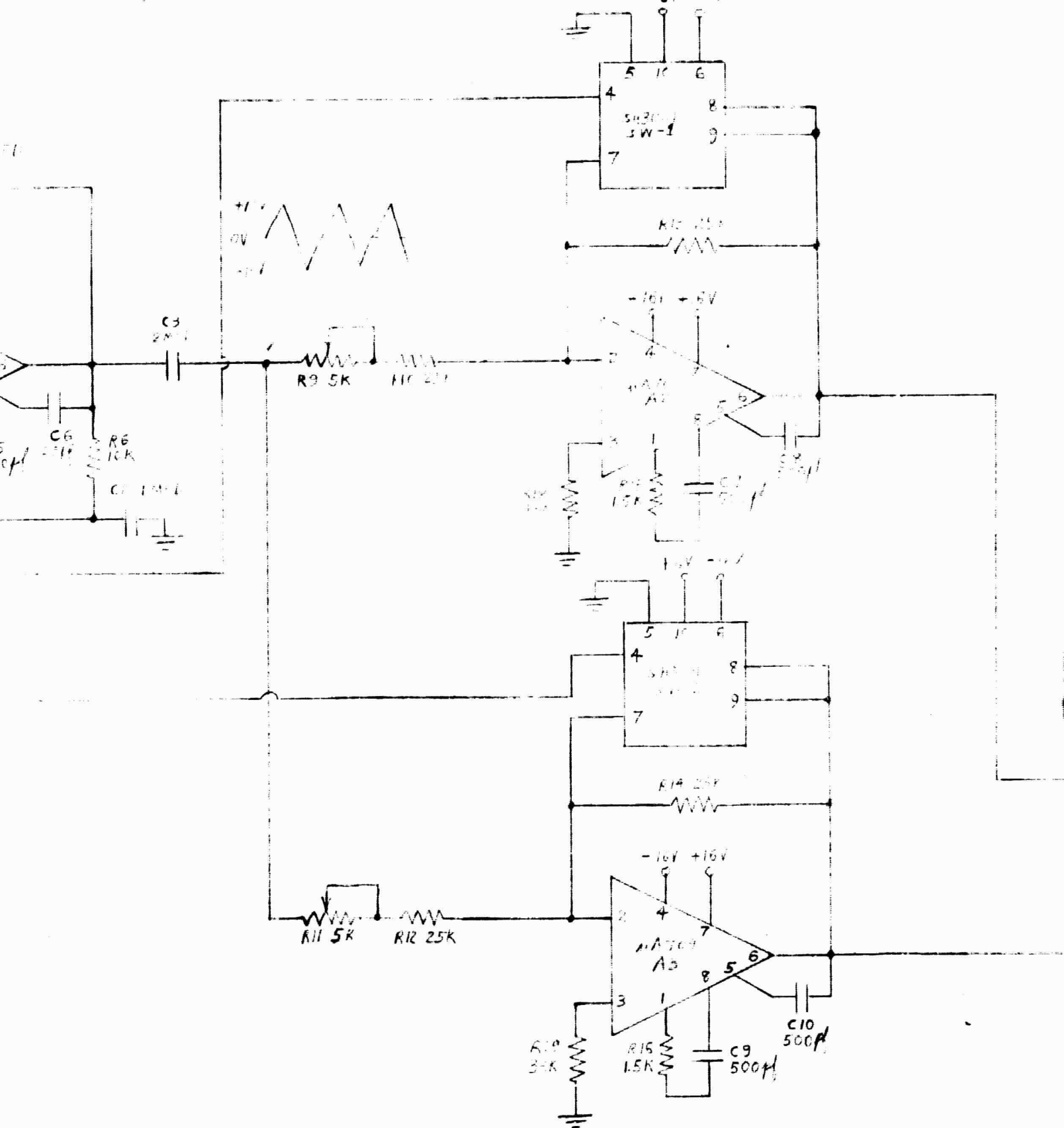
HANDLE

HOLE #11/12
DRILL FOR 2-5%

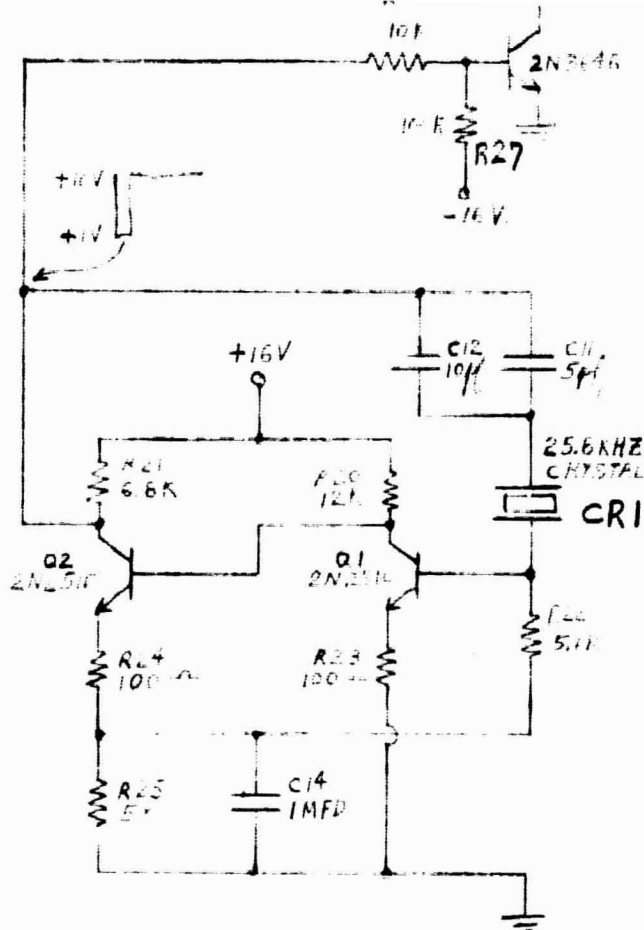


- | | |
|---|---------------------|
| A | |
| B | |
| C | |
| D | |
| E | |
| F | |
| G | |
| H | |
| J | |
| K | |
| L | 400 HZ OUTPUT |
| M | \bar{C} |
| N | \bar{B} |
| P | I - INHIBIT |
| R | B 100 HZ OUTPUT |
| S | C 200 HZ OUTPUT |
| T | +6V, 87MA. |
| U | GROUND |
| V | |
| W | HORIZ. OUTPUT |
| X | VERT. OUTPUT |
| Y | -16V. (-15V, 14MA.) |
| Z | +16V. (+15V, 14MA.) |

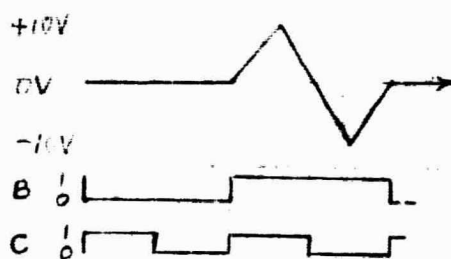
Y



		SCALE	NONE
		PROJ. NO.	01114
		DRAWN BY	T. FATTINSCA
		DATE	2-19-68
		FOR ASSEMBLY	
		MATERIAL	
A	B+C WAVESHAPES ADDED	2-20-68	
LET.	CHANGE	DATE	WEIGHT CAL. ACT.



HORIZ. SWP

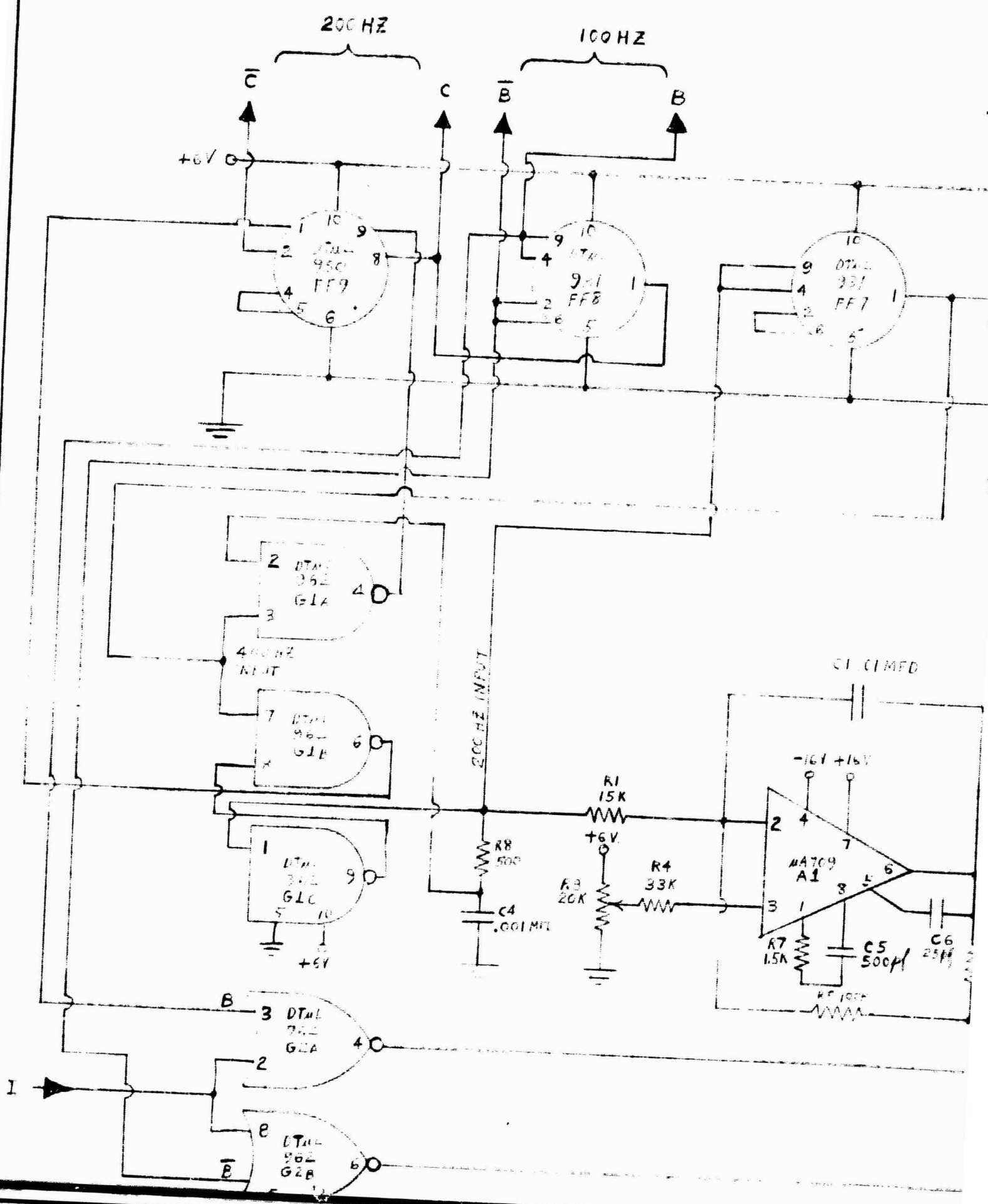


VERT. SWP

DATE	2-17-68	HIGH ALTITUDE ENGINEERING LABORATORY UNIVERSITY OF MICHIGAN DEPARTMENT OF AERO. AND ASTRO. ENGINEERING ANN ARBOR MICHIGAN
BY		
NAME	ATWILL SCAN GENERATOR	DRAWING NO. H3-52010
AL.		
ACT.		

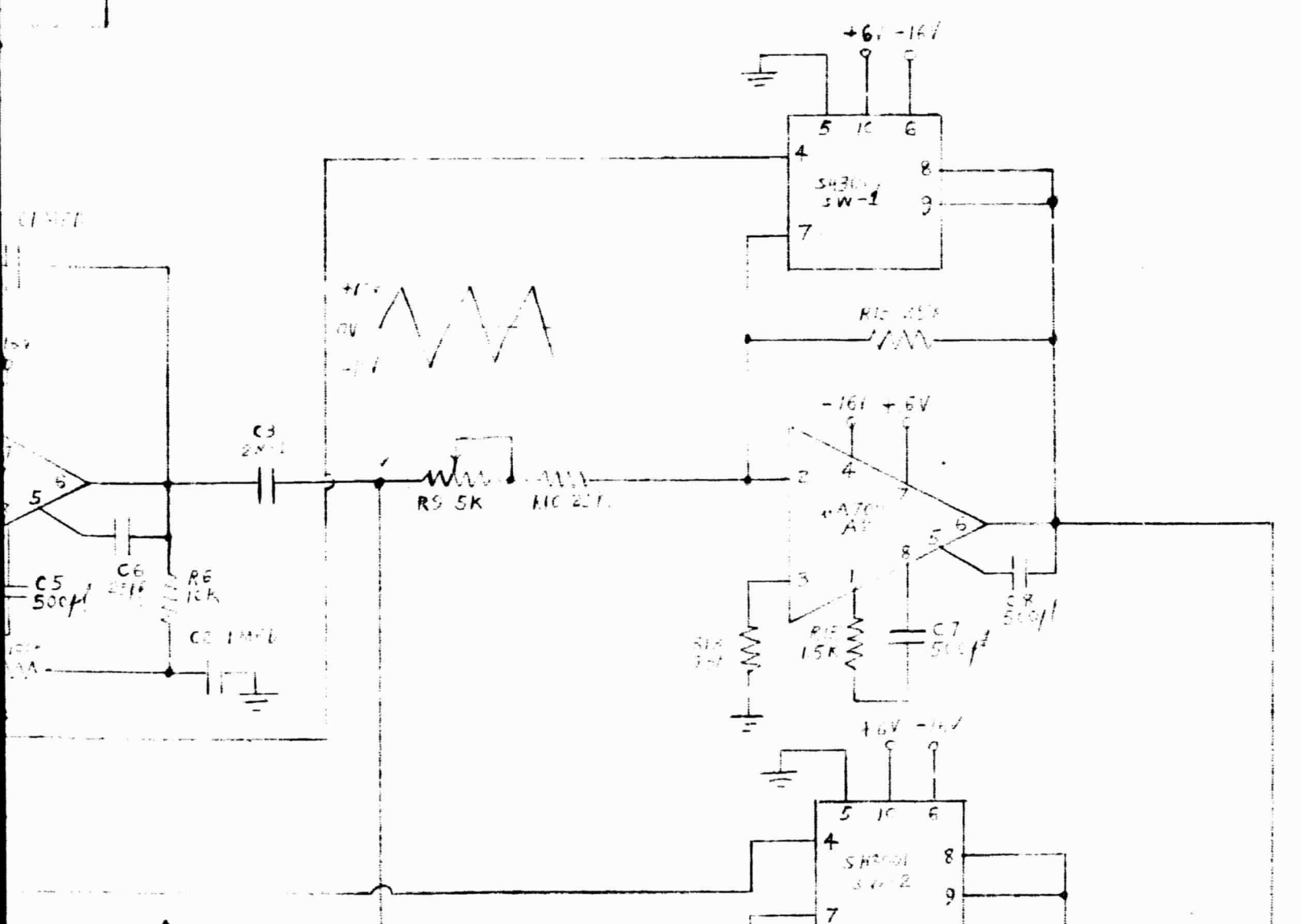
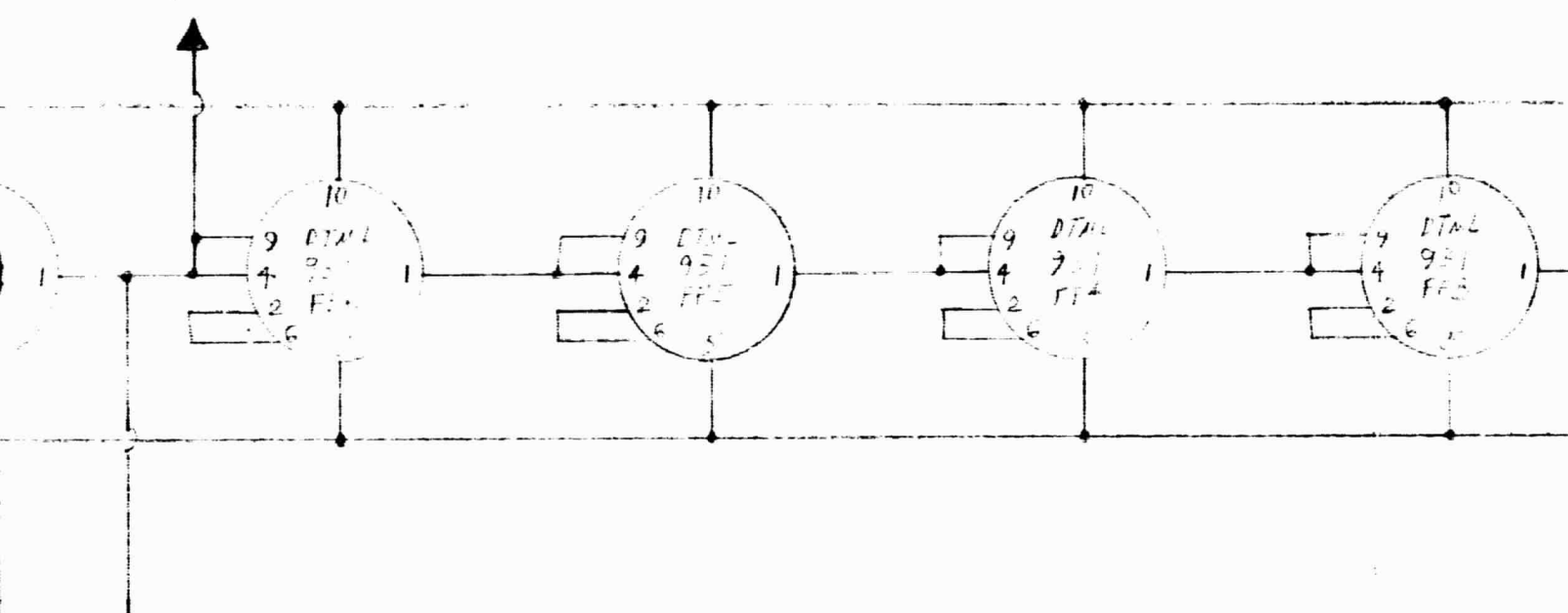
III

IV

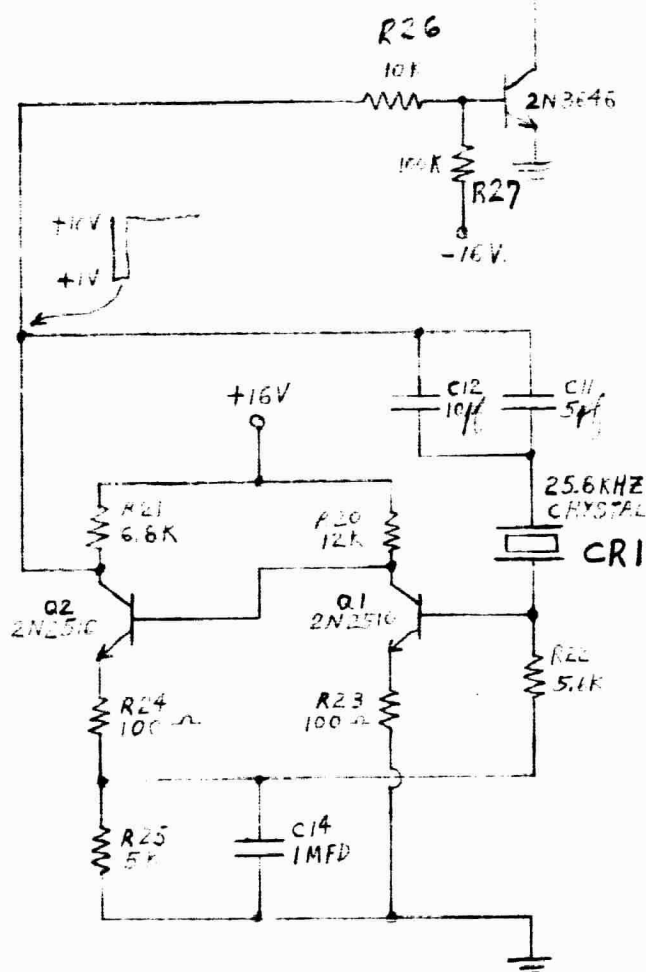
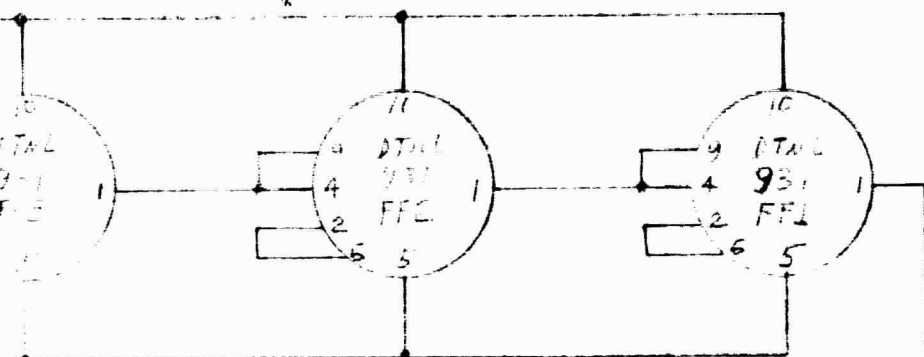


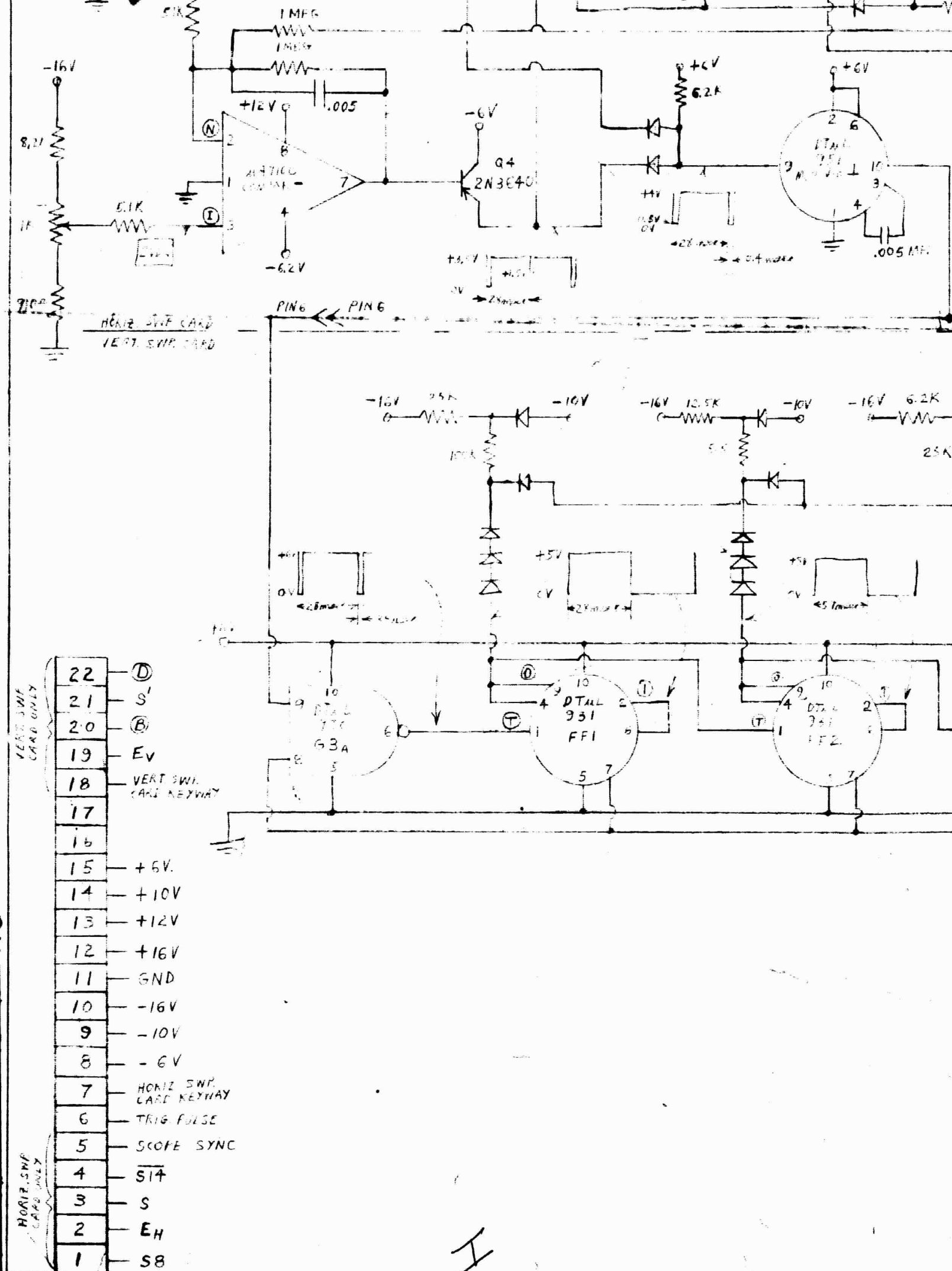
IV

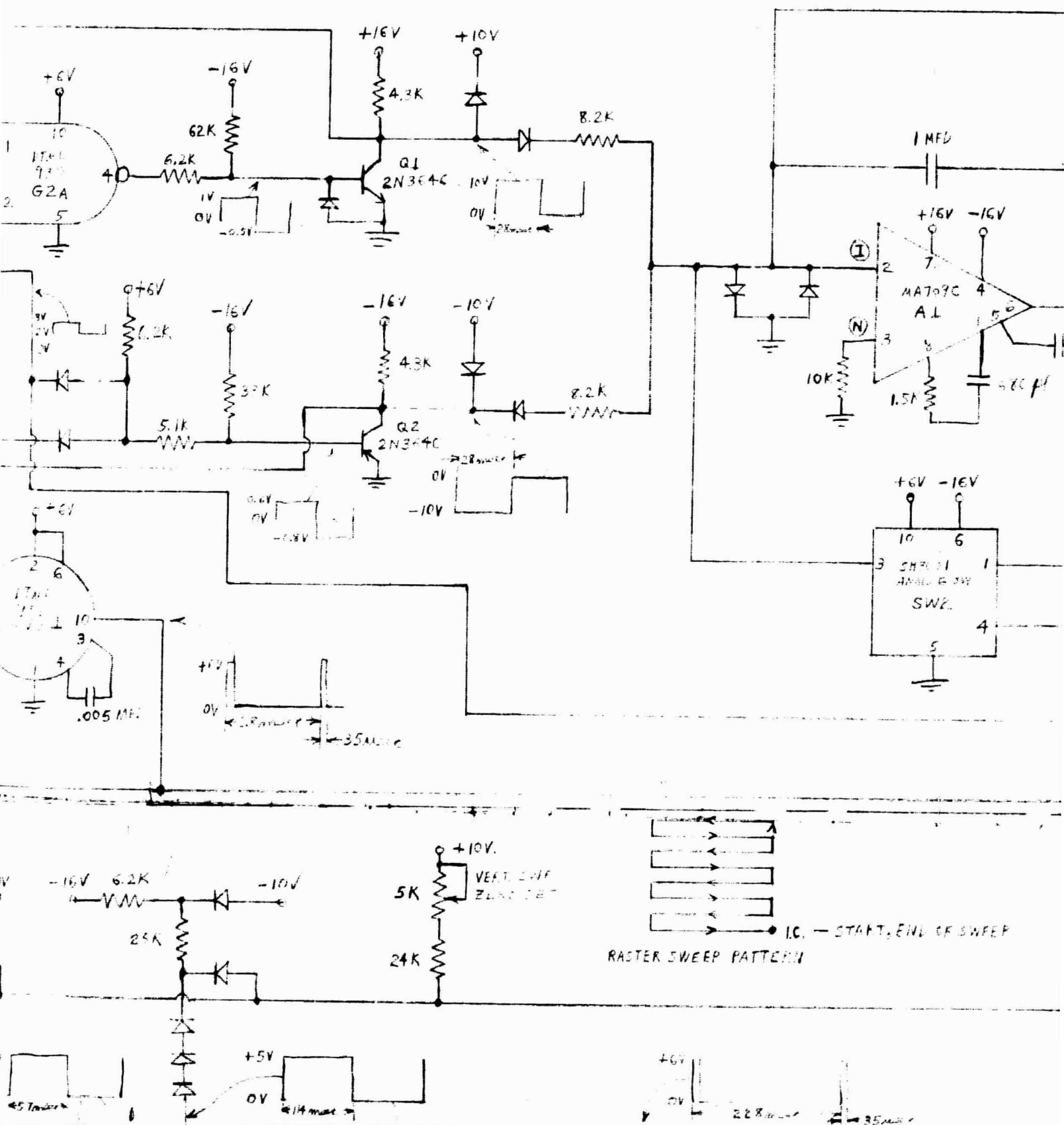
400HZ

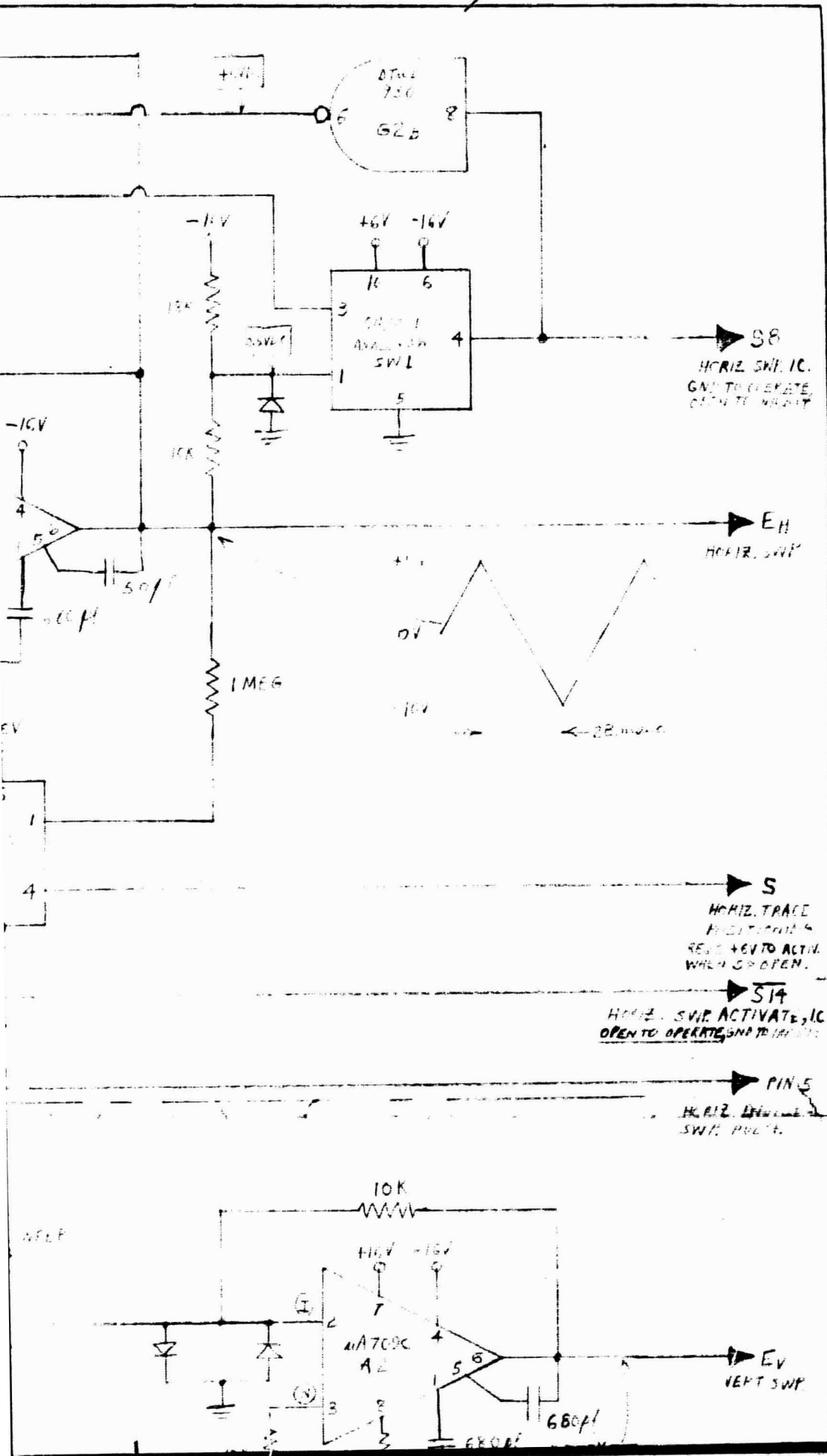


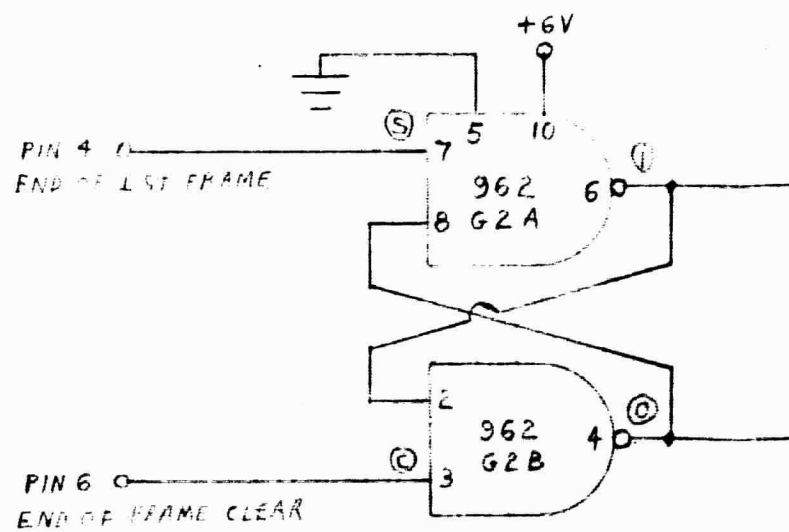
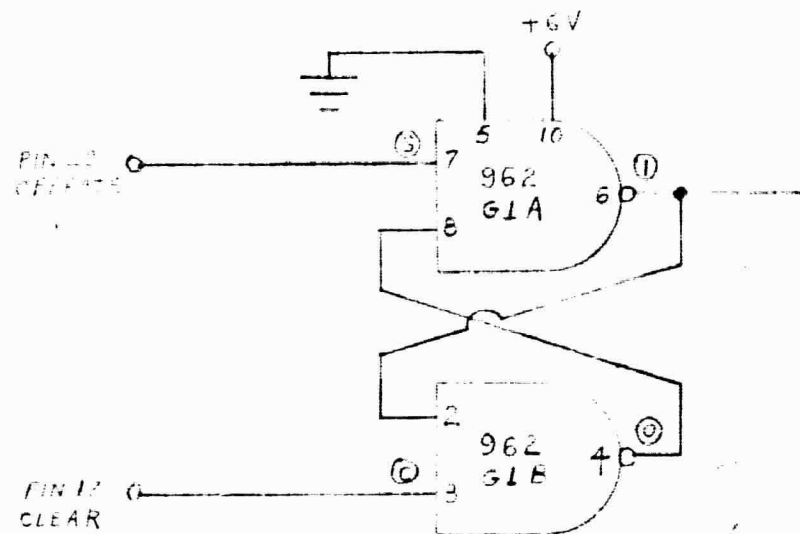
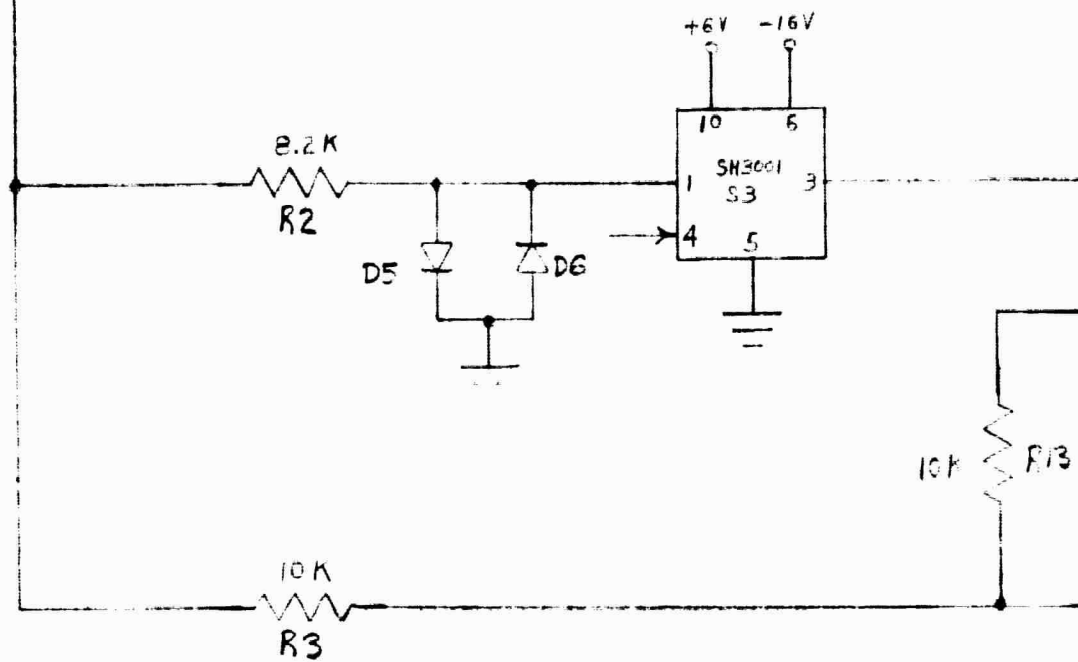
VI





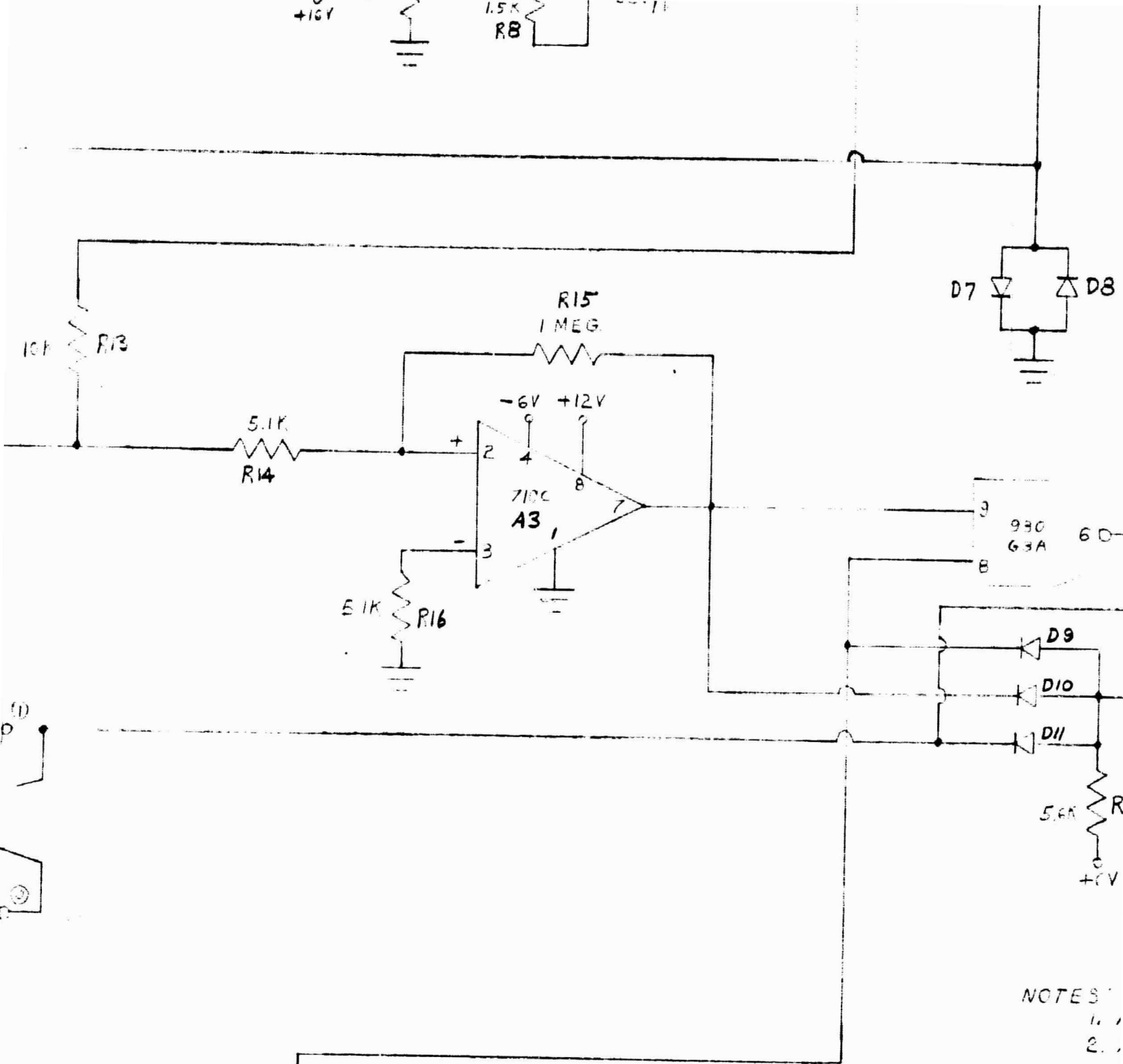






22	— OPERATE
21	
20	
19	
18	
17	— CLEAR
16	— SIGNAL INPUT
15	— +6V
14	— +10V
13	— +12V
12	— +16V
11	— GND
10	— -16V
9	— -10V
8	— -6V
7	
6	— ENL OF FRAME CLEAR
5	
4	— END OF 1ST FRAME
3	
2	
1	— OUTPUT

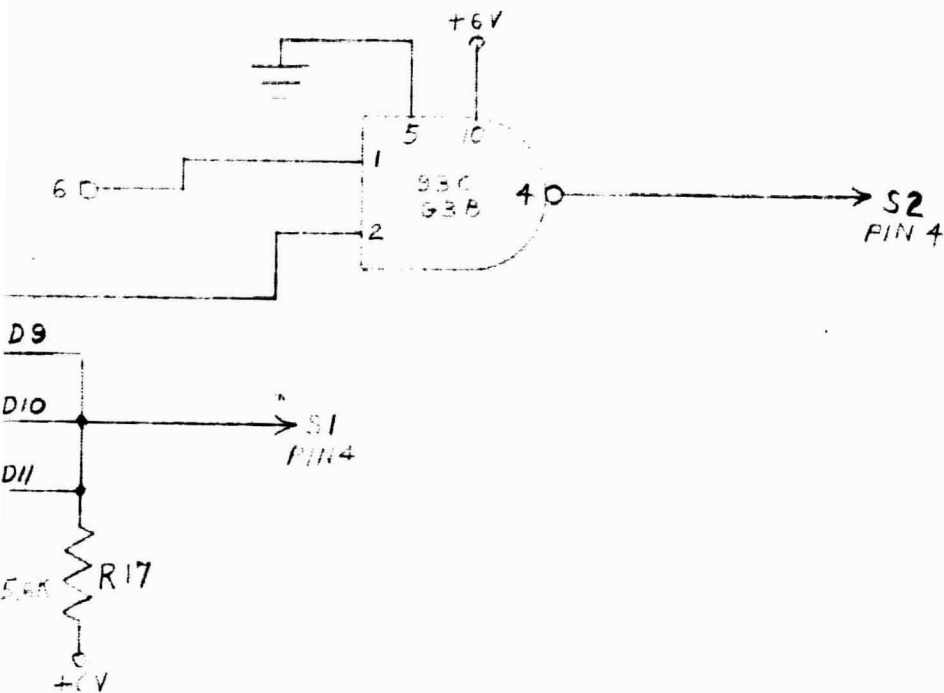
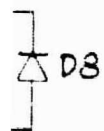
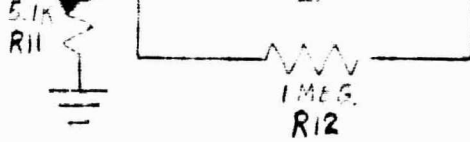
I



NOTES:
1.
2.

		SCALE	NONE
		PROJ. NO.	01114
		DRAWN BY	T. PATTER
		DATE	4-2-61
		FOR ASSEMBLY	
		MATERIAL	
LET.	CHANGE	DATE	WEIGHT CAL. ACT.

II



- NOTES:
1. ALL RESISTORS $\frac{1}{4}$ W 5% UNLESS NOTED
 2. ALL DIMENSIONS ARE IN INCHES

NAME	HIGH ALTITUDE ENGINEERING LABORATORY UNIVERSITY OF MICHIGAN DEPARTMENT OF AERO. AND ASTRO. ENGINEERING ANN ARBOR MICHIGAN
114	
ATTN: JASON	
-2-68	NAME PEAK LIGHT INTENSITY HOLD DETECTOR
	DRAWING NO. H3-52016

PIN 16
SIGNAL INPUT

1K
R1

D1

D2

+6V -16V

10 6
1 5
SH3001
S1

8.2K
R2

D5

D6

+6V -16V

10 6
1 5
SH3001
S3

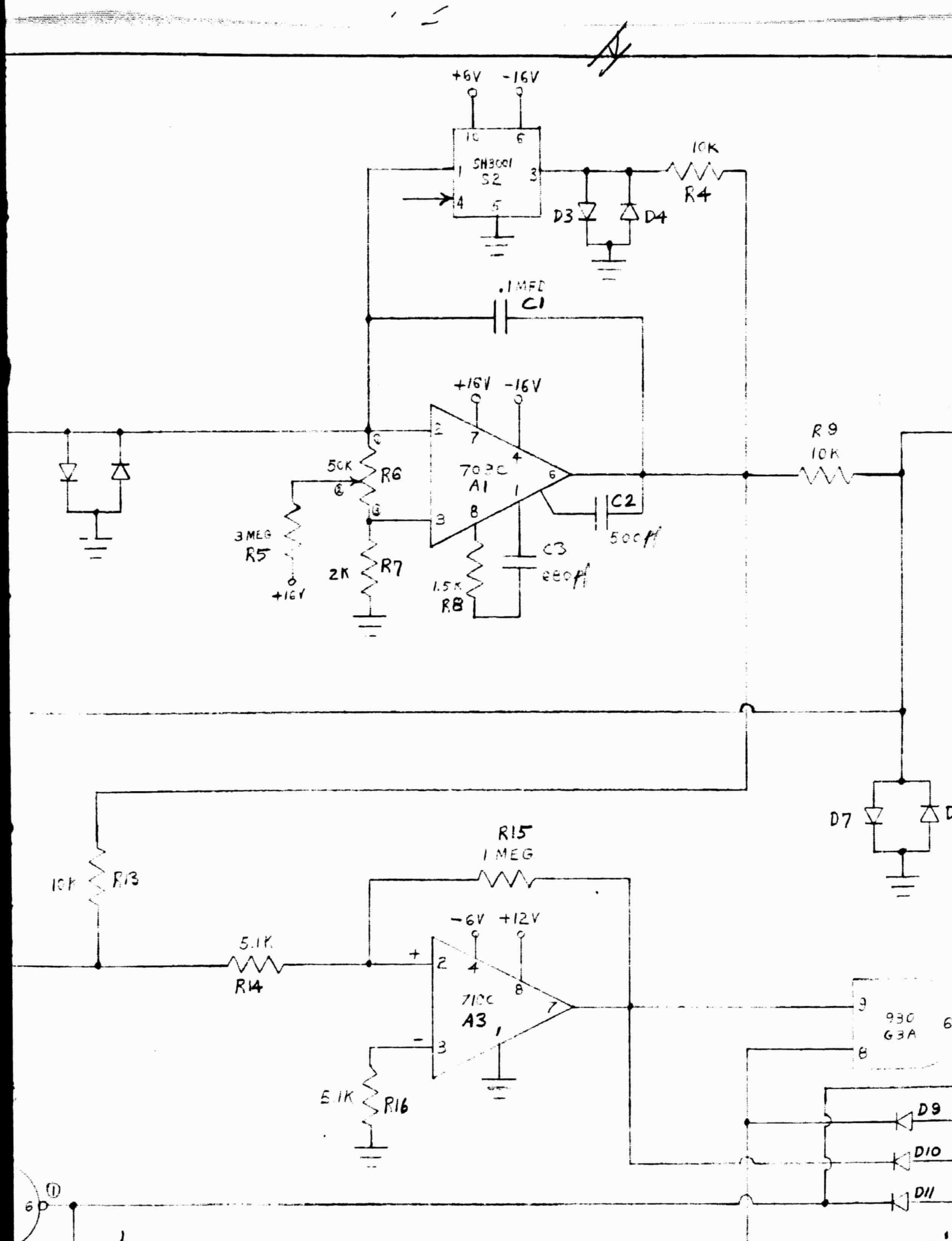
10K
R3

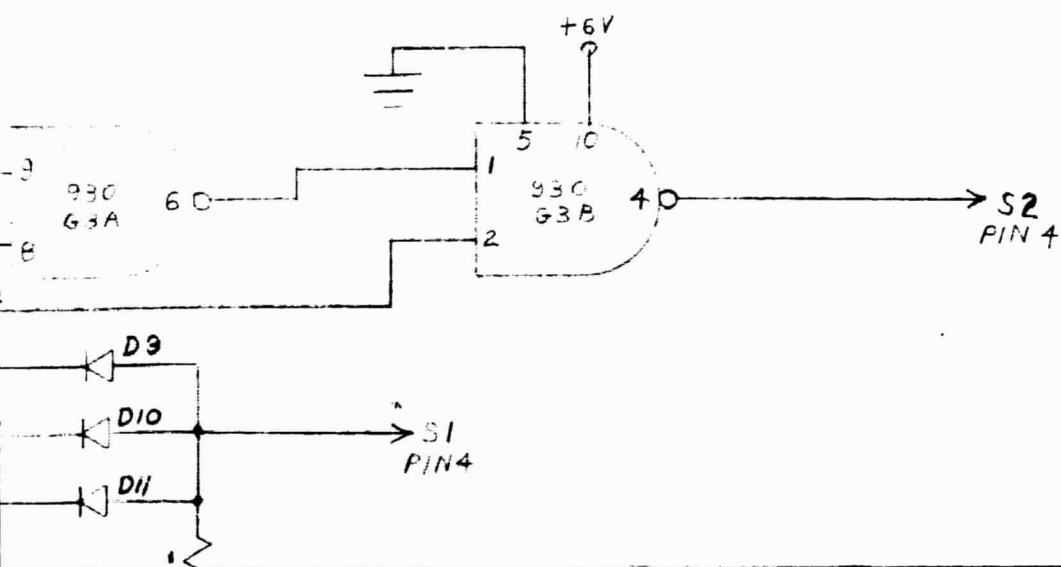
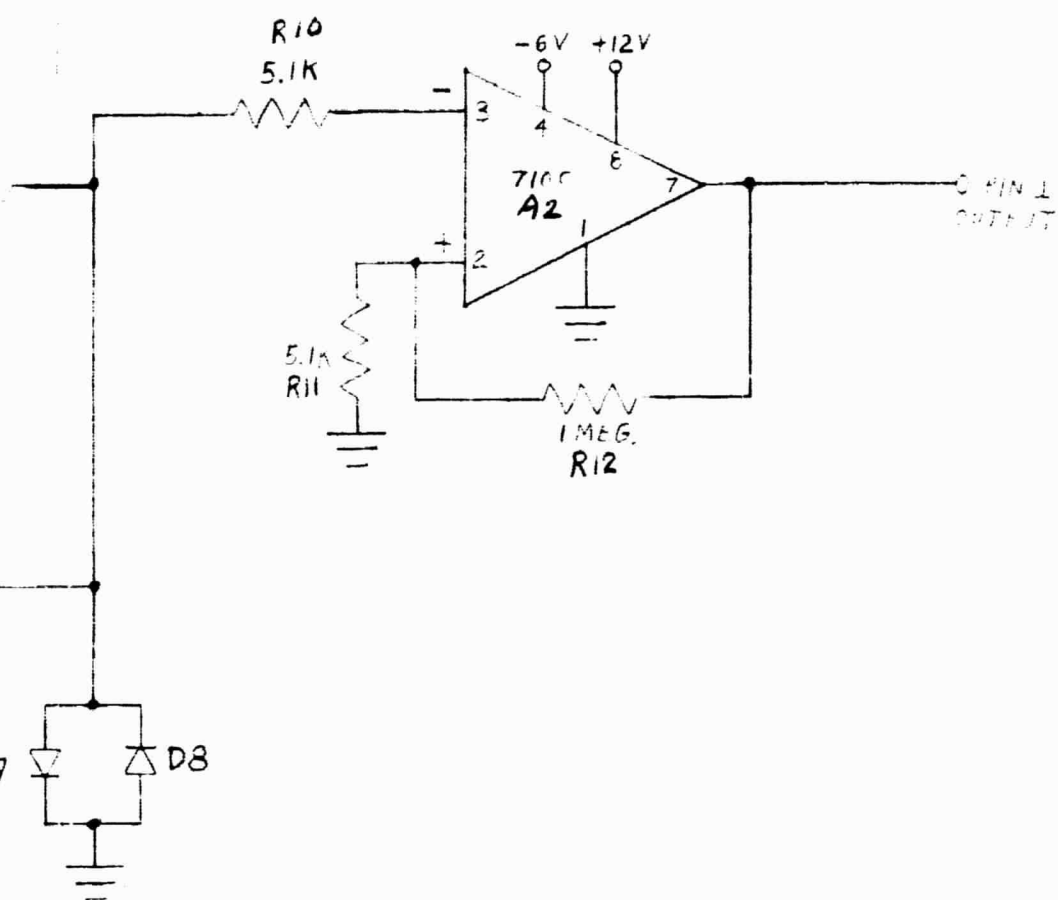
10K

PIN 40
OPERATE

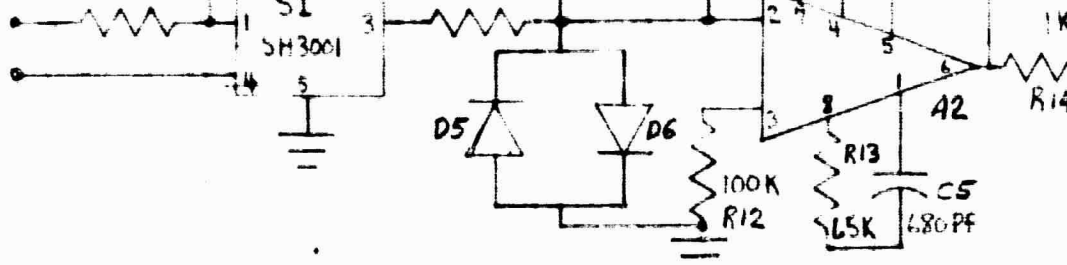
+6V

5 10
7 6
962
G1A





VERT. DEFL.
S1 CONTROL



SIMULATED
HOR. STAR MOT.

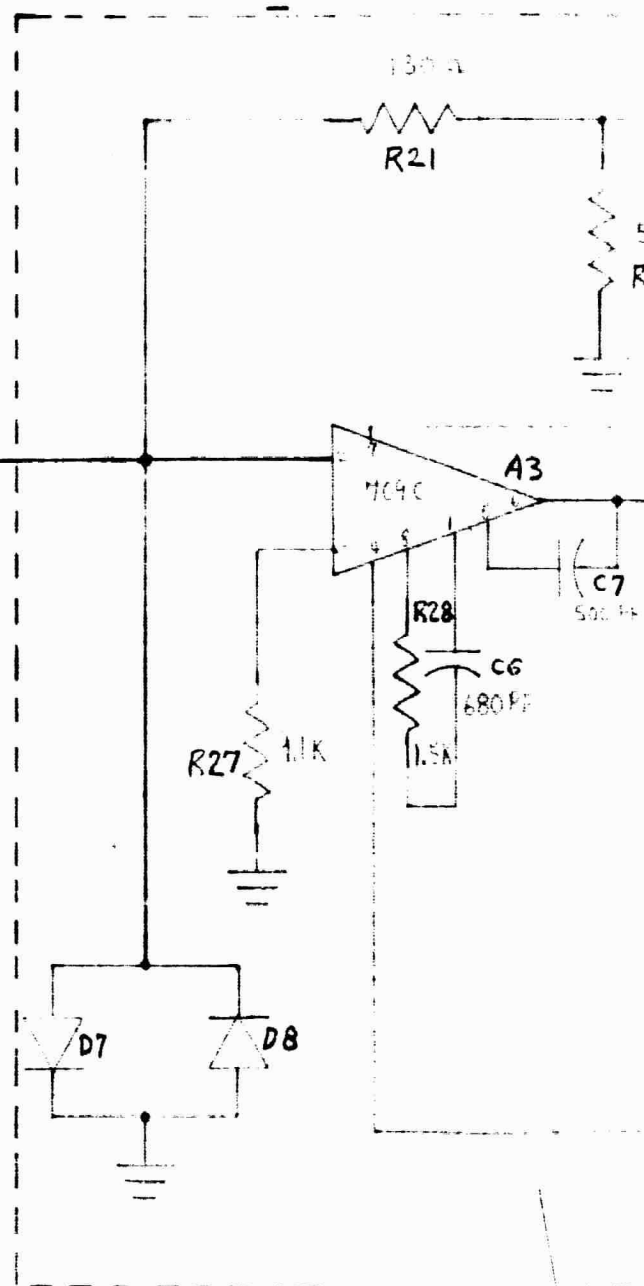
10K
R18

H.F.
VARIABLE

22K
R19

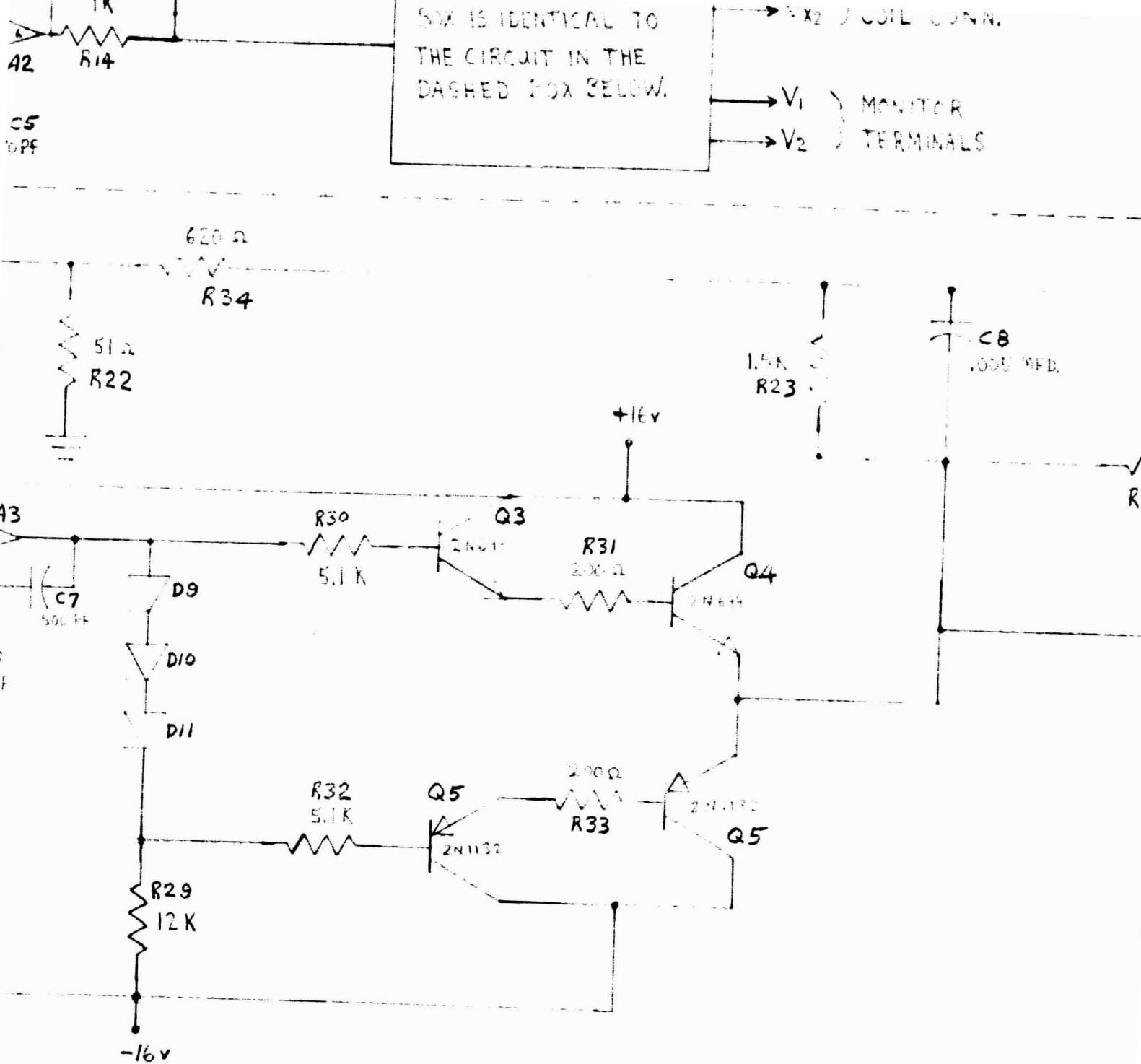
HOR. DEFL.

22K
R20



17	HX ₁
16	HX ₂
15	F
14	H. B.W. CH. L.P.
13	H. DEFL.
12	HOR. STAR MOT.
11	+6V
10	
9	
8	
7	
6	
5	
4	
3	
2	
1	
18	+11V
17	GND
16	-11V
15	
14	
13	
12	
11	
10	
9	
8	
7	
6	
5	
4	
3	
2	
1	

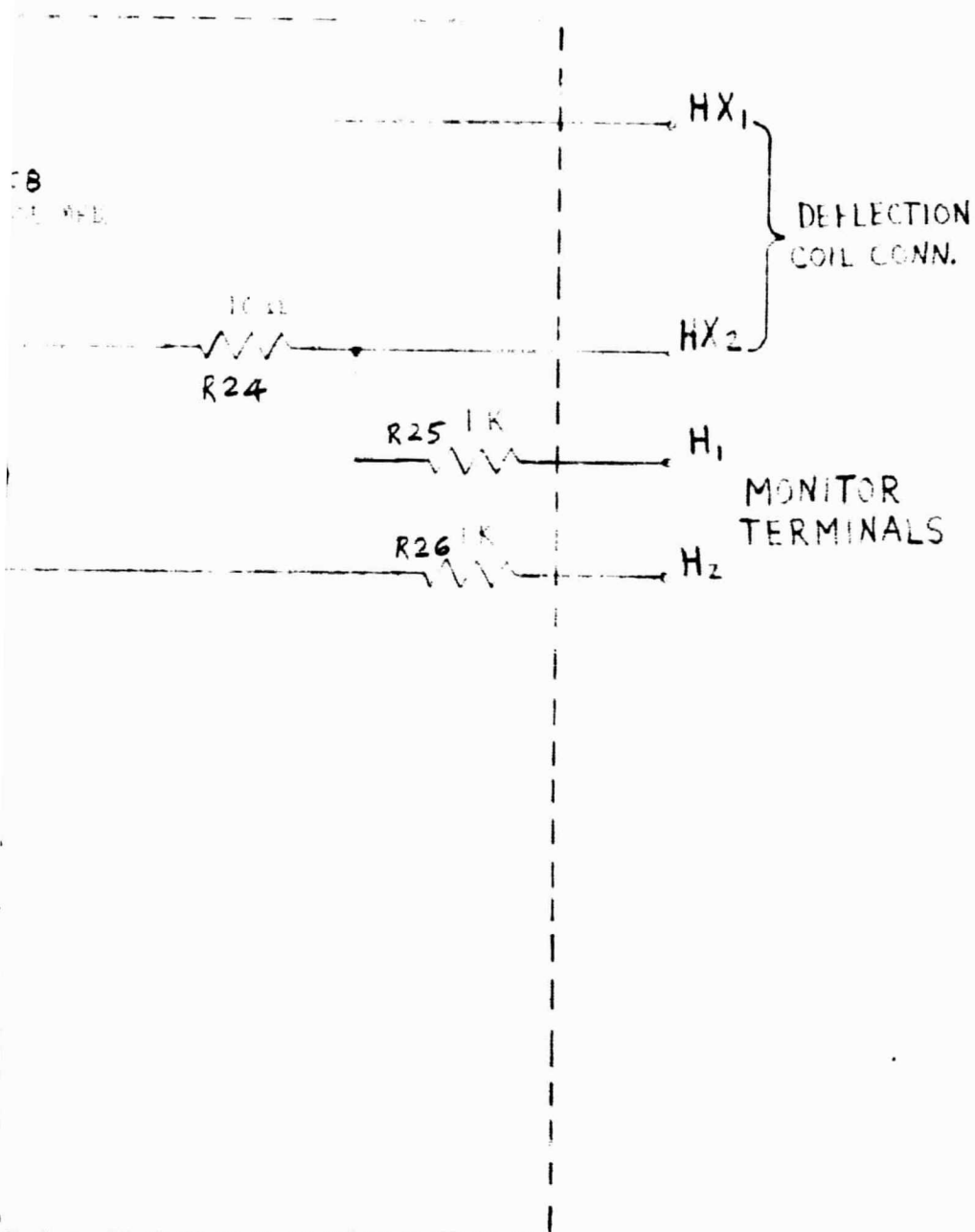
ALL DIODES ARE 1N486B UNLESS NOTED
ALL RESISTORS ARE 1/4W 5% UNLESS NOTED



ED
TED

II

		SCALE	NONE
		PROJ. NO.	01114
		DRAWN BY	E. GILREATH
		DATE	4-2-68
		FOR ASSEMBLY	
		MATERIAL	
LET.	CHANGE	DATE	WEIGHT CAL. ACT.



NAME	HIGH ALTITUDE ENGINEERING LABORATORY UNIVERSITY OF MICHIGAN DEPARTMENT OF AERO. AND ASTRO. ENGINEERING ANN ARBOR MICHIGAN
1114	
ALLEATH	
-2-68	
NAME	FOCUS REGULATOR AND DEFLECTION COIL DRIVERS
DRAWING NO.	H3-52017

SIMULATED
VERT. STAR MOT.

R1 10K

VERT.
AT WILL SWEEP

R2 39K

R3
390Ω
1/2W 5%

D1

VERT. DEFL.

S1 CONTROL

R9
1MEG

+6V -4V

S1
SH3001

D5

+16V -16V

50PF

C3

500PF

C4

680PF

C5

1.5K

100K

R12

100K

R13

42

100K

R10

100Ω

1MEG

C9

10K

R18

SIMULATED
HOR. STAR MOT.

10K

R18

HOR.
AT WILL SWEEP

10K

R19

130Ω

R21

704C

A3

1.5K

R28

680PF

C6

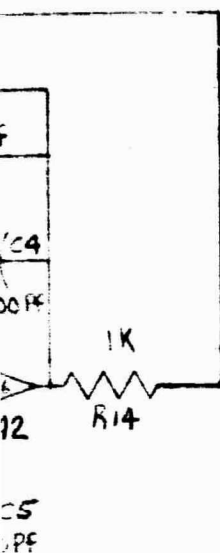
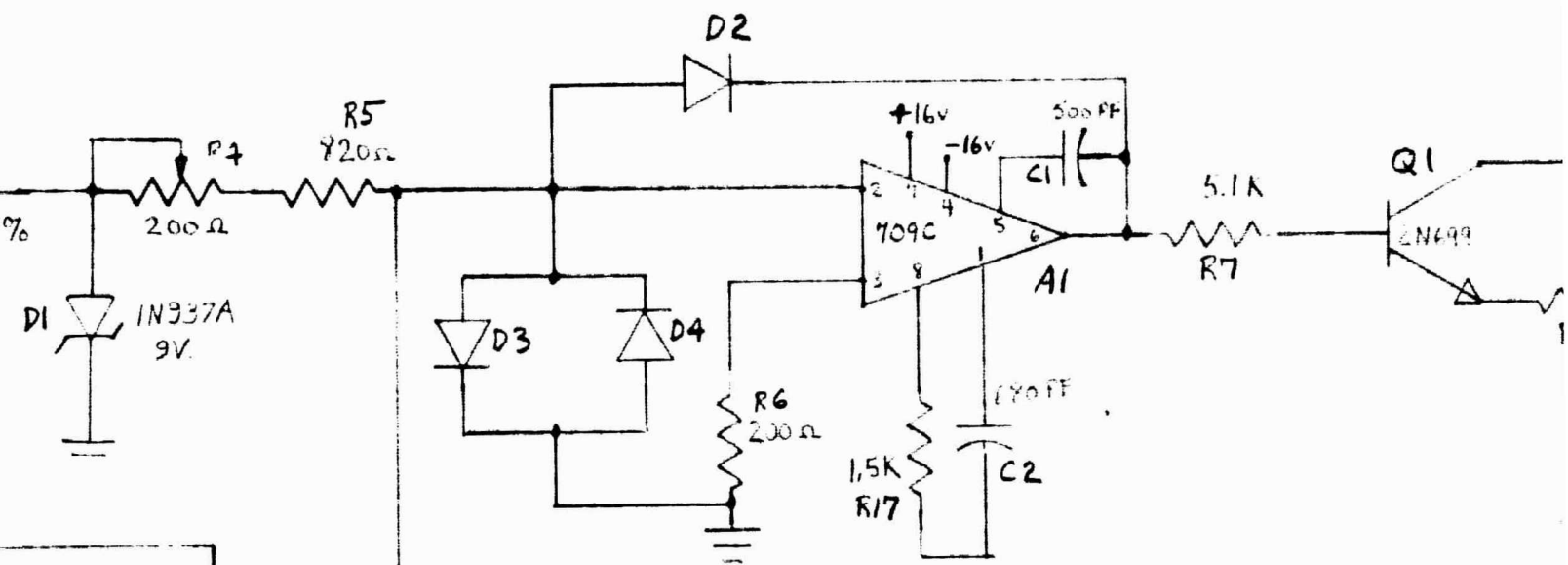
500

C7

R27 1.1K

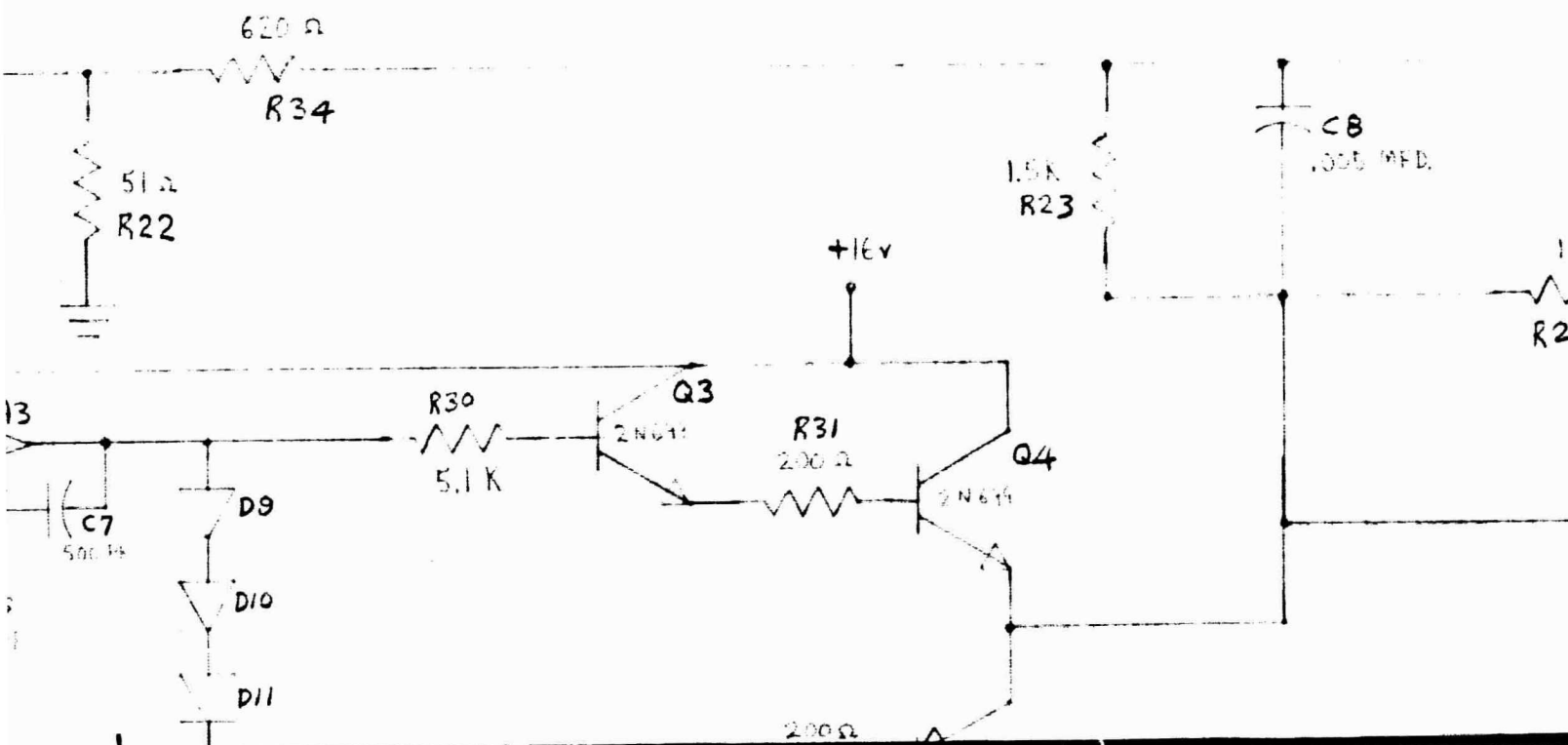
2.2	HX1
1.1	HX2
0.5	A1

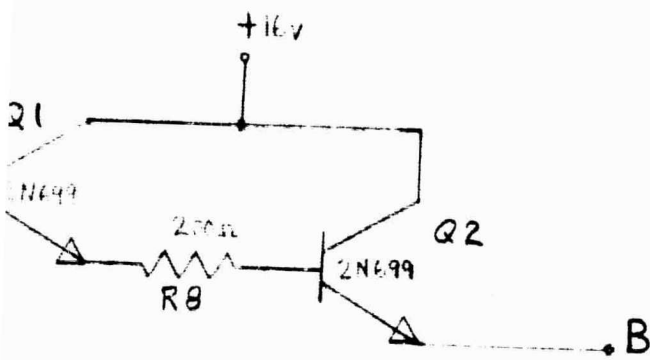
HOR. DEFL.



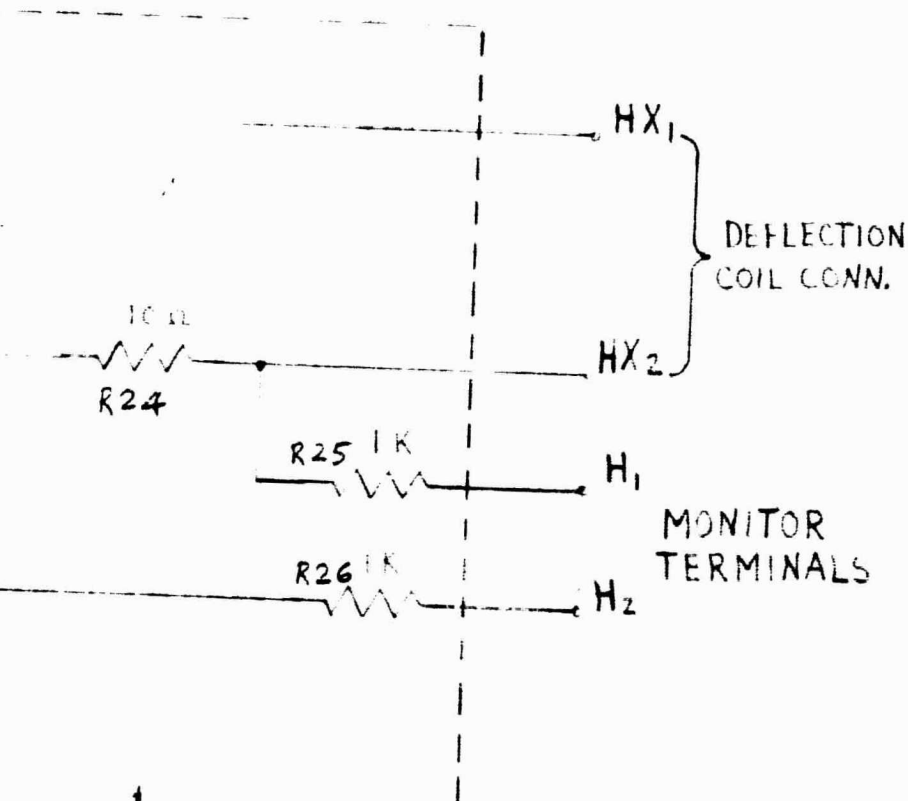
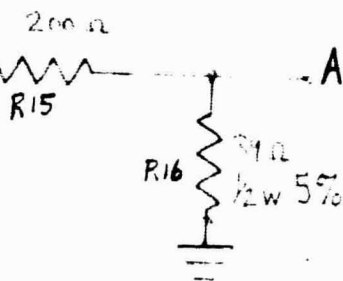
THE CIRCUIT IN THIS BOX IS IDENTICAL TO THE CIRCUIT IN THE DASHED BOX BELOW.

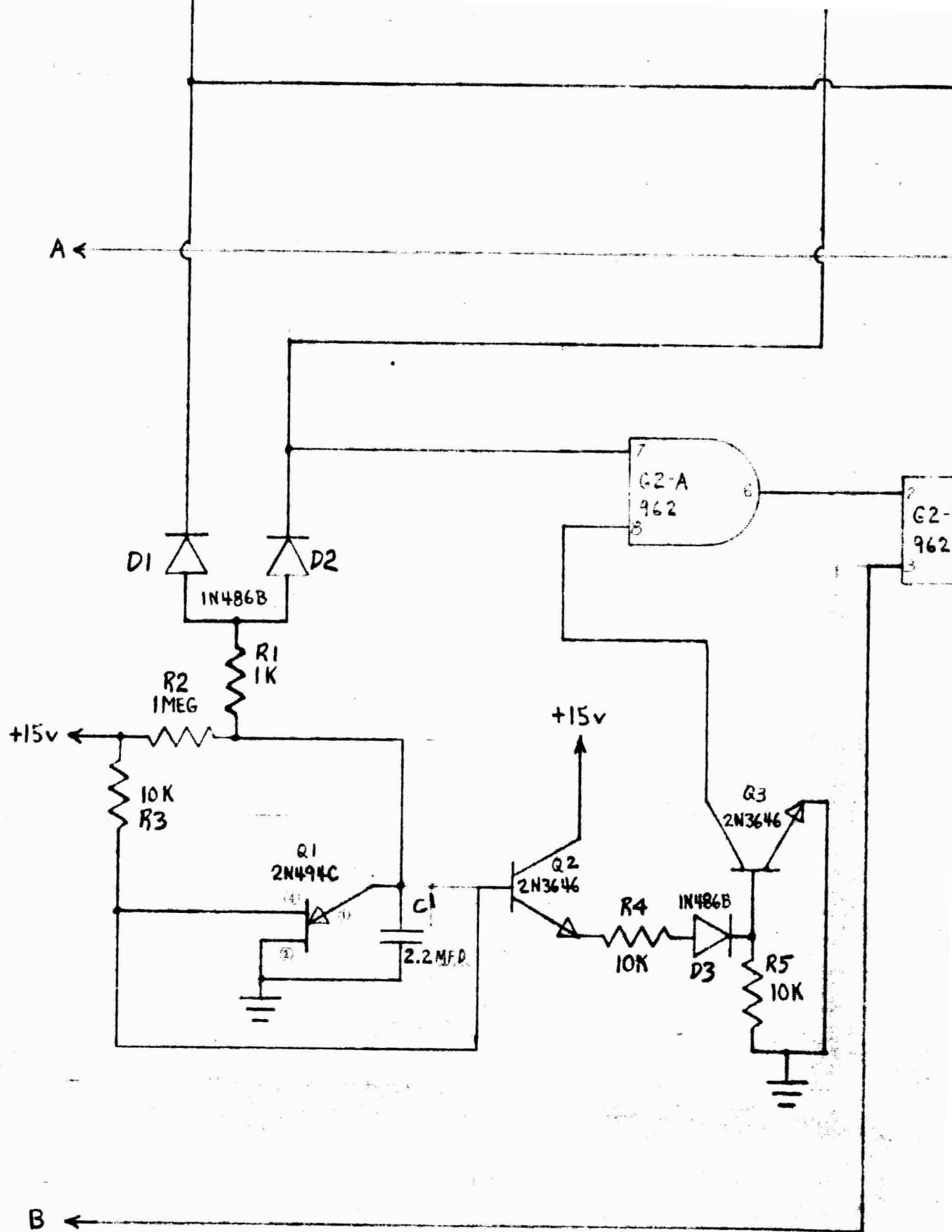
V_{x1} } DEFLECTION
 V_{x2} } COIL CONN.
 V_1 } MONITOR
 V_2 } TERMINALS

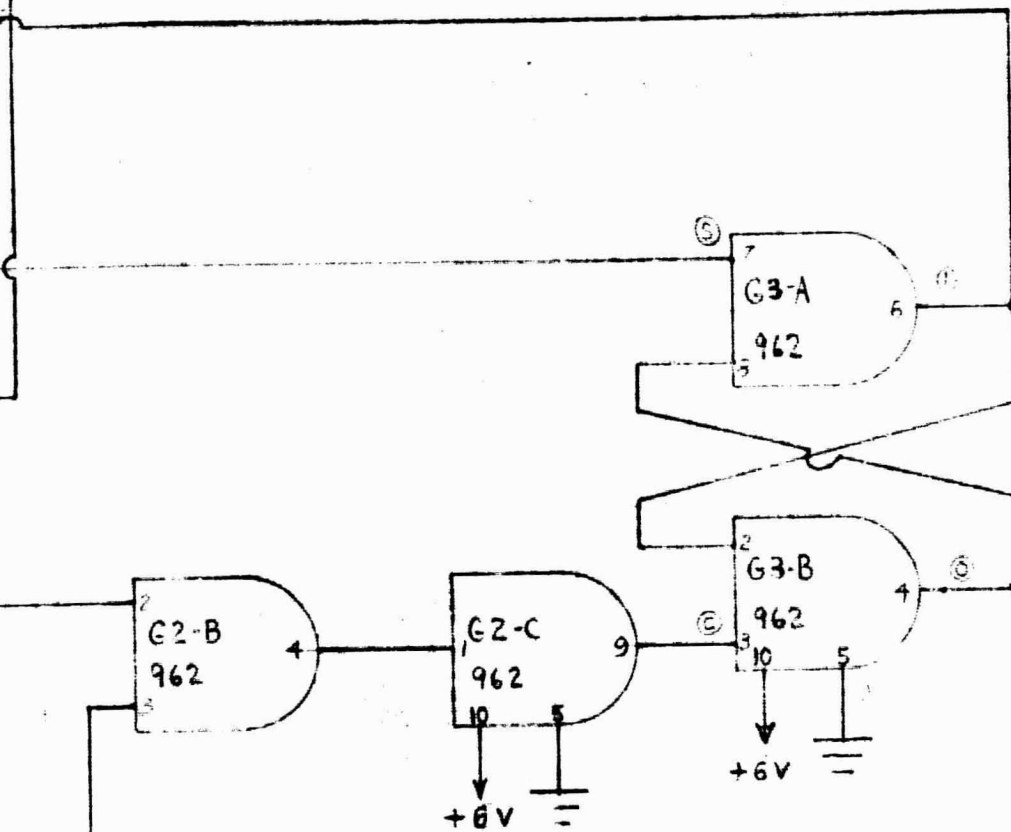




FOCUS COIL
DRIVE CONN.







NOTES:
1. ALL RESISTORS 1/4W, 5%

		SCALE	NONE
		PROJ. NO.	01114
		DRAWN BY	ED GILREATH TED PATTERSON
		DATE	4-5-68
		FOR ASSEMBLY	
		MATERIAL	
LET.	CHANGE	DATE	WEIGHT CAL. ACT.

→ H

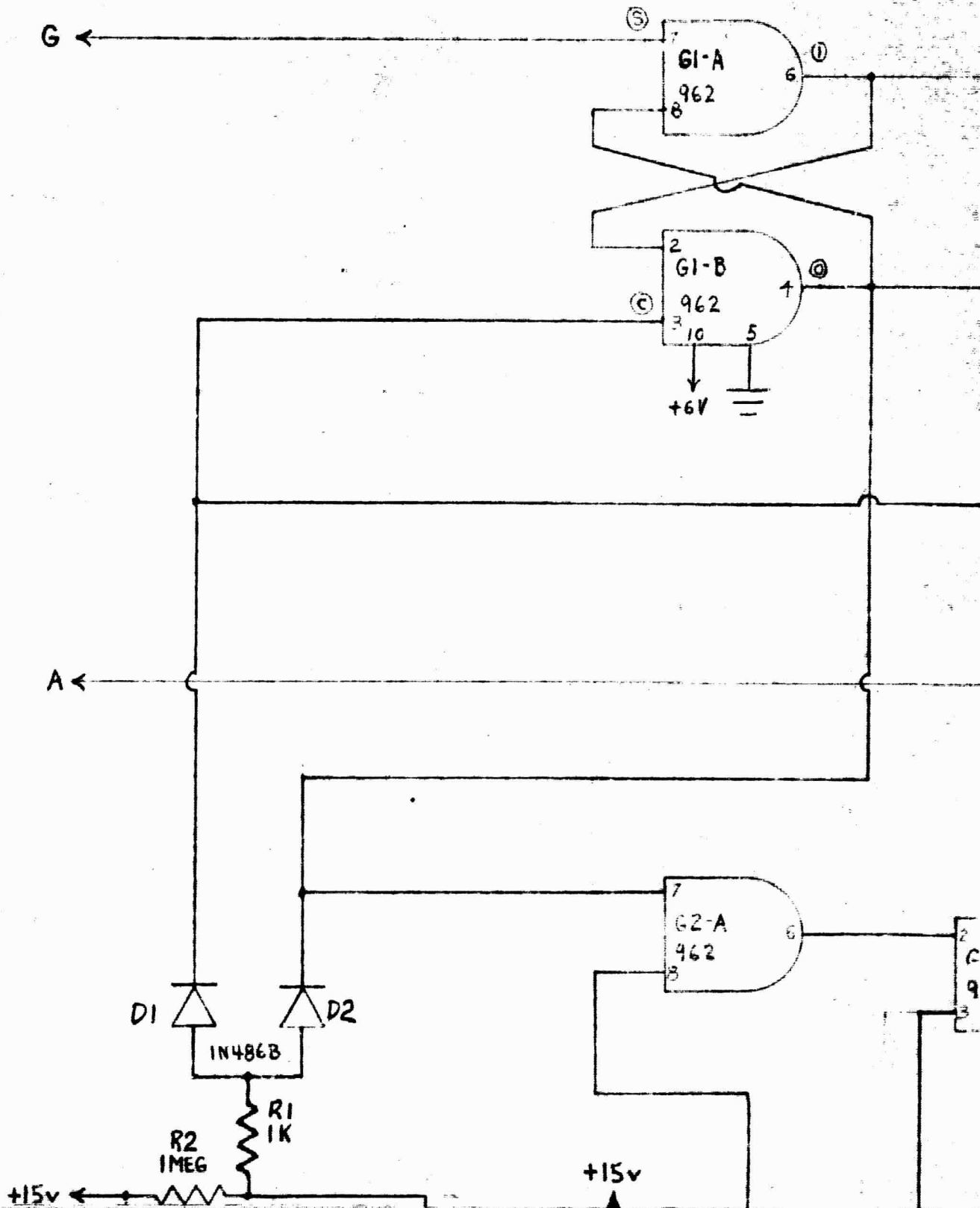
→ J-C

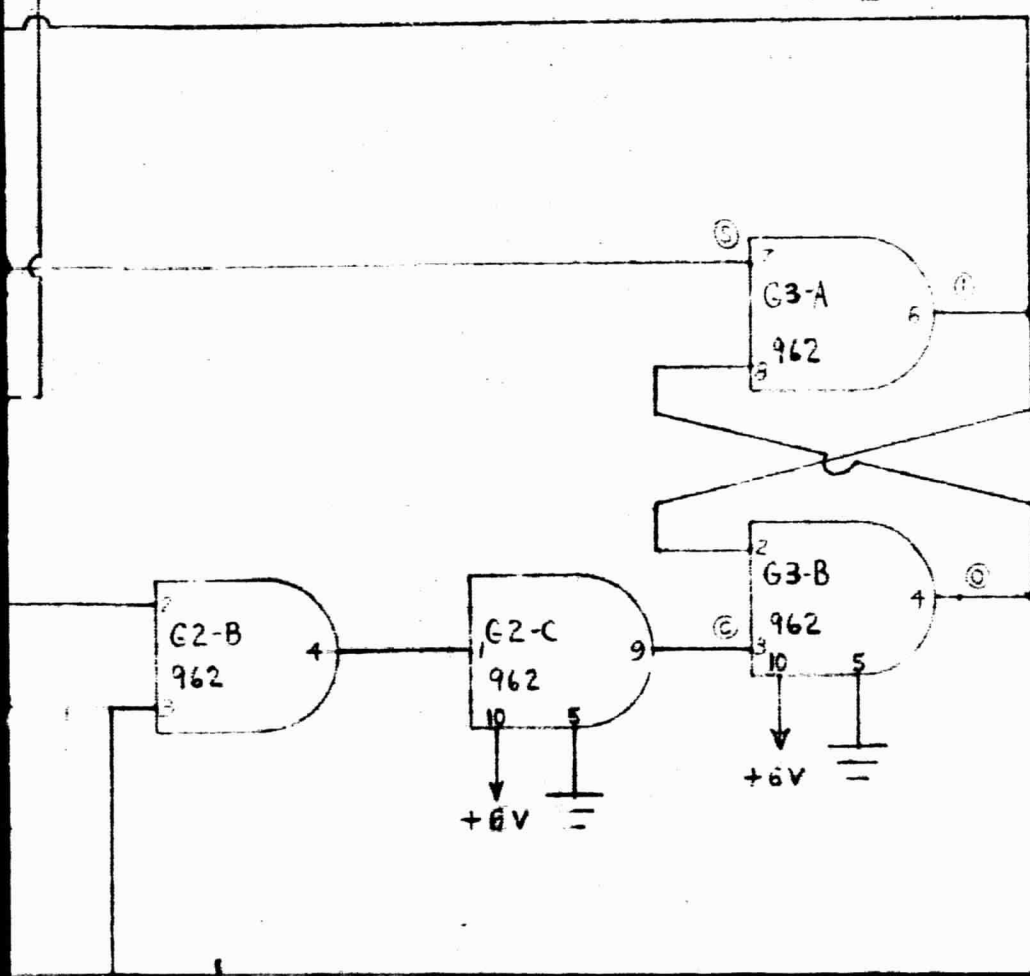
22	KEYWAY
21	G
20	K-D
19	L-F
18	J-C
17	H
16	B
15	+6V
14	
13	
12	+16V
11	GND
10	
9	
8	
7	A
6	
5	
4	
3	
2	
1	

NONE	HIGH ALTITUDE ENGINEERING LABORATORY UNIVERSITY OF MICHIGAN DEPARTMENT OF AEROSPACE ENGINEERING ANN ARBOR MICHIGAN
01114	
ED GILREATH TED PATTINSON	
4-5-68	
	NAME DATA TELESCOPE LOGIC CARD
	DRAWING NO. H3-52018

III

IV





VI

→ K-D

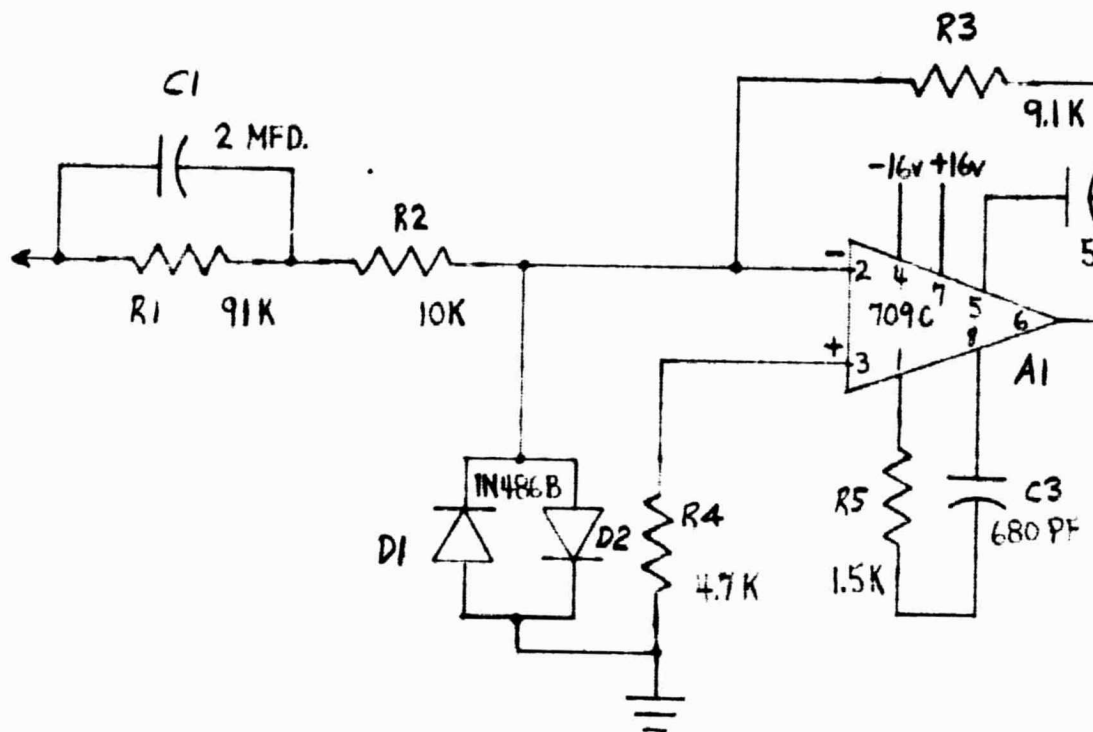
→ L-F

→ H

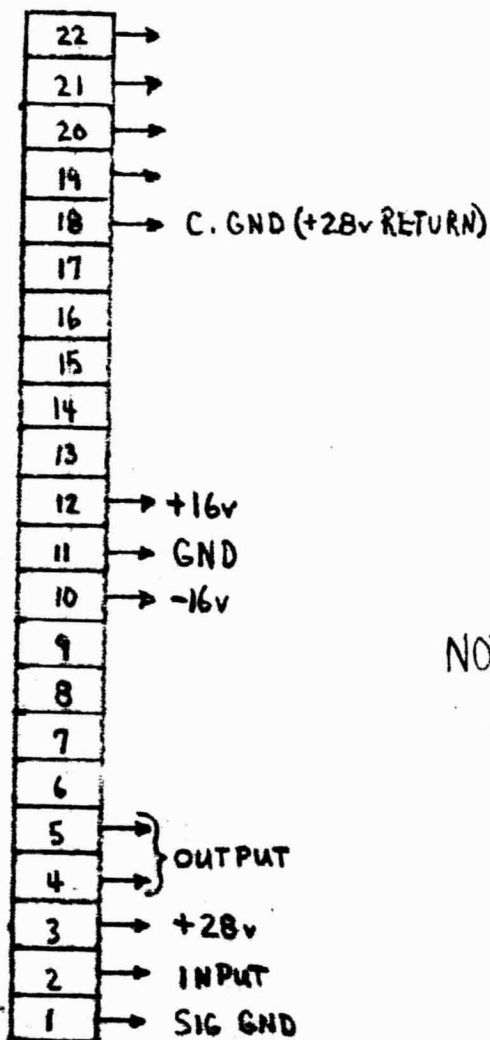
→ J-C

22	KEYWAY
21	G
20	K-D
19	L-F
18	J-C
17	H
16	B

INPUT
PIN 2

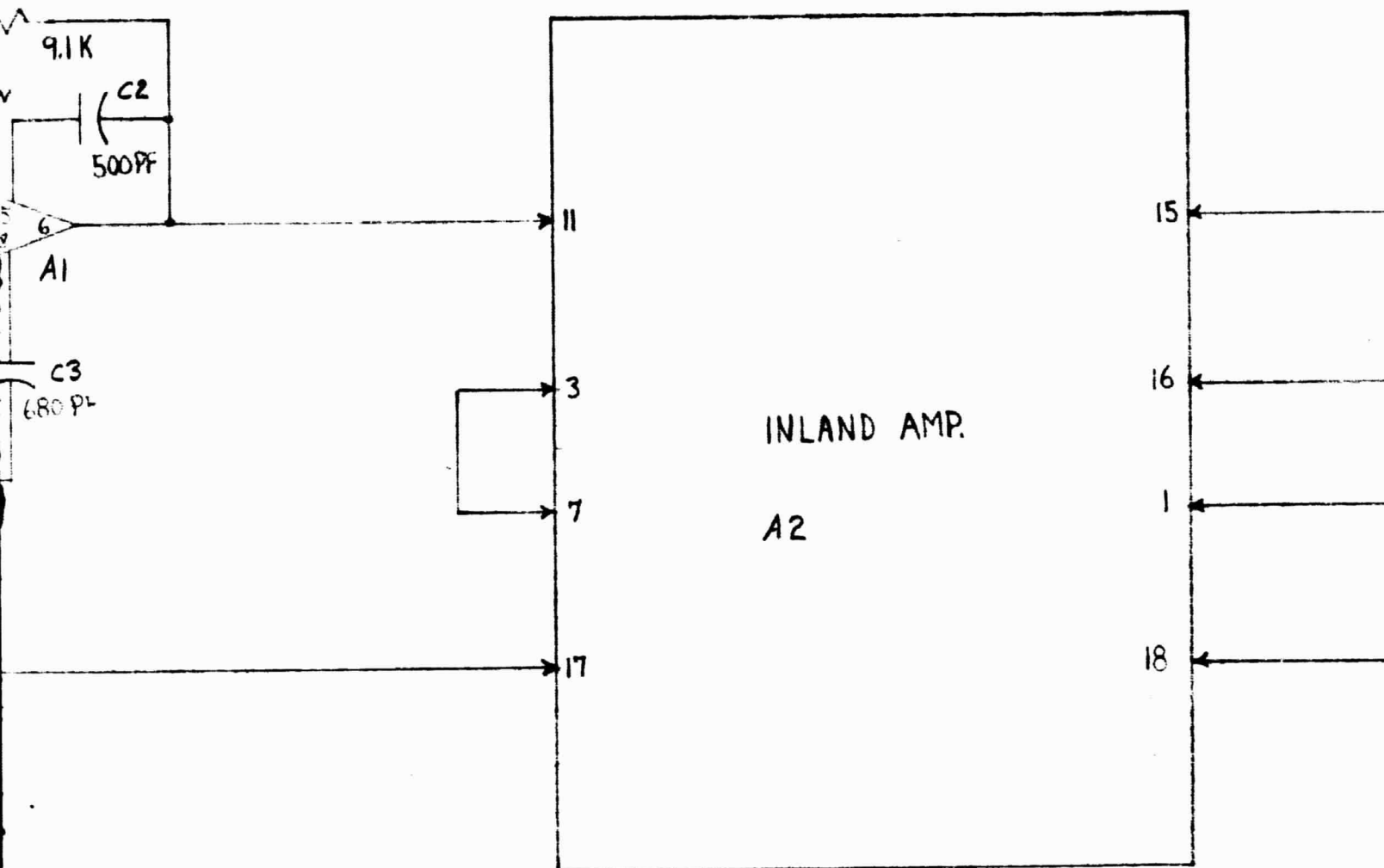


+28 v
PIN 3



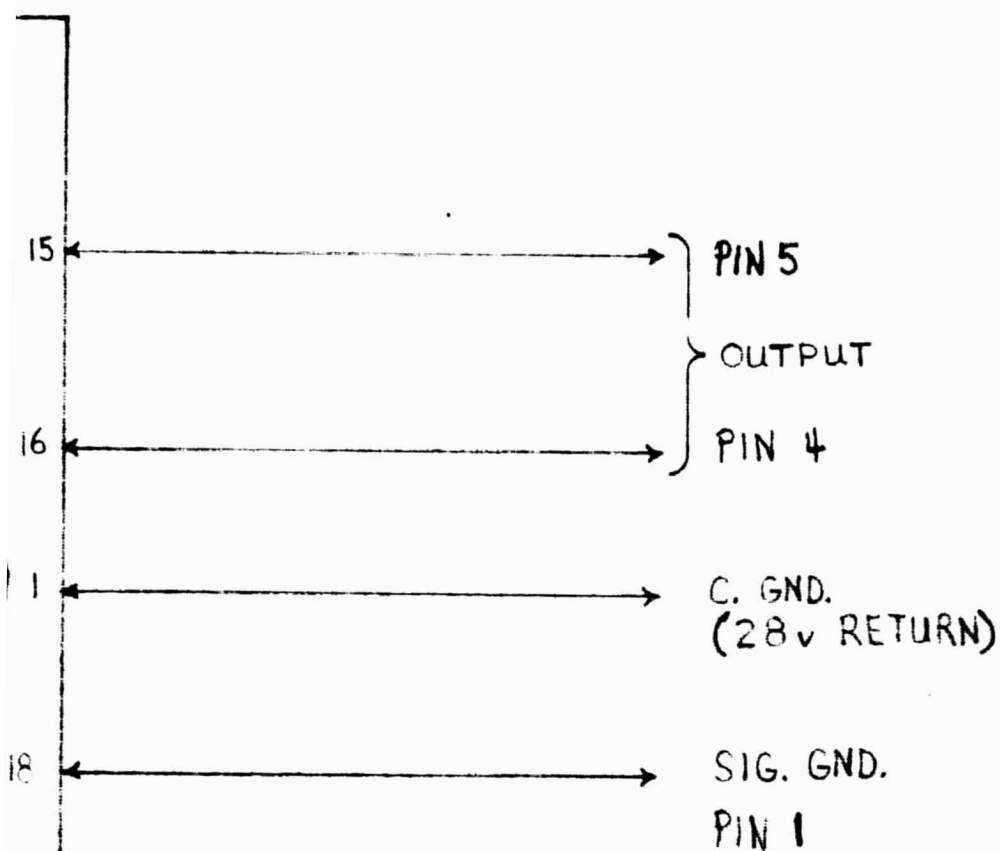
NOTE:

ALL RESISTORS $\frac{1}{4}w$ 5% UNLESS NOTED.



			SCALE	
			PROJ. NO.	
			DRAWN BY	<i>CE 5/10/68</i>
			DATE	APRIL 15 1968
			FOR ASSEMBLY	
			MATERIAL	
LET.	CHANGE	DATE	WEIGHT CAL. ACT.	

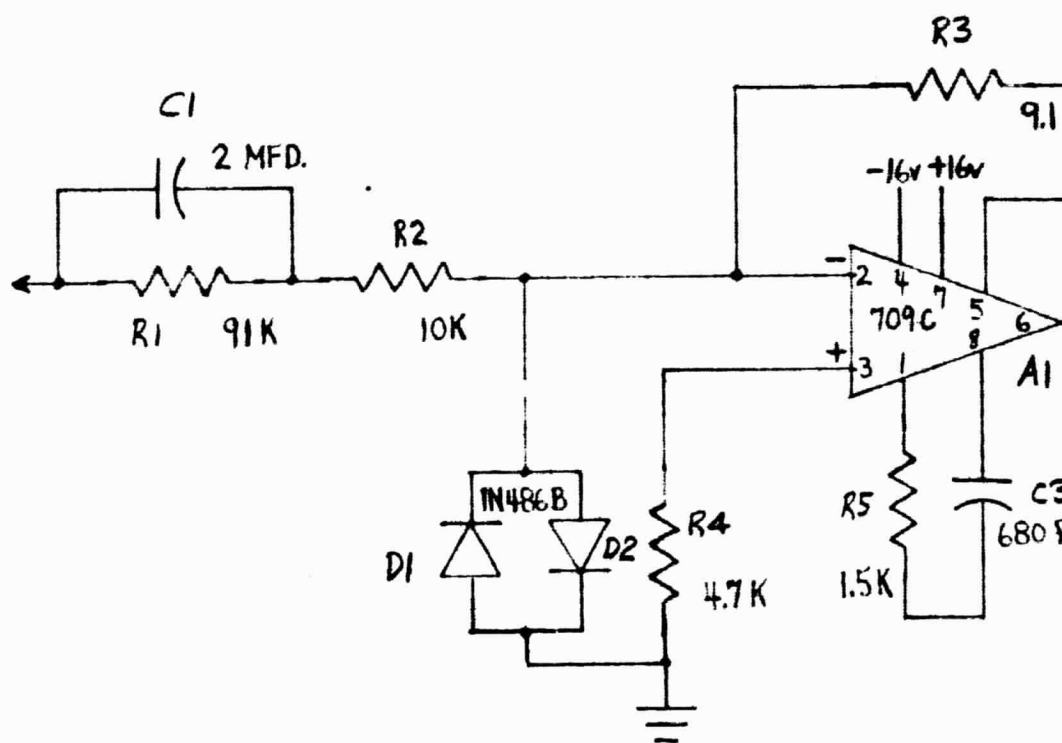
II



	HIGH ALTITUDE ENGINEERING LABORATORY UNIVERSITY OF MICHIGAN DEPARTMENT OF AEROSPACE ENGINEERING ANN ARBOR MICHIGAN
<i>E. A. Smith</i> APRIL 15 1968	
	NAME TORQUE MOTOR DRIVE AMP.
	DRAWING NO. H3-52021

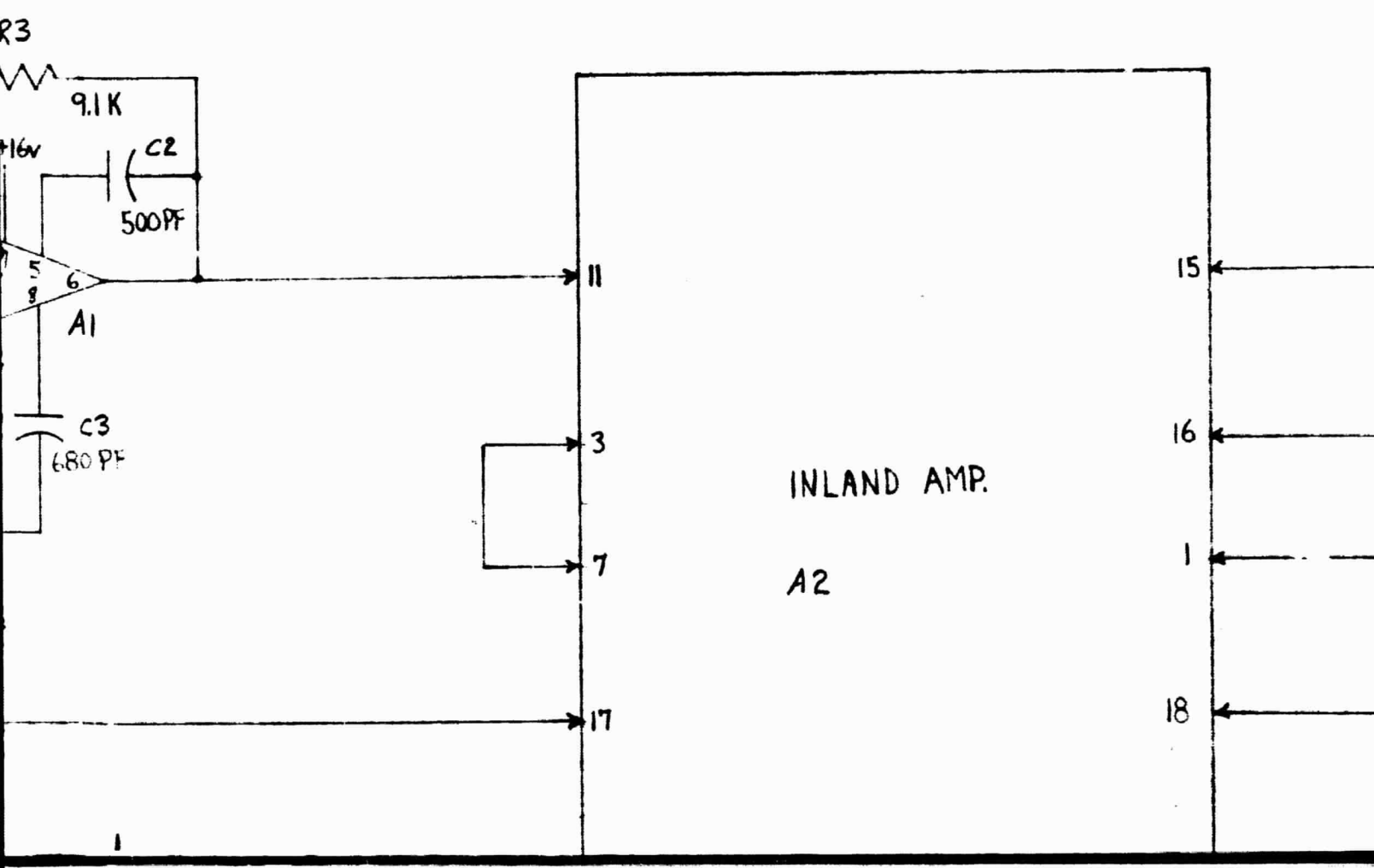
IV

INPUT
PIN 2

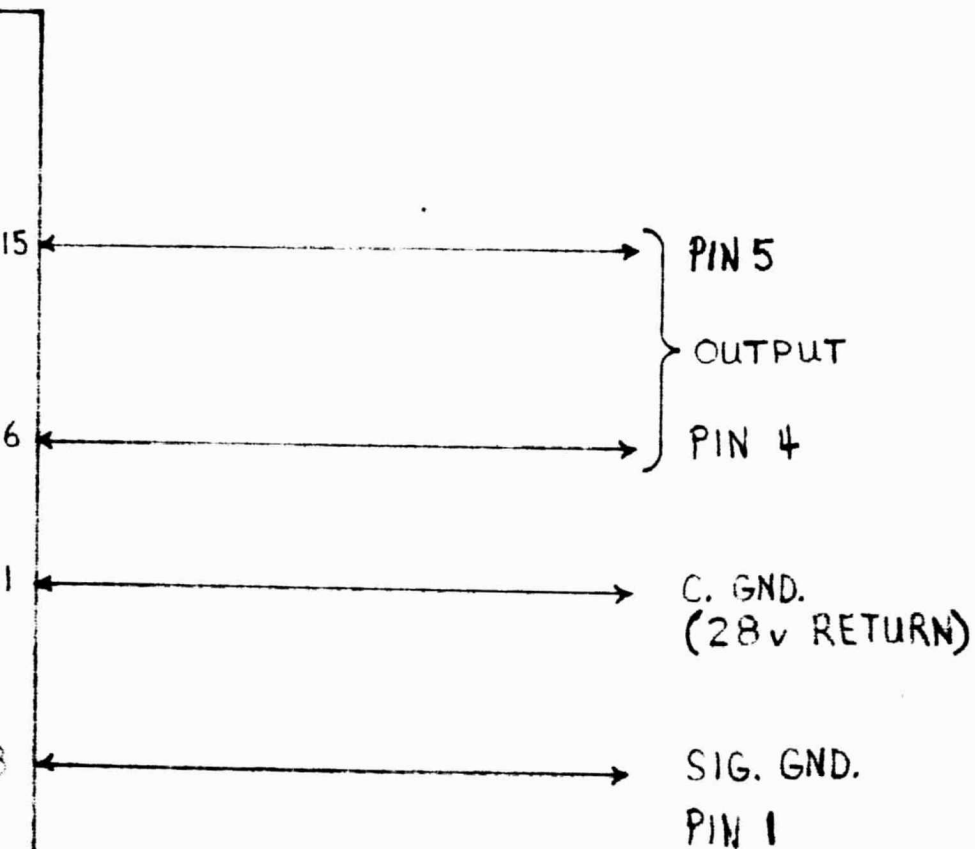


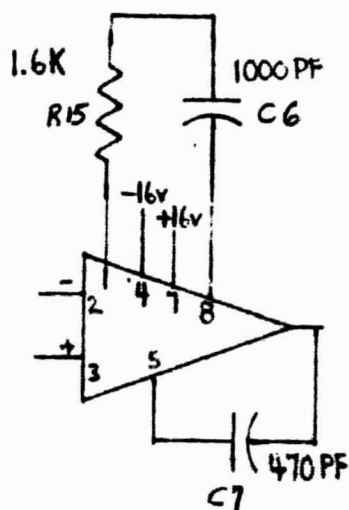
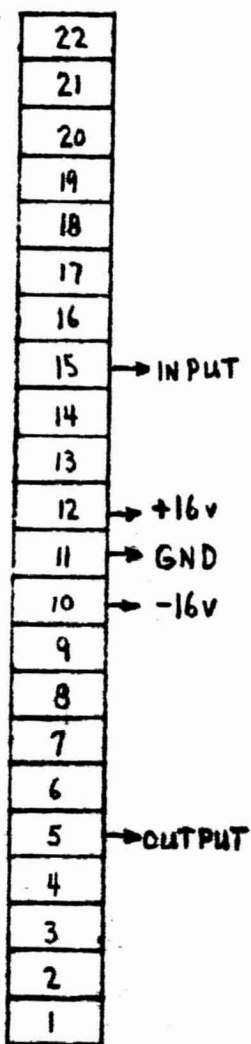
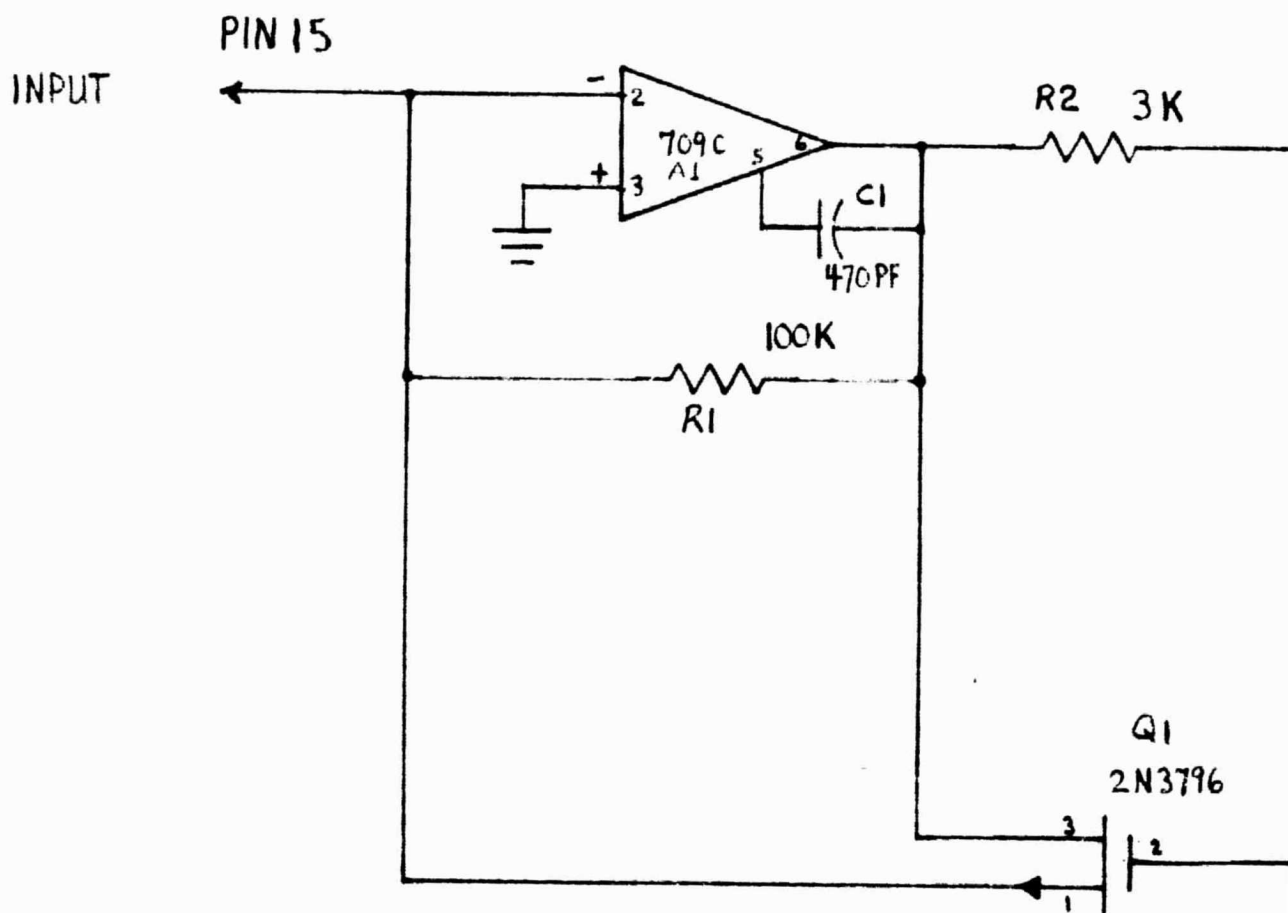
+28 v
PIN 3

IV



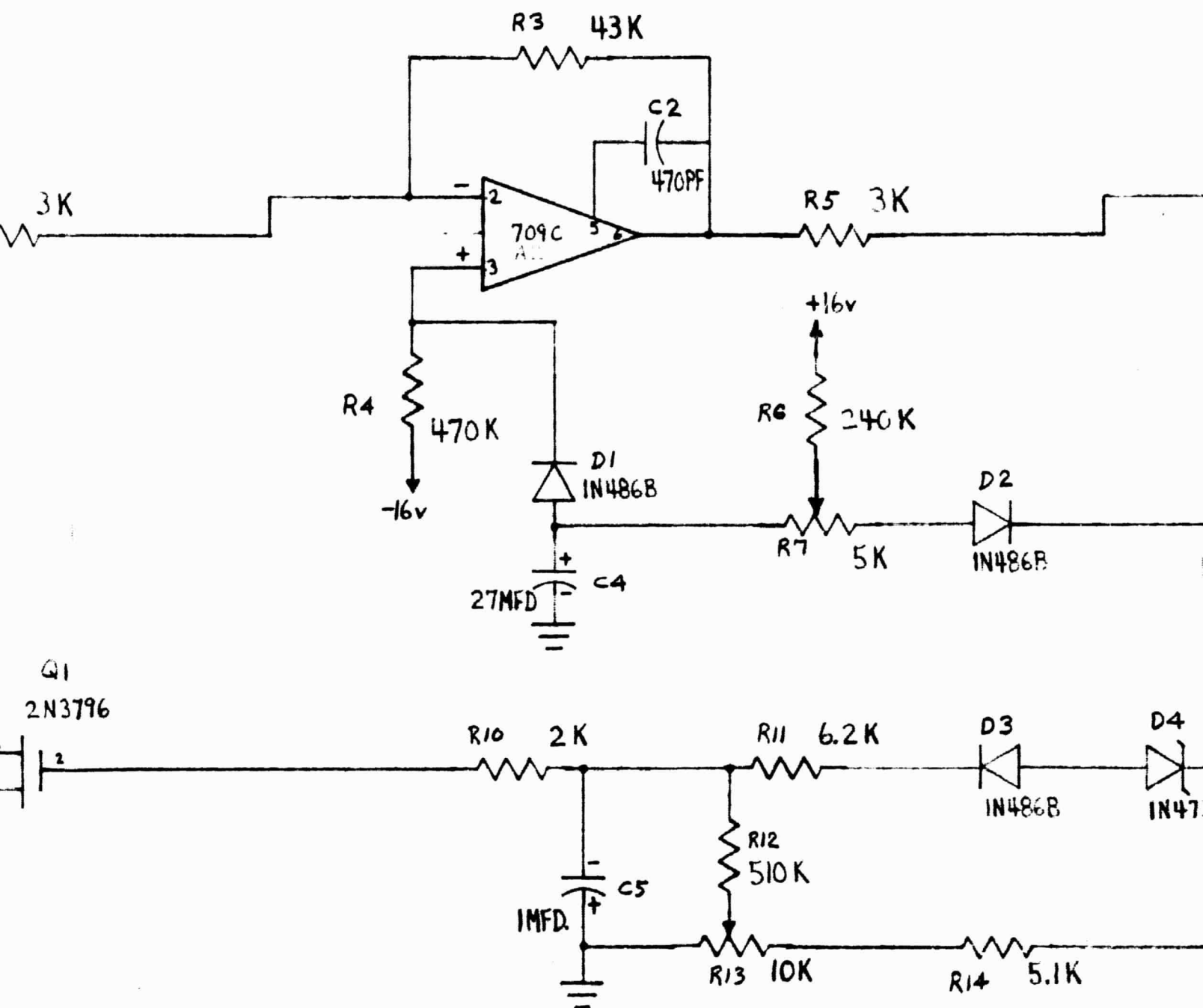
~~VI~~





TYPICAL AMP. CONNECTIONS

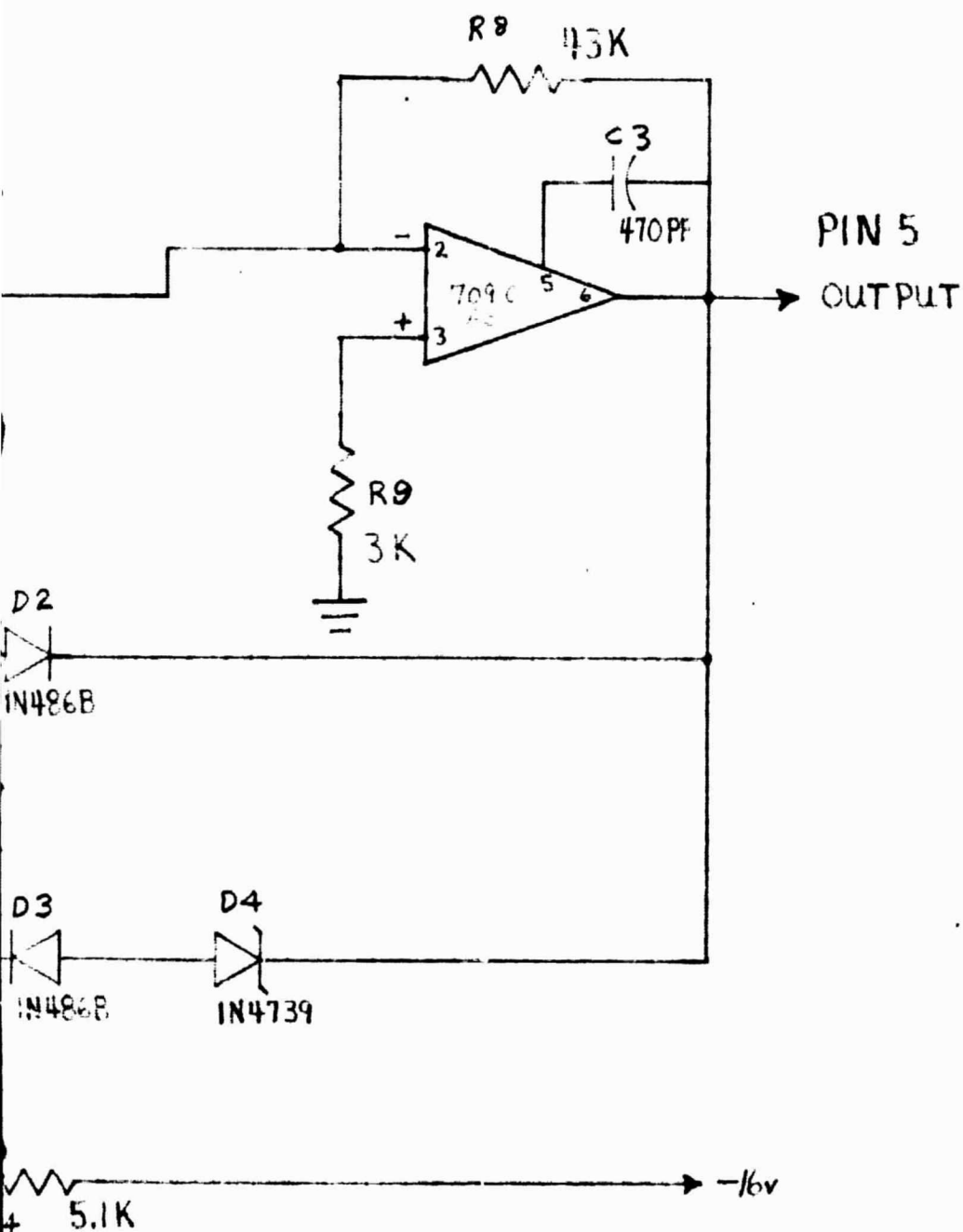
ALL RESISTORS $\frac{1}{4}$ W 5% UNL



INSTRUCTIONS

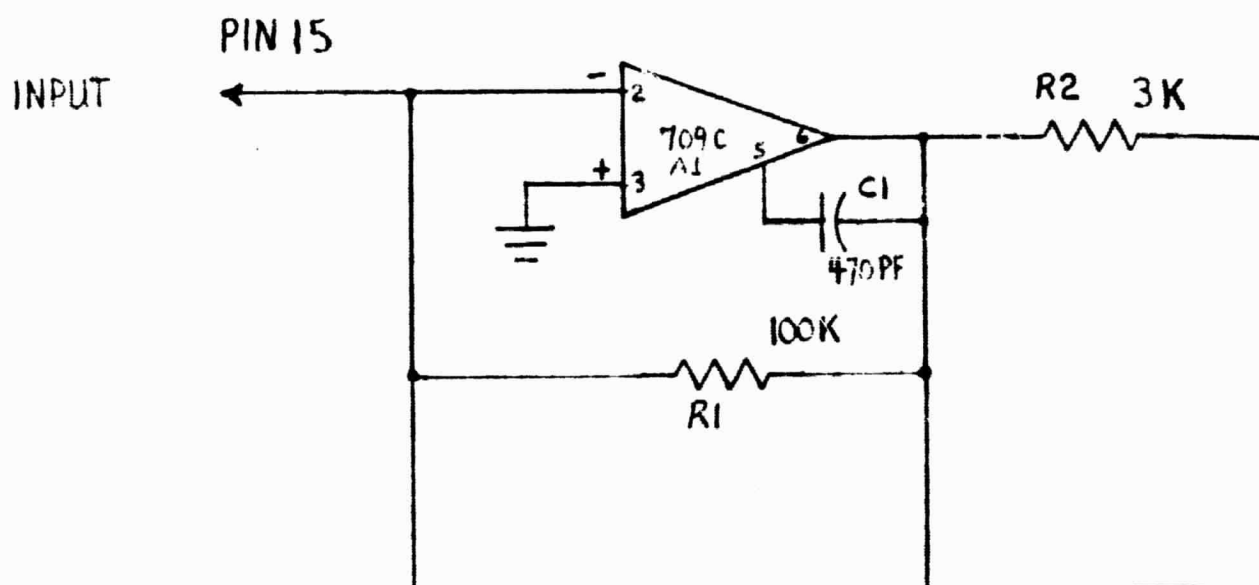
5% UNLESS NOTED

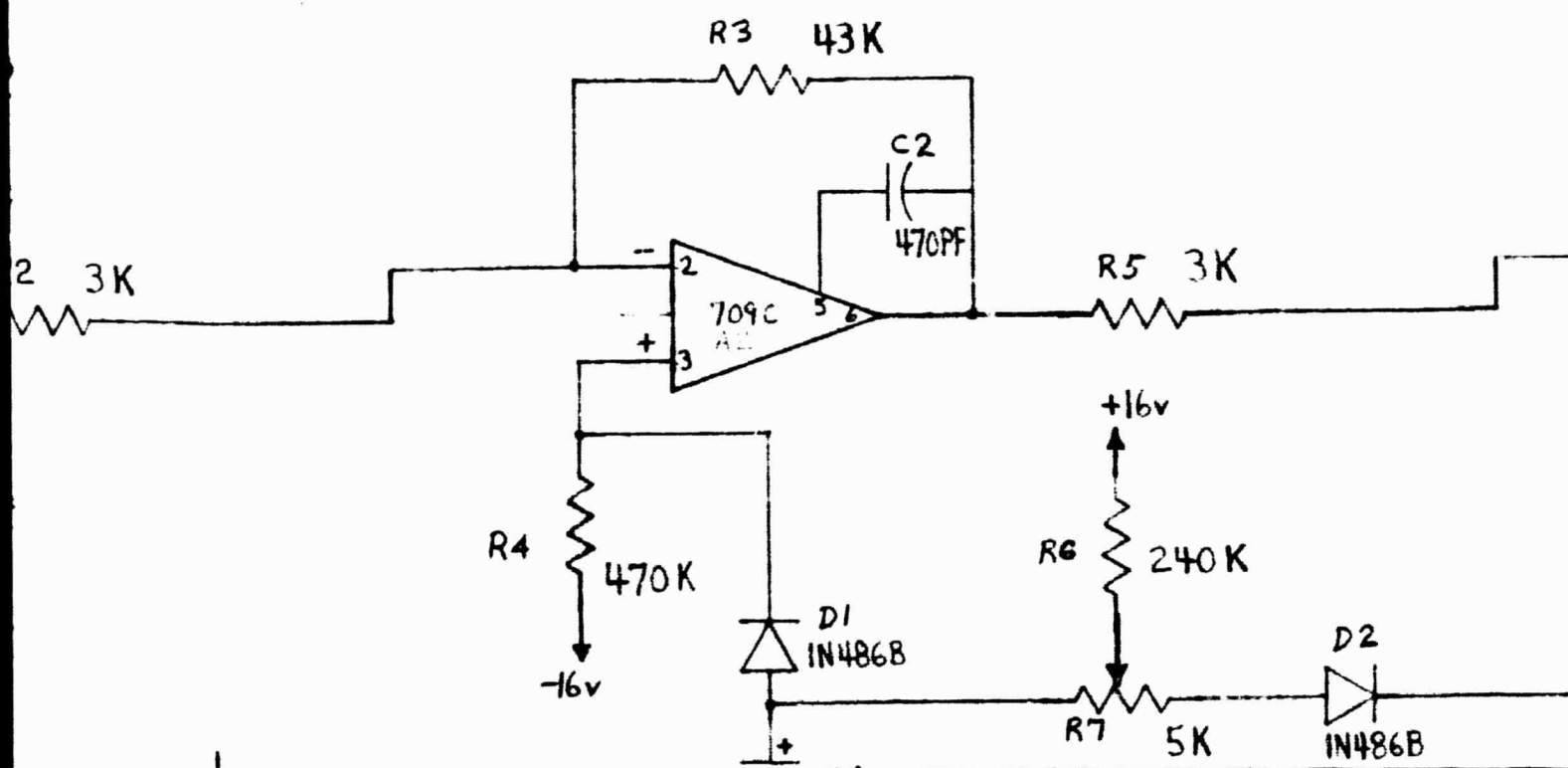
		SCALE	
		PROJ. NO.	01114
		DRAWN BY	<i>E. J. Smith</i>
		DATE	4-15-1968
		FOR ASSEMBLY	
		MATERIAL	
	CHANGE	DATE	WEIGHT CAL. ACT.



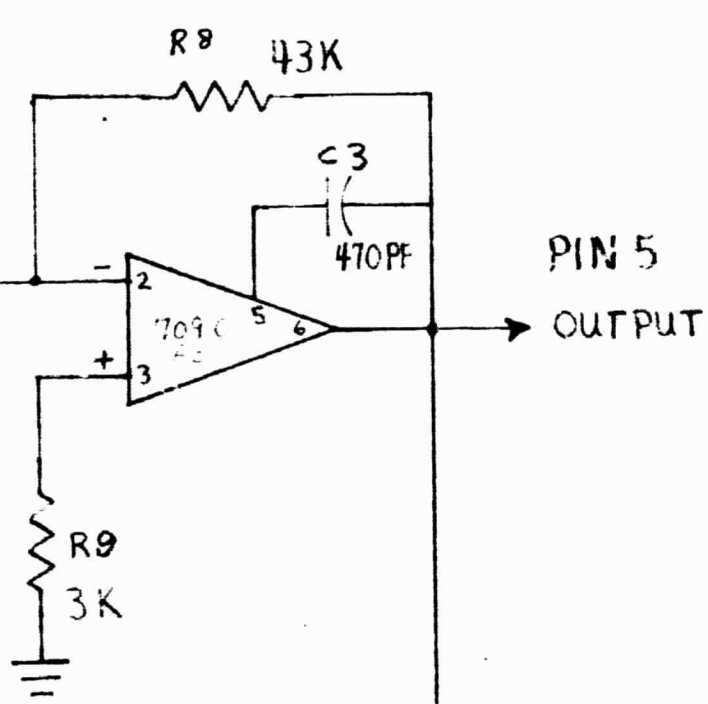
DATE		HIGH ALTITUDE ENGINEERING LABORATORY UNIVERSITY OF MICHIGAN DEPARTMENT OF AEROSPACE ENGINEERING ANN ARBOR MICHIGAN
NO.	01114	
AWN BY	<i>[Signature]</i>	
DATE	4-15-1968	
FOR EMBLY		NAME PRE-AMPLIFIER, SIG. DISSECTOR
SERIAL		DRAWING NO. H3-52022
MT CAL. ACT.		

III





~~VI~~



CENTER
WITHIN .001

3.5

30°

NOTE 2

1.0
RUM.

$\frac{1}{4}$

$\frac{7}{32}$

$\frac{3}{4}$

$\frac{3}{4}$

1.951
1.949

3.902
3.898

NOTES:

1. SLIT WITH $\frac{1}{32}$ SAW
OTHER MACHINING
2. DRILL THRU (3) PLAC.
LIMITS .174 - .180
COIL PART NO. 20
NOT TAP THRU.) C

4

30°

NOTE 1.

$\frac{7}{32}$

$\frac{5}{8}$

5.746
5.744

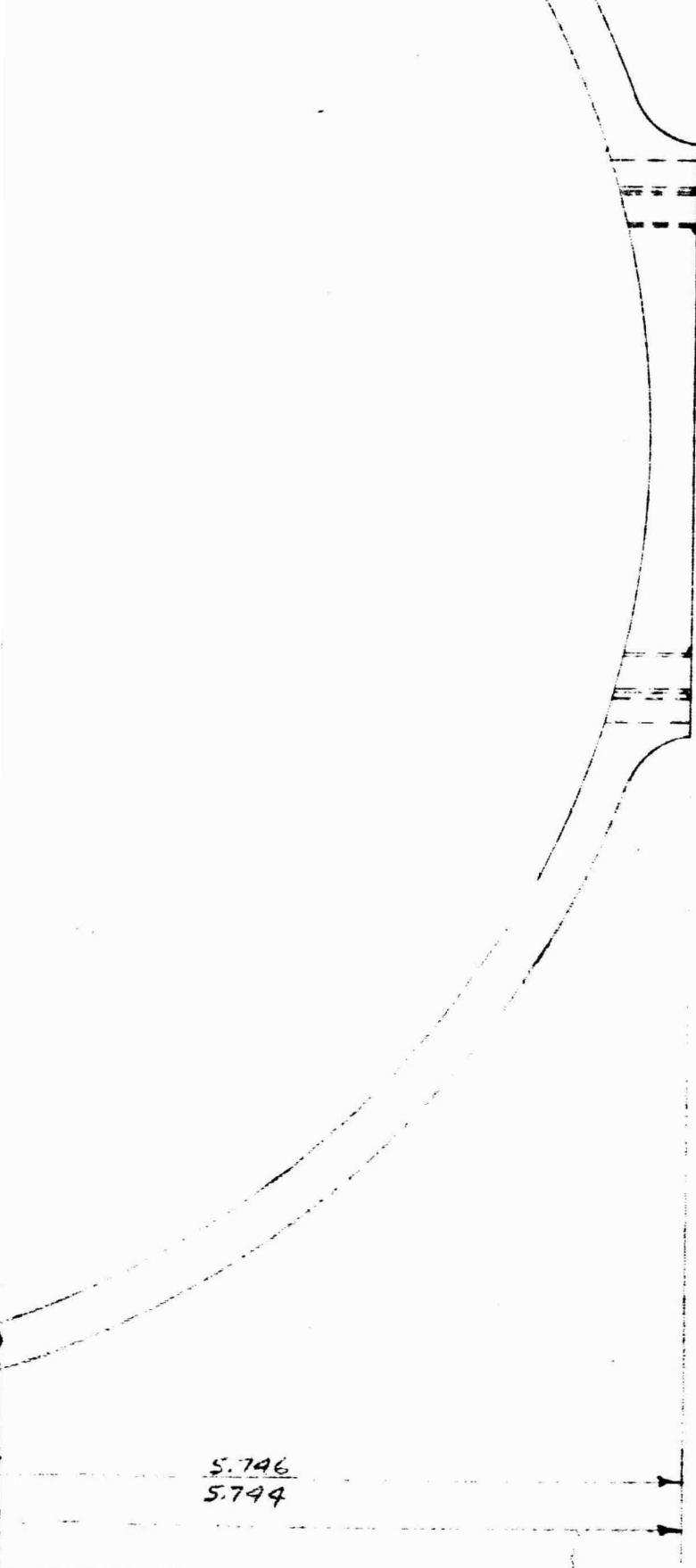
11.491
11.484

5.746
5.744

32 SAW AFTER COMPLETION
CHINING & INSPECTION.
3) PLACES #16 DRILL. DIA.
-.180. TAP WITH HELI-
NO. 2 CPA-H3. (TAP WILL
RU.) C'BORE .270 DIAM.

11/1

		SCALE	FULL
		PROJ. NO.	01114
		DRAWN BY	F3
		DATE	9/20/68
		FOR ASSEMBLY	
		MATERIAL	AZ-31B
LET.	CHANGE	DATE	WEIGHT CAL. ACT.



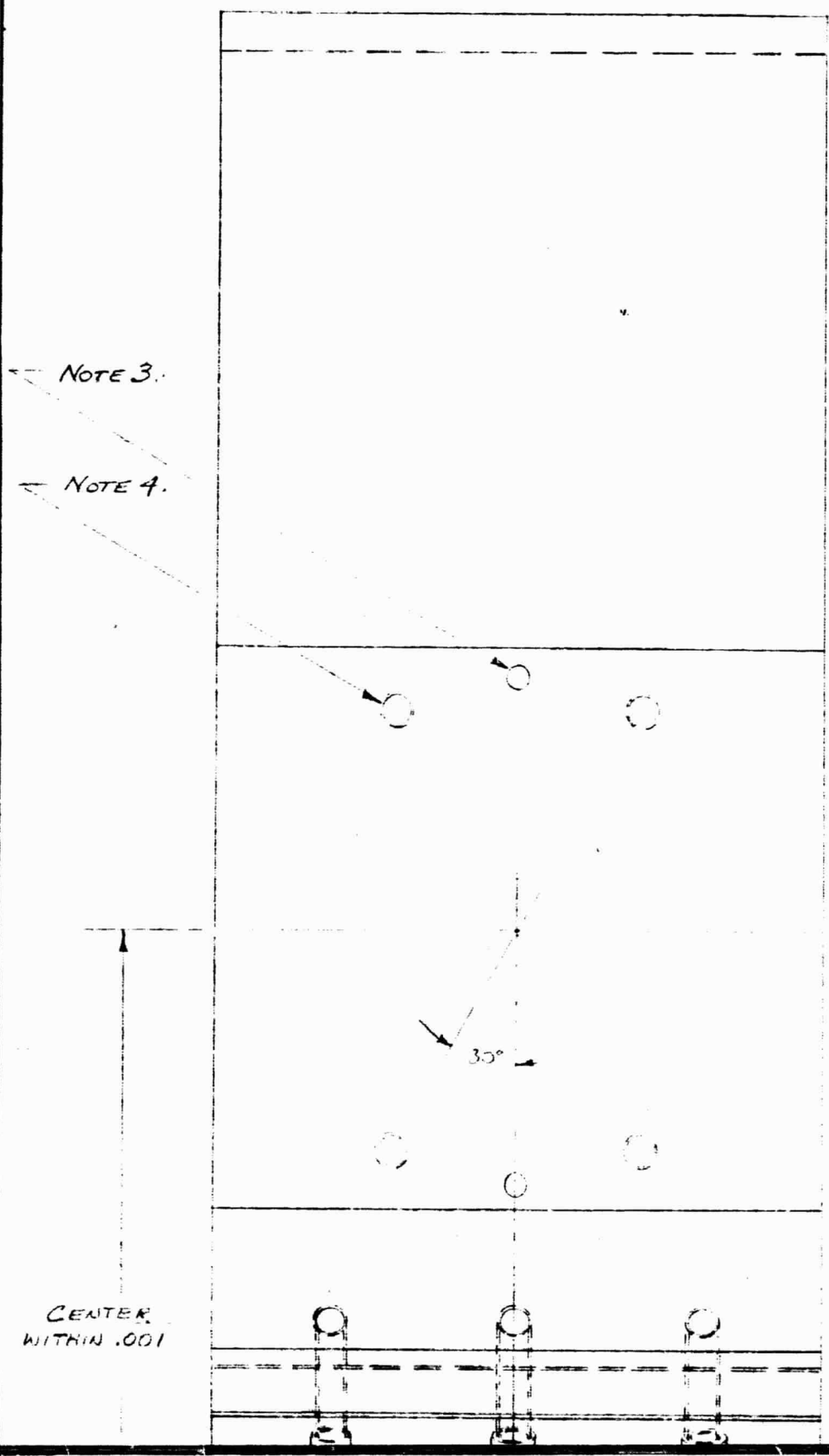
5.746
5.744

	FULL	HIGH ALTITUDE ENGINEERING LABORATORY UNIVERSITY OF MICHIGAN DEPARTMENT OF AERO. AND ASTRO. ENGINEERING ANN ARBOR MICHIGAN
NO.	01114	
N	F3	
	4/20/68	NAME
LY		INNER GIMBAL
AL	AZ-31B	DRAWING
CAL		NO. H3-52023
ACT.		

III

NOTES

- 3. DRILL TH
ON CIRC
- 4. DRILL TH
TAP WITH
DIAM. .20
- 5. ANODIZE.



11.5

10.9985
11.0000

7/16 R. NOM
TYPICAL
(5) PLACES.

3.5

NOTE 2.

CENTER
WITHIN .001

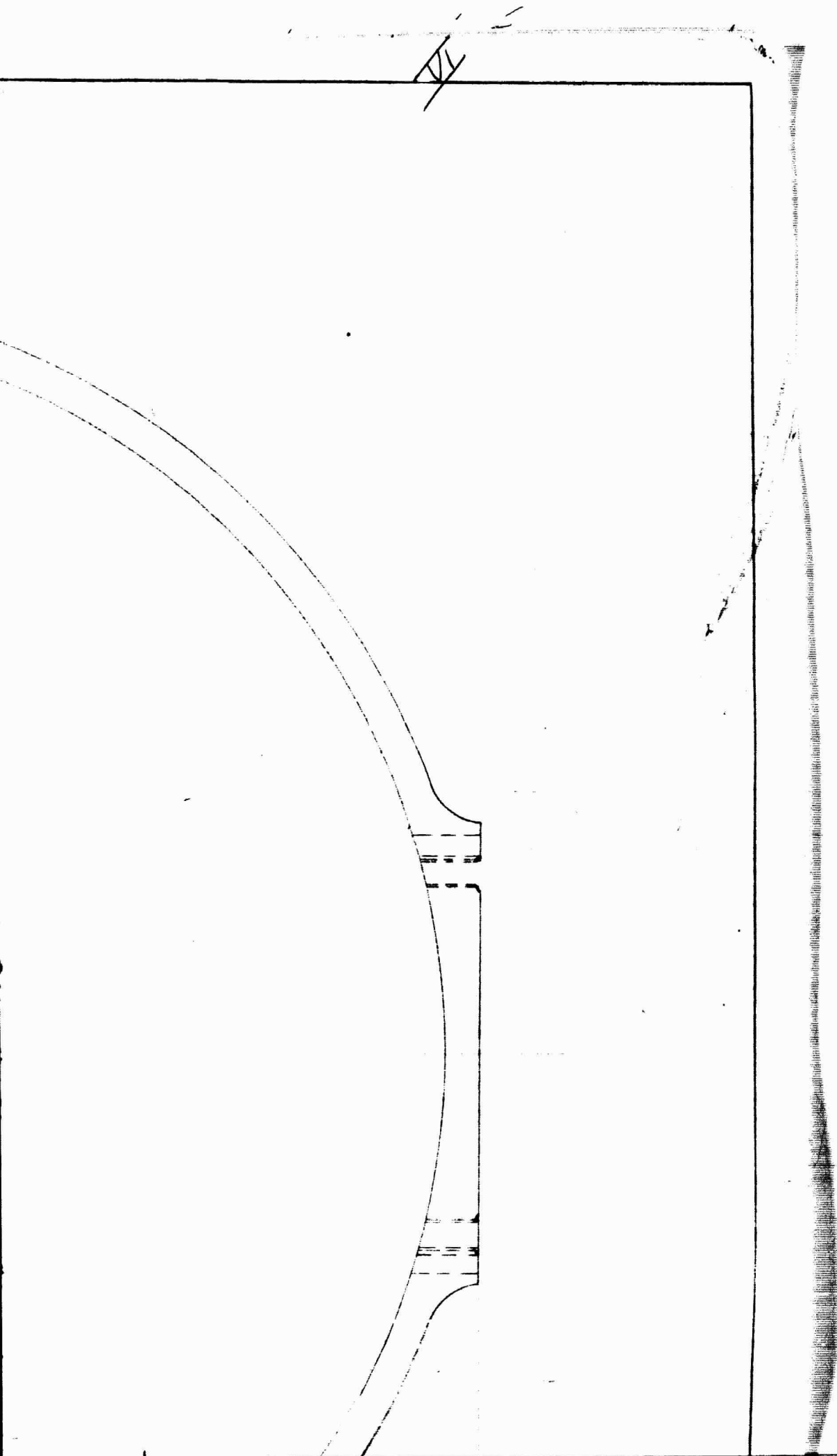
N

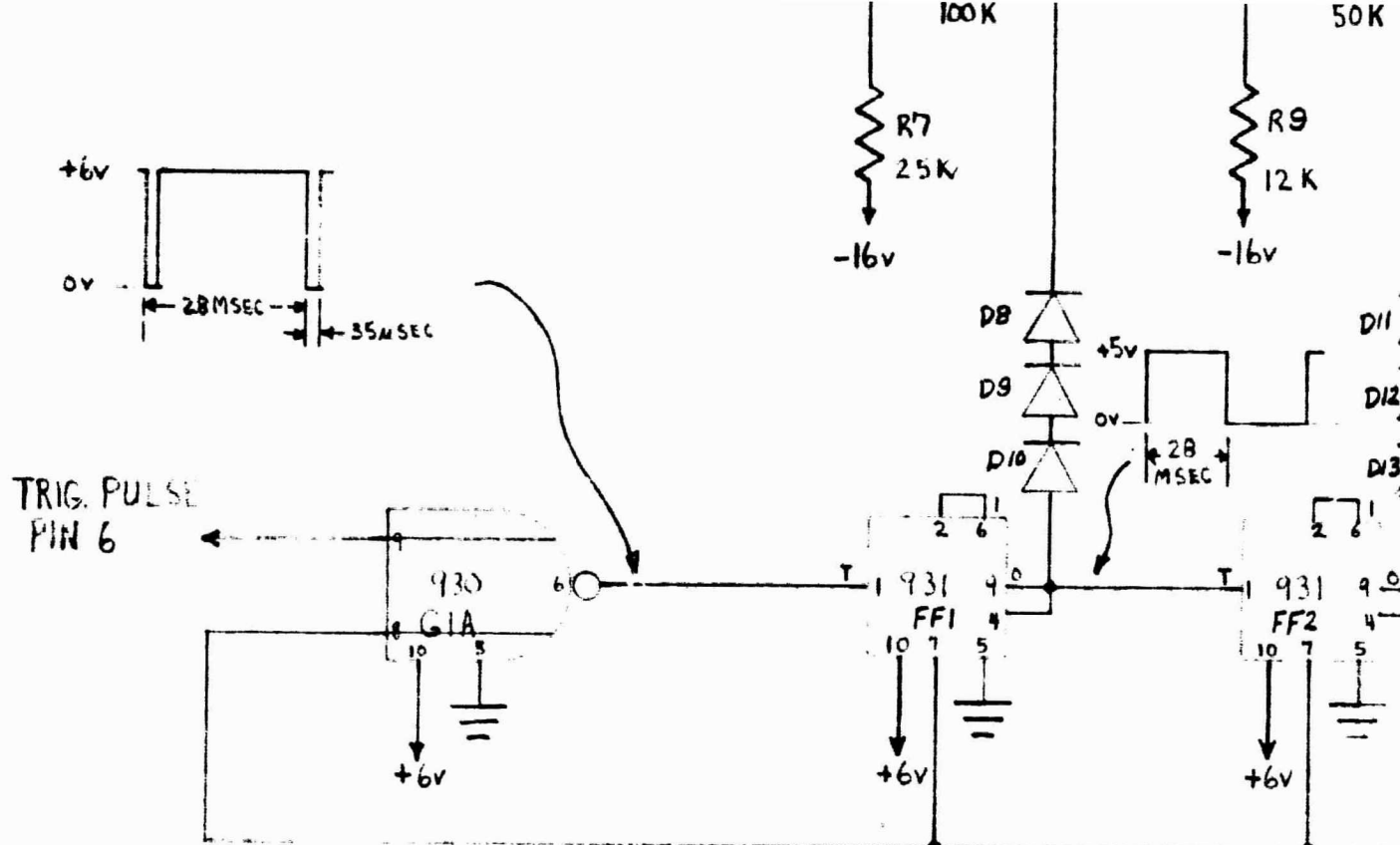
KILL THRU (2) HOLES $.1254 \pm .0002$ DIA. ON $3.1570 \pm .0002$ B.C.
ON CIRCLE CONCENTRIC WITH NOTE 4 HOLES. TYPICAL (2) PLACES.
KILL THRU (4) HOLES #16 DRILL DIA. LIMITS $.174-.180$. $3.157 \pm .001$ B.C.
F WITH HELI-COIL PART #2 CPA-H3 AFTER C'SINK 120° TO
AM. $.20-.23$. TYPICAL (2) PLACES.
MODIZE. $.0001-.0003$ THICK.

NOM
CAL
PLACES.

30°

NOTE 1.

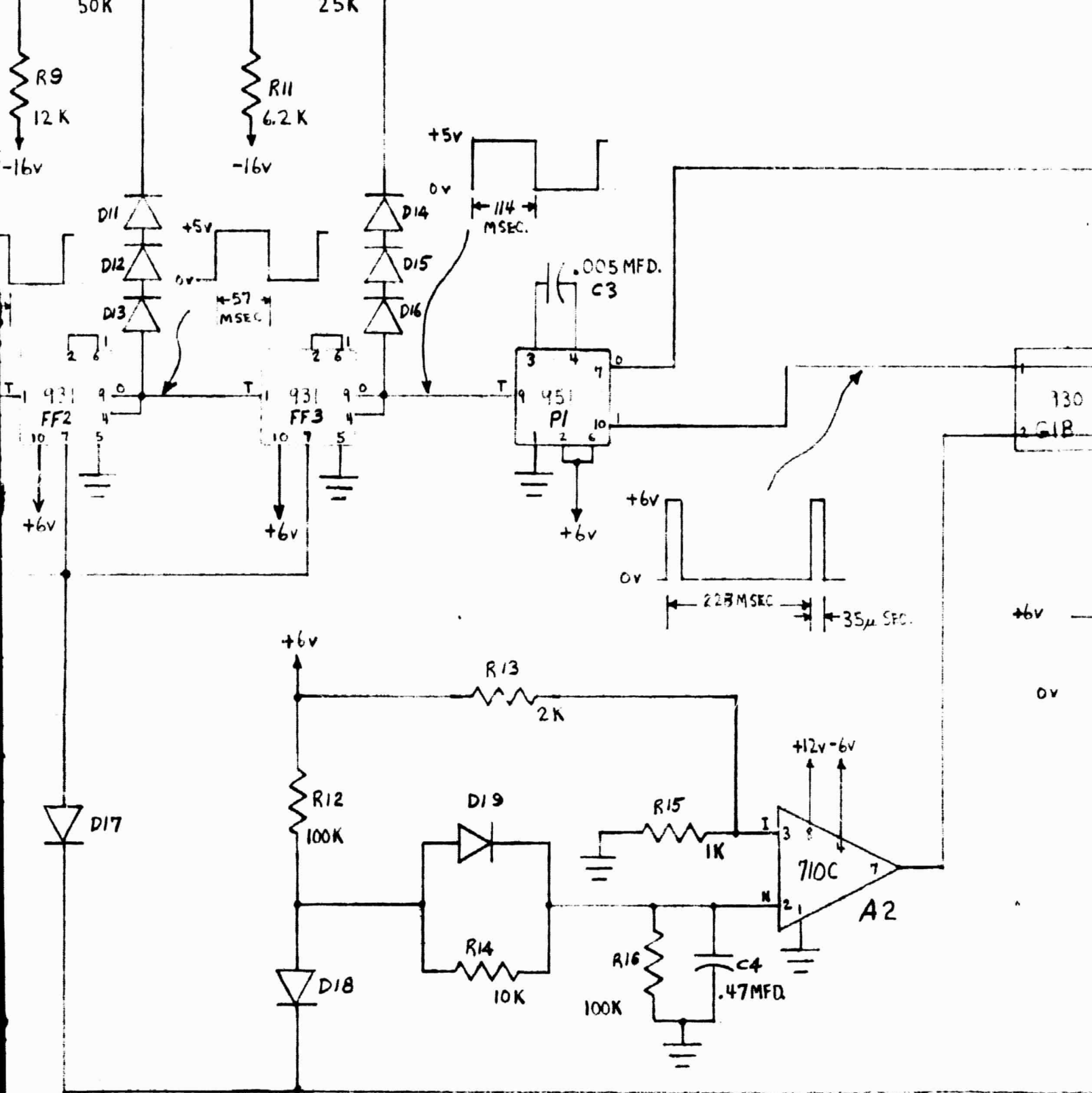




22	VERT. RESET PULSE ①
21	VERT. TRACE POSITIONING ⑤
20	VERT. END OF FRAME PULSE ③
19	EV - VERT. SWEEP
18	KEY
17	
16	
15	+6v
14	+10v
13	+12v
12	+16v
11	GND
10	-16v
9	-10v
8	-6v
7	
6	TRIG. PULSE
5	
4	
3	
2	
1	

NOTE

- ALL DIODES ARE IN486B
- ALL RESISTORS ARE 1/4w 5%
- TO RESET VERT. TRACE TO BOTTOM OF RASTE
BOTH OF THE FOLLOWING CONDITIONS MUST BE MET
- 3A S' GROUNDED
- 3B ST4 INHIBITED

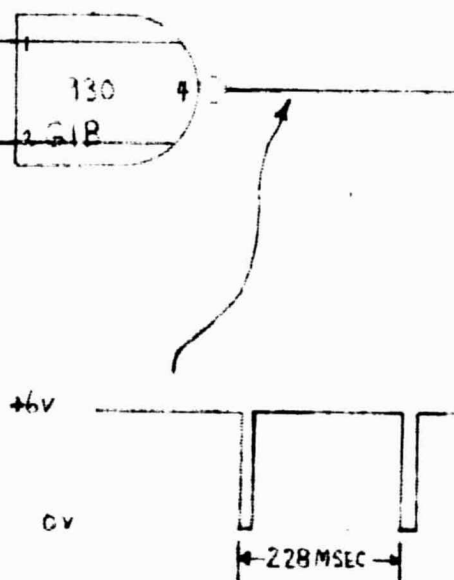


IF RASTER (I.C.S.W.),
ONS MUST EXIST.

		SCALE	
		PROJ. NO.	01114
		DRAWN BY	ED GILREA
		DATE	4-29-68
		FOR ASSEMBLY	
		MATERIAL	
LET.	CHANGE	DATE	WEIGHT CAL. ACT.

→ VERT. RESET PULSE
PIN 22 (D)
SAME AS END OF FRAME
PULSE, EXCEPT ALL PULSES
ARE SEEN.

→ VERT. END OF FRAME
PULSE - PIN 20 (E)
NO INITIAL PULSE WHEN
CIRCUITS RESET TO I.C.
AND THEN INITIATED.

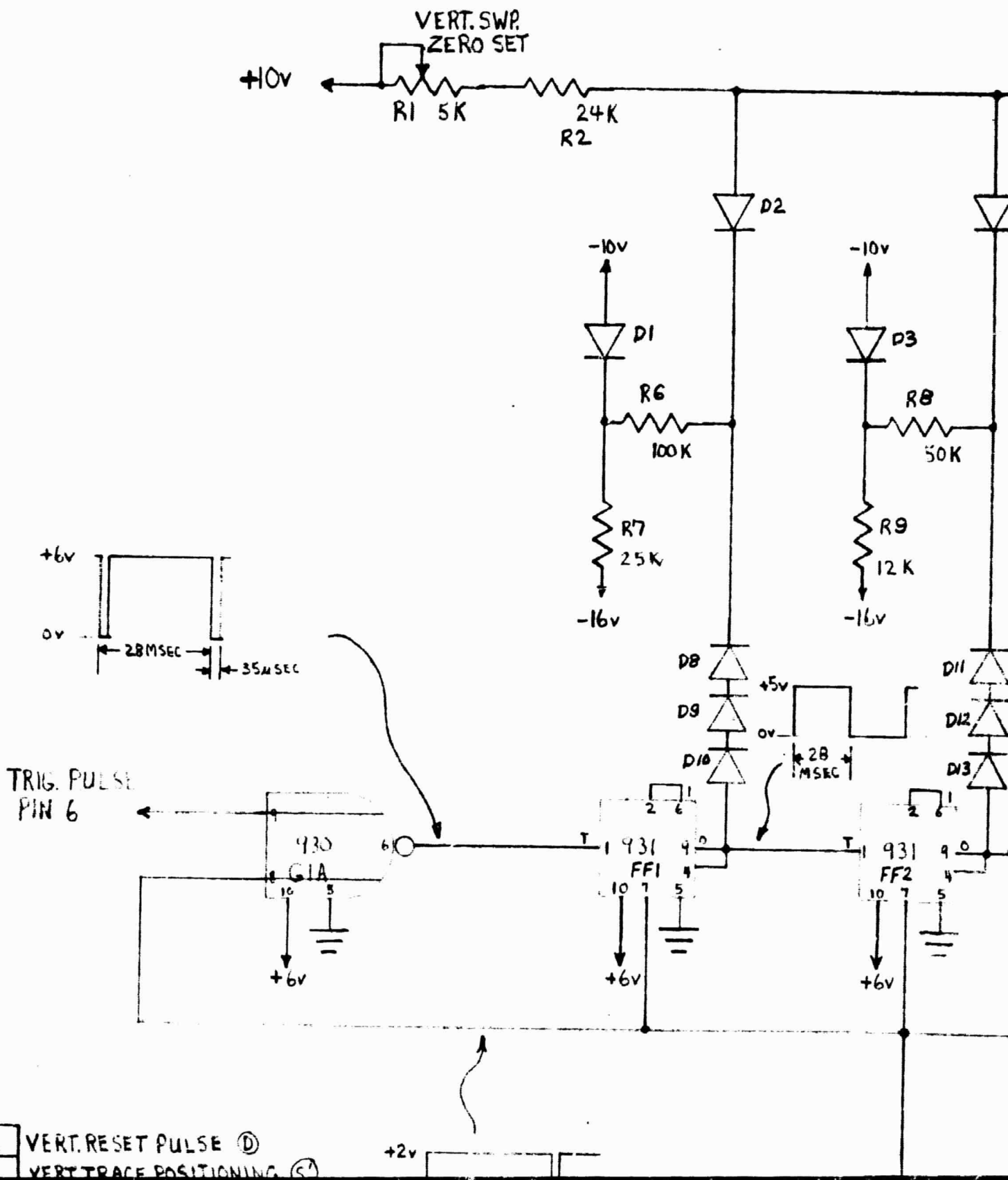


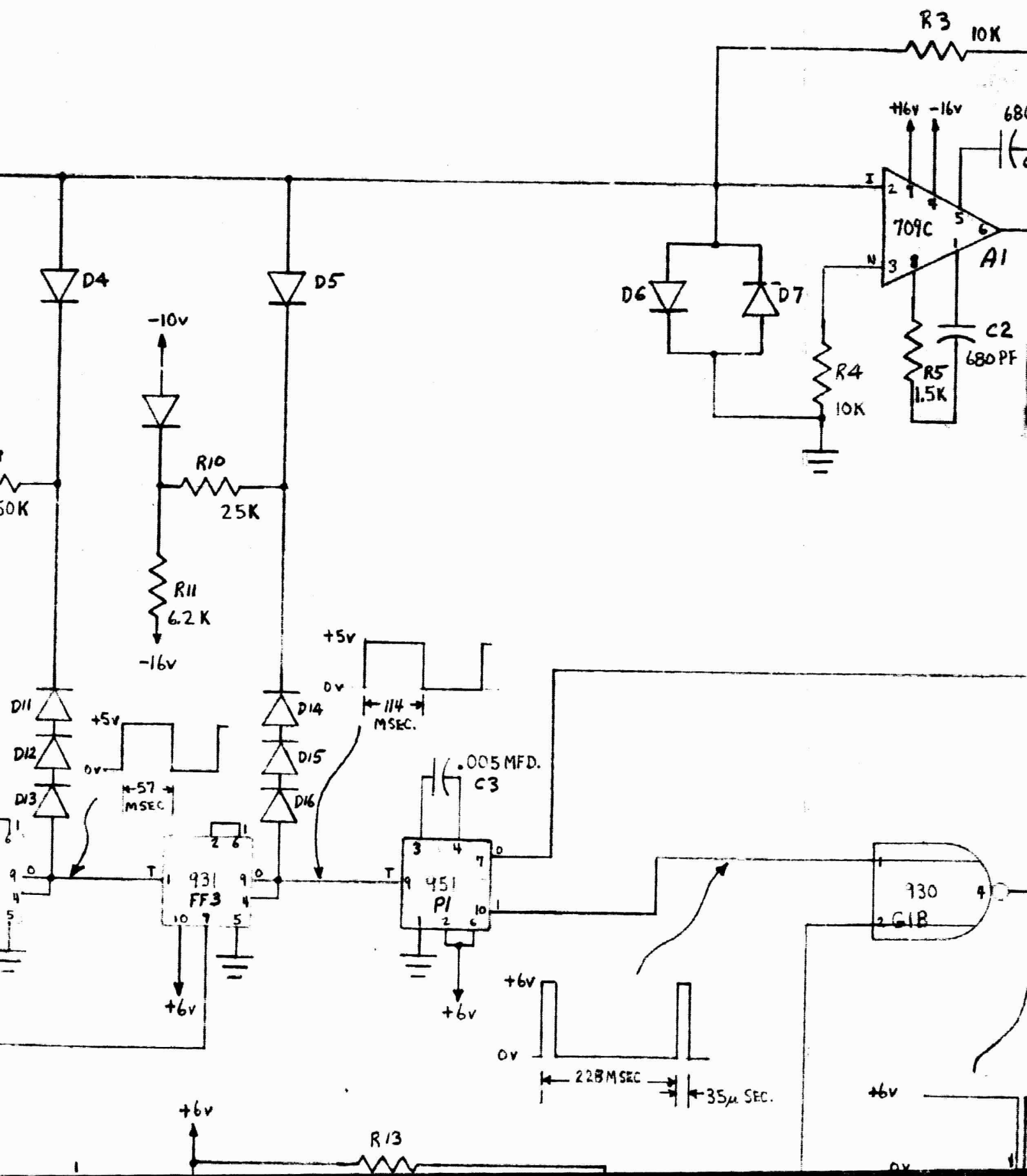
→ (S') VERT. TRACE
POSITIONING
PIN 21
OPEN TO OPER., GND TO ACT.

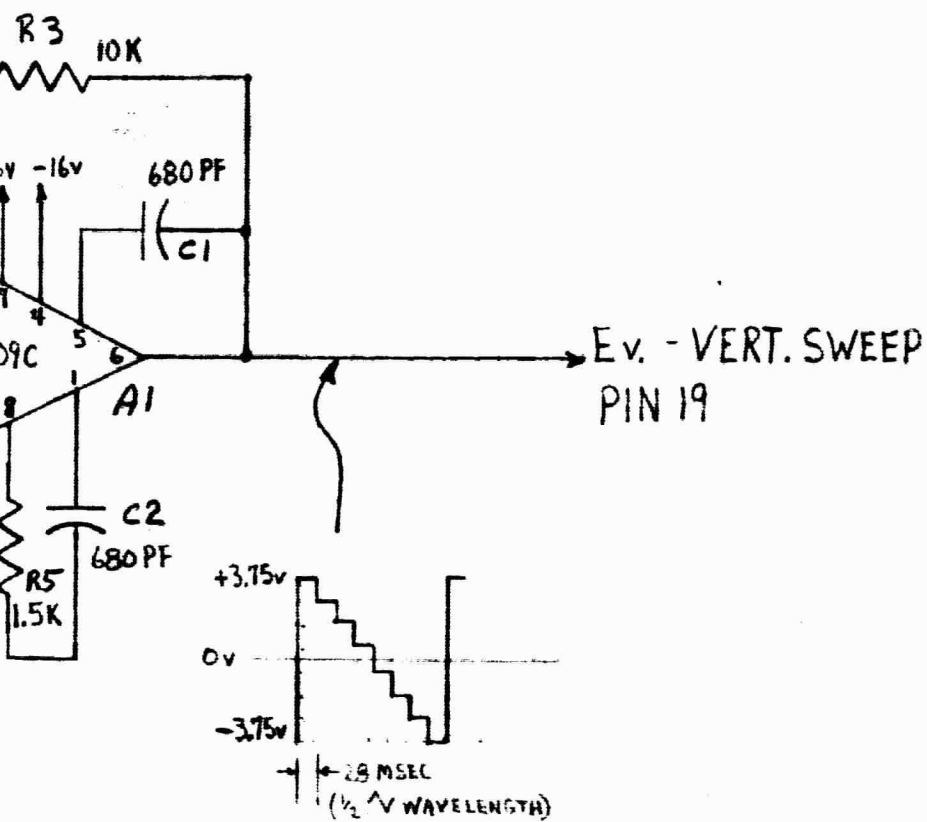
	<p align="center">HIGH ALTITUDE ENGINEERING LABORATORY UNIVERSITY OF MICHIGAN DEPARTMENT OF AEROSPACE ENGINEERING ANN ARBOR MICHIGAN</p>
01114	
ED GILREATH	<p>NAME VERT. RASTER SCAN GENERATOR</p>
4-29-68	
	<p>DRAWING NO. H3-52025</p>

J7

IV

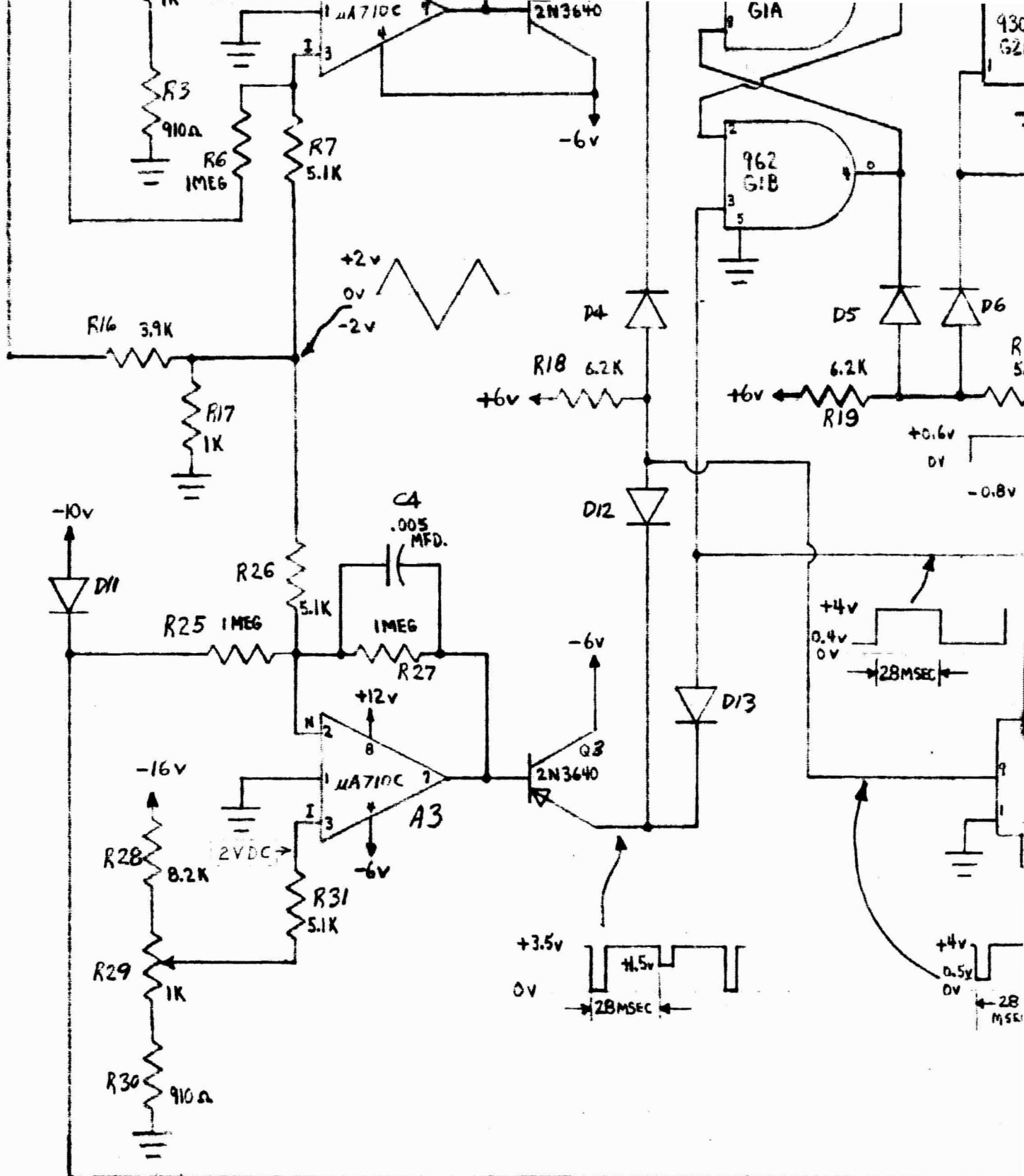






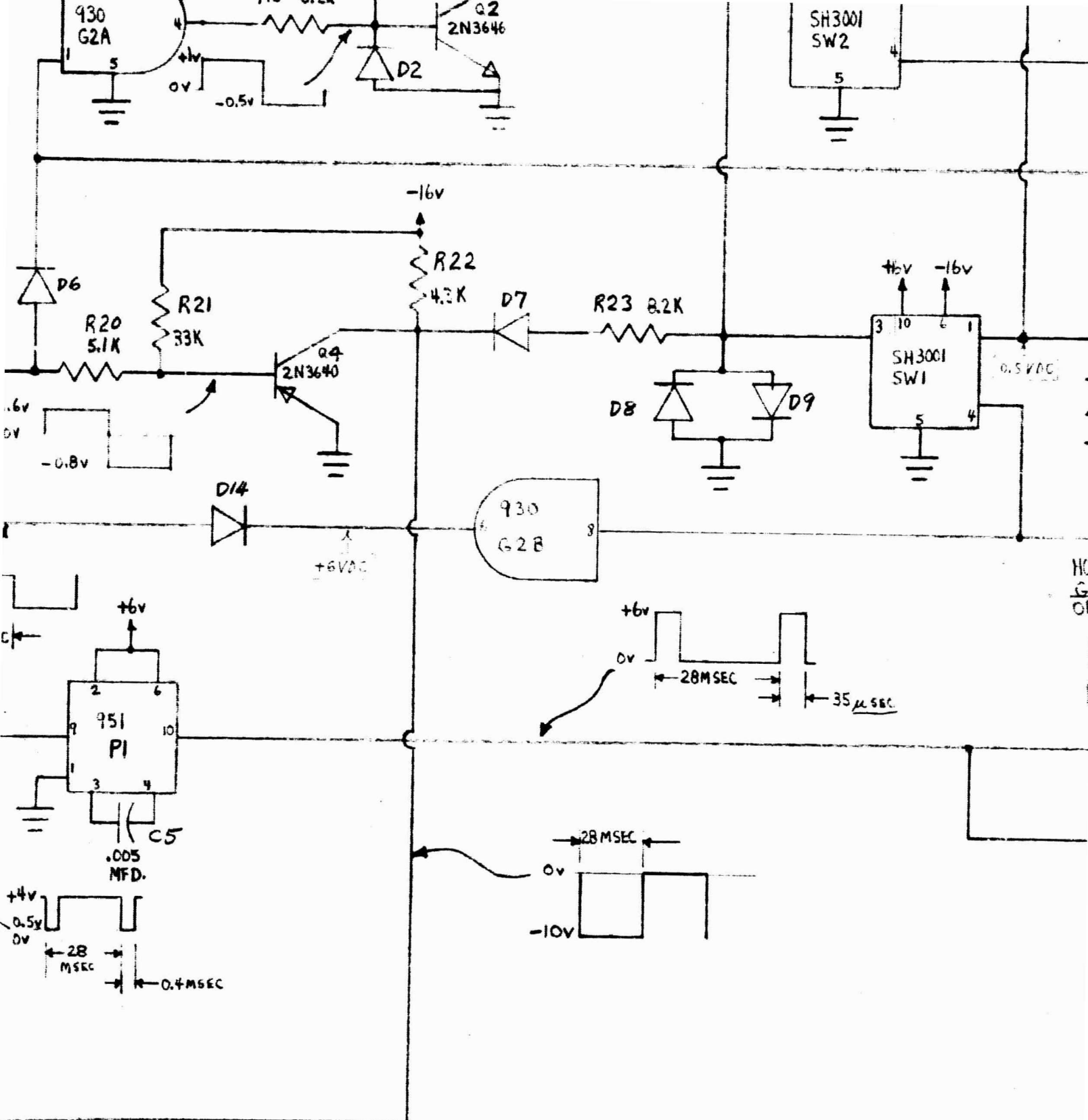
VERT. RESET PULSE
PIN 22 (D)
SAME AS END OF FRAME
PULSE, EXCEPT ALL PULSES
ARE SEEN.

VERT. END OF FRAME
PULSE - PIN 20 (B)
NO INITIAL PULSE WHEN
CIRCUITS RESET TO I.C.
AND THEN INITIATED.



NOTE:

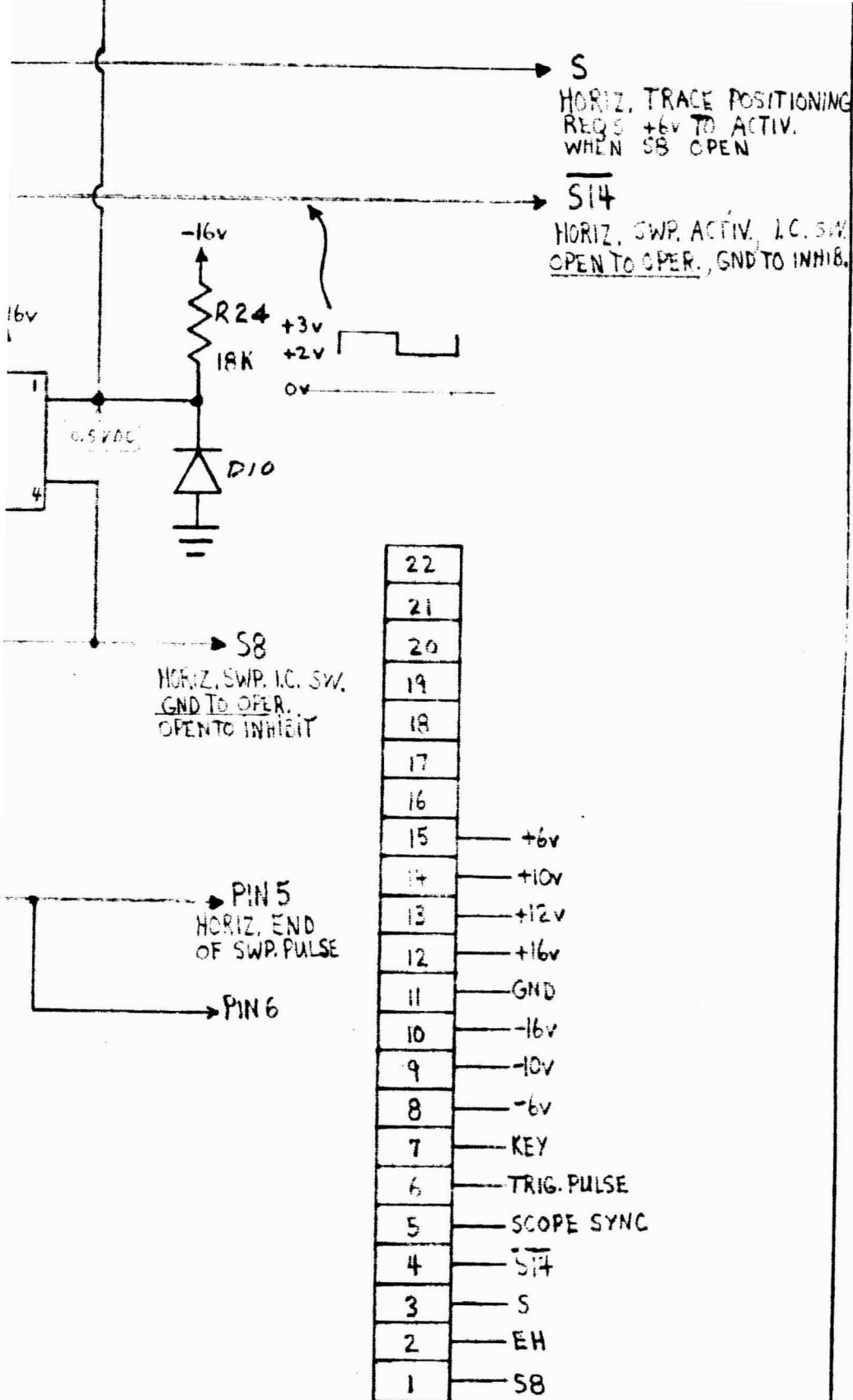
1. ALL DIODES IN486B UNLESS NOTED.
2. ALL RESISTORS $\frac{1}{4}$ W 5% UNLESS NOTED
3. SB IS IC (INITIAL CONDITION) SW TO RETURN HORIZ. SWP. TO RIG GROUND TO OPER., OPEN TO INHIBIT
4. CLOSING S AND INHIBITING $\overline{514}$ ALLOWS HORIZ. TRACE TO D REQUIRES +6v TO ACTIVATE WHEN SB IS INHIBITED.



P. TO RIGHT.

E TO DRIFT TO CEN. OF RASTER.
LIMITED.

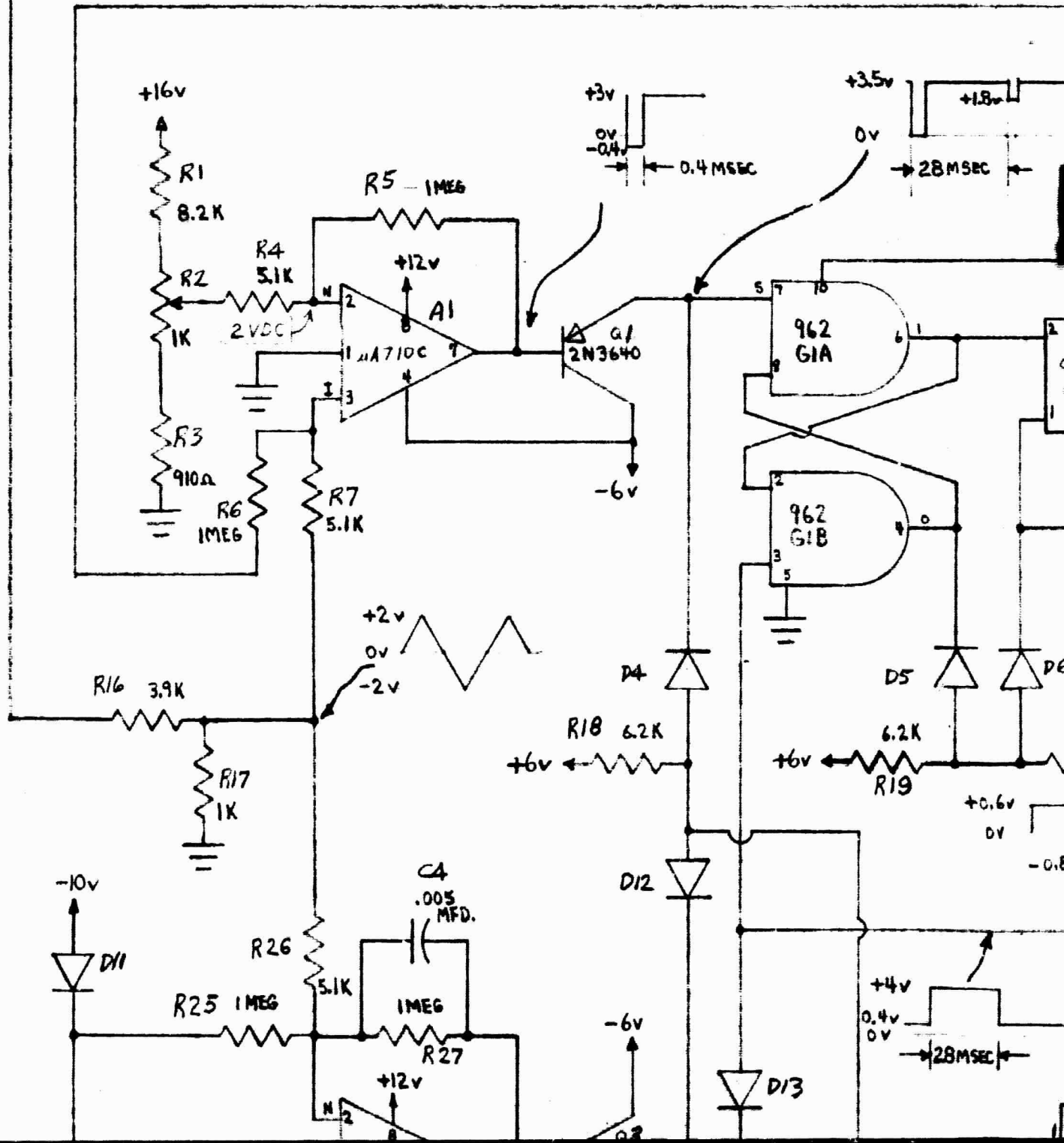
			SCALE	
			PROJ. NO.	01114
			DRAWN BY	<i>Ed. Smith</i>
			DATE	5-9-68
			FOR ASSEMBLY	
			MATERIAL	
LET.	CHANGE	DATE	WEIGHT CAL. ACT.	

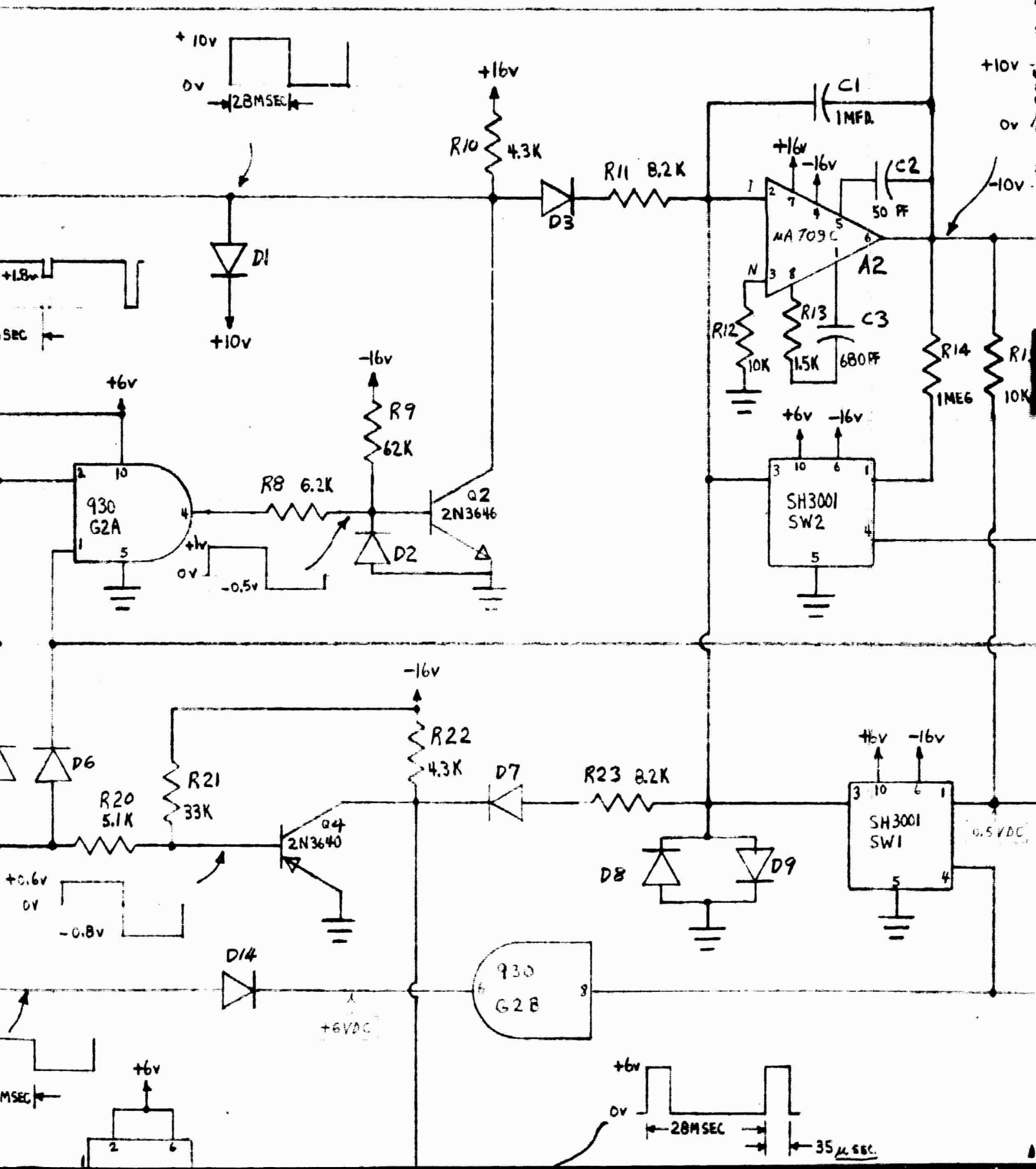


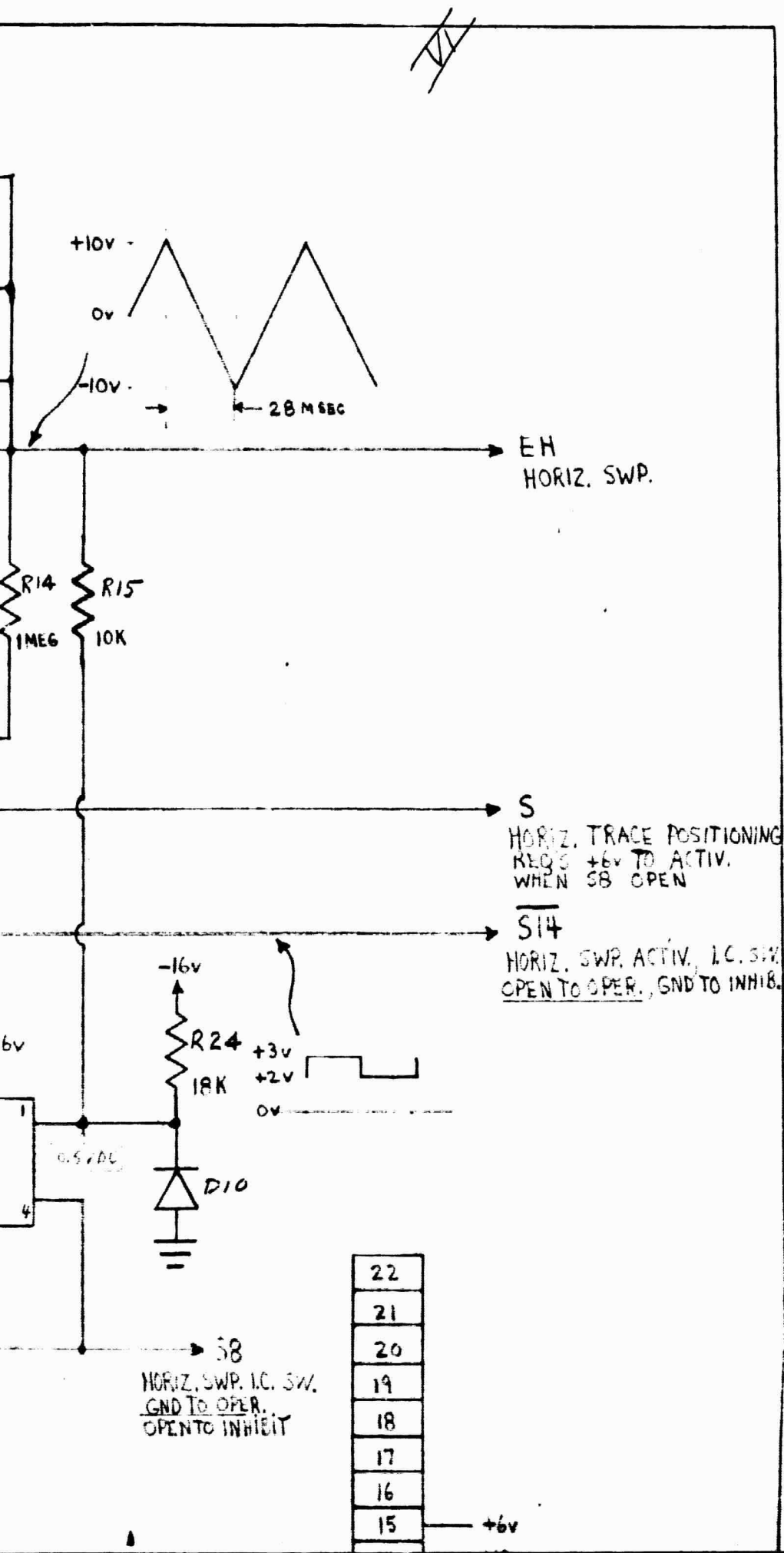
HIGH ALTITUDE ENGINEERING LABORATORY
UNIVERSITY OF MICHIGAN
DEPARTMENT OF AEROSPACE ENGINEERING
ANN ARBOR MICHIGAN

NAME HORIZ. RASTER SCAN GENERATOR

DRAWING
NO. H3-52026







#28 DRILL.

DRILL THRU (4) HOLES EQUALLY SPACED
ON $.750 \pm .001$ B.C. LOCATE CENTER TO $.001$.

B2' C'SINK TO $.280$ DIA.

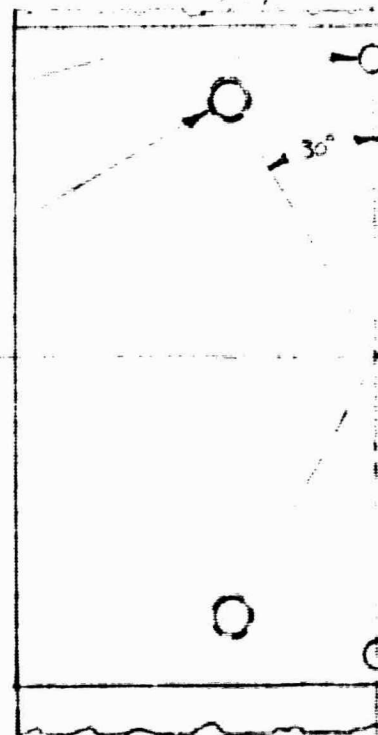
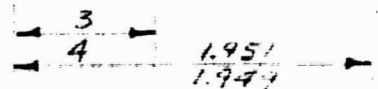
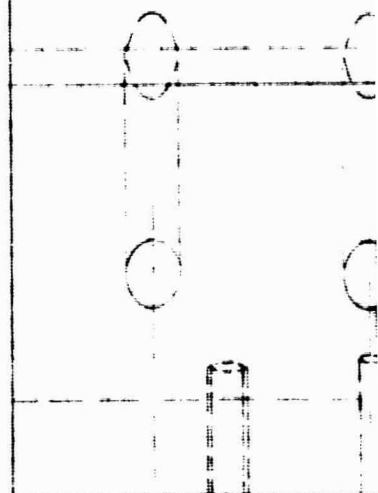
TYPICAL (2) PLACES

$.3752 - .3754$ DIAM. HOLE

C'FLA $\frac{1}{16}$ NOM.

LOCATE CENTER TO $.001$

TYPICAL (2) PLACES



(2) HOLES ON $3.1570 \pm .0002$ B.C.

$.1252 - .1255$ DIA. LOCATE CENTER TO $.001$.

CHAMFER $\frac{1}{16}$ NOM.

TYPICAL (2) PLACES.

DRILL THRU (4) HOLES.

#16 DRILL. DIAM. LIMITS $.174 - .180$

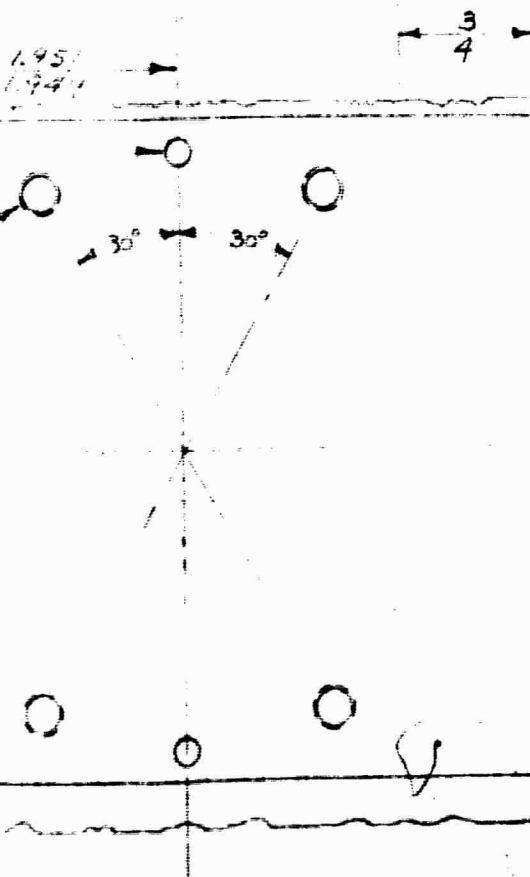
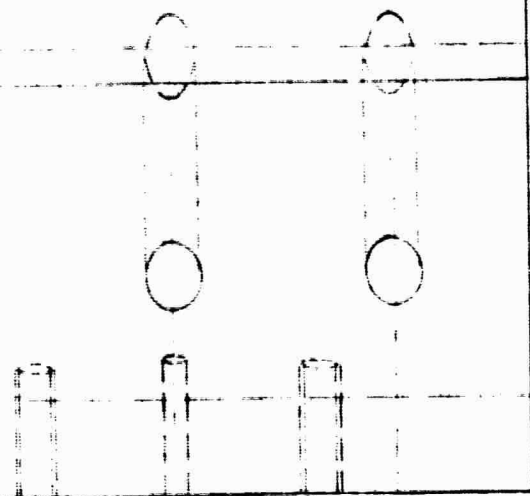
$3.157 \pm .001$ B.C. LOCATE CENTER TO $.001$.

C'SINK 120° TO $.20 - .23$ DIA. TAP WITH HELI-COIL

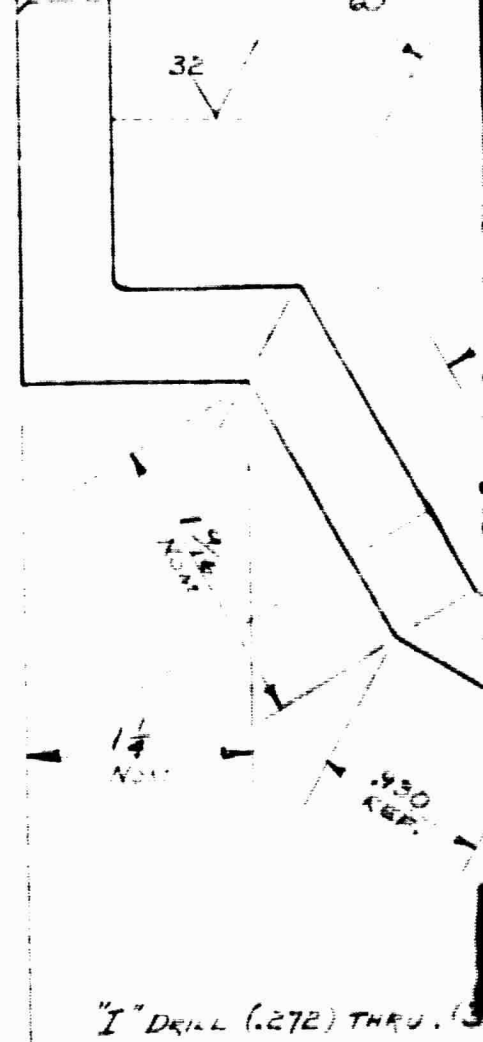
PART NO. 2-CRA-H3. TYPICAL (2) PLACES

4

12.0
NOM.



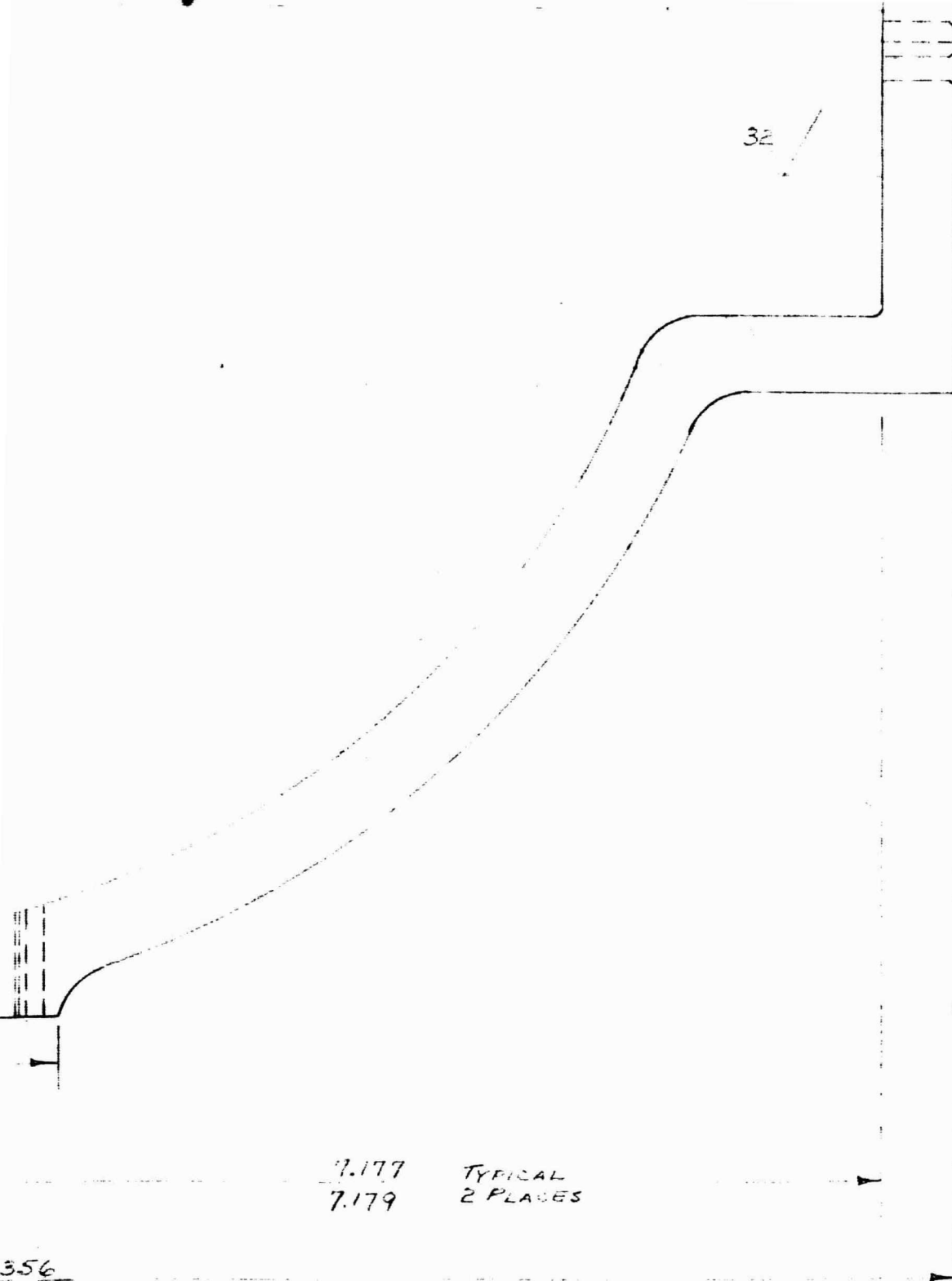
VIEW SHOWS TOP & BOTTOM BOLDS ONLY.



"I" DRILL (.272) THRU.

II

LET



356
M.

			SCALE	FULL	HIGH ALTITUDE ENGINEERING UNIVERSITY OF MICHIGAN DEPARTMENT OF AERO. AND ASTRO. ENG. ANN ARBOR
			PROJ. NO.	01114	
			DRAWN BY	F3	
			DATE	4-23-68	
			FOR ASSEMBLY		NAME MIDDLE G
			MATERIAL	AZ-31B	DRAWING NO. H5-52
LET.	CHANGE	DATE	WEIGHT CAL. ACT.		

IV

UDE ENGINEERING LABORATORY
NIVERSITY OF MICHIGAN
OF AERO. AND ASTRO. ENGINEERING
BOR MICHIGAN

DDLE GIMBAL

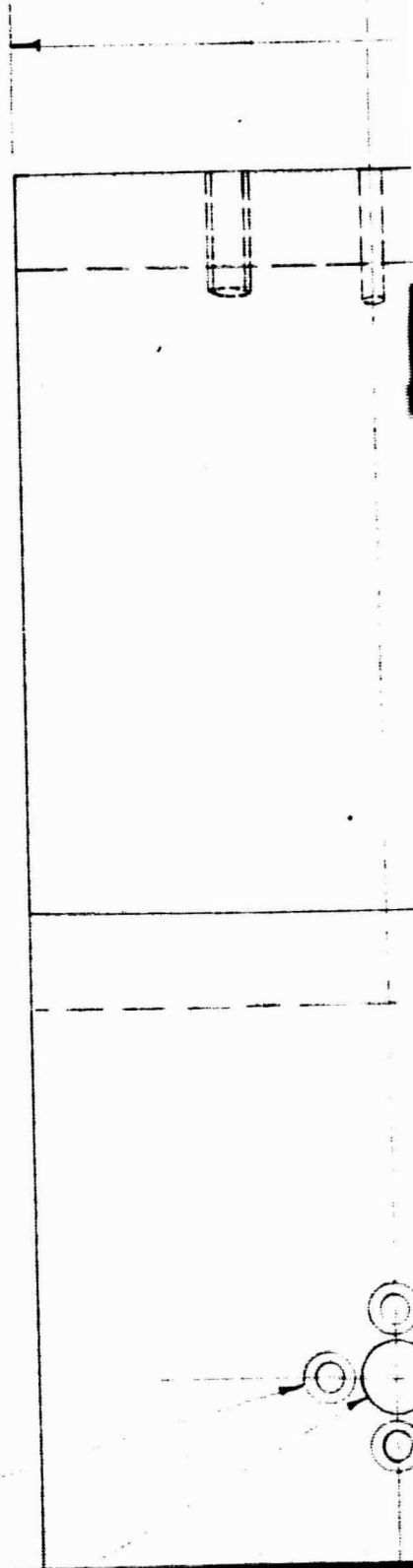
45-52001

1

IV

NOTES:

1. BREAK EDGES.
2. ANODIZE.



3.902
3.898

13.001
12.999

6.501
6.499

6.0
NOM

5.0
NOM

4.0
NOM

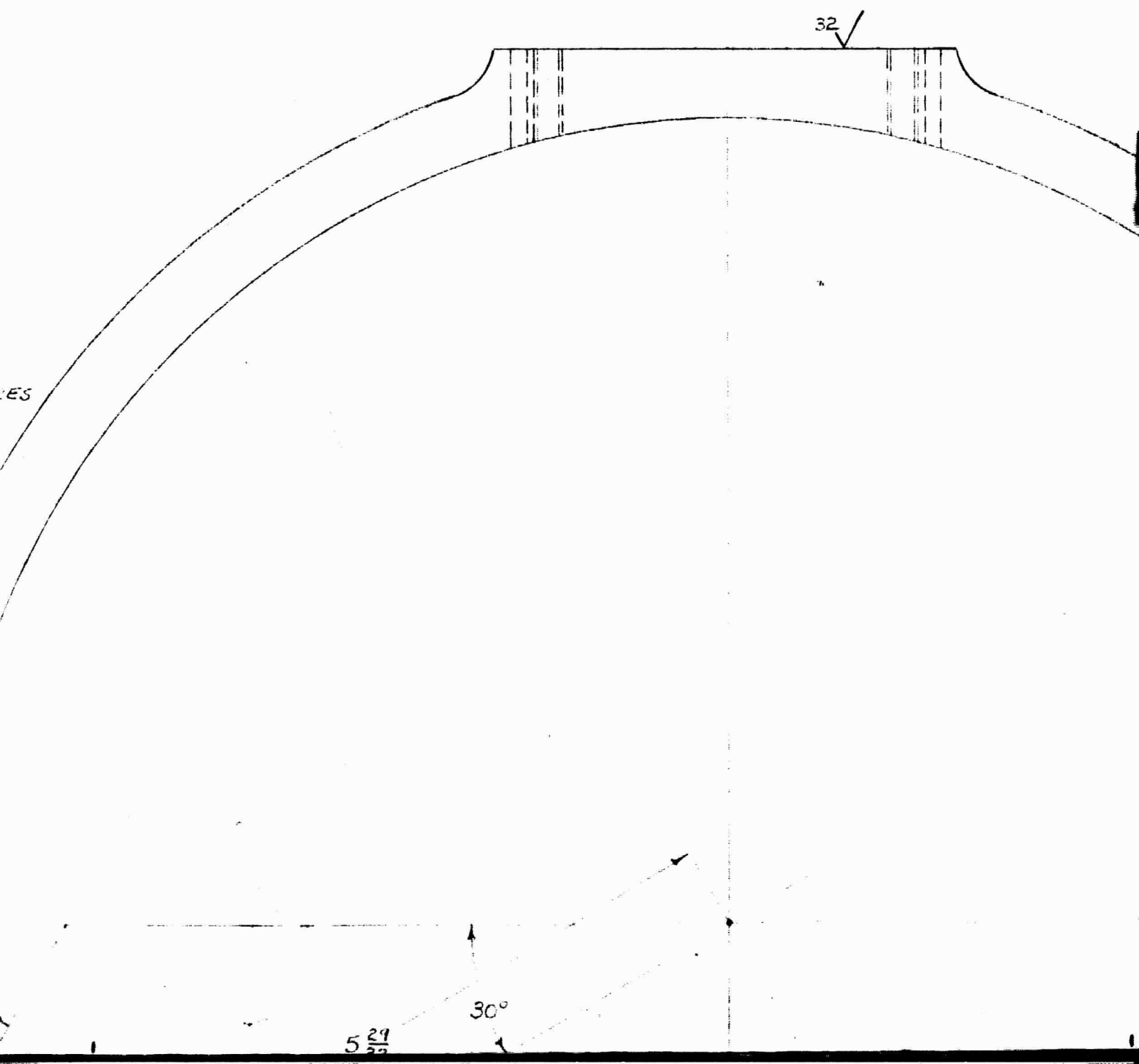
$\frac{1}{16}$ R. NOM.
TYP. (4) PLACES

$\frac{7}{16}$ R. NOM.
TYP. (10) PLACES

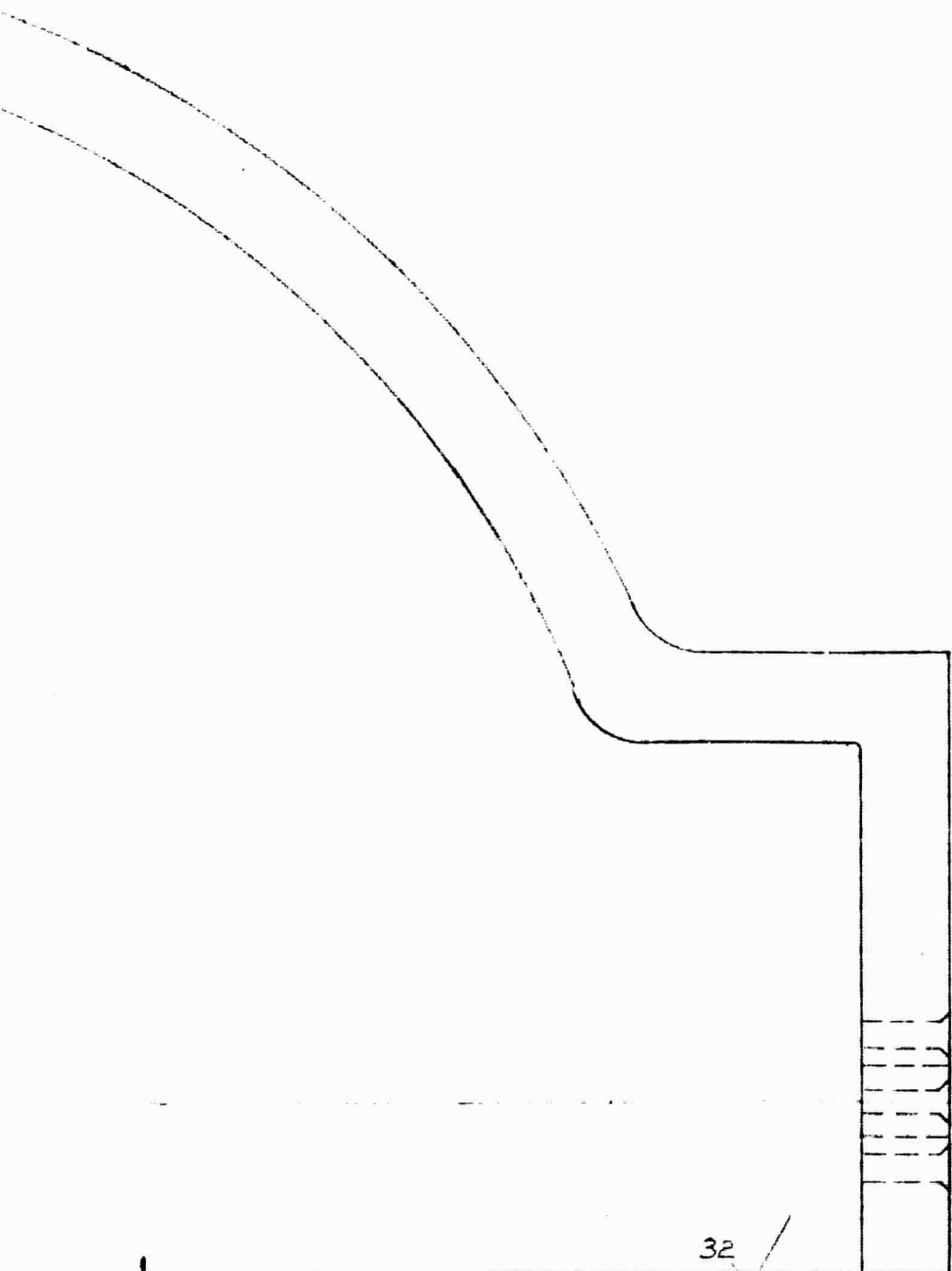
60°

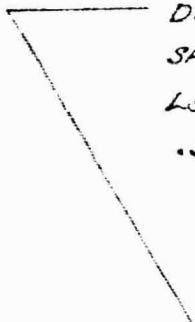
32

VIII

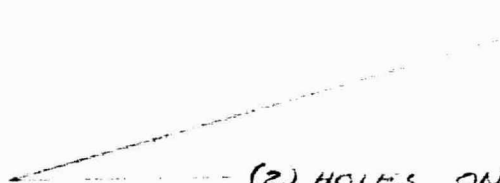


IV





DRILL THRU (4) HOLES. #19 DRILL
SPACED AS ON HI-52007. $3.157 \pm .001$ B.C.
LOCATE CENTER TO .001. C'SINK 82° TO
.340 DIAM.



(2) HOLES ON $3.1570 \pm .0002$ B.C.
.1252 - .1256 DIAM. LOCATE CENTER TO .001
CHAMFER $\frac{1}{16}$ NOM.

I

32



15.088
15.056

45
NOM

32



II

32 ✓

40
NOM.

FINISH SPEC.
APPLIES

32 ✓

15.868
15.844

16.856
NOM.

LET.	

III

FINISH SPEC.
APPLIES

32 ✓

7.940
7.916

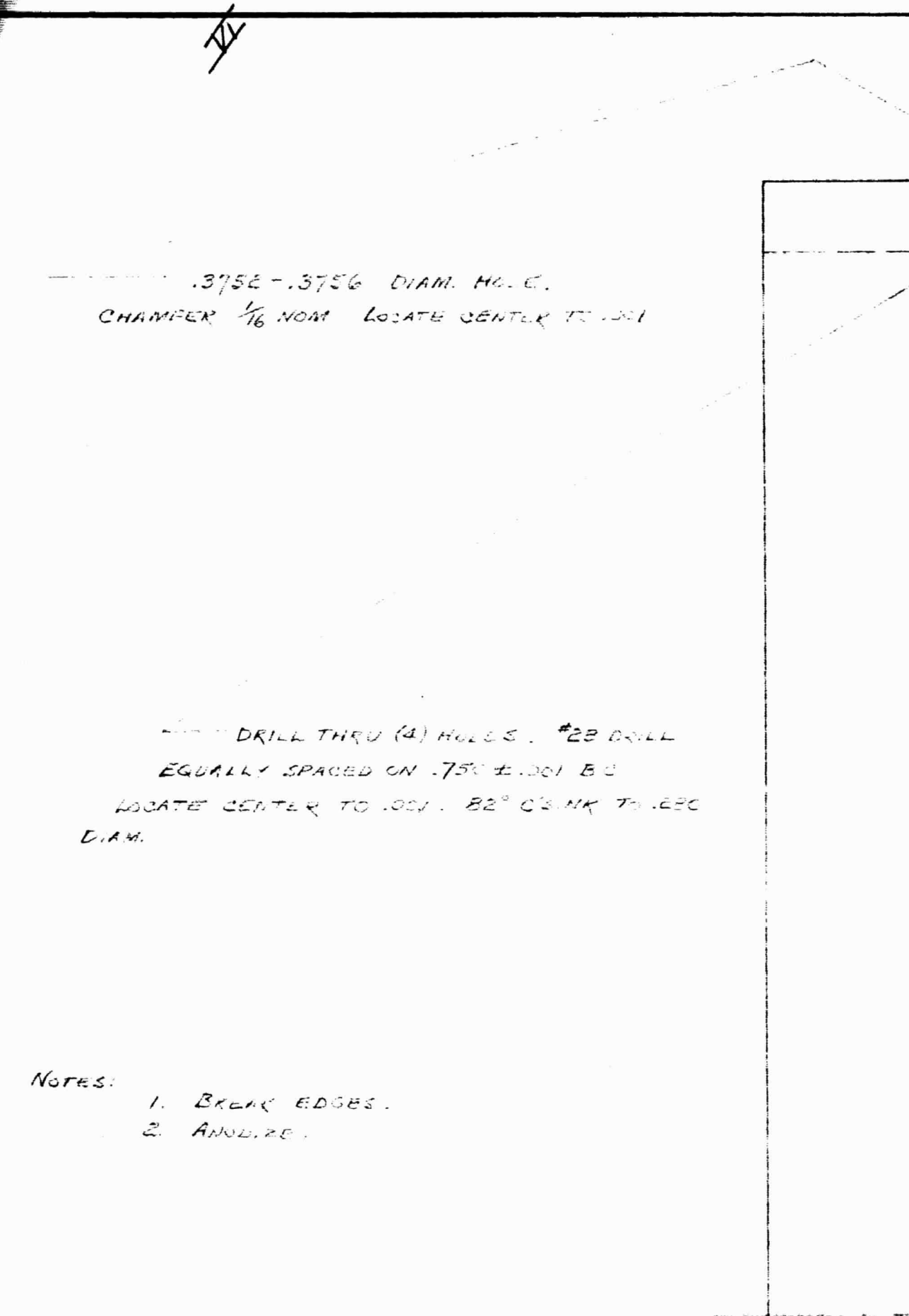
			SCALE	FULL	HIGH ALTITUDE ENGINE UNIVERSITY OF DEPARTMENT OF AERO. ENGR. ANN ARBOR	
			PROJ. NO.	01114		
			DRAWN BY	F3		
			DATE	4-23-68		
			FOR ASSEMBLY		NAME	OUTER
			MATERIAL	AZ-31B	DRAWING NO.	H5-
LET.	CHANGE	DATE	WEIGHT	CAL. ACC.		

36 ✓
TITUDE ENGINEERING LABORATORY
UNIVERSITY OF MICHIGAN
OF AERO. AND ASTRO. ENGINEERING
ARBOR MICHIGAN

UTER GIMBAL

H5-52002

IV

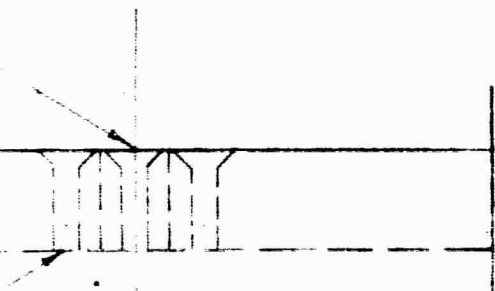

----- .375E-.3756 DIAM. HOLE.
CHAMFER $\frac{1}{16}$ NOM LOCATE CENTER TO .001

----- DRILL THRU (4) HOLES. #28 DRILL
EQUALLY SPACED ON .750 \pm .001 B.C.
LOCATE CENTER TO .001. 82° C'SINK TO .000
DIAM.

NOTES:

1. BREAK EDGES.
2. ANODIZE.

~~VII~~



7.933
REF.

16.087
NOM.

VIII

32 ✓

32 ✓



2.71 M
FINISH

~~IX~~